Platinum(II) complexes of heteroaromatic derivatives

by

JANINE CHANTSON

Submitted in partial fulfilment of the degree

PHILOSOPHIAE DOCTOR

in the Faculty of Natural and Agricultrual Sciences

UNIVERSITY OF PRETORIA

PRETORIA

Supervisor: S. Lotz

December 2002

ACKNOWLEDGEMENTS

With sincere thanks to

Prof S. Lotz for his mentorship.

Prof R. Vleggaar and his workgroup for sharing laboratory equipment and expertise.

Prof. P.L. Wessel and Mr. E. Palmer for assistance with the NMR facilities.

Dr. Helmar Görls and Dr. V.V.H Ichharam for the determination of crystal structures.

Mr. L. Engelbrecht, Mr. R. Muir and Mr R. Dumas for technical support.

Prof. J. Boeyens and Prof. T. Modro for their belief in me and for allowing me the time to complete the project.

Friends and colleagues in the Department for their moral support.

My dearest daugher, Tyra Jane, for the many hours spent over weekends and holidays in my office, affording me the time to complete this dissertation.

CONTENTS

SUMMARY

Platinum(II) complexes of heteroaromatic derivatives

Candidate: Janine Chantson

Supervisor: S. Lotz

Degree: Ph.D. Chemistry

Department of Chemistry, Faculty of Natural and Agricultrual Sciences

University of Pretoria, Pretoria

Date: December 2002

The central theme of this thesis is the preparation and characterisation of novel platinum(II) organometallic complexes of heteroaromatic ligands, where the heteroatom is sulfur, nitrogen or oxygen. These complexes were obtained primarily through oxidative addition reactions of zerovalent platinum.

The first example of a double oxidative addition reaction of platinum(0) to a heteroaromatic substrate is reported: tetrakis(triethylphosphine)platinum(0) reacted with 4,6-dibromodibenzothiophene to yield μ-dibenzothienyl-1κC^4:2κC^6-bis[*trans*-bromobis(triethylphosphine)platinum(II). A related binuclear platinum(II) complex, μ-dibenzothienyl-1κC^4:2κC^6-bis[*cis*-chloro(η^4-1,5-cyclooctadiene)platinum(II)], was also prepared, but was obtained via double transmetallation rather than double oxidative addition, by reacting 4,6-bis(trimethylstannyl)dibenzothiophene with the *cis*-directing precursor dichloro(η^4-1,5-cyclooctadiene)platinum(II). The 4,6-substituted dibenzothiophene ligands used in these reactions were novel and methods for the synthesis of 4,6-bis(trimethylstannyl)-dibenzothiophene, 4,6-bis(trimethylsilyl)dibenzothiophene and 4,6-dibromodibenzothiophene were designed. The crystal structures of the latter two compounds were obtained. An improved method of synthesis of 2,8-dibromodibenzothiophene was also developed.

The reactivities of various types of heteroaromatic compounds with platinum(0) were investigated. Carbon-sulfur bond activation in 3,6-dimethylthieno[3,2-*b*]thiophene produced a six-membered thiaplatinacycle. The X-ray crystal structure established that the C(vinyl)-S rather than the C(aryl)-S bond was the site of attack. Analogous thiaplatinacycles were obtained with 2,2′-bithiophene and 1-methyl-2-(2-thienyl)pyrrole. These molecules also underwent carbon-hydrogen bond activation at the α-carbon of the thienyl rings to generate platinum(II) hydrides with *trans* phosphine groups.

Oxidative insertion into the nitrogen-hydrogen bonds of nitrogen heteroaromatic compounds (*eg.* indole, imidazole, pyrazole, benzimidazole and indazole) occurred readily to form *trans*-[PtH(1-azolyl)$(PEt_3)_2$] complexes. Activation of the relatively weaker N-H bonds occurs more readily than C-S or C-H insertion. However, the reactivity of pyrrole with tetrakis(triethyl)-phosphineplatinum(0) was appreciably poorer. Tris(triphenylphosphine)platinum(0) was generally not a strong enough nucleophile to produce complexes analogous to that obtained with tetrakis(triethylphosphine)platinum(0).

Oxygen-containing heterocycles such as furan, dibenzofuran and benzoxazole reacted with tetrakis(triethylphosphine)platinum(0) through C-H bond activation, generating platinum(II) hydrides similar to those obtained with the azoles *i.e. trans* isomers. The greater strength of C-O bonds did not allow for the formation of six-membered platinacycles, whereas the weaker C-S bonds in thiophene-containing compounds led to the formation of thiaplatinacycles. Despite benzothiazole having a C-S bond, oxidative insertion occurred at a C-H bond.

Displacement of cyclooctadiene from dichloro(η^4-1,5-cyclooctadiene)platinum(II) by two equivalents of novel heteroarylphosphine ligands afforded complexes of the type *cis*-[$Pt(PXR_2)_2Cl_2$] where X is a thienyl, pyrrolyl or pyridinyl derivative and R is a phenyl or isopropyl group. An exception was [Pt(P{2-(1-methylpyrrolyl)}$^iPr_2)_2Cl_2$] which has a *trans* geometry.

The platinum(II) complexes were characterised by NMR spectroscopy, mass spectrometry and single crystal X-ray studies. Platinum coupling constants were particularly useful in assigning the geometries of the square planar complexes.

LIST OF ABBREVIATIONS

bipy	2,2′-bipyridine
BT	benzothiophene
cod	1,5-cyclooctadiene
COSY	correlated spectroscopy
Cy	cyclohexyl
dba	dibenzylideneacetone
DBT	dibenzothiophene
dppe	bis(diphenylphosphino)ethane
dppf	1,1′-bis(diphenylphosphino)ferrocene
dppm	bis(diphenylphosphino)methane
EI	electron impact
eq	equivalents
FAB	fast atom bombardment
HDN	hydrodenitrogenation
HDO	hydrodeoxygenation
HDS	hydrodesulfurisation
HETCOR	heteronuclear correlation spectroscopy
IUPAC	International Union of Pure and Applied Chemistry
MS	mass spectrometry
m/z	mass to charge ratio
NBS	*N*-bromosuccinimide
NMR	nuclear magnetic resonance
ORTEP	Oak Ridge Thermal Ellipsoid Program
T	thiophene
Tol	toluyl
thf	tetrahydrofuran
tmeda	*N,N,N′,N′*-tetramethylethylenediamine

CHAPTER 1

Introduction

Platinum chemistry is an attractive field of study as a vast array of platinum complexes displaying a variety of different coordination modes can be found. The principle formal oxidation states of zero, two and four exhibit bonding to σ- and π-bonding ligands. In oxidation state two, platinum forms square planar complexes, and depending on the combination of ligands involved, *cis*- and *trans*- isomers are obtained.

Important organometallic homogeneous catalysts are found in the early and late transition metal groups; examples thereof include titanocene derivatives, *ansa*-metallocenes[1], which catalyse olefin polymerisations and nickel allyls which catalyse olefin oligomerisations. Of special interest in our laboratories are the catalytic reactivities of Group 10 transition metals. A key step in catalysis is the oxidative addition reaction which is best studied for Group 10 transition metals. By focussing on platinum complexes, it is possible to isolate key oxidative addition complexes and to study their composition, where the analogous complexes of nickel and palladium are merely unstable intermediates.

1.1 Catalysis

The chemistry of platinum is often studied in order to model the behaviour of its lighter, more

[1] For examples, see *Metallocenes Volume 1*, edited by A. Togni and R. L. Halterman, Wiley-VCH, 1998

CHAPTER 1

labile 3*d* and 4*d* analogues of nickel and palladium respectively. Zerovalent Group 10 metals complexes are electron-rich nucleophiles and readily susceptible to oxidation. The transition state involves the promotion of electrons from the d^{10} to the d^9s^1 state [1]. *Ab initio* molecular orbital calculations for the oxidative addition of zerovalent palladium and platinum to C-H bonds have shown that the activation energy barrier is larger for palladium than platinum [2]. Since the d^9s^1 state is more accessible for platinum than palladium, this results in a more exothermic / less endothermic oxidation addition reaction for platinum(0). Oxidative addition reactions are therefore generally easier for platinum. Conversely, reductive elimination is easier for palladium by the same argument. For this reason palladium enjoys widespread use as a catalyst for amongst others, carbon-carbon coupling processes and transmetallation reactions [3]. For example, transmetallation from tin is known as Stille Coupling and is one of the most broadly developed processes in organopalladium chemistry. A search for "Stille Coupling" in the Science Citation Index for the three year period 1997 - 1999 yielded 102 hits alone [4]. A general catalytic cycle for a palladium-catalysed cross-coupling reaction is given in Scheme 1.1.

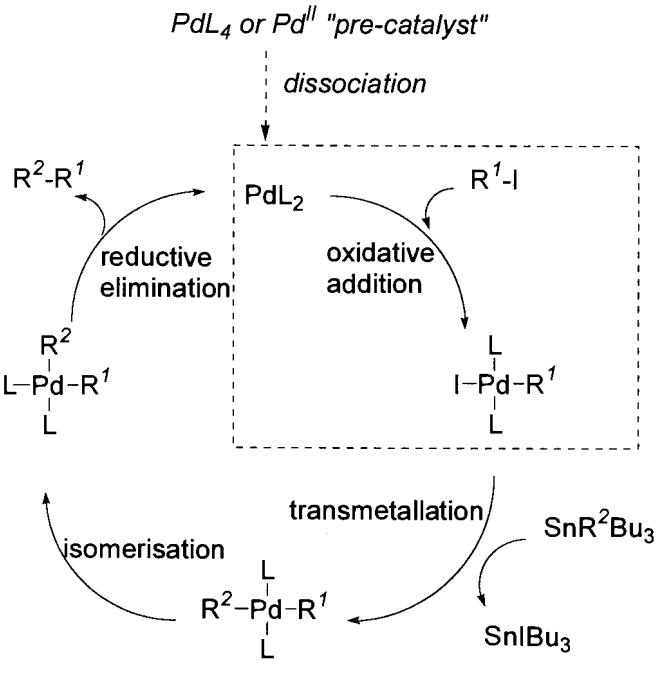

Scheme 1.1 A cross-coupling catalytic cycle *eg.* Stille

The initial step involves the oxidative addition of an arylhalide (or pseudohalide) to a zerovalent palladium complex. This "active" complex may arise from the dissociation of a coordinatively saturated zerovalent palladium precursor, or from a divalent palladium complex which is converted to an active zerovalent palladium catalyst [3]. Palladium catalysts have been applied for R^1/R^2 coupling of heteroaromatic substrates. Although the catalytic reactions which lead to the final coupled products have been investigated, the individual reactions steps (*i.e.* oxidative addition of the heteroaromatic substrate to the metal catalyst complex) have not yet been thoroughly explored. The basis of this study was to obtain more information about the oxidative addition reactions of heteraromatic substrates using platinum.

1.2 Oxidative addition

The oxidation state of the metal increases by two units during an oxidative addition reaction. The metal complex will first vacate a coordination site and formally transfer electrons during bond cleavage of the oxidising agent, AB; one electron to each of the atoms A and B. Two new bonds, M-A and M-B, are formed and the metal ends up as a coordinatively saturated complex (Scheme 1.2).

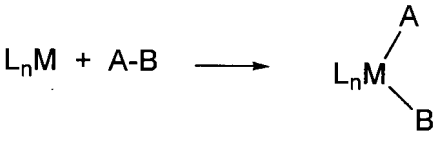

Scheme 1.2 Oxidative addition to $[ML_n]$

The enthalpy change for the reaction is a function of the bond dissociation energies (*D*) according to Equation 1.1

Equation 1.1 $$\Delta H_{o.a} = D\,(A\text{-}B) - \{\, D\,(L_nM\text{-}A) + D\,(L_nM\text{-}B)\,\}$$

The $T\Delta S$ term is of the order of 42 kJ / mol [5], and it is thus the relative strengths of the bonds involved that determine whether the oxidative addition is energetically favourable or not. The thermochemistry of M-C σ-bonds and M-H bonds have been reviewed [6]. Pt-C bonds are relatively strong, usually stronger than Pt-H bonds.

Dissociation of a ligand(s) from the metal starting complex (Scheme 1.1) may provide a kinetic barrier before oxidation can proceed.

The term "activation" is often used in conjunction, or interchangeably with oxidative addition. The literal meaning of what it means to activate a σ-bond (A-B) is to increase the reactivity of this bond towards a reagent. The bond is therefore more readily capable of being cleaved. This bond breakage is itself referred to as "activation", and results in the oxidative addition product A-M-B. The terms "insertion" or "oxidative insertion" are also used to describe the same process.

1.3 Mechanisms of oxidative addition

A brief overview of the possible mechanisms of oxidative addition reactions follows [7]:

Various types of C-H (and Si-H) bonds can oxidatively add to metals, via a three centre transition state or intermediate (Figure 1.1). "Agostic" C-H type bonds can sometimes occur. A *cis* isomer would be formed first, which subsequently rearranges to the *trans* isomer. Usually the polarity of the solvent is not a determining factor, although an electron-rich phosphine may accelerate the oxidative addition reaction.

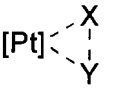

Figure 1.1 A three-centre intermediate in oxidative addition

A non-chain, radical mechanism has been recognised for the oxidative addition of certain alkyl halides to $[Pt(PPh_3)_3]$ (Figure 1.2).

$$PtL_3 \xrightarrow{-L} PtL_2$$

$$PtL_2 + XY \longrightarrow \cdot PtXL_2 + \cdot Y$$

$$\cdot PtXL_2 + \cdot Y \longrightarrow PtXYL_2$$

Figure 1.2 Radical mechanism for oxidative addition of alkylhalides, XY, to PtL_3

An S_N^2 reaction mechanism for oxidative addition has a rate that is more solvent-dependent, as it involves the formation of polar intermediates by ligand (anion) dissociation (Figure 1.3).

$$L_3Pt{:}\ X{-}Y \longrightarrow L_3\overset{+}{P}t{-}X + Y^- \xrightarrow{-L} PtXYL_2$$

Figure 1.3 An S_N^2 oxidative addition reaction mechanism

Ionic mechanisms occur with hydrogen halides, which are often dissociated in solution. Polar solvents thus facilitate this type of mechanism. The first step involves protonation of the metal complex followed by coordination of the anion (Figure 1.4).

$$PtL_3 + X^+ + Y^- \longrightarrow XPtL_3^+ + Y^- \xrightarrow{-L} PtXYL_2$$

Figure 1.4 Ionic mechanism of oxidative addition *eg.* XY = hydrogen halide

For a specific oxidative addition reaction, detailed mechanistic studies must be preformed before it can be speculated as to which mechanism is involved. The kinetically favoured reaction product forms first, but it may undergo spontaneous rearrangement to the thermodynamically more stable product. The isolated or postulated products of an oxidative addition of palladium(0) or platinum(0) to alkyl and aryl halides or pseudohalides are commonly *trans* isomers [8]. For palladium the oxidative addition has been established to

proceed usually via a concerted mechanism which necessitates the initial formation of the *cis*-isomer, with further isomerisation occurring rapidly.

1.4 *Cis-trans* isomerisation

The nature of the metal precursor, the nature of the ligands and even the solvent play a role in *cis-trans* isomerisations. Various mechanisms for the isomerisation of square planar complexes have been identified and studied [9]. Non-photochemical isomerisation routes fall into three broad categories [10]:

The consecutive displacement mechanism (Figure 1.5) involves the replacement of an anionic ligand, Y, by a neutral ligand, L, or a solvent molecule and the formation of $[PtXL_3]^+Y^-$ [11,12]. Subsequent attack of Y^- may form the original isomer, or it may produce the other isomer. Complexes of the type *cis*-$[PtRX(PR'_3)_2]$, where X = halide and R = alkyl, isomerise in this way in the presence of free phosphine, PR'_3. A polar solvent should favour this type of isomerisation as it would solvate the ionic intermediates.

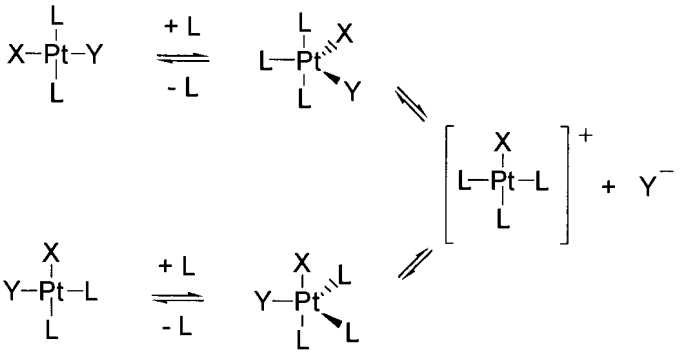

Figure 1.5 Consecutive displacement *cis-trans* isomerisation

Another way in which isomerisation occurs is through the formation of a five-coordinate species by association of a ligand or solvent molecule (Figure 1.6). Subsequent pseudorotation

of and dissociation from this five-coordinate intermediate yields the other isomer. Louw has provided evidence for this type of mechanisms in studies of the isomerisation of $[PtX_2(PEt_3)_2]$ where X is a halide, catalysed by PEt_3 or X [13]. Five-coordinate $[PtM_2L_3]$ complexes have been isolated and their geometries have been found to be close to square-pyramidal or trigonal-bipyramidal [14]. If the five-coordinate species has an appreciable lifetime in the solvent used, pseudorotation may be the chosen method of isomerisation.

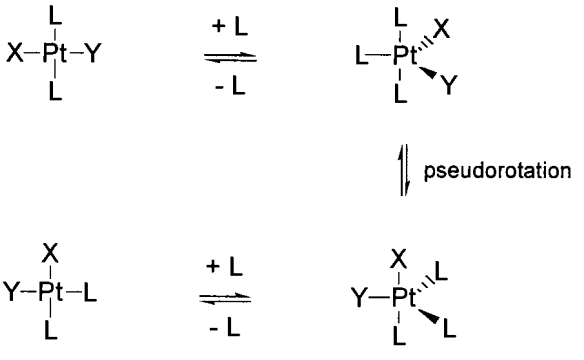

Figure 1.6 Consecutive displacement *cis-trans* isomerisation

Lastly, the isomerisation may proceed via the dissociation of a ligand to form a "T-" or "Y-" shaped intermediate (Figure 1.7). Some controversy concerning this mechanism exists [15].

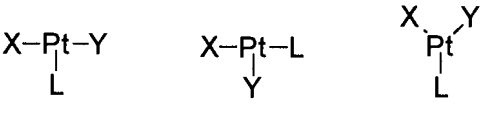

Figure 1.7 T- and Y- shaped intermediates

The thermodynamic stability of the favoured isomer is determined, in part, by the trans influence.

1.5 The trans influence

For platinum(II) square planar complexes, certain ligands facilitate the replacement or substitution of the ligand *trans* to it. The more effective the ligand at labilising the *trans* ligand, the stronger its trans effect. Ligands which tend to form particularly strong M-L σ-bonds *eg.* H^-, Me^- and $SnCl_3^-$, or those that form very strong π-bonds *eg.* CO and C_2H_4 have strong trans effects [8b,16]. A comparison of the rates of substitution for a series of analogous compounds gives an indication of the relative trans effect of ligands. The trans influence is related to the trans effect as the same ligands which exert a strong trans effect will also exercise a stronger trans influence. The trans influence relates to the capability of a ligand to weaken the *trans* M-L bond. This is manifested as an $M\text{-}L_{(trans)}$ bond lengthening, which is evident from M-L coupling constants in the NMR spectrum (where M-L = $^{195}Pt\text{-}^{31}P$) or in M-L stretch frequencies in the IR spectrum. Thus, in platinum phosphine complexes, the one bond $^{195}Pt\text{-}^{31}P$ coupling, $^1J_{Pt\text{-}P}$, can provide useful information regarding, amongst others, the trans influence of co-ligands in the complex.

1.6 $^1J_{Pt\text{-}P}$ in platinum phosphine complexes

The $^1J_{Pt\text{-}P}$ coupling constant in platinum phosphine complexes is sensitive to factors such as the type of phosphine ligand, the ligand *trans* to the phosphorus atom, the platinum oxidation state and the chelating ring size, where applicable. It is thus a useful parameter for characterising platinum complexes. Larger values for the coupling constant has been correlated to stronger Pt-P bonds (and consequently shorter Pt-P bond lengths) [17].

Theoretical calculations for a general one-bond coupling constant between atoms A and B, $^1J_{A\text{-}B}$, have shown the coupling to be largely a function of the Fermi contact interaction between the nuclear spin and the *s* electron [16,18]. Thus, $^1J_{Pt\text{-}P}$ can be described by the following expression:

Equation 1.2 $$^{1}J_{Pt\text{-}P} \propto \gamma_{Pt}\ \gamma_{P}\ (\Delta E)^{-1}\ \alpha_{Pt}^{2}\ \alpha_{P}^{2} \mid \psi_{Pt(6s)}(0) \mid^{2} \mid \psi_{P(3s)}(0) \mid^{2}$$

where γ_{Pt} and γ_{P} are the gyromagnetic ratios for atoms Pt and P respectively; $(\Delta E)^{-1}$ is the mean singlet-triplet excitation energy; α_{Pt}^{2} and α_{P}^{2} relate to the *s*-character of the bonding hybrid orbital used by Pt and P respectively in the Pt-P bond; $\mid \psi_{Pt(6s)}(0) \mid^{2}$ and $\mid \psi_{P(3s)}(0) \mid^{2}$ are the electron densities of the n*s* valence orbital at the Pt and P nuclei respectively. In a series of related compounds, Pidcock *et.al.* [17] showed that $(\Delta E)^{-1}$ and $\alpha_{P}^{2} \mid \psi_{P(3s)}(0) \mid^{2}$ change only slightly and that the terms α_{Pt}^{2} and $\mid \psi_{Pt(6s)}(0) \mid^{2}$ varied most. Therefore, a decrease in covalency (or conversely, an increase in ionic character) of the Pt-P bond reduces the coupling constant. The couplings are also related to the trans influence. Stronger trans influence ligands in the *trans* position to the phosphine weakens the Pt-P bond and results in a smaller $^{1}J_{Pt\text{-}P}$ [20].

For complexes of the type *cis*-$[PtCl_2L_2]$ and *cis*-$[PtMeClL_2]$ (where L = $P(C_6H_4Z\text{-}4)_3$ and Z = NMe_2, OMe, Me, H, Cl, CF_3), $^{1}J_{Pt\text{-}P}$ values have been plotted against the respective Hammet substituent constants [19] and it was found that the more electron-withdrawing substituents are associated with smaller $^{1}J_{Pt\text{-}P}$ values as a result of a decrease in the P→Pt(II) σ-donation. In other words, an increase in $^{1}J_{Pt\text{-}P}$ is related to an increase in the *s*-character in the Pt-P σ-bond [20], as was shown by Equation 1.2.

1.7 Project objectives

A large part of this project concentrates on the oxidative addition reactions of platinum(0), in particular tetrakis(triethylphosphine)platinum(0). In the first instance, oxidative insertions into C(heteroaryl)-Br bonds are manipulated in order to construct binuclear platinum(II) complexes with a rigid backbone and in which the metals centres are directly opposite each other and at a non-bond distance of 4-6 Å (Figure 1.8).

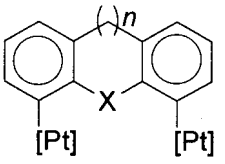

n = 0,1
X = S, O

Figure 1.8 Proposed binuclear Pt(II) complexes with rigid backbone spacers

This distance would allow for the activation of an allyl or butadiyne group in the intermetal area. In typical A-frame binuclear complexes (*eg.* with bis(diphenylphosphino)methane, dppm, bridges) the distance between the platinum centres is less than 3 Å (Figure 1.9) [21]. The close proximity of the two metal centres allows for the activation of organic substrates in the intermetal region by cooperative interaction of the two metals through the bridging atom, X, of the organic substrate. In our proposed systems the metals are too far apart for this type of interaction. "Communication" is only possible through the conjugated ring system of the rigid spacer.

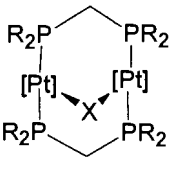

Figure 1.9 Dppm-bridged A-frame dinuclear platinum complexes

In the second instance, a systematic study of bond activation processes occurring in heteroaromatic sulfur-, nitrogen- and oxygen containing compounds was undertaken. The removal of sulfur (as hydrogen sulfide) and nitrogen (as ammonia) is practised on a large scale in the petroleum industry in order to meet stringent environmental regulations on fuel emissions. Generally, unsaturated heterocyclic rings are the most difficult to treat and remove. While sulfur has received the most attention because of its relatively high concentration, hydrodenitrogenation and hydrodeoxygenation processes compete with hydrodesulfurisation

in the consumption of hydrogen gas [22]. The importance of model systems for C-heteroatom cleavage is crucial to understanding and subsequently developing improved processes for the removal of heteroatoms [23]. Therefore, studies into the activation of C-S bonds in aromatic thiophene and thiophene-like molecules with homogenous metal complexes have been undertaken in order to gain understanding into the role of the metal in heterogenous systems [24]. This project aims to expand on the study of thiophenic substrates, as well as to do a systematic study of related heteroaromatic compounds (pyrrole and related azoles, and furan-like compounds) (Figure 1.10).

X = S, O
R = H, alkyl

R = H, alkyl
R' = H

Figure 1.10 Possible sites for bond activation by platinum(0)

The reaction of thiophene with low-valent transition metals, *eg.* tetrakis(triethylphosphine)-platinum(II) results in the insertion of the metal fragment into the C-S bond [24]. An investigation will be carried out to see if the analogous reaction occurs for furan-like molecules, *i.e.* C-O activation. Other possible bonds which may be activated in these heteroaromatic compounds are the C-H and C-C(alkyl) bonds in the α-position. In the case of pyrroles, activation at the N-H bond of pyrrole, or at the N-C(alkyl) bond on 1-alkylpyrrole are also possible insertion sites. If C-H activation is found to be a favourable process, the formation of platinum(II) hydrides would provide interesting NMR spectra, as hydride protons resonate far upfield in a region clear of other proton resonances.

Continuing on the theme of effectively using dibenzothiophene as a spacer in binuclear platinum complexes, the aim is also to use thiophene as a spacer via diphosphine substituents. Platinum(II) compounds will be prepared by substitution rather than by oxidative addition.

1.8 References

[1] A. Dedieu; *Chem. Rev.*, **2000**, *100*, 543-600

[2] S.Sakaki, B. Biswas and M. Sugimoto; *J. Chem. Soc., Dalton Trans.*, **1997**, 803-809

[3] L. S. Hegedus in *Organometallics in Synthesis: A Manual*, Ed. M. Schlosser, John Wiley and Sons Ltd, Chichester, UK, 2002, pp 1150-1208

[4] For some applications of the Stille- or modified Stille-coupling reactions see (a) C. Losterzo; *Synlett*, **1999**, 1704-1711 (b) E. Antonelli, P. Rosi, C. Losterzo and E. Viola; *J. Organomet. Chem.*, **1999**, *578*, 210-222 (c) A. Hucke and M.P. Cava; *J. Org. Chem.*, **1998**, *63*, 7413-7417 (d) B. Dominguez, B. Iglesias and A.R. Delera; *Tetrahedron*, **1999**, *55*, 15071-15098 (e) E. Fouquet and A.L. Rodriguez; *Synlett*, **1998**, 1323-1324

[5] Y.-S Lin and A. Yamamoto; *Topics in Organometallic Chemistry*, Vol3, Ed. S. Murai, 1999, 99 162-192

[6] J.A. Martinho Simões and J.L. Beauchamp; *Chem. Rev.*, **1990**, *90*, 629-688

[7] R. H. Crabtree in *The Organometallic Chemistry of the Transition Metals*, John Wiley and Sons, New York, 1988, (a) pp 121-132 and (b) pp 5-6

[8] (a) C. Amatore, G. Broeker, A Jutand and F. Khalil; *J. Am. Chem. Soc.*, **1997**, *119*, 5176-5185 (b) C. Amatore, A. Jutand and A. Suarez; *ibid*, **1993**, *115*, 9531-9541

[9] G.K. Anderson and R.J. Cross; *Chem. Soc. Rev.*, **1980**, *9*, 185-215

[10] D.L. Packett and W.C. Trogler; *Inorg. Chem.*, **1988**, *27*, 1768-1775

[11] (a) D.G. Cooper and J. Powell; *J. Am. Chem. Soc.*, **1973**, *95*, 1102-1108 (b) R. Favez, R. Roulet, A.A. Pinkerton and D. Schwarzenbach; *Inorg. Chem.*, **1980**, *19*, 1356-1365

[12] (a) J.H. Price, J.P. Birk and B.B. Wayland; *Inorg Chem.*, **1978**, *17*, 2245-2250 (b) D.A. Redfield and J.H. Nelson; *ibid.*, **1973**, *12*, 15-19

[13] (a) W.J. Louw; *Inorg. Chem.*, **1977**, *16*, 2147 (b) M.S. Holt, J.H. Nelson; *Inorg. Chem.*, **1986**, *25*, 1316-1320

[14] (a) W.J. Louw, D.J.A. de Waal and G.J. Kruger; *J.Chem. Soc., Dalton Trans.*, **1976**, 2364 (b) C.A. McAuliffe, I.E. Niven and R.V. Parish; *Inorg. Chim. Acta*, **1975**, *15*, 67-70

[15] (a) R. Romeo, D. Minniti and S. Lanze; *Inorg. Chem.*, **1980**, *19*, 3663-3668 (b) S. Komiya, T.A. Albright, R. Hoffmann and J.K. Kochi; *J. Am. Chem. Soc.*, **1976**, *98*, 7255-7265

[16] T.G. Appleton, H.C. Clark and L.E. Manzer; *Coord. Chem. Rev.*, **1973**, *10*, 335-422

[17] (a) G.G. Mather, A. Pidcock and G.J.N Rapsey; *J. Chem. Soc., Dalton Trans.*, **1973**, 2095 (b) A. Crispini, K.N. Harrison, A.G. Orpen, P.G. Pringle and J.R. Wheatcroft; *ibid.*, **1996**, 1069-1076

[18] (a) J.A. Pope and D.P. Santry; *Mol. Phys.*, **1964**, *8*, 1 (b) A. Pidcock, R.E. Richards and L.M. Venanzi; *J. Chem. Soc. (A)*, **1966**, 1707-1710

[19] C.J. Cobley and P.G. Pringle; *Inorg. Chim. Acta*, **1997**, *265*, 107-115

[20] P.S. Pregosin and R.W. Kuntz in *^{31}P and ^{13}C NMR of Transition Metal Complexes*, Ed. P. Diehl, E. Fluck and R. Kosfeld, Springer, New York, 1979, p378

[21] (a) J.K. Stille in *The Chemistry of the Metal-Carbon Bond*, Ed. F.R. Hartley and S. Patia, John Wiley and Sons Ltd., 1985, pp 716-717 (b) H.-K. Yip, C.M. Che and S.-M. Peng; *J. Chem. Soc., Dalton Trans.*, **1993**, 179-187 (c) P.K. Byers; *Coord. Chem. Rev.*, **1995**, *146*, 431-450 (d) R. Huang, I.A. Guzei and J.H. Espenson; *Organometallics*, **1999**, *18*, 5420-5422

[22] (a) J.G. Speight in *The Desulfurization of Heavy Oils and Residua*, Chemical Industries Vol.4 Ed. H. Heinemann, Marcell Dekker Inc., New York, 1981 (b) R.M. Laine; *Catal. Rev.-Sci. Eng.*, **1983**, *25*, 459-474 (c) E. Furimsky; *Catal. Rev.- Sci. Eng.*, **1983**, *25*, 421-458

[23] R.J. Angelici; *Polyhedron*, **1997**, *16*, 3073-3088

[24] C. Bianchini and A. Meli; *Acc. Chem. Res.*, **1998**, *31*, 109-116

/ End of Chapter 1 //

CHAPTER 2

Binuclear Platinum(II) Complexes of Dibenzothiophene Derivatives

2.1 INTRODUCTION

Palladium(0) precursors catalyse a wide range of coupling reactions via oxidative addition / transmetalation / reductive elimination cycles (*eg.* Heck, Stille and Suzuki couplings) [1]. The palladium(0) complexes $[Pd(PPh_3)_4]$ and $[Pd_2(dba)_3.dba]$ (dba = dibenzylideneacetone) in the presence of triphenylphosphine are widely used. Palladium(II) precursors such as $[PdCl_2(PPh_3)_2]$, $[Pd(OAc)_2]$ (where OAc = acetate) and $[PdCl_2(NCMe)_2]$ are also used as they are readily reduced to a catalytically active palladium(0) species in the catalytic cycle.

The first step in these catalytic sequences commonly involves an oxidative addition reaction to an organohalide substrate, RX. The oxidation state of the metal formally increases from zero to two and the oxidising agent (the RX) adds to the metal. The order of reactivity is I >> OTf (triflate) > Br >>> Cl [2]. Although the use of chlorides is limited, progress has been made during the past decade towards the functionalisation of inert carbon-chlorine bonds in chloroarenes [3].

Of the Group 10 triad, platinum is more kinetically inert than palladium or nickel and platinum organometallic complexes are readily accessible and tunable. For this reason it is useful to study the stoichiometric reactions of platinum in order to model catalytic reactions that its lighter, more labile triad analogues undergo. Oxidation addition requires the promotion of the metal to an intermediate electronic state [4]. Platinum attains this state more readily than palladium and the oxidation addition reaction for platinum is more exothermic / less endothermic with a lower activation energy barrier [5].

Many examples of σ-carbon-bonded complexes of the type *trans*-[MXR′$(PR_3)_2$], where X = halide and R′ = alkyl, aryl, alkenyl or acyl [6], have been isolated. Insertions into Si-X bonds by platinum(0) have also been reported [7]. The oxidative insertion of platinum(0) into alkyl halides is much easier than into aryl halides, while only a few examples of insertion into carbon-halide bonds of heteroaromatic compounds are known. Studies of palladium(0) insertion reactions with aryl halides have shown that electron-withdrawing groups (*eg.* NO_2 and CF_3) *para* to the C-X bond enhance the activation of the C-X bond. On the other hand, electron-donating groups in the *para* position decrease the reactivity [8]. Furthermore, triethyl-phosphine metal precursors react under milder conditions than when the phosphine is triphenylphosphine. The latter is a weaker base, thus rendering the "$M(PR_3)_2$" species a weaker nucleophile [9].

Binuclear complexes synthesised by a double oxidative addition to a dihalo aromatic compound are relatively rare [10]. Double oxidative addition reactions of this type have found application in the preparation of organometallic macrocycles like metalloporphyrins (Figure 2.1) [11].

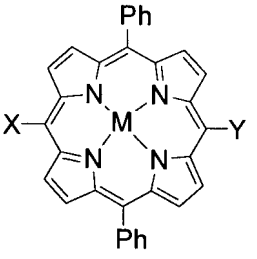

M = Ni, 2 H; X = H; Y = $Pd(PPh_3)_2Br$, *cis*- or *trans*-$Pt(PPh_3)_2Br$

M = Ni; X = $Pd(PPh_3)_2Br$; Y = $Pd(PPh_3)_2Br$, *trans*-$Pt(PPh_3)_2Br$

Figure 2.1 *meso*-η^1-Palladio- and Platinioporphyrins

The catalytic processes of C-C and C-heteroatom (nitrogen, sulfur and oxygen) coupling have been studied but much less attention has been given to the stoichiometric reactions which lead to the isolation of the metal(II) oxidation products of heteroaromatic substrates. Hor *et. al.* studied the oxidation addition reactions of $[Pd(PPh_3)_4]$ with bromothiophenes and the formation of *trans*-$[PdBr(\sigma\text{-thienyl})(PPh_3)_2]$ complexes [12]. In 1999, Lin and co-workers prepared heterobimetallic compounds from halothiophene substituted ferrocene molecules (Figure 2.2) [13].

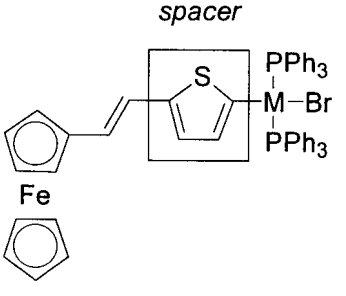

M = Pt or Pd; spacer = thiophene, bithiophene, dithienylethylene

Figure 2.2 Ferrocene end-capped Pd(II) and Pt(II) complexes with thiophene spacers

The authors claim that this is the first reported case of the oxidative addition of $[Pt(PPh_3)_4]$ to a heteroaromatic compound. In fact, Chin and McWhinnie reported the isolation of *trans*-

$[PtBr(2\text{-}C_4H_3S)(PPh_3)_2]$, based on elemental analysis and ^{31}P NMR data [14]. The $^1J_{Pt\text{-}P}$ coupling was reported as 1870 Hz, which is an unusually small value for *trans* PtP_2 systems of this type (see later discussion).

Many examples of A-frame complexes containing the bridging ligands bis(diphenyl-phosphino)methane, dppm, and diphenylphosphinoethane, dppe, have been recorded [15]. Cowie and co-workers studied the transformation reactions which alkynes undergo with binuclear Ir/Ir and Rh/Ir A-frame complexes of dppm [16]. Mixed symmetrical and unsymmetrical palladium and platinum dimers bridged by two dppm molecules are also known [15a]. These complexes can undergo oxidative addition reaction without disruption of the binuclear complex [15b,d] (Figure 2.3). The Pt-Pt separation in dppm bridged complexes are typically of the order of 2.58 to 2.64 Å [15b,c], comparable to but slightly shorter than in elemental platinum (2.77 Å).

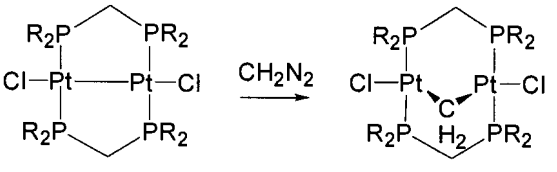

Figure 2.3

This chapter focusses on the preparation of rigid "A-frame" type binuclear complexes in which the two metal centres are set at a distance of *ca.* 4 to 6 Å apart. The alignment of the metal centres is brought about by the geometry of the planar condensed aromatic ring system and the position of attachment of the metal fragments to the rings. This set distance is rather long for metal-metal bonding to occur, but through the electron conjugated, aromatic ring system, the metals may still "communicate" in a cooperative way. Such a system would allow enough space for the possible activation of larger organic substrates such as butadiyne and allyls in the intermetal region.

It is proposed that the binuclear complexes be constructed via a double oxidative addition

reaction at the two carbon-bromine bonds of dibromo molecules such as 4,6-dibromo-dibenzothiophene and 1,8-dibromoanthracene, the structures of which are given below.

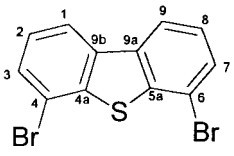

4,6-dibromodibenzothiophene

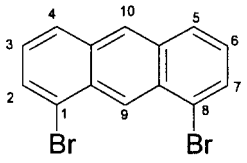

1,8-dibromoanthracene
(or 4,5-dibromoanthracene)

Note: The same type of numbering system is used for both dibenzothiophene and dibenzofuran. However, when the fused ring system consists of three six-membered rings, the numbering system changes, so that anthracene, acridine and xanthene have the same numbering order.

The pyridine analogue of anthracene, *viz.* 4,5-dibromoacridine, was not considered in this study. A double oxidative insertion at the C-Br bonds of 4,5-dibromoacridine would be complicated by the presence of a pyridine-like nitrogen atom; platinum has a strong tendency to form *N*-bonded complexes of pyridine-like derivatives[1].

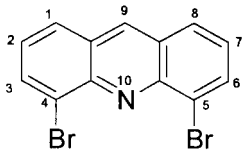

4,5-dibromoacridine

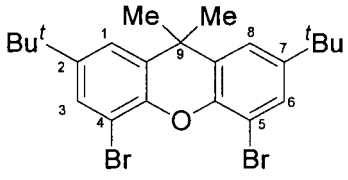

4,5-dibromo-2,7-di-*tert*-butyl-9,9-dimethylxanthene

The interatomic distance between the two bromine atoms is expected to be quite similar to

[1] Refer to Table 4.1, Chapter 4, for examples

that in 1,8-dibromoanthracene as a result of the structural similarity of their aromatic fused-ring systems. The related compound 4,5-bis(diphenylphosphino)acridine has a P-P non-bond separation of 4.338(1) Å [17].

Although the molecule, 4,5-dibromo-2,7-di-*tert*-butyl-9,9-xanthene, is not fully conjugated and non-aromatic, it would be of interest to compare the intermetal distance in the diplatinum complex that may arise from a double oxidative insertion reaction into the C-Br bonds. The nonplanarity of the ring system is clearly observed in the X-ray crystal structure of the related compound, 9,9-dimethyl-4,5-(diphenylphosphino)xanthene. The folding-in of the two benzenoid rings results in a relatively short P-P nonbond distance of 4.045(1) Å [18].

Once the binuclear complex has been constructed, fine-tuning of the co-ligands will render the complex more amenable to further oxidative addition reactions at the platinum(II) centres. Complexes of the type $[PtXY(PR_3)_2]$ are relatively inert to further oxidation to form an octahedral platinum(IV) complexes. Substitution of the phosphines by amines or imines enhances the susceptibility to oxidative addition [19].

2.2 RESULTS AND DISCUSSION

2.2.1 Synthesis of Dibenzothiophene-based Ligands

While the syntheses of 2,8-; 3,7- and 2,4-dibromodibenzothiophene (Figure 2.4) are recorded in the literature [20, 21], no reference to the 4,6-dibromo isomer could be found. While investigating methods of preparing 4,6-dibromodibenzothiophene, an improved method for the synthesis of 2,8-dibromodibenzothiophene, **1**, was developed. Compound **1** has previously been prepared by the treatment of dibenzothiophene with bromine [20]. The method of Neumoyer and Amstutz [22] requires prolonged reflux in carbon disulfide (40% yield). Campaigne and Ashby improved this method to obtain a better yield (62%) in a much shorter

reaction time [23]. Boekelheide *et. al.* [24] reported a 75% yield by repeating the procedure of Neumoyer, but no further experimental details were given. Very low yields of **1** were obtained by the bromination of dibenzothiophene in dichloromethane [25], but the reaction of 5-methyldibenzo[*b,d*]thiophenium tetrafluoroborate [25, 26] with bromine gave **1** in satisfactory yields. The use of *N*-bromosuccinimide as a free radical brominating agent for heteroaromatic compounds in chloroform under mild conditions has become more common [27] and we have incorporated it in an improved method of synthesis of **1**.

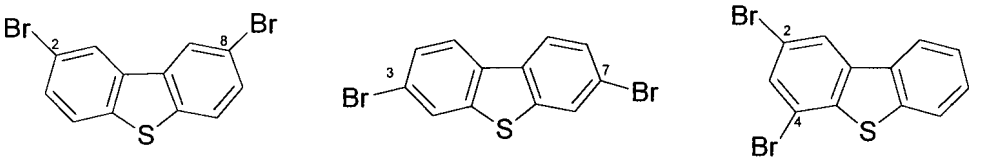

1

Figure 2.4 2,8-, 3,7- and 2,4-dibromodibenzothiophene

In contrast to the synthesis of 2,8-dibromodibenzothiophene, the preparation of 3,7-dibromo-dibenzothiophene involves the bromination of dibenzothiophene-5,5-dioxide followed by a lithium aluminum hydride reduction [21a], and 2,4-dibromodibenzothiophene, together with other products, is prepared by an intramolecular homolytic aromatic *ipso* substitution of an aryl radical generated from 2-(2,4,6-tribromophenylsulfanyl)aniline [21b].

The approach used to prepare 4,6-dibromodibenzothiophene involved the dilithiation of dibenzothiophene. Derivatisation at positions 4 and 6 of dibenzothiophene via metallation is inherently problematic. Caubère and co-workers optimised the monolithiation reaction and were able to isolate 4-methyldibenzothiophene in 94 % yield (by gas chromatography) under the following conditions: 3 eq. *n*-BuLi, thf / hexane solvent, temperature -78 °C, 5 hr reaction time, and 3 eq. of the electrophile (MeI) [28]. An excess of organolithium base is essential otherwise appreciable amounts of dibenzothiophene remains unconverted. Attempts at dilithiation by different research groups have in the past led to mixtures of monolithiated (major) and dilithiated (minor) products [29, 33]. Schroth and co-workers battled to separate

4,6-bis(diphenylphosphino)benzothiophene and 4-(diphenylphosphino)dibenzothiophene which were obtained by an attempted dilithiation reaction followed by treatment with chlorodiphenylphosphine [29]. Meille *et. al.* experienced similar problems with 4-methyl- and 4,6-dimethyldibenzothiophene mixtures [33]. Caubère and co-workers found that the activation of *n*-butyllithium with *N,N,N′,N′*-tetramethylethylenediamine, tmeda, only becomes effective at 60 °C in hexane. By employing 3 eq. n-BuLi and 3 eq tmeda for 2 hr at 60 °C, they were able to obtain 4,6-disubstituted dibenzothiophene in yields of 50-60 % depending on the electrophile used.

.

Following the dilithiation of dibenzothiophene using the method of Caubère, subsequent reaction of 4,6-dilithiodibenzothiophene with bromine could be expected to give the desired 4,6-dibromosubstituted compound. However, it was found that bromination of 4,6-dilithio-dibenzothiophene with two equivalents of bromine gave a mixture of brominated dibenzothiophene products. It was not possible to separate these products by column chromatography on silica gel. To overcome this problem, the 4,6-dilithiodibenzothiophene intermediate was treated with chlorotrimethylsilane which led to the isolation of 4,6-bis-(trimethylsilyl)dibenzothiophene, **2**. When **2** was reacted with bromine, pure 4,6-dibromo-dibenzothiophene, **3**, was obtained in a quantitative yield (Scheme 2.1). The structures of **2** and **3** were confirmed by single crystal X-ray crystallography.

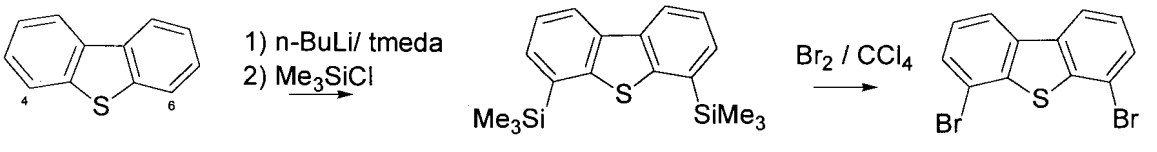

2 **3**

Scheme 2.1 Synthetic route for 4,6-dibromodibenzothiophene, **3**

The tin analogue of **2** *viz.* 4,6-bis(trimethylstannyl)dibenzothiophene, **4**, was also synthesised (Scheme 2.2). It was isolated as a yellow oil which underwent extensive protodestannylation

on silica gel. The yield was also diminished through bulb-to-bulb distillation under high vacuum as **4** degraded to dibenzothiophene. NMR spectroscopy and mass spectrometry (MS) were used to characterise **4**.

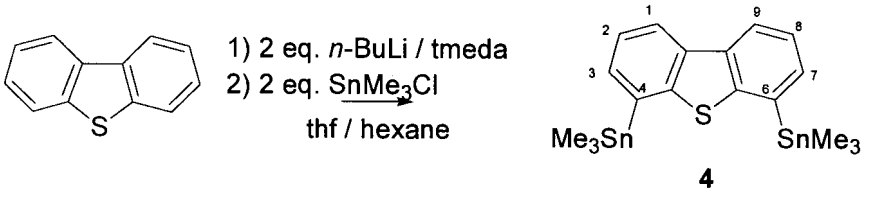

Scheme 2.2 Synthesis of 4,6-bis(trimethylstannyl)dibenzothiophene, **4**

2.2.2 Crystal structures of 4,6-bis(trimethylsilyl)dibenzothiophene, 2, and 4,6-dibromo-dibenzothiophene, 3

The molecular structures of **2** and **3** are highly symmetrical. For comparative purposes, the bond lengths and internal bond angles of free dibenzothiophene are given in Figure 2.5 [30].

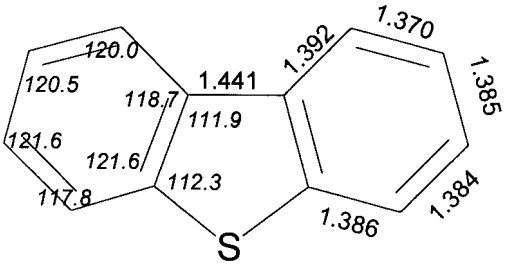

Figure 2.5 Bond lengths and bond angles of dibenzothiophene

2.2.2.1 *Crystal structure of 4,6-bis(trimethylsilyl)dibenzothiophene,* **2**

Compound **2** crystallises from a hexane solution in the space group $P2_1/n$ with monoclinic unit cells. An ORTEP diagram **2** of is given in Figure 2.6.

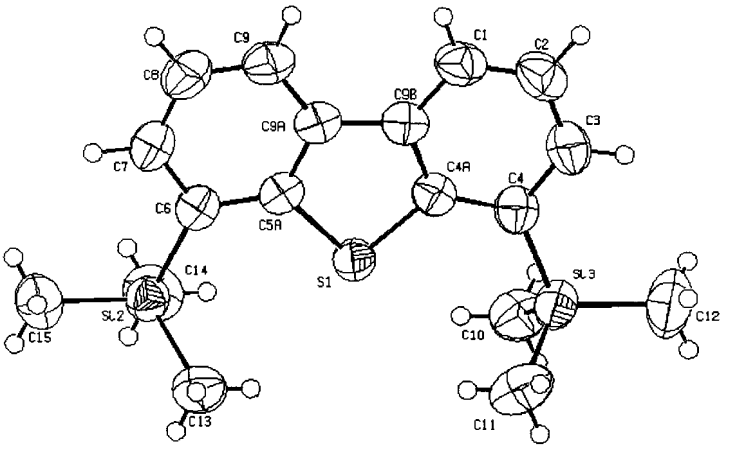

Figure 2.6 ORTEP diagram of **2**

Table 2.1 summarises some of the important bond lengths and angles. For a complete list of bond lengths and angles, refer to the Appendix. Bond lengths of the dibenzothiophene ring fall within the range of typical values reported in the Cambridge Structural Database [31]. Bond angles also compare favourably with the exception of C(3)-C(4)-C(4a) and C(7)-C(6)-C(5a); 114.5(2)° and 114.7(2)° respectively. These angles are smaller than the values typically reported (mean bond angle approximately 118° with range of approximately 6° based on 71 structures in the Cambridge Structural Database [31]) and with the corresponding angle in free dibenzothiophene *viz.* 117.8° [30]. Compounds substituted at positions 4 and 6 report similar C(3)-C(4)-C(4a) and C(7)-C(6)-C(5a) bond angles. Examples include 116.13(7)° in 4,6-bis(diphenylphosphino)dibenzothiophene [32a] and 117.6(4)° in 4,6-dimethyldibenzothiophene [33]. The five-membered thienyl ring in **2** remains essentially undistorted by the introduction of the trimethylsilyl substituents. The non-bonding separation between the two silicon atoms in **2** was found to be 6.77 Å.

Table 2.1 Selected bond lengths (Å) and bond angles (°) for **2**

Si(3)-C(4)	1.890(2)	C(4a)-S(1)-C(5a)	92.24(8)
S(1)-C(4a)	1.756(2)	C(9b)-C(4a)-S(1)	111.1(1)
C(9a)-C(9b)	1.448(2)	C(4a)-C(9b)-C(9a)	112.8(2)
C(1)-C(2)	1.370(3)	C(9b)-C(4a)-C(4)	123.8(2)
C(2)-C(3)	1.390(3)	C(1)-C(9b)-C(4a)	118.5(2)
C(3)-C(4)	1.396(3)	C(2)-C(1)-C(9b)	119.4(2)
C(4)-C(4a)	1.406(2)	C(1)-C(2)-C(3)	120.6(2)
C(4a)-C(9b)	1.401(2)	C(2)-C(3)-C(4)	123.1(2)
C(1)-C(9b)	1.398(2)	C(3)-C(4)-C(4a)	114.5(2)
Si(3)-C(10)	1.854(2)	C(3)-C(4)-Si(3)	121.6(1)
Si(3)-C(11)	1.859(3)	C(4a)-C(4)-Si(3)	123.9(1)
Si(3)-C(12)	1.861(3)	C(4)-C(4a)-S(1)	125.0(1)
		C(1)-C(9b)-C(9a)	128.8(2)

2.2.2.2 *Crystal structure of 4,6-dibromodibenzothiophene,* **3**

Atom numbering for **3** is shown below and the molecular shape is represented by a ball-and-stick model in Figure 2.7, which also shows the packing of molecules in the crystal. Selected bond lengths and angles for the planar molecules of **3** are given in Table 2.2. Refer to the Appendix for full details of the aquisition and structural data.

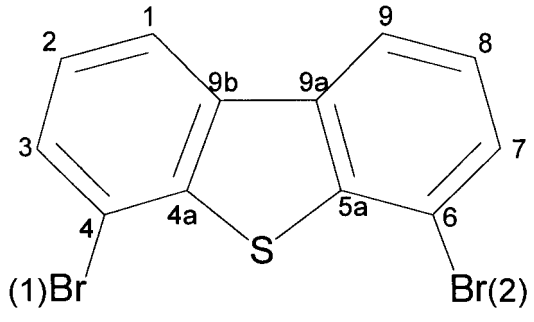

Table 2.2 Selected bond lengths (Å) and bond angles (°) for **3**

Br(1)-C(4)	1.894(5)	C(4a)-S(1)-C(5a)	90.6(2)
S(1)-C(4a)	1.753(4)	S(1)-C(4a)-C(9b)	112.8(3)
C(9)-C(9a)	1.402(6)	C(4a)-C(9b)-C(9a)	111.9(4)
C(1)-C(2)	1.374(7)	C(4)-C(4a) -C(9b)	120.9(4)
C(2)-C(3)	1.403(7)	C(4a)-C(9b)-C(1)	118.2(4)
C(3)-C(4)	1.381(6)	C(9b)-C(1)-C(2)	119.9(5)
C(4)-C(4a)	1.379(6)	C(1)-C(2)-C(3)	121.5(5)
C(4a)-C(9b)	1.416(6)	C(2)-C(3)-C(4)	119.0(5)
C(1)-C(9b)	1.407(6)	C(3)-C(4)-C(4a)	120.5(4)
		C(4a)-C(4)-Br(1)	118.8(3)
		C(3)-C(4)-Br(1)	120.6(4)
		S(1)-C(4a)-C(4)	126.3(3)
		C(1)-C(9b)-C(9a)	129.9(4)

The internal bond angles of the benzene rings show only a small deviation from the bond angles of pure dibenzothiophene. In particular, the C(3)-C(4)-C(4a) angle is 120.5(4)°. Consequently the external C(4a)-C(4)-Br(1) and C(3)-C(4)-Br(1) angles are larger than for the corresponding angles about silicon in **2**. The thienyl ring in **3** is somewhat distorted compared to free dibenzothiophene, as well as to **2**. The angle at sulfur is smaller (90.6° vs 91.5°) and C(9)-C(9a) is longer while C(4a)-C(9b) is shorter. The Br(1)-C(4) bond distance in **3** is almost identical to the Si(3)-C(4) separation in **2**; 1.894(5) Å and 1.890(2) Å respectively.

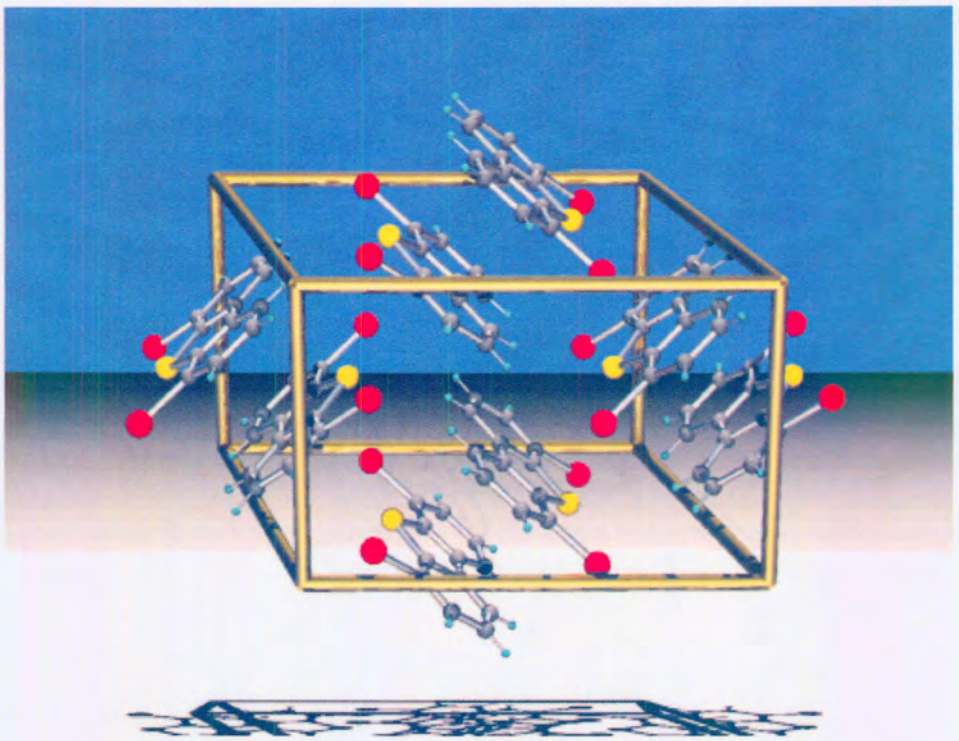

Figure 2.7 Packing of molecules of **3** in the crystal lattice

In the solid state, molecules of **3** are grouped in twos (Figure 2.7). The molecules are planar and each pair of molecules are parallel, but face opposite directions. Furthermore, each pair is orientated perpendicular to neighbouring pairs so that the sulfur and two bromine atoms of a particular molecule point directly at the centres of the three conjugated rings of the dibenzothiophene unit in an adjacent molecule.

The distance between the two bromine atoms is 6.51 Å. This is shorter than in **2** (6.77 Å), but both are longer than the P-P non-bond distance in 4,6-bis-(diphenylphosphino)dibenzothiophene *viz.* 6.383(1)Å [32a]. The P-P separation in the analogous 4,6-bis(diphenylphosphino)dibenzofuran molecule is 5.741(1)Å [32b]. As expected, these non-bond distances are all longer than the P-P separation in 4,5-dibromoacridine (4.338Å) (Page 18,19) [17]. The substituents at position 4 and 6 of the two benzene rings of dibenzothiophene (or dibenzofuran) point away from each

other as a result of the geometry of the five-membered thiophene (or furan) ring. In acridine, the substituents at positions 4 and 5 are parallel because the benzene rings are supported by a six-membered internal ring.

2.2.3 1,8-dibromoanthracene

The preparation of 1,8-dibromoanthracene has been reported previously in the literature (Scheme 2.3) [34].

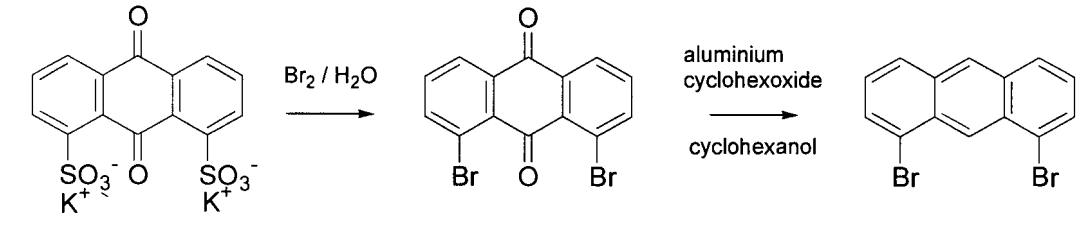

9,10-anthraquinone-1,8-disulfonate 1,8-dibromo-9,10-anthraquinone 1,8-dibromoanthracene

Scheme 2.3 Synthesis of 1,8-dibromoanthracene

Unfortunately 9,10-anthraquinone-1,8-disulfonate is no longer commercially available; the closest related compound being 1,8-dichloro-9,10-anthraquinone. We designed an alternative multi-step procedure for the synthesis of 1,8-dibromoanthracene, Scheme 2.4, but have to date not fully optimised all the steps of the procedure in order to obtain 1,8-dibromoanthracene in a suitable yield for further use in reactions with platinum(0).

Steps 1 and 2 in Scheme 2.4 were reported in the literature [35, 36]. The use of zinc as a reducing agent has been reported for 1,8-diiodo-, but not for 1,8-dibromo-9,10-anthraquinone [36]. Reduction of the 1,8-diiodo compound is inefficient as it is accompanied by C-I bond cleavage to yield anthracene in 68% yield.

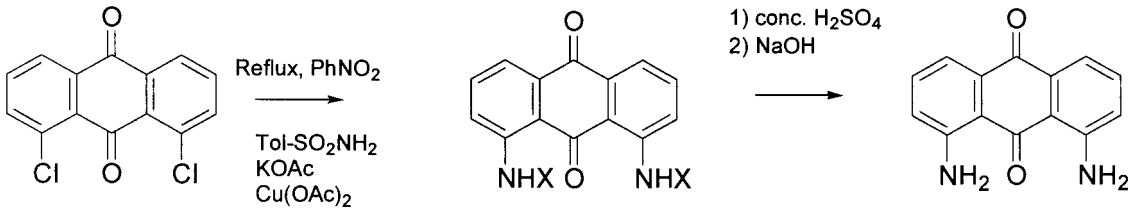

X = SO_2Tol

Step 1

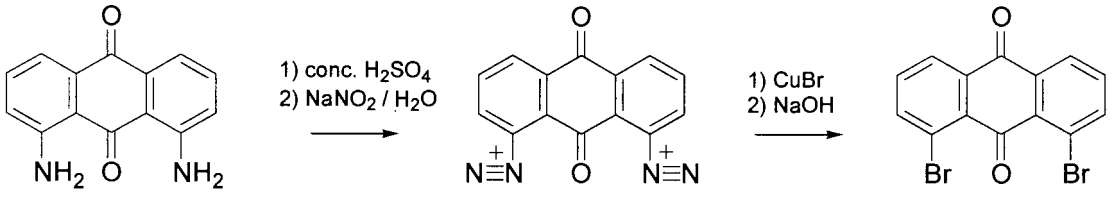

Step 2

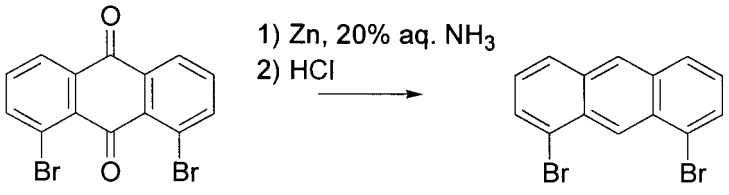

Step 3

Scheme 2.4 Synthetic procedure proposed for the preparation of 1,8-dibromoanthracene

2.2.4 Preparation of Binuclear Platinum(II) Complexes

2.2.4.1 *μ-dibenzothienyl-1κC⁴:2κC⁶-bis[*trans-*bromobis(triethylphosphine)-platinum(II)]*

Compound **3** reacted with two equivalents of tetrakis(triethylphosphine)platinum(0) in refluxing toluene after 1 hour to give μ-dibenzothienyl-1κ*C*⁴:2κ*C*⁶-bis[*trans*-bromobis(triethylphosphine)platinum(II)], **2-1**, so named according to IUPAC rules [37] (Reaction 2.1)

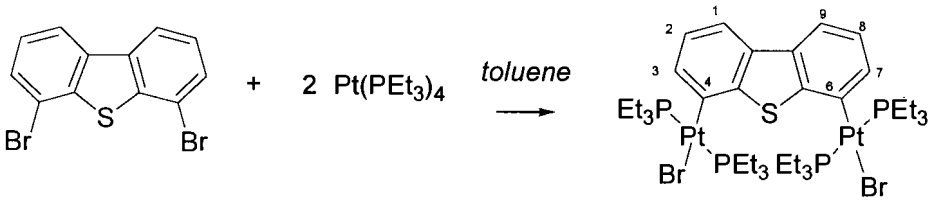

3 **2-1**

Reaction 2.1

A concerted effort was made to obtain crystals of **2-1** in order to determine the Pt-Pt non-bond distance by X-ray crystallography. Colourless prisms were grown from a cold saturated solution of **2-1** in toluene / hexane. However, the crystals readily become opaque when handled and were thus unsuitable for crystallographic studies.

The $^{31}P\{^{1}H\}$ NMR spectrum displays a single resonance at 12.47 ppm with accompanying ^{195}Pt satellites ($^{1}J_{Pt-P}$ = 2694 Hz), indicating the presence of two equivalent phosphorus atoms. This data compares favourably with other *trans*-"$PtX(PR_3)_2$" compounds, where X = I or Br and R = Et or Ph (Table 2.3). In light of this data it appears that the compound reported by Chin and McWhinnie [14] *viz.* *trans*-$[PtBr(2\text{-}C_4H_3S)(PPh_3)_2]$ may have been incorrectly assigned, as their reported

$^{1}J_{Pt\text{-}P}$ coupling of 1870 Hz is an anomalous value. No other NMR data was provided.

[$PtXY(PR_3)_2$]-type complexes (X = halide, Y = anionic ligand) occur predominantly as *trans*-isomers [38]. The *trans* isomers are thermodynamically more stable and steric factors may play a role here to minimise crowding around the phosphine groups.

Table 2.3 $^{31}P\{^{1}H\}$ NMR for *trans*-[$PtXY(PR_3)_2$] type complexes

		$^{31}P\{^{1}H\}$ NMR δ /ppm	$^{1}J_{Pt\text{-}P}$ / Hz	Reference
spacer 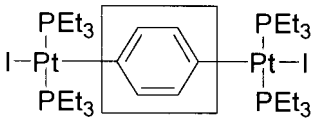	*spacer*			
	1,4-benzene	10.3	2787	[10]
	4,4′-diphenyl	24.3	3095	
	4,4″-ter-*p*-phenyl	24.0	3075	
	4,4′-benzophenone	22.2	3040	
trans-[$PtBr(SiMe_3)(PEt_3)_2$]		19.2	2864	[7]
trans-[$PtBr(SiPhMe_2)(PEt_3)_2$]		17.1	2780	
spacer 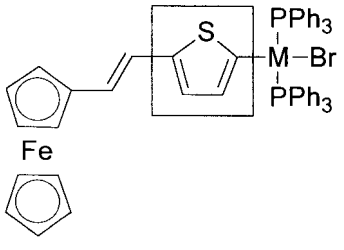	*spacer*			
	thiophene	23.8	2874	[13]
	bithiophene	23.9	2858	
	dithienylethylene	23.8	2842	

A rare example of a *cis* isomer is formed by the reaction of [$Pt(PPh_3)_2(C_2H_4)$] with the α-bromoglycine derivative, *N*-benzoyl-2-bromomethylglycinate (Figure 2.8) [39].

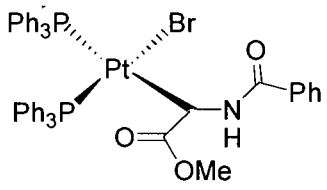

Figure 2.8 Example of a *cis*-[PtBrY(PR_3)$_2$] type complex

This compound displays two separate singlet resonances, attributed to two nonequivalent phosphorus atoms in its ^{31}P NMR spectrum; δ 17.90 ppm ($^2J_{P\text{-}P}$ = 16.5 Hz, $^1J_{Pt\text{-}P}$ 1903 Hz) and 20.45 ppm ($^2J_{P\text{-}P}$ = 16.5 Hz, $^1J_{Pt\text{-}P}$ 4482 Hz)

Thienyl bonded diplatinum complexes similar to **2-1** have been prepared by reacting thienyltin compounds with *cis*-(η^4-1,5-cyclooctadiene)dichloroplatinum(II) and subsequently substituting the η^4-1,5-cyclooctadiene (η^4-cod) with phosphine ligands (Scheme 2.5) [40].

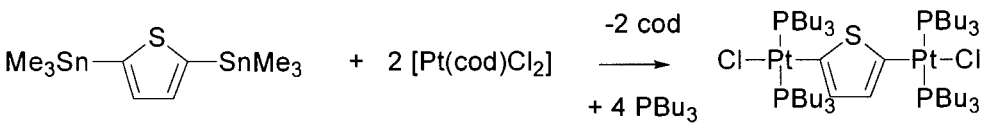

Scheme 2.5 A diplatinum compound bridged by 2,5-thienylene

A similar type of double transmetallation reaction was carried out using **4** instead of 2,5-bis(trimethylstannyl)thiophene (See next section 2.2.4.2).

2.2.4.2 *μ-dibenzothienyl-1κC⁴:2κC⁶-bis[*cis*-chloro(η⁴-1,5-cyclooctadiene)-platinum(II)]*

Complex **2-2** was prepared according to Reaction 2.2. It was isolated as a yellow oil and characterised by NMR spectroscopy and MS. The cod ligand can readily be replaced by phosphines, or amines (mono- or bidentate).

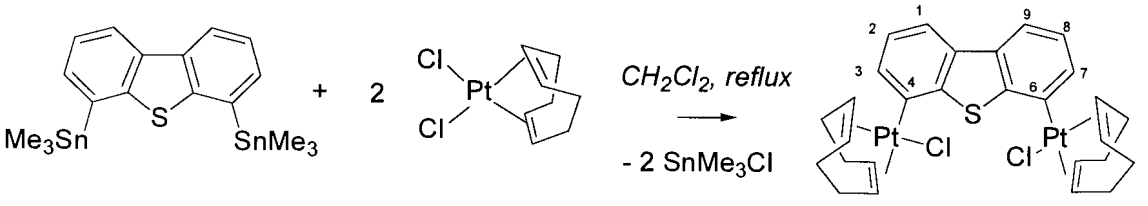

2-2

Reaction 2.2

[PtXR(η⁴-cod)] type complexes (where X = Br or Cl and R = alkyl) are commonly prepared by a halide exchange reaction between [Pt(η⁴-cod)X_2] and organolithium substrates [41]. This methodology is not applicable to dibenzothiophene because of the difficulty in the dilithiation of dibenzothiophene. An excess of organolithium reagent is required to achieve a double lithiated product and to avoid appreciable contamination by monolithiated dibenzothiophene. It is also not practical and cost-effective to use an excess of the electrophile (in this case [Pt(η⁴-cod)X_2]) to quench the reaction.

2.2.5 Oxidative addition to 4,5-dibromo-2,7-di-*tert*-butyl-9,9-dimethylxanthene

Out of interest, the oxidative addition of tetrakis(triethylphosphine)platinum(II) to 4,5-dibromo-2,7-di-*tert*-butyl-9,9-dimethylxanthene was also investigated. The reactivity of 4,5-

dibromo-2,7-di-*tert*-butyl-9,9-dimethylxanthene proved to be more sluggish than for 4,6-dibromodibenzothiophene. The latter produced the binuclear platinum insertion product **2-1** after ninety minutes in reluxing toluene. For the 4,5-dibromoxanthene analogue, a single oxidation reaction was observed under the same reaction conditions *viz.* two equivalents of $[Pt(PEt_3)_4]$ and one equivalent of the dibromo substrate in refluxing toluene (Figure 2.9): ^{1}H NMR δ / ppm: 7.394 (d, CH, 1H), 7.309(d, CH, 1H), 7.295 (d, CH, 1H), 6.924 (m, CH, 1H), 1.687 (m, PCH_2, 12H), 1.555 (s, Me, 6H), 1.263 (s, ^{t}Bu, 18H), 1.028 (m, PCH_2CH_3, 18H). ^{31}P NMR δ / ppm 10.96 (Pt-sat., $^1J_{Pt-P}$ 2739 Hz). The similarity in ^{31}P NMR data with that of **2-1** indicates a *trans* diphosphine geometry at the platinum(II) centre. When the reaction mixture was allowed to reflux for twenty-four hours, the mono-oxidation product was once again detected by NMR spectroscopy. However, a second phosphine resonance was detected in the ^{31}P NMR spectrum (δ / ppm: 13.06, $^1J_{Pt-P}$ 2752 Hz) - due to the presence of a small amount of the binuclear platinum(II) complex. Increasing the reaction time to one week still yielded a mixture of mono- and binuclear products (4:1 based on ^{31}P NMR peak intensities).

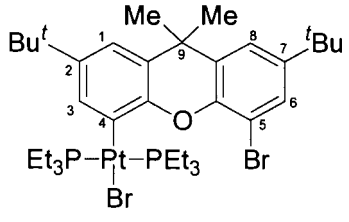

Figure 2.9 Mono-nuclear Pt(II) complex of 4,5-dibromo-2,7-di-*tert*-butyl-9,9-dimethylxanthene.

2.2.6 Oxidation Addition of Platinum(II) to Platinum(IV)

Platinum(II) diimine complexes such as $[PtMe_2(N,N\text{-}2,2'\text{-bipyridine})]$ and $[PtMe_2(N,N\text{-}1,10\text{-phenanthroline})]$ are known to be extremely reactive toward oxidative insertion of alkyl halides, producing octahedral platinum(IV) products [19]. In an attempt to obtain a similar

C-Br activation product, [$PtMe_2$(*N,N*-2,2′-bipyridine)] was reacted with 4,6-dibromo-benzothiophene at elevated temperatures for extended periods. Unfortunately the aryl-halide bonds in 4,6-dibromodibenzothiophene are too inert to undergo oxidative addition under these conditions. Puddephatt and co-workers have shown, though, that it is possible for an intramolecular aryl-halogen bond to be activated: Platinum-bonded Schiff base ligands were so tailored that oxidative addition of a pendant aryl-halogen bond attached to the Schiff base could be driven by the formation of five-membered metallacycle [42]. Such systems can even lead to the activation of an aromatic carbon-flourine bond [43].

2.2.7 Oxidation Addition of Palladium(0) to Palladium (II)

The oxidative addition of bromothiophenes to tetrakis(triphenylphosphine)palladium(II) has been reported by Hor and co-workers and complexes of the type *trans*-[$PdBr(C_4H_{3-n}Br_nS$-*C*)$(PPh_3)_2$] where n = 1 - 3 were isolated [12]. There reactions occurred readily at room temperature using benzene as a solvent.

It was thus attempted to achieve a double oxidative C-Br insertion to generate the palladium analogue of **2-1**. The following compounds were each reacted with two equivalents of [$Pd(PPh_3)_4$] in benzene: 2,5-dibromothiophene, 4,5-dibromo-2,7-di-*tert*-butyl-9,9-dimethyl-xanthene and 4,6-dibromodibenzothiophene. None of the reactions resulted in the formation of a binuclear palladium(II) complex (NMR spectroscopy and MS). [$Pd(PPh_3)_4$] readily catalyses cross-coupling reactions and it is suspected that this is what occurred in the reaction solution containing excess palladium(0).

Oxidative addition reactions were also attempted using [$Pd_2(dba)_3$.dba] (also known as "$Pd(dba)_2$"). The dba ligand readily dissociates in the presence of suitable neutral ligands such as amines or phosphines. P.G. Jones *et. al.* was able to isolate complexes of the type [Pd(2-C_6H_4Y)BrL_2] where Y = CHO, CN and L = PPh_3, L_2 = tmeda, dppe [44]. Using a similar

method, "$Pd(dba)_2$" was reacted with 2,5-dibromothiophene, firstly in the presence of tmeda, and then again with dppe. A palladium(II) oxidative addition product could not be isolated. The reactivity of palladium in comparison to platinum is a complicating issue and more experience is needed to trap the intermediate complexes. One contributing factor to the complexity of the product mixtures obtained with palladium is the ease with which palladium(II) undergoes reductive elimination (Refer to Chapter 1).

2.2.8 NMR Spectroscopy

Tables 2.4 -2.6 contain ^1H NMR data for compounds **1**, **2**, **3** and **4** and complexes **2-1** and **2-2**.

Table 2.4 ^1H NMR data for dibenzothiophene and **1** (in $CDCl_3$), δ / ppm (J in Hz)

	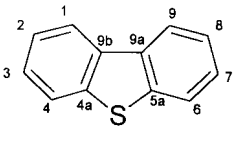	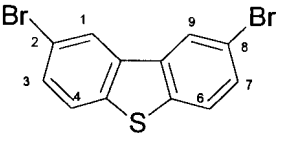 **1**
H-1, H-9	8.173 dd, $^3J_{HH}$ = 5.7, $^4J_{HH}$ = 3.4	8.20 d, $^4J_{HH}$ = 1.80
H-2, H-8	7.50 - 7.47 m	-
H-3, H-7	7.50 - 7.47 m	7.55 dd, $^3J_{HH}$ = 8.53, $^4J_{HH}$ = 2.05
H-4, H-6	7.891 dd, $^3J_{HH}$ = 5.7, $^4J_{HH}$ = 2.9	7.68 d, $^3J_{HH}$ = 8.52

The NMR data for dibenzothiophene is included for comparative purposes; this data corresponds closely to that reported by D.W. Jones *et. al.* [45]. Protons H-1/H-9 and H-3/H-7 in compounds **1** to **4** were assigned by comparing their chemical shifts to that of the corresponding protons in free dibenzothiophene.

Table 2.5 ^{1}H NMR data for **2**, **3** and **4** (in $CDCl_3$) δ / ppm

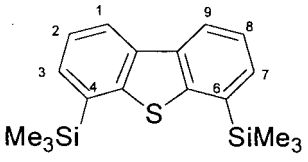 **2**	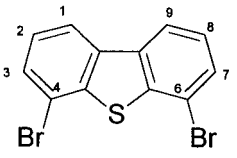 **3**	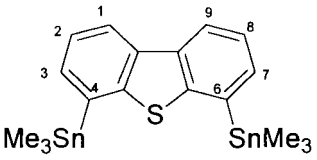 **4**
8.173 dd, H-1, H-9 $^3J_{HH}$ = 7.82 Hz $^4J_{HH}$ = 1.14 Hz	8.050 dd, H-1, H-9 $^3J_{HH}$ = 7.82 Hz $^4J_{HH}$ = 0.95 Hz	8.087 dd, H-1, H-9 $^3J_{HH}$ = 7.76 Hz $^4J_{HH}$ = 1.29 Hz
7.455 t, H-2, H-8 $^3J_{HH}$ = 7.05 Hz $^3J_{HH}$ = 7.8 Hz	7.356 t, H-2, H-8 $^3J_{HH}$ = 7.82 Hz	7.397 t, H-2, H-8 $^3J_{HH}$ = 7.4 Hz
7.610 dd, H-3, H-7 $^3J_{HH}$ = 7.05 Hz $^4J_{HH}$ = 1.3 Hz	7.631 dd, H-3, H-7 $^3J_{HH}$ = 7.82 Hz $^4J_{HH}$ = 0.96 Hz	7.501 dd, H-3, H-7 $^3J_{HH}$ = 6.80 Hz $^4J_{HH}$ = 1.29 Hz
0.516 s, Me		0.457 s with Sn-sat.,Me $^2J_{119Sn-H}$ = 56.1 Hz $^2J_{117Sn-H}$ = 53.5 Hz

Bromo-substituents at positions 2 and 8 have only a small effect on the proton chemical shift values of **1**. The chemical shift of the H-1 and H-9 protons in **2**, **3** and **4** shift are relatively unaffected by substitution with respect to the corresponding chemical shift for free dibenzothiophene. Protons H-2 and H-8 in **2**, **3** and **4** are slightly more shielded than in free dibenzothiophene. The chemical shift of protons H-3 and H-7 in **2** and **3** exhibit an enhanced

deshielding effect and move somewhat downfield with respect to free dibenzothiophene, while that of **4** is relatively unchanged. The methyl protons attached to the silicon atom in **2** resonate at a frequency typical of silyl derivatives. Isotope ^{29}Si is a spin- ½ nucleus, but has a very low natural abundance of 4.7 %. Thus, two-bond ^{29}Si-H coupling was not observed. Two isotopes of tin also have spin-½ nuclei and are NMR-active, *viz.* ^{119}Sn (natural abundance 8.58 %) and ^{117}Sn (natural abundance 7.61 %). Coupling of methyl protons in **4** to both these nuclei could be detected: $^{2}J_{119Sn-H}$ = 56.1 Hz and $^{2}J_{117Sn-H}$ = 53.5 Hz. These values are in agreement with other reported alkyltin compounds [46].

Table 2.6 ^{1}H NMR data for **2-1** and **2-2** (in $CDCl_3$) δ / ppm

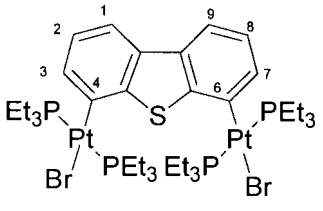 **2-1**	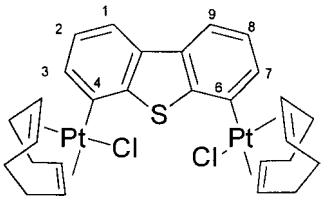 **2-2**
7.62 d, 2H, H-1 and H-9	7.647 dd, 2H, H-1 and H-9
$^{3}J_{HH}$ = 7.76 Hz	$^{3}J_{HH}$ = 6.72 Hz, $^{4}J_{HH}$ = 2.31 Hz
6.983 t, 2H, H-2 and H-8	7.13-7.15 m, 4H, H-2 H-8 and H-3 H-7
$^{3}J_{HH}$ = 7.50 Hz	5.903 s, br, Pt-sa., 4H, cod CH
7.381 d with Pt-sat., 2H, H-3 and H-7	$^{2}J_{Pt-H}$ unresolved
$^{3}J_{HH}$ = 7.24 Hz, $^{3}J_{Pt-H}$ = 70.5 Hz	4.756 s, br, Pt-sat., 4H, cod CH
1.696 m, 24H, CH_2	$^{2}J_{Pt-H}$ = 74.5 Hz
1.013 m, 36H, CH_3	2.69-2.65 m, 8H, cod CH_2
	2.44-2.38 m, 8H, cod CH_2
$^{31}P\{^{1}H\}$ NMR δ / ppm	
12.5 s with Pt.sat.,	
$^{1}J_{Pt-P}$ 2694 Hz	

The assignments of the protons for **2-1** and **2-2** were aided by comparing the chemical shifts with that obtained for related monoplatinum-substituted dibenzothiophene compounds [46]. The protons are relatively more shielded and shift upfield relative to the corresponding protons in the free 4,6-dibromodibenzothiophene and 4,6-bis(trimethylstannane)dibenzothiophene ligands and in dibenzothiophene. The $^{3}J_{Pt\text{-}H}$ coupling of 70.5 Hz for H-3 / H-7 falls into the usual range [10, 47]. The chemical shift values of the 1,5-cyclooctadiene protons are typical of [PtClR(cod)] systems [48].

$^{13}C\{^{1}H\}$ NMR data for compounds **1**, **2**, **3** and **4** and complexes **2-1** and **2-2** are arranged in Tables 2.7 - 2.9. Assignments were based on two-dimensional ^{13}C /^{1}H correlation (HETCOR) NMR experiments.

Table 2.7 ^{13}C NMR data for dibenzothiophene and **1** (in $CDCl_3$) δ / ppm

	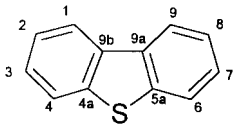	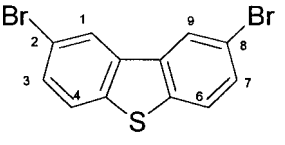 **1**
C-4a, C-5a	139.37	138.67
C-9a, C-9b	135.47	136.12
C-1, C-9	121.48	124.68
C-2, C-8	124.25	118.58
C-3, C-7	126.59	130.26
C-4, C-6	122.71	124.16
	Corresponds to literature values [45]	

Substitution at positions 4 and 6 of dibenzothiophene causes a marked change in the ^{13}C NMR chemical shifts of C-4 / C-6 (δ 122.71 ppm in free dibenzothiophene). The -$SiMe_3$ and -$SnMe_3$

groups in **2** and **4** deshield carbons C-4 and C-6 (δ 133.76 and 134.45 ppm respectively), while the bromine atoms provide shielding so that these carbons exhibit an upfield resonance in **3** (δ = 116.36 ppm). The *ipso* C-2 and C-8 carbon atoms in **1** are also shielded by the attached bromine atoms and resonate at 118.58 ppm. The chemical shift and coupling constants of the methyl groups in **4** correspond well with other reported organotrimethylstannanne compounds [49].

Table 2.8 ^{13}C NMR data for **2**, **3** and **4** (in $CDCl_3$) δ / ppm

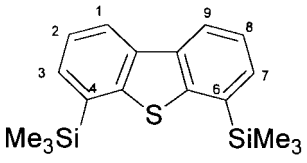 **2**	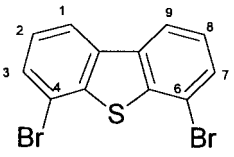 **3**	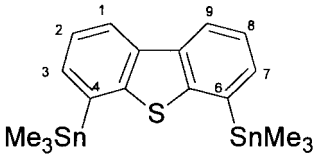 **4**
145.03 C-4a, C-5a	141.08 C-4a, C-5a	148.04 C-4a, C-5a
134.45 C-9a, C-9b	137.07 C-9a, C-9b	135.52 C-9a, C-9b
133.76 C-4, C-6	116.36 C-4, C-6	134.45 C-4, C-6 $^{1}J_{Sn-C}$ unresolved
122.29 C-1, C-9	120.96 C-1, C-9	121.72 C-1, C-9
123.74 C-2, C-8	126.16 C-2, C-8	123.81 C-2, C-8
132.39 C-3, C-7	129.96 C-3, C-7	134.18 C-3, C-7
-1.182 Me		-9.07 Me, $^{1}J_{Sn-C}$ = 347 Hz

Coordination of the platinum fragments to C-4 and C-6 in **2-1** and **2-2** causes a noticeable downfield chemical shift of the C-4 / C-6, C-3 / C-7 and C-4a / C-5a carbon atoms (Table 2.9). Atoms C-1 / C-9 are relatively more shielded and the chemical shifts of C-2 / C-8 are essentially unchanged.

Table 2.9 ^{13}C NMR data for **2-1** and **2-2** (in $CDCl_3$) δ / ppm

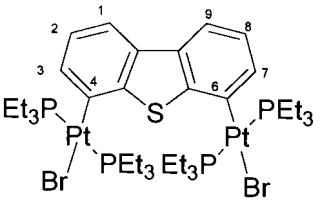 **2-1**		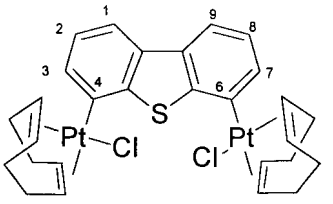 **2-2**	
147.92	C-4a, C-5a	147.00	C-4a, C-4b
134.84	C-9a, C-9b	140.19	C-9a, C-9b
133.29	C-4, C-6	135.61	C-4, C-6
133.15	C-3, C-7	130.90	C-3,C-7
123.56	C-2, C-8, $^{3}J_{Pt-C}$ = 75.4 Hz	124.63	C-2, C-8
115.34	C-1, C-9	117.85	C-1, C-9
14.41	CH_2, t, $^{1}J_{P-C}$ = 17.1 Hz)	115.80	cod CH
8.05	CH_3	99.98	cod CH
		32.16	cod CH_2
		28.23	cod CH_2

Certain J_{Pt-C} couplings for complexes **2-1** and **2-2** were not resolved.

2.2.9 Mass spectrometry

The electron impact method of ionization was used in the mass spectrometry analyses (EI-MS); the results of which are presented in Tables 2.10 and 2.11.

Table 2.10 EI-MS data for the dibenzothiophene derivatives **1**, **2**, **3** and **4**

	m/z (intensity) [fragment ion]		m/z (intensity) [fragment ion]
1	342 (28) [M^+] 182 (31) [M^+ - 2Br] 149 (21) [M^+ - 2Br - SH]	**2**	328 (65) [M^+] 313 (100) [M^+ - Me] 298 (2) [M^+ - 2Me] 256 (10) [M^+ - 3Me - Si] 241 (22) [M^+ - 4Me - Si]] 73 (28) [$SiMe_3^+$]
3	342 (32) [M^+] 263 (8) [M^+ - Br] 182 (17) [M^+ - 2Br]	**4**	510 (6) [M^+] 494 (20) [M^+ - Me] 348 (20) [$DBTSnMe_3H^+$] 333 (100) [$DBTSnMe_2H^+$] 301 (36) [$DBTyl^{119}Sn$] 184 (13) [DBT^+] 151 (28) [$SnMe_2^+$]

The molecular ion peaks were resolved for compounds **1** - **4**. The two dibromo compounds tend to fragment by loss of bromine atoms. Compounds **2** and **4** lose successive methyl groups followed by the loss of silicon and tin atoms respectively.

Complexes **2-1** and **2-2** have relatively high molecular weights and their molecular ions were not detected in the spectrometer.

Table 2.11 EI-MS data for the Pt(II) complexes **2-1** and **2-2**

m/z (intensity) [fragment ion]

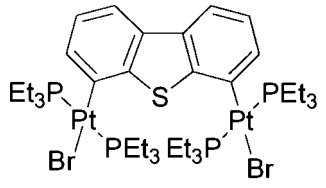 **2-1**	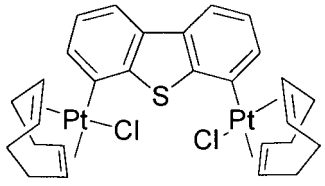 **2-2**
[M^+] of 1205 not detected	M^+ of 858 not detected
773 (45) [M^+ - $Pt(PEt_3)_2$]	520 (5) [M^+ - Pt(cod)Cl]
694 (66) [M^+ - $Pt(PEt_3)_2$ - Br]	377 (6) [DBTylPt$^+$]
431 (68) [$Pt(PEt_3)_2$]	338 (19) [Pt(cod)Cl$^+$]
118 (39) [PEt_3^+]	303 (20) [Pt(cod)$^+$]
	184 (57) [DBT$^+$]

2.3 CONCLUSIONS

To the best of our knowledge, **2-1** is the first reported example of a binuclear platinum compound generated from double oxidative addition into two C-Br bonds of a heteroaromatic compound. In contrast, the reactivity of a 4,5-dibromoxanthene molecule was considerably different as to prevent the isolation of an analogous binuclear complex under similar reaction conditions. For **2-1** to act as a catalyst, it is necessary for the Pt(II) centre(s) to undergo oxidative addition to Pt(IV). The phosphine co-ligands in **2-1** are sufficiently basic to facilitate this oxidation. Furthermore, *trans* phosphines are not readily replaced by more basic amines. The cod ligand in compound **2-2**, however, is readily substituted by chelating diamines. This is expected to render **2-2** more susceptible to oxidative addition to Pt(IV).

In the light of these results, it became interesting to investigate the oxidative addition reactions of Pt(0) with various types of heteroaromatic compounds.

2.4 REFERENCES

[1] (a) V. Farina in *Comprehensive Organometallic Chemistry II*, Vol. 12, Ed. E.W. Abel, F.G.A. Stone and G. Wilkinson, Pergamon, Oxford, U.K., 1995, 161-240 (b) L. S. Hegedus in *Organometallics in Synthesis: A Manual*, Ed. M. Schlosser, John Wiley and Sons Ltd, Chichester, UK, 2002, pp 1150-1208

[2] A Jutand and A. Mosleh; *Organometallics*, **1995**, *14*, 1810-1817

[3] V.V. Grushin and H. Alper in *Topics in Organometallic Chemistry*, Vol 3., Ed. S. Murai, Springer-Verlag, Berlin, 1999, 194-219

[4] A. Dedieu; *Chem. Rev.*, **2000**, *100*, 543-600

[5] S.Sakaki, B. Biswas and M. Sugimoto; *J. Chem. Soc., Dalton Trans.*, **1997**, 803-809

[6] (a) J.K. Stille in *The Chemistry of the Metal-Carbon Bond*, Ed. F.R. Hartley and S. Patia, John Wiley and Sons Ltd., 1985, pp 656-666 (b) R.J. Puddephatt, *ibid.*, 1982, pp 250-252

[7] H. Yamashita, M. Tanaka and M. Goto; *Organometallics*, **1997**, *16*, 4696-4704

[8] P. Fitten and E.A. Rick; *J. Organomet. Chem.*, **1971**, *28*, 287-291

[9] G.W. Parshall; *J. Am. Chem. Soc.*, **1974**, *96*, 2360-2366

[10] J. Manna, C.J. Kuehl, J.A. Whiteford and P.J. Stang; *Organometallics*, **1997**, *16*, 1897-1905

[11] D.P. Arnold, Y. Sakata, K. Sugiura and E.I. Worthington; *Chem. Commun.*, **1998**, 2331-2332

[12] (a) Y. Xie, S.-C. Ng, B.-M. Wu, F. Xue, T.C.W. Mak and T.S.A. Hor; *J. Organomet. Chem.*, **1997**, *531*, 175-181 (b) Y. Xie, B. Wu, F. Xue, S.-C. Ng, T.C.W. Mak and T.S.A. Hor; *Organometallics*, **1998**, *17*, 3988-3995

[13] K.R. J. Thomas, J.T. Lin and K.-J. Lin; *Organometallics*, **1999**, *18*, 5285-8591

[14] L.-Y. Chia and W.R. McWhinnie; *J. Organomet. Chem.*, **1980**, *188*, 121-128

[15] (a) K.A. Fallis, C. Xu and G.K. Anderson; *Organometallics*, **1993**, *12*, 2243- (b) J.K. Stille in *The Chemistry of the Metal-Carbon Bond*, Ed. F.R. Hartley and S. Patia, John Wiley and Sons Ltd., 1985, pp 716-717 (c) H.-K. Yip, C.M. Che and S.-M. Peng; *J. Chem. Soc., Dalton Trans.*, **1993**, 179-187 (d) P.K. Byers; *Coord. Chem. Rev.*, **1995**, *146*, 431-450 (e) R. Huang, I.A. Guzei and J.H. Espenson; *Organometallics*, **1999**, *18*, 5420-5422

[16] (a) J.R. Torkelson, R. McDonald and M. Cowie; *Organometallics*, **1999**, *18*, 4134-4146 (b) D.S. A. George, R.W. Hilts, R. McDonald and M. Cowie; *ibid.*, **1999**, *18*, 5330-5343 (c) F.H. Antwi-Nsaiah, J.R. Torkelson and M. Cowie; *Inorg. Chim. Acta*, **1997**, *259*, 213-226 (d) D.S.A. George, R. McDonald and M. Cowie; *Organometallics*, **1998**, *17*, 2553-2566

[17] S. Hillebrand, B. Bartkowska, J. Bruckmann, C. Krüger and M.W. Haenel; *Tetrahedron Lett.*, **1998**, *39,* 813-816

[18] S. Hillebrand, J. Bruckmann, C. Krüger and M.W. Haenel; *Tetrahedron Lett.*, **1995**, *36,* 75-78

[19] (a) R.H. Hill and R.J. Puddephatt; *J. Am. Chem. Soc.*, **1985**, *107*, 1218-1225 (b) P.K. Monaghan and R.J. Puddephatt; *Organometallics*, **1986**, *5*, 439-442 (c) M Crespo and R.J. Puddephatt; *Organometallics*, **1987**, *6*, 2548-2550 (d) P.K. Monaghan and R.J. Puddephatt; *J.Chem. Soc., Dalton Trans.*, **1988**, 595-599

[20] J. Ashby and C.C. Cook in *Advances in Heterocyclic Chemistry*; Eds. A.R. Katritzky and A.J. Boulton, Vol. 16, Academic Press, New York, 1974, p 254

[21] (a) R. Gerdil and E.A.C. Lucken; *J. Am. Chem. Soc.*, **1965**, *87*, 213-217 (b) L. Benati, P.C. Montevecchi and A. Tundo; *J. Chem. Soc. Chem. Commun.*, **1978**, 53

[22] C.R. Neumoyer and E.D. Amstutz; *J. Am. Chem. Soc.*, **1947**, *69*, 1920-1921

[23] E. Campaigne and J. Ashby; *J. Heterocycl. Chem.*, **1969**, *6*, 517-522

[24] R.B. DuVernet, O. Wennerström, J. Lawson, T. Otsubo and V. Boekelheide; *J. Am. Chem. Soc.*, **1978**, *100*, 2457-2464

[25] R.M. Acheson and D.R. Harrison; *J. Chem. Soc. (C),* **1970**, 1764-1784

[26] F. Sauter and P. Stütz in *Houben-Weyl Methoden der organischen Chemie*, Vol. E6a, Georg Thiem Verlag, Stuttgart, 1994, pp 903-904

[27] R.H. Mitchell, Y. Chen and J. Zhang; *Org. Prep. Proced. Int.*, **1997**, *29*, 715-719

[28] C. Cuehm-Caubère, S. Adach-Becker, Y. Fort and P. Caubère; *Tetrahedron*, **1996**, *52*, 9087-9092

[29] M.W. Haenel, D. Jakubik, E. Rothenberger and G. Schroth; *Chem. Ber.*, **1991**, *124*, 1705-1710

[30] R.M. Schaffrin and J. Trotter; *J. Chem. Soc. A*, **1970**, 1561

[31] F.H. Allen and O. Kennard; *Chem. Design Autom. News*, **1993**, *8*, 1 and 31-37

[32] (a) M.W. Haenel, H. Fieseler, D. Jakubik, B. Gabor, R. Goddard and C. Krüger; *Tetrahedron Lett.*, **1993**, *34*, 2107-2110 (b) E.M. Vogl, J. Bruckmann, C. Krüger and M.W. Haenel; *J. Organomet. Chem.*, **1996**, *520*, 249-252

[33] V. Meille, E. Schulz, M. Lemaire, R. Faure and M. Vrinat; *Tetrahedron*, **1996**, *52*, 3953-3960

[34] M.W. Haenel, D.Jakubik, C. Krüger and P. Betz; *Chem. Ber.*, **1991**, *127*, 333-336

[35] H.O. House, D.G. Koepsell and W.J. Campbell; *J. Org. Chem.*, **1972**, *37*, 1003-1011

[36] H.O. House, D.G. Koepsell and W.Jaeger; *J. Org. Chem.*, **1973**, *38*, 1167-1173

[37] Compounds were named according to IUPAC's Nomenclature of Inorganic Chemistry -

Recommendations for 1990, Ed. G.J. Leigh, Blackwell Scientific Publications, Oxford, 1990

[38] J.K. Stille and K.S.Y. Lau; *Acc. Chem. Res.*, **1977**, *10*, 434

[39] B. Kayser, C. Missling, J. Knizek, H. Nöth and W. Beck; *Eur. J. Inorg. Chem.*, **1998**, 375-379

[40] S. Kotani, K. Shiina and K. Sonogashira; *J. Organomet. Chem.*, **1992**, *429*, 403-413

[41] (a) H.A. Brune, R. Hess and G. Schmidtberg; *Chem. Ber.*, **1985**, *118*, 2011-2019 (b) H.C. Clark and L.E. Manzer; *J. Organomet. Chem.*, **1973**, *59*, 411-428

[42] (a) M. Crespo, X. Solans and M. Font-Bardía; *J. Organomet. Chem.*, **1996**, *518*, 105-113 (b) S.D. Perera and B.L. Shaw; *J. Chem. Soc., Dalton Trans.*, **1995**, 641-647

[43] C.M. Anderson, M. Crespo, G. Ferguson, A.J. Lough and R.J. Puddephatt; *Organometallics*, **1992**, *11*, 1177-1181

[44] J. Vicente, J.A. Abad, E. Martinez-Viviente, M.C.R. Dearello and P.G. Jones; *Organometallics*, **2000**, *19*, 752-760

[45] K.D. Bartlet, D.W. Jones and R.S. Matthews; *Tetrahedron*, **1971**, *27*, 5177-5189

[46] R. Meyer, Ph.D thesis, **1998**

[47] W.-D. Muller and H.A. Brune; *Chem. Ber.* **1986**, *119*, 759-761

[48] C. Eaborn, K.J. Odell and A. Pidcock; *J. Chem. Soc. Dalton Trans.*, **1978**, 357-368

[49] C.D. Schaeffer Jr. and J.J. Zuckerman; *J. Organomet. Chem.*, **1973**, *55*, 97-10

CHAPTER 3

Homogeneous C-S Activation by Platinum(0)

3.1 INTRODUCTION

It is becoming increasingly important for a world that makes higher demands for energy that advanced technologies are developed to make better use of ever dwindling resources. For sustainable development to be realised, the principles of "Green Chemistry" [1] will need to be adopted on a larger scale. "Green Chemistry" has been defined as the design of chemical products and processes that reduce or eliminate the use and generation of hazardous substances. It implies the use of processes that show atom economy, avoid the formation of undesirable by-products and are mindful of the environment[1]. The combustion of fossil fuels is particularly deleterious to the planet. Carbon dioxide emissions are believed to play a role in global warming, while nitrogen oxide and sulfur oxide emissions lead to acid rain which in turn affect forests, lakes and buildings. Improved fuel quality and cleaner exhaust gases are two areas being targeted on an ongoing basis to improve air quality. The removal of sulfur and nitrogen from fossil fuels is necessary to reduce noxious emissions as well as to prevent the poisoning of catalysts during further petroleum hydrotreating and hydrocracking processes.

---

[1] For more information on Green Chemistry visit the following websites:
The Green Chemistry Network (RSC-affliated) www.chemsoc.org/gcn
The Green Chemistyr Institute (ACS-affliated) www.chemistry.org/greenchemistryinstitute

The controlled removal of sulfur (as hydrogen sulfide) and nitrogen (as ammonia) from petroleum feedstocks is know as hydrodesulfurisation (HDS) and hydrodenitrogenation (HDN) respectively (also collectively referred to as hydrotreating). It occurs by treating the feedstocks with hydrogen gas (up to 200 atm) over heterogeneous catalysts at 300-450 °C. Commercial catalysts typically consist of alumina oxide-supported cobalt, molybdenum or tungsten sulfides (or combinations thereof) as the main component with late transition metals (Ni, Co, Ru, Ir, Rh, Pt, Pd, Os, Re) as promoters [2]. In addition to HDS and HDN, hydrodeoxygenation and hydrogenation of unsaturated hydrocarbons also occur. These processes compete with each other for hydrogen and this additional consumption of hydrogen increases the overall expense of hydrotreating.

Organosulfur compounds present in fossil fuels vary widely in their reactivities during catalytic HDS. Thiols, sulfides and disulfides generally react under milder conditions and more rapidly than aromatic thiophenes (Table 3.1 [3]). Mono- and particularly disubstituted dibenzo-thiophenes are more problematic and require deep catalytic HDS [4].

The sulfur content may vary considerably depending on the type of crude oil, typically 0.2 % to 4 % by mass. In the United States diesel fuel must be < 500ppm in sulfur, although even lower specifications have been proposed. The petroleum refining industry thus faces a huge challenge to fully optimise fuel processing and catalyst performance, or to develop alternatives (*eg.* biodesulfurisation using enzyme-catalysed reactions [5]). The understanding of the underlying chemistry is essential for meeting this challenge.

Modelling studies of desulfurisation processes using supported catalysts [6], clean single-crystal transition metal surfaces [7] and organometallic complexes in homogeneous solution [8] have been undertaken in order to predict the structure of possible intermediates and the nature of kinetics on heterogeneous catalysts. In particular, the mechanisms of C-S bond cleavage in homogeneous solutions could provide insights into the mechanism of heterogeneous catalytic C-S scission that could lead to the design of better catalysts with improved desulfurisation capabilities.

Table 3.1 Organosulfur compounds present in petroleum feedstocks

Sulfur compound classification	Structure
Non-thiophene (thiols, sulfides and disulfides)	R-S-H, R-S-R, R-S-S-R
Thiophenes	
Benzothiophenes	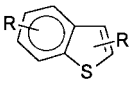
Non-β-substituted dibenzothiophenes	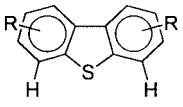
β-substituted dibenzothiophenes	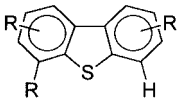
Di-β-substituted dibenzothiophenes	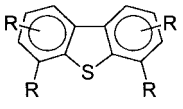
3,4-rings containing S	variable
1,2-rings containing S	variable

Thiophene can coordinate to transition metal centres in various ways. The modes of coordination together with representative examples are given in Figure 3.1.

Figure 3.1 Coordination modes of thiophene to transition metal complexes [9a]

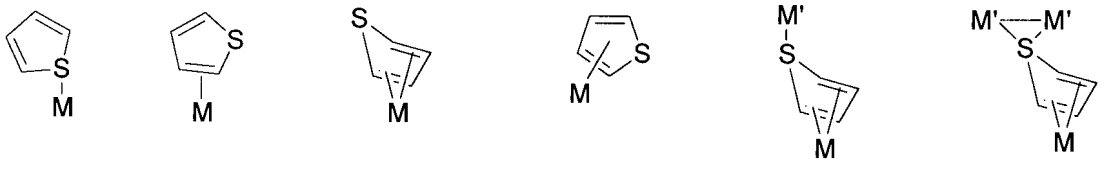

η^1(S)	η^2	η^4	η^5	η^4,S-μ_2	η^4,S-μ_3

Examples

η^1 (S)	$[Re(Cp^*)(BT)(CO)_2]$, where $Cp^* = C_5Me_5^-$	[9b]
η^2	$[Os(2,3-\eta^2-C_4H_4S)(NH_3)_5]^{2+}$ (based on NMR)	[9c]
η^4	$[IrCp^*(\eta^4-2,5-Me_2C_4H_2S)]$	[9d]
η^5	$[Ru(\eta^5-SC_4Me_4)_2]^{2+}$	[9e]
η^4,S-μ_2	$[(CO)_3Fe(\eta^4,S-\mu_2-SC_4H_4)Re(CO)_2Cp^*]$	[9f]
η^4,S-μ_3	$[Cp^*Ir(\eta^4,S-\mu_3-2,5-Me_2C_4H_2S)\{Mo_2(CO)_4Cp_2\}]$	[9g]

Electron-rich iridium(I), rhodium(I) and platinum(0) complexes react with thiophene (T), benzothiophene (BT) and dibenzothiophene (DBT) to form thiametallacycles in which the metal has oxidatively inserted into a C-S bond of the heterocycle [10]. Maitlis *et. al.* [11] has studied the thiaplatinacycles in particular. In the case of BT, the metal fragment inserts into a C(vinyl)-S bond rather than the C(aryl)-S bond [11a]. Pre-coordination of the metal to the sulfur atom is thought to be a key step leading to C-S bond cleavage. The X-ray crystal structure of the η^1(S)-bonded rhenium complex, $[Re(\eta^5-C_5Me_5)(BT)(CO)_2]$, shows that the C(vinyl)-S bond is weakened relative to the C(aryl)-S bond [9b]. This provides an explanation for the regioselectivity of the insertion reaction, in addition to the role of steric effects.

C(aryl)-S bonds can, however, be activated: $[Mn(\eta^6-BT)(CO)_3]^+$ and $[Mn(\eta^5-T)(CO)_3]^+$ are reduced by cobaltacene, $[Co(\eta^5-C_5H_5)_2]$, in the presence of carbon monoxide to give products in which Mn inserts into the S-C(aryl) bond rather than the S-C(vinyl) bond (Figure 3.2) [12].

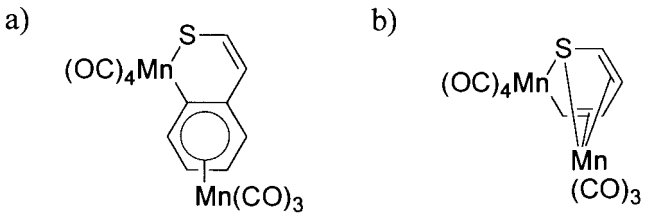

Figure 3.2 S-C(aryl) insertion in $Mn(CO)_3$-coordinated a) benzothiophene and b) thiophene

Photolysis of *cis*-$[Fe(H)_2(dmpe)_2]$, where dmpe = bis(dimethylphosphino)ethane, in the presence of thiophene (or 2-methylthiophene) gives a mixture of two products; a C-S insertion product, $[Fe(SCMeCHCHCH)(dmpe)_2]$ as well as a C-H insertion product *trans*-$[Fe(H)(2\text{-}C_4H_3S)(dmpe)_2]$ [13].

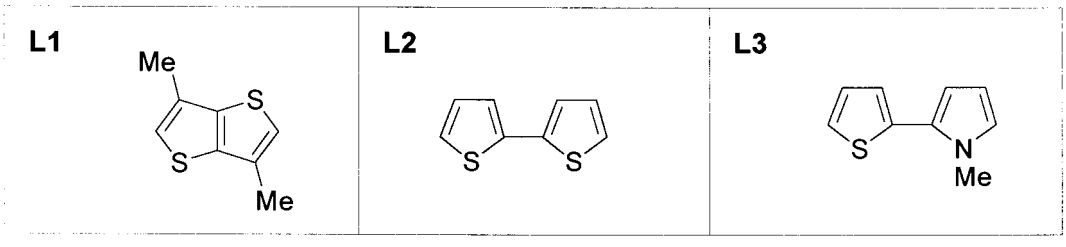

Continuing with the theme of oxidative insertion into thiophene-like molecules [12], the reactions of platinum(0) with 3,6-dimethylthieno[3,2-*b*]thiophene **L1**, 2,2′-bithiophene **L2** and 1-methyl-2-(2-thienyl)pyrrole **L3** were investigated.

3.2 RESULTS AND DISCUSSION

3.2.1 Reaction of $[Pt(PEt_3)_4]$ with 3,6-dimethylthieno[3,2-*b*]thiophene

The ligand 3,6-dimethylthieno[3,2-*b*]thiophene **L1**, was prepared by heating a mixture of 2,5-dimethyl-3-hexyne-2,5-diol, elemental sulfur and benzene in an autoclave according to the

method of Choi *et. al.* (Scheme 3.1) [14]. The ligand was crystallized from hexane.

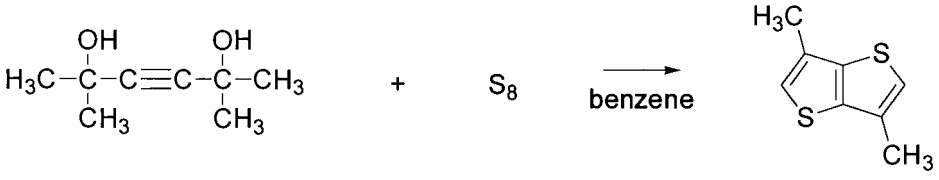

Scheme 3.1 Synthesis of 3,6-dimethylthieno[3,2-*b*]thiophene **L1**

A twofold excess of **L1** was refluxed with tetrakis(triethylphosphine)platinum(0) in toluene for three hours to obtain complex **3-1**, as characterised by NMR and mass spectrometry. The structure was confirmed by a single crystal X-ray diffraction study. Both the NMR data and the crystal structure correspond well with related thiaplatinacycles reported in the literature [11].

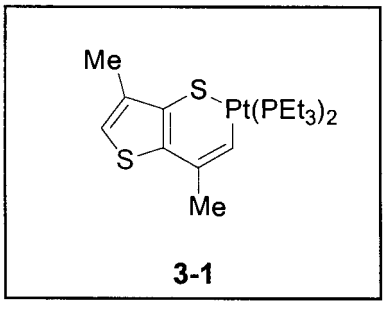

3-1

A six-membered metallacycle was obtained. This thiaplatinacycle has the platinum σ-bonded to the C(vinyl)-atom and to the S-atom. Thus, as could be anticipated, the platinum inserted into the C(vinyl)-S bond rather than the C(aryl)-S bond.

The presence of two thienyl rings allows for the possibility of a double oxidative insertion occurring to form a dithiaplatinacycle (Figure 3.3).

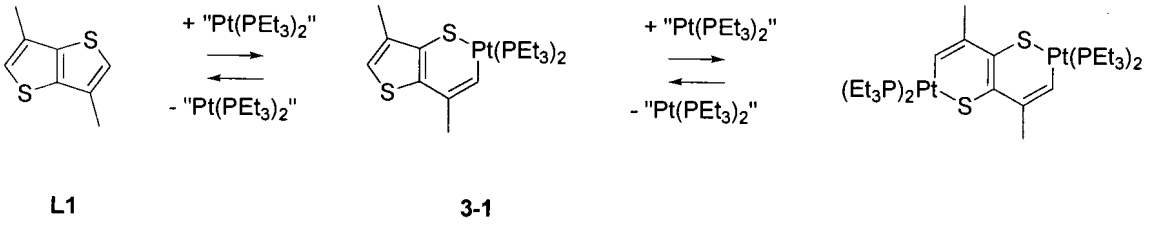

L1 **3-1**

Figure 3.3 Equilibria between the free thiophene-based ligand and the thiaplatinacycle(s)

Thiaplatinacycle **3-1** probably exists in equilibrium with **L1**, but it precipitated out of a toluene solution. The presence of a dithiaplatinacycle was not detected, despite heating **3-1** with an excess of $[Pt(PEt_3)_4]$.

3.2.1.1 *NMR Spectroscopy of* **3-1**

The ^{1}H, $^{13}C\{^{1}H\}$ and $^{31}P\{^{1}H\}$ NMR data are arranged in Table 3.2. The $^{31}P\{^{1}H\}$ NMR data is particularly informative.

In the $^{13}C\{^{1}H\}$ NMR spectrum the J_{Pt-C} couplings were generally not resolved. The C(vinyl)H resonance appeared as a doublet at 131.9 ppm. Coupling to the *cis*-phosphine, $^{2}J_{Pa-C}$ = 9.4 Hz, is considerably smaller in magnitude than the coupling to the *trans*-phosphine, $^{2}J_{Pb-C}$ = 100.1 Hz.

The two phosphorous atoms are nonequivalent and in *cis*-positions. They thus give rise to two doublets with chemical shifts of 11.98 ppm (P_a) and 0.20 ppm (P_b) (Figure 3.4), and are coupled to each other by a two-bond coupling of 24.3 Hz. This value is typical of *cis*-phosphines [15b]. The respective one-bond ^{31}P couplings to ^{195}Pt are 3139 Hz and 1696 Hz. The large dissimilarity in these two coupling constants is a result of the different *trans* influences of the S- and the C-bound thiaplatinacycle, the *trans* influence of the σ-bonded C-atom being greater. Generally, a larger $^{1}J_{Pt-P}$ coupling for related

complexes indicates a weaker *trans* influence of the ligand coordinated *trans* to the relevant phosphorus atom [15a].Therefore, atom P_a is *trans* to the S-atom and atom P_b is *trans* to the C-atom.

Table 3.2 NMR data for **L1** and **3-1** (in $CDCl_3$)

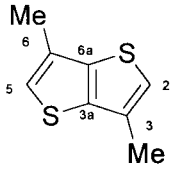 **L1**	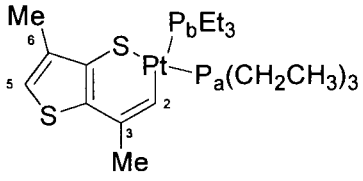 **3-1**
^{1}H NMR δ / ppm	
6.949 s, H-2, H-5 2.354 d, Me, $^4J_{HH}$ = 0.8 Hz	7.278 dd, H-2, $^3J_{P-H}$ = 7.8 Hz, $^3J_{P-H}$ = 25.4 Hz 6.784 s, broadened base H-5 (long range J_{Pt-H}) 2.462 s, Me-3 2.368 d, Me-6, $^4J_{HH}$ = 0.8 Hz 2.00 m, PCH_2 1.13 m, PCH_2CH_3
^{13}C{^{1}H} NMR δ / ppm	
140.08 *ipso*-C 130.37 *ipso*-C 121.80 CH 14.63 Me	139.04 d, *ipso*-C, $^3J_{P-C}$ = 7.2 Hz 137.70 s, *ipso*-C 137.57 s, *ipso*-C 131.86 dd, C-2, $^2J_{Pa-C}$ = 9.4 Hz, $^2J_{Pb-C}$ = 100.1 Hz 128.80 s with Pt-sat., *ipso*-C, J_{Pt-C} = 17.9 Hz 116.24 s, C-5 28.44 d with Pt-sat, Me-3, $^3J_{P-C}$ = 11.7 Hz, $^2J_{Pt-C}$ = 60.1 Hz 16.56 s, Me-6 16.6 m, PCH_2 8.4 m, PCH_2CH_3

$^{31}P\{^{1}H\}$ NMR δ / ppm	
11.98	d with Pt-sat., P_a
	$^{2}J_{Pa\text{-}Pb}$ = 24.2 Hz, $^{1}J_{Pt\text{-}Pa}$ = 3139 Hz
0.20	d with Pt-sat., P_b
	$^{2}J_{Pa\text{-}Pb}$ = 24.2 Hz, $^{1}J_{Pt\text{-}Pb}$ = 1696 Hz

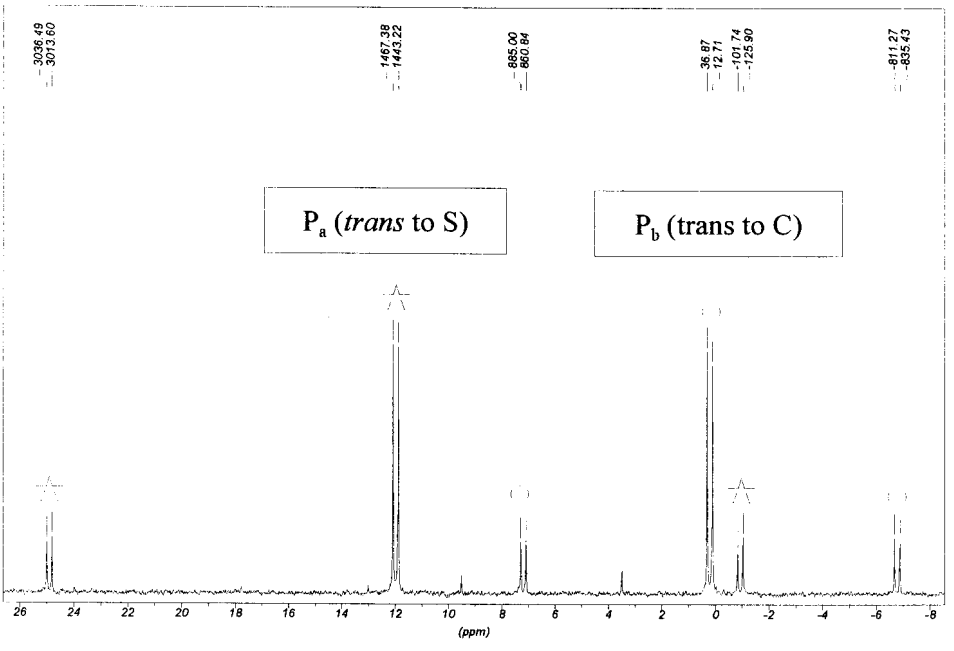

Figure 3.4 $^{31}P\{^{1}H\}$ NMR spectrum of **3-1** (in $CDCl_3$)

3.2.1.2 Crystal structure of **3-1**

Ivory-coloured crystals suitable for single-crystal X-ray diffraction were grown from a cold (-20°C), saturated solution of **3-1** in toluene / hexane (1:1). Complex **3-1** has an orthorhombic crystal system and crystallizes in the $P2_12_12_1$ space group. Refer to the Appendix for the relevant acquisition and refinement data, as well as full details of the structural parameter data (bond lengths, bond angles and torsion angles). Figure 3.5 is

an ball-and-stick depiction of the molecular structure of **3-1**.

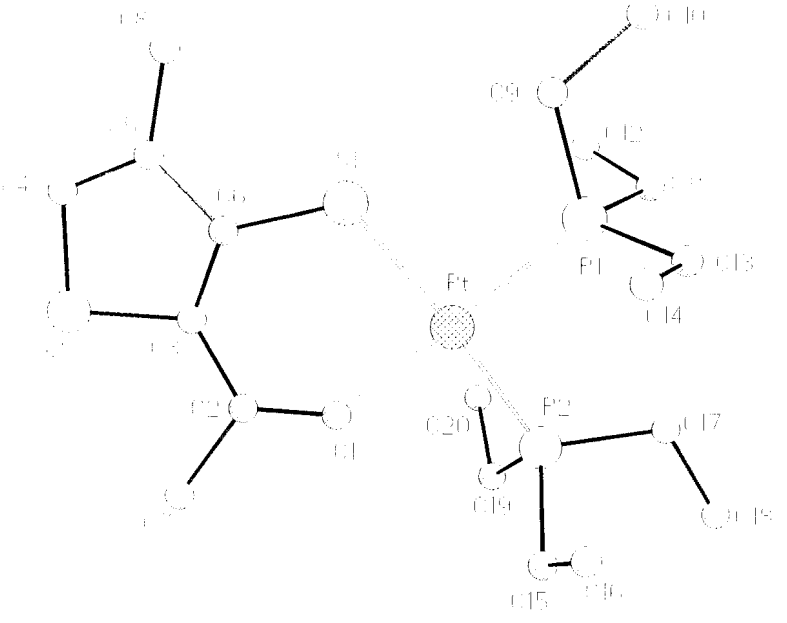

Figure 3.5 Ball-and-stick diagram of **3-1**

The six-membered thiaplatinacycle is close to planar (Refer to the selected torsion angles in Table 3.3), while the five-membered thiophene ring is planar.

Table 3.3 Selected torsion angles (°) for **3-1**

C(1)-Pt-S(1)-C(6)	-13.8(5)	C(4)-S(2)-C(3)-C(6)	-0.5(8)
S(1)-Pt-C(1)-C(2)	9.2(11)	C(3)-S(2)-C(4)-C(5)	1.6(10)
C(1)-C(2)-C(3)-C(6)	-13.5(18)	S(2)-C(4)-C(5)-C(6)	-2.1(14)
S(1)-C(6)-C(3)-C(2)	3.3(17)	S(2)-C(3)-C(6)-C(5)	-0.6(12)
Pt-S(1)-C(6)-C(3)	12.0(10)		

Table 3.4 Selected bond lengths (Å) and angles (°) for **3-1**

Pt-C(1)	2.04(1)	C(1)-Pt-P(2)	85.4(4)
Pt-P(2)	2.279(3)	C(1)-Pt-S(1)	89.8(4)
Pt-S(1)	2.290(2)	P(2)-Pt-S(1)	173.7(1)
Pt-P(1)	2.342(2)	C(1)-Pt-P(1)	176.1(3)
		P(2)-Pt-P(1)	97.73(9)
S(1)-C(6)	1.75(1)	S(1)-Pt-P(1)	87.24(9)
S(2)-C(3)	1.74(1)		
S(2)-C(4)	1.73(2)	C(6)-S(1)-Pt	112.0(4)
		C(2)-C(1)-Pt	138.(1)
C(1)-C(2)	1.29(2)	C(1)-C(2)-C(3)	123.(1)
C(2)-C(3)	1.42(2)	C(3)-C(6)-S(1)	125.7(9)
C(3)-C(6)	1.37(2)	C(6)-C(3)-C(2)	129.4(9)
C(4)-C(5)	1.33(2)		
C(5)-C(6)	1.43(2)	C(3)-S(2)-C(4)	90.8(6)
		C(6)-C(3)-S(2)	110.(1)
		C(4)-C(5)-C(6)	111.(1)
		C(3)-C(6)-C(5)	115.(1)
		C(5)-C(4)-S(2)	114.(1)
		C(1)-C(2)-C(7)	122.(1)
		C(3)-C(2)-C(7)	115.(1)
		C(2)-C(3)-S(2)	121.(1)
		C(5)-C(6)-S(1)	119.(1)
		C(4)-C(5)-C(8)	125.(1)
		C(6)-C(5)-C(8)	124.(1)

The platinum atom is in a near square planar coordination geometry. The bond angle ∠P(1)-Pt-P(2) of 97.73(9)° is considerably larger than the ideal square planar value of 90°. This is most likely due to the steric repulsion of the phosphine ethyl substituents (cone angle of PEt_3 = 132° [16]).

The ∠C(1)-Pt-S(1) bond angle is almost exactly 90°, with the remaining two angles being smaller than 90° (Table 3.4). The insertion of the Pt-centre causes the C(6)-S(1)-Pt bond angle to expand to 112.0(4)°, compared to the C(3)-S(2)-C(4) angle of 90.8(6)°. The remaining angles are all larger than the 120° expected for benzene.

On comparing the Pt bond lengths, S(1)-Pt is 2.290 Å and Pt-P(2) is 2.279 Å whereas C(1)-Pt is 2.035 Å and Pt-P(1) is 2.342 Å (Table 3.4). This illustrates the higher *trans* influence of C(1) over S, which was also manifested in the $^{1}J_{Pt\text{-}P}$ coupling constants. The localisation of the double bonds is evident when comparing C-C bond lengths. The C(1)-C(2) distance of 1.29(2) Å is considerably shorter than the 1.42(2) Å for C(2)-C(3), which in turn is similar to the 1.43(2) Å for C(5)-C(6). The latter two are thus single bonds. The remaining two double bonds, C(3)-C(6) and C(4)-C(5) have bond lengths of 1.37(2) Å and 1.33(2) Å respectively.

The thiaplatinacycle can be constructed in various ways (Figure 3.6).

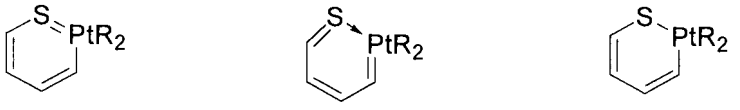

I II III

Figure 3.6 Canonical forms of a thiaplatinacycle

Structure I is a metallathiabenzene *i.e.* a heterobenzene analogue where a CH group has been replaced by a transition metal and its associated ligands. Angelici *et. al.* obtained a crystal structure of an iridathiabenzene (Figure 3.7); both the X-ray results and the NMR spectra indicated a planar, delocalized π-system [17]. In the resonance structure IV, the iridium is a 16-electron centre, whereas in V it is an 18-electron centre.

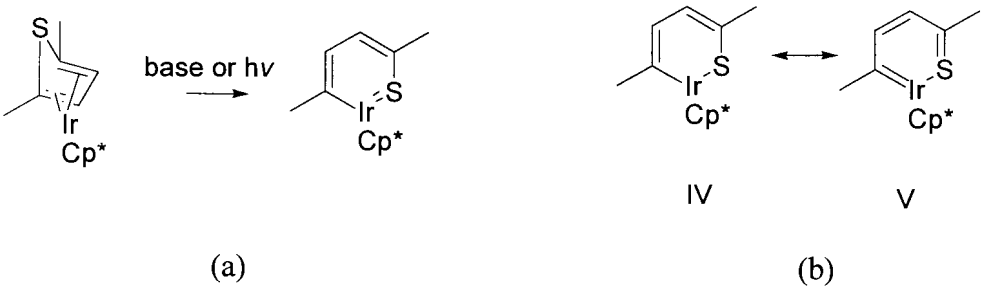

Figure 3.7 (a) Preparation of an iridathiabenzene and (b) resonance forms of the iridathiabenzene

Metallabenzenes [18], metallapyryliums [19] and metallapyridines [20] are related compounds that are also regarded as aromatic in nature. Only very recently has the first platinabenzene molecule been isolated [21] (Figure 3.8). The crystal structure of this compound shows that the bond lengths of the Pt-C bonds are 1.959(3) Å and 1.929(4) Å.

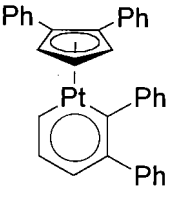

Figure 3.8 The first reported platinabenzene

From an electronic standpoint, the electron-rich nature of the platinum centre is not favourable for the formation of structure I.

Structure II is a conjugated platinum(0) carbene complex. A brief survey of the nature of Pt=C carbene bonds was undertaken (Table 3.5).

Table 3.5 Summary of selected Pt=C carbene bond attributes

		Pt=C bond length / Å	^{13}C NMR δ / ppm	$^{1}J_{Pt-C}$ (carbene) / Hz	Ref.
A	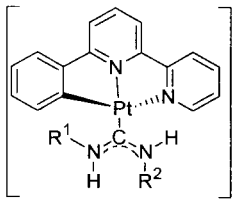	1.997 (2) 1.992 (4) 1.989 (6) 1.996 (8)	193.7 185.2 194.0 188.4 (CD_3CN)	1363 1274 - 1321	[22a]
B	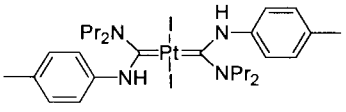	2.051 (4)	190.2 ($CDCl_3$)	810	[22b]
C	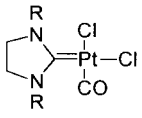	1.97(1) for R = benzyl	168.2 ($CDCl_3$)	1134	[22c]
D	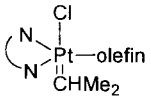	2.006 for NN = dmphen, olefin=dimethyl -maleate	181 (CD_3NO_2)	1006	[22d]
E	a mononuclear bis(carbene) platinum(IV) complex	2.050 (7) and 2.057 (7)	185 (CD_2Cl_2)	733	[22e]
F	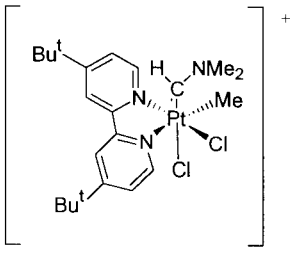	1.991 (21)	177.9 (CD_2Cl_2)	932	[22f]

The Pt=C bond lengths of platinum(II) carbenes average 2.00 Å. Panunzi and co-workers also noted average distances of 2.00 Å for Pt-C(carbene) as well as 2.05 Å for Pt-C(alkyl) bond lengths [23]. The Pt-C bond length of 2.035 Å in **3-1**, is rather long for a Pt-C(carbene) bond. More telling however, is the absence of a carbene carbon resonance with attendant ^{195}Pt satellites at $\delta \geq 170$ ppm in the ^{13}C NMR spectrum of **3-1**. Structure II (Figure 3.6) is thus not an accurate depiction of the bonding in **3-1**.

In structure III the π-electrons are localised. The C-C bond lengths in **3-1** clearly show that the double bonds are localised and that structure III is the "best-fit" representation of **3-1**.

Attempts to insert a second platinum moiety into the second thienyl ring was unsuccessful. It is known that insertion reaction of tris(triethylphosphine)platinum(0) with thiophene is reversible [11a] and that free thienylthiophene, the $[Pt(PEt_3)_4]$ / $[Pt(PEt_3)_3]$ precursor, dissociated phosphine molecules and the thiaplatinacycle exist in equilibrium.

3.2.2 Reaction of $[Pt(PEt_3)_4]$ with 2,2′-bithiophene, L2

Reaction of 2,2′-bithiophene with tetrakis(triethylphosphine)platinum(0) led to the formation of two types of compounds. *Trans*-{5-(2,2′-bithienyl)}hydridobis(triethylphosphine)-platinum(II), **3-2a**, (NMR Table 3.6) is a product of a C-H activation on the unsubstituted α-position of one of the thienyl rings.

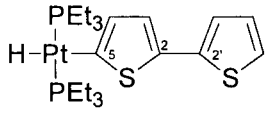

3-2a

The platinum is attached to the ring system via a σ-bond to the α-carbon. The α-position is

more susceptible to metallation than the β-position, and this holds true for five-membered heteroaromatic rings in general [24].

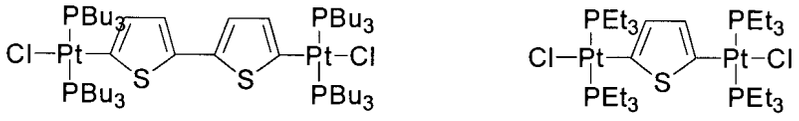

(a) (b)

Figure 3.9 Diplatinum complexes with bridging (a) 5,5'-di(2,2'-thienylene) and (b) 2,5-thienylene ligands

A diplatinum complex of 2,2'-bithiophene, *viz.* *trans,trans*-$[Cl(PBu_3)_2Pt(\mu\text{-}2,5'\text{-}C_4H_2SC_4H_2S)Pt(PBu_3)_2Cl]$ (Figure 3.9a) has been reported in the literature. However, no ^{31}P NMR data was provided [25]. The related diplatinum thienyl derivative, *trans,trans*-$[Cl(PEt_3)_2Pt(\mu\text{-}2,5\text{-}C_4H_2S)Pt(PEt_3)_2Cl]$ (Figure 3.9b) has a chemical shift of 18.91 ppm in the ^{31}P NMR spectrum, with $^1J_{Pt\text{-}P} = 2673$ Hz [26]. This is remarkably similar to the ^{31}P NMR data for **3-2a** (Table 3.6).

The high-field region of the ^1H NMR spectrum of **3-2a** showed a 1:2:1 triplet resonance at -7.300 ppm with coupling to two equivalent ^{31}P-nuclei. The resonance was flanked by two satellite 1:2:1 triplet systems due to coupling to the ^{195}Pt nucleus with coupling constants of 17.4 Hz ($^2J_{P\text{-}H}$) and 713 Hz ($^1J_{Pt\text{-}H}$). This type of pattern is characteristic of a *trans* "H-Pt-C" bonded complex where the C-atom is part of an aromatic heterocyclic ring[2].

A single phosphorus resonance was observed at 18.66 ppm in the $^{31}P\{^1H\}$ NMR spectrum, with a one-bond coupling to ^{195}Pt of 2674 Hz. The chemical shift falls into the region typical of phosphine complexes. The single resonance indicates that the two phosphine groups are equivalent and therefore in *trans*-positions. Furthermore, the value of $^1J_{Pt\text{-}P}$ is characteristic of a *trans*-phosphine platinum(II) hydrido species[2].

[2] Refer to Chapter 5 (Table 5.7)

The hydride complex decomposes in deuterated chloroform, presumably due to trace amounts of hydrogen chloride in the solvent. With time the hydride peak in the ^{1}H NMR spectrum disappears and a new peak at 3.537 ppm ($^{1}J_{Pt-P}$ = 3470 Hz) replaces the original resonance in the $^{31}P\{^{1}H\}$ NMR spectrum (This is typical of a *cis*-$[PtX_2(PEt_3)_2]$ complex.[3]).

The second product that was obtained, was a thiaplatinacycle **3-2b**.

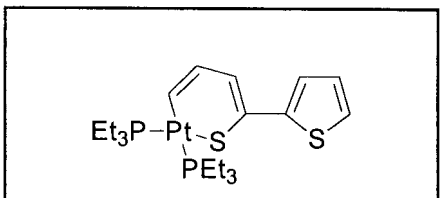

3-2b

The ^{31}P NMR data of **3-2b** (Table 3.6) is very similar to that of the thiaplatinacycle **3-1**: 11.98 ppm, P_a, $^{2}J_{Pa-Pb}$ = 24.2 Hz, $^{1}J_{Pt-Pa}$ = 3139 Hz and 0.20 ppm, P_b, $^{2}J_{Pa-Pb}$ = 24.2 Hz, $^{1}J_{Pt-Pb}$ = 1696 Hz. Once again P_a is *trans* to the sulfur atom and P_b is *trans* to carbon.

The assignments of the ^{1}H NMR resonances for **3-2a** and **3-2b** were aided by two-dimensional (^{1}H, ^{1}H) homonuclear chemical shift correlation (COSY) experiments and integration values, as well as comparing the data to the NMR spectrum of **3-1**. The broadened doublet signal (flanked by satellites) at 6.55 ppm is similar in appearance to the resonance at 6.784 ppm for **3-1**, and was taken to be characteristic of thiaplatinacycles. From the COSY NMR spectrum, the protons belonging to each of the different ring systems could be identified. The rings are labelled a and b in **3-2a**, and a′ and b′ in **3-2b** respectively (Table 3.6)

The $^{13}C\{^{1}H\}$ NMR resonances could not be unambiguously assigned due to overlapping of signals and the *ipso*-carbon atoms were obscured by low intensity resonances from decomposition of the platinum(II) complexes in solution.

---

[3] Refer to Chapter 6, Table 6.9

Table 3.6 NMR data for **L2** and **3-2** (in $CDCl_3$)

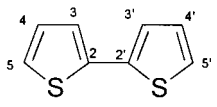 **L2**	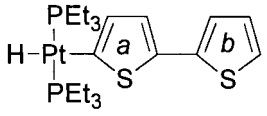 **3-2a**	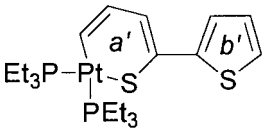 **3-2b**
^{1}H NMR δ / ppm		
7.243-7.223 m, 4H	7.51 m, H_a	7.39 d, H_b, J_{HH} 3.27Hz
7.049 dd, 2H	7.42 m, H_b	7.18 m, $H_{a'}$
J_{HH} 3.88Hz	7.13 m, H_a	7.11 m, $H_{a'}$
J_{HH} 4.92 Hz	7.08 m, H_b	7.08 m, $H_{b'}$
	6.97 m, H_b	6.92 m, $H_{b'}$
	1.68 CH_2	6.55 d, br, Pt-sat.$H_{a'}$
	1.10 CH_3	J_{HH} 3.27 Hz
	-7.300 t, Pt-sat, PtH	J_{Pt-H} 27.4 Hz
	$^2J_{P-H}$ 17.4Hz	1.96 CH_2
	$^1J_{Pt-H}$ 713 Hz	1.17 CH_3
	^{31}P{^{1}H} NMR δ / ppm	
	18.66 s, Pt-sat, $^1J_{Pt-P}$ 2674 Hz	11.36 d, Pt-sat, $^1J_{Pt-P}$ 3145 Hz, $^2J_{P-P}$ 22.9 Hz (*trans* to S)
		0.50 d, Pt-sat, $^1J_{Pt-H}$ 1676 Hz, $^2J_{P-P}$ 22.9 Hz (*trans* to C)

When a mixture of two equivalents of 2,2′-thiophene and one equivalent of $[Pt(PEt_3)_4]$ is heated for 20 hours in refluxing toluene, a mixture of approximately 1: 1.3 of **3-2a** / **3-2b** was obtained. When the same mixture was refluxed for 72 hours, **3-2b** was still obtained, but the ^{31}P{^{1}H} NMR resonance signal at -18.67 ppm decreased significantly in intensity, and broadening of the peak occurred. A new doublet resonance appeared at 18.24 ppm ($^1J_{Pt-H}$ 2277 Hz, $^2J_{P-P}$ 19.1 Hz) Similarly, the hydride region of the ^{1}H NMR spectrum showed that the hydride resonance had changed in appearance from a triplet (with accompanying satellites) to

a broadened resonance at -7.325 ppm, still flanked by satellites ($^1J_{Pt-H}$ 713 Hz). The NMR resonances of **3-2b** were unchanged.

The molecular ion of m/z = 597 observed in the mass spectrum was consistent with the formula for **3-2a** / **3-2b** (Table 3.8).

3.2.3 Reaction of $[Pt(PEt_3)_4]$ with 1-methyl-2-(2-thienyl)pyrrole, L3

The ligand, 1-methyl-2-(2-thienyl)pyrrole **L3**, was prepared via a palladium-catalysed cross-coupling reaction of 2-metallated 1-methylpyrrole and 2-bromothiophene (Scheme 3.2) [27]. The resulting oil, **L3**, was purified by distillation and kept under argon before use. The compound does not store well and decomposes over time. It is also decomposed by column chromatography on silica gel.

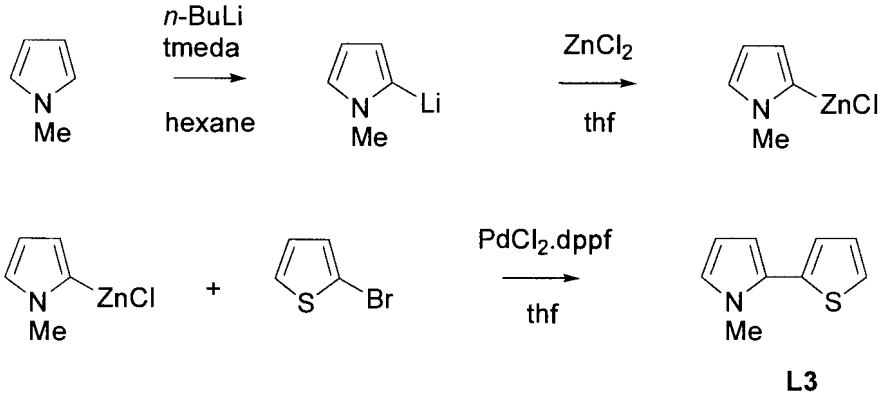

Scheme 3.2 Synthetic route for 1-methyl-2-(2-thienyl)pyrrole

The reaction of **L3** with tetrakis(triethyl)phosphineplatinum(0) yielded a mixture of two products. These products could not be separated without causing decomposition thereof. Interpretation of the NMR spectra led to the identification of the two products as a *trans*-diphosphine platinum(II) hydride complex **3-3a** and a thiaplatinacycle **3-3b**.

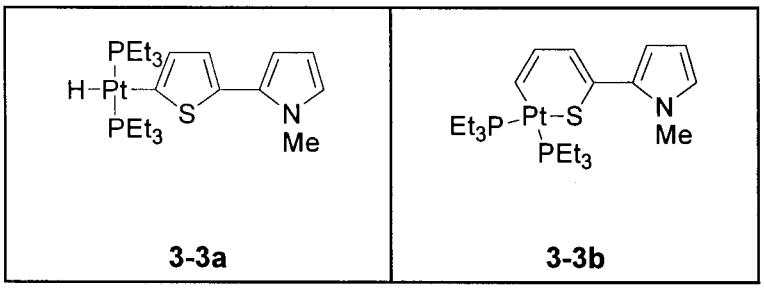

3-3a **3-3b**

Both compounds have the same molecular formula and hence the same molar mass. FAB-MS analysis of the mixture identified the molecular ion and the observed accurate mass was found to be 594.1928 (calculated mass = 594.1926) (Table 3.8).

Evidence for **3-3a** was provided by the high-field region of the ^{1}H NMR spectrum (Table 3.7). A triplet pattern, with accompanying ^{195}Pt satellites, due to a hydride proton, appeared at -7.241 ppm. This hydride proton is coupled to two equivalent phosphine groups ($^{2}J_{P\text{-}H}$ = 17.5 Hz) and to the platinum centre ($^{1}J_{Pt\text{-}H}$ = 713 Hz). The two equivalent phosphorus atoms resonate at 18.71 ppm in the $^{31}P\{^{1}H\}$ NMR spectrum with a $^{1}J_{Pt\text{-}P}$ coupling of 2680 Hz. These chemical shifts and coupling constants are almost identical to that of **3-2a** and therefore support the hydride structure **3-3a**.

In addition to the resonance at 18.71 ppm (arising from **3-3a**), two other resonance patterns were observed in the $^{31}P\{^{1}H\}$ NMR spectrum. The two doublet patterns at 10.32 ppm (P_a *trans* to S, $^{2}J_{Pa\text{-}Pb}$ = 22.9 Hz, $^{1}J_{Pt\text{-}Pa}$ = 3094 Hz) and 0.93 ppm (P_b *trans* to C, $^{2}J_{Pa\text{-}Pb}$ = 23.9 Hz, $^{1}J_{Pt\text{-}Pb}$ = 1671 Hz) are reminiscent of the $^{31}P\{^{1}H\}$ NMR spectrum.for **3-1**, and **3-2b**. This data thus provides evidence for the presence of **3-3b**.

Table 3.7 NMR data for **L3** and **3-3a / 3b** (in $CDCl_3$)

L3 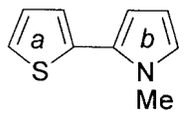	**3-3a** 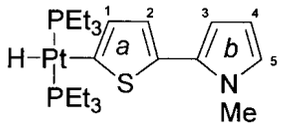	**3-3b** 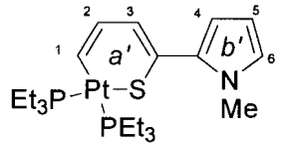
^{1}H NMR δ / ppm		
7.244 dd, CH_a $^3J_{HH}$ 5.1 Hz, $^4J_{HH}$ 1.3 Hz 7.051 m, CH_a 7.010 dd, CH_a $^3J_{HH}$ 3.6 Hz, $^4J_{HH}$ 1.3 Hz 6.687 t, CH_b $^3J_{HH}$ 2.3 Hz 6.316 dd, CH_b $^4J_{HH}$ 3.6 Hz, $^3J_{HH}$ 1.8 Hz 6.512 dd, CH_b $^4J_{HH}$ = 3.6 3.703 Me	6.733 m, H_a1 6.979 m, H_a2 6.659 m, H_b3 6.113 m, H_b4 6.271 dd, H_b5, $^3J_{HH}$ 3.2 Hz, $^4J_{HH}$ 1.9 Hz 3.711 s, Me 1.67 m, PCH_2 1.05 m, PCH_2CH_3 -7.241 t, Pt-sat., PtH, $^2J_{P\text{-}H}$ 17.5 Hz, $^1J_{Pt\text{-}H}$ 713 Hz	6.594 m, Pt-sat. obscured by overlapping peaks, $H_{a'}$ 7.034 m, $H_{a'}$ 7.214 dd, $H_{a'}$ 6.56-6.54 m, $H_{b'}$ 6.18 m, $H_{b'}$ 6.08-6.03 m, $H_{b'}$ 3.673 s, Me 1.92 m, PCH_2 1.10 m, PCH_2CH_3
	$^{31}P\{^1H\}$ NMR δ / ppm	
	18.71 s with Pt-sat., $^1J_{Pt\text{-}P}$ 2680 Hz	10.32 d with Pt-sat., P_a *trans* to S $^2J_{Pa\text{-}Pb}$ 22.9 Hz $^1J_{Pt\text{-}Pa}$ 3094 Hz 0.93 d with Pt-sat., P_b *trans* to C $^2J_{Pa\text{-}Pb}$ 23.9 Hz, $^1J_{Pt\text{-}Pb}$ 1671 Hz

Surprisingly, the C(2)-C(2') insertion product, **3-3c**, was not obtained; a second singlet resonance with attendant ^{195}Pt satellites due to equivalent phosphines was not detected in the ^{31}P NMR spectrum.

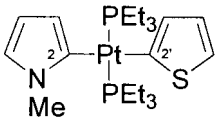

3-3c

Although C-H activation is generally easier to achieve than C-C oxidative insertion, the C(2)-C(2') bond in 1-methyl-2-(2-thienyl)pyrrole has been found to readily labilized when attempting to obtain chromium, molybenum and tungsten carbene derivatives of 1-methyl-2-(2-thienyl)pyrrole [28]. The molecule underwent C-C bond scission with two to three equivalents of *n*-butyllithium to form two separate carbene complexes (2-butylthienyl and 1-methylpyrrolyl derivatives).

3.2.4 Reactions of $[Pt(PPh_3)_3]$

Unlike $[Pt(PEt_3)_4]$, the less nucleophilic tris(tripheylphosphine)platinum(0) complex does not react with 3,6-dimethylthieno-[3,2-*b*]thiophene **L1**, or with thiophene, despite prolonged reluxing. A mixture of orange-red and orange crystals were isolated from the mixtures. These crystals were formed by the thermal decomposition of tris(triphenylphosphine)platinum(0). Benzene solutions of $[Pt(PPh_3)_3]$ are known to undergo thermal P-C bond cleavage of the coordinated phosphine to yield the orange-red complex, $[Pt_2(\mu\text{-}PPh_2)(PPh_3)]$ and the orange complex, $[Pt_3(\mu\text{-}PPh_2)_3(Ph)(PPh_3)_2]\cdot C_6H_6$ [29]. In toluene, thermal degradation leads to the formation of a similar dinuclear species, $[Pt_2(\mu\text{-}PPh_2\text{-}\{\mu\text{-}C_6H_4(PPh_2)\text{-}2\}(PPh_3)_2]$ as well as the same unsolvated trinuclear species [30].

Swiegart *et. al.* was able to achieve C-S activation with $[Pt(PPh_3)_3]$ by using the π-bonded benzothiophene, $[(\eta^6\text{-}C_8H_6S)Mn(CO)_3^+]$ [31]. Insertion of $Pt(PPh_3)_2$ occurred at the C(vinyl)-S

bond, whereas $Mn(CO)_4$ inserts into the C(aryl)-S bond [12].

3.2.5 Mass spectrometry

The mass spectrometry results for **3-1**, **3-2** and **3-3** are summarised in Table 3.8. The latter complex was analysed using a fast-atom bombardment mass spectrometer, rather than an electron impact mass spectrometer. The fragmentation pattern in both cases involved the loss of successive ethyl fragments.

Table 3.8 Mass peaks m/z (% Intensity) [Fragment]

3-1 EI-MS $C_{20}H_{38}P_2S_2Pt$	**3-2** EI-MS $C_{20}H_{36}P_2S_2Pt$
599 (48)[M^+]	597 (2)[M^+]
431 (76) [M^+ - $S_2C_8H_8$] *ie* [$Pt(PEt_3)_2$]$^+$	431 (2)[M^+ - $S_2C_8H_6$] *ie* [$Pt(PEt_3)_2$]$^+$
402 (76) [M^+ - $S_2C_8H_8$ - Et]	402 (3) [$Pt(PEt_3)_2^+$ - Et]
374 (87) [M^+ - $S_2C_8H_8$ - 2Et]	375 (3) [$Pt(PEt_3)_2^+$ - 2 Et]
168 (100) [$S_2C_8H_8^+$]	348 (1) [$Pt(PEt_3)_2^+$ - 3 Et]
118 (34) [[PEt_3]$^+$	166 (100) [$S_2C_8H_6^+$]

3-3 FAB-MS $C_{21}H_{39}NP_2S_2Pt$	
594 (17) [M^+]	164 (11) [C_9H_9NSH]$^+$
537 (18) [M^+ - Et - C_2H_4]	163 (7) [C_9H_9NS]$^+$
476 (5) [M^+- PEt_3]	135 (100) [$HOPEt_3$]$^+$
431 (30) [M^+- C_9H_9NS] *ie* [$Pt(PEt_3)_2$]$^+$	119 (20) [$HPEt_3$]$^+$
402 (19) [$Pt(PEt_3)_2$ - Et]$^+$	Accurate mass (calculated)
375 (16) [$Pt(PEt_3)_2$ - 2 C_2H_4]$^+$	594.1926
347 (10) [$Pt(PEt_3)_2$ - Et - C_2H_3 - C_2H_4]$^+$	Accurate mass (observed) 594.1928

3.3 CONCLUSIONS

The reaction of the thienothiophene, **L1**, with [$Pt(PEt_3)_4$] yielded a thiaplatinacycle, **3-1**, via an oxidative insertion into a C(vinyl)-S bond. The structure of **3-1** was confirmed by single crystal X-ray diffraction studies. While the thiophene-containing molecules 2,2′-bithiophene and 1-methyl-2-(2-thienyl)pyrrole both formed analogous thiaplatinacycles, **3-2b** and **3-3b**, as deduced from NMR spectra, these molecules also underwent C-H activation to generate *trans*-$PtH(PEt_3)_2$ type complexes (**3-2a** and **3-3a**). In the case of 1-methyl-2-(2-thienyl)pyrrole it was concluded that the site of C-H activation was at the thienyl rather than the 1-methylpyrrolyl ring. (Refer to Chapter 4 for C-H activation of 1-methylpyrrole.)

3.4 REFERENCES

[1] P.T. Anastas and J.C. Warner in *Green Chemistry: Theory and Practice*, Oxford University Press, New York, **1998**, p. 30

[2] R.J. Angelici in *Encyclopedia of Inorganic Chemistry*, ed. R.B. King, Vol. 3, 1994, p 1433

[3] T. Halpert, A. Anderson and G. Markeley; *Proc. World Petr. Congr.*, **1997**, 15

[4] B.C. Gates and H. Topsøe; *Polyhedron*, **1997**, *16*, 3213-3217

[5] D.J. Monticello; *Chemtech*, **1998**, *28*, 38-45

[6] J.W. Benson, G.L. Shrader, R.J. Angelici; *J. Molec. Cat. A: Chem.*; **1995**, *96*, 283-299

[7] (a) T.E. Caldwell and D.P. Land; *Polyhedron*, **1997**, *16*, 3197-3211 (b) C.M. Friend and D.A. Chen; *Polyhedron*, **1997**, *16*, 3165-3175

[8] (a) C. Bianchini, J.A. Casares, A. Meli, V. Sernau, F. Vizza, and R.A. Sanchez-Delgado; *Polyhedron*, **1997**, *16*, 3099-3114 (b) W.D. Jones, D.A. Vicic, R.M. Chin, J.H. Roache and A.W. Myers; *Polyhedron*, **1997**, *16*, 3115-3128

[9] (a) R.J. Angelici; *Coord. Chem. Rev.*, **1990**, *105*, 61-76 (b) M.-G. Choi and R.J. Angelici; *Organometallics*, **1992**, *11*, 3328-3334 (c) M.L. Spera and W.D. Harman; *Organometallics*, **1995**, *14*, 1559-1561 (d) J. Chen and R.J. Angelici; *Organometallics*, **1989**, *8*, 2277-2279 (e) J.R. Lockemeyer, T.B. Rauchfuss, A.L. Rheingold and S.R. Wilson; *J. Am. Chem. Soc.*, **1989**, *111*, 8828-8834 (f) M.-G. Choi and R.J. Angelici; *J. Am. Chem. Soc.*, **1989**, *111*, 8753-8754 (g) J. Chen and R.J. Angelici; *Organometallics*, **1990**, *9*, 879-880

[10] R.J. Angelici; *Polyhedron*, **1997**, *16*, 3073-3088

[11] (a) J.J. Garcia, B.E. Mann, H. Adams, N.A. Bailey and P.M. Maitlis; *J. Am. Chem. Soc.*, **1995**, *117*, 2179-2186 (b) J.J. Garcia, A. Arevalo, S. Capella, A. Chehata, M. Hernandez, V. Montiel, G. Picazo, F. Del Rio, R.A. Toscano, H. Adams and P.M. Maitlis; *Polyhedron*, **1997**, *16*, 3185-3195 (c) A. Iretskii, H. Adams, J.J. Garcia, G. Picazo and P.M. Maitlis; *Chem. Commun.*, **1998**, 61-62 (d) A. Arévalo, S. Bernès, J.J. Garcia and P.M. Maitlis; *Organometallics*, **1999**, *18*, 1680-1685

[12] C.A. Dullaghan, S. Sun, G.B. Carpenter, B. Weldon and D.A. Sweigart; *Angew. Chem. Int. Ed.*, **1996**, *35*, 212-214

[13] I.E. Buys, L.D. Field, T.W. Hambley and A.E.D. McQueen, *J. Chem. Soc., Chem. Commun.*, **1994**, 557-558

[14] K.S. Choi, K. Sawada, H. Dong, M. Hoshino and J. Nakayama; *Heterocycles*, **1994**, *38*, 143-148

[15] (a) T.G. Appleton, H.C. Clark and L.E. Manzer; *Coord. Chem. Rev.*, **1973**, *10*, 335-422 (b) G.N. Glavee, L.M. Daniels and R.J. Angelici; *Organometallics*, **1989**, *8*, 1856-1865

[16] N.N. Greenwood and A. Earnshaw in *Chemistry of the Elements*, Pergamon Press, **1984**, p567

[17] J. Chen, L.M. Daniels and R.J. Angelici; *J. Am. Chem. Soc.*, **1990**, *112*, 199-204

[18] J.R. Bleeke; *Chem. Rev.*, **2001**, *101*,

[19] (a) J.R. Bleeke and J.M.B. Blanchard; *J. Am. Chem. Soc.*, **1997**, *119*, 5443-5444 (b) J.R. Bleeke, J.M.B. Blanchard and E. Donnay; *Organometallics*, **2001**, *20*, 324-336

[20] K.J. Weller, I. Filippov, P.M. Briggs and D.E. Wigley; *Organometallics*, **1998**, *17*, 322-329

[21] V. Jacob, T.J.R. Weakley and M.M. Haley; *Angew. Chem. Int. Ed.*, **2002**, *41*, 3470-3172

[22] (a) S.-W. Lai, M.C.-W. Chan, K.-K. Cheung and C.-M. Che; *Organometallics*, **1999**, *18*, 3327-3336 (b) S.-W. Zhang, R. Ishii, F. Motoori, T. Tanaka, Y. Takai, M. Sawada and S. Takahashi; *Inorg. Chim. Acta*, **1997**, *265*, 75-82 (c) R.-Z. Ku, J.-C. Huang, J.-Y. Cho, F.-M. Kiang, K.R. Reddy, Y.-C. Chen, K.J. Lee, J.H. Lee, G.-H. Lee, S.-M. Peng and S.-T. Liu; *Organometallics*, **1999**, *18*, 2145-21464 (d) M.E. Cucciolito, A. Panunzi, F. Ruffo, V.G. Albano and M. Monari; *Organometallics*, **1999**, *18*, 3482-3489 (e) S.-W. Zhang and S. Takahashi; *Organometallics*, **1998**, *17*, 4757-4759 (f) L.M. Redina, J.J. Vittal and R.J. Puddephatt; *Organometallics*, **1995**, *14*, 1030-1038

[23] V.G. Albano, G. Natile and A. Panunzi; *Coord. Chem. Rev.*, **1994**, *133*, 67

[24] T. Eicher and S. Hauptmann in *The Chemistry of Heterocycles*, Georg Tieme Verlag, Stuttgart, 1995, pp 52-218

[25] S. Kotani, K. Shiina and K. Sonogashira; *J. Organomet. Chem.*, **1992**, *429*, 403-416

[26] K. Onitsuka, K. Murakami, K. Matsukawa, K. Sonogashira, T. Adachi and T. Yoshida; *J. Organomet. Chem.*, **1995**, *490*, 117-123

[27] L. Brandsma, S.F. Vasilevsky and H.D. Verkruijsse in *Applications of Transition Metal Catalysts in Organic Synthesis*, Springer-Verlag, Berlin, 1998, p 264

[28] C. Crause and S. Lotz; unpublished results

[29] N.J. Taylor, P.C. Chieh and A.J. Carty; *J. Chem. Soc. Chem. Commun.*, **1975**, 448

[30] M.A. Bennett, D.E. Berry, T. Dirnberger, D.C.R. Hockless and E. Wenger; *J. Chem. Soc., Dalton Trans.*, **1998**, 2367-2371

[31] C.A. Dullaghan, X. Zhang, D.L. Greene, G.B. Carpenter, D.A. Sweigart, C. Camiletti and E. Rajaseelan; *Organometallics*; **1998**, *17*, 3316-3322

/ End of Chapter 3 //

CHAPTER 4

Reactions of Pt(0) with five-membered *N*-Heteroaromatic Compounds

4.1 INTRODUCTION

The activation of C-S bonds is a key step in the removal of sulfur (hydrodesulfurisation, HDS [1]) from oil and petroleum feedstocks. The homogeneous chemistry of various transition-metals with thiophene and thiophene-like molecules has been extensively studied [2] in order to gain understanding into the role of the metal in heterogeneous desulfurisation catalysts. Increasing interest is being focussed on the hydrodenitrogenation, HDN, process [3], which results in the removal of nitrogen from oil and petroleum feedstocks in the form of ammonia. This process is essential in reducing NO_x emissions from coal-derived fuel and while the commercial importance cannot be underestimated, the actual mechanisms of metal-catalysed hydrodenitrogenation is poorly understood. The nitrogen-containing contaminants in fuelstocks are aromatic heterocyles (mainly the pyridine and pyrrole derivatives of quinoline and indole respectively) and aliphatic amines and anilines. The latter, nonheterocyclic compounds undergo hydrodenitrogenation rapidly, while the heterocyclic compounds are more problematic. Studies on hydrodenitrogenation have focussed mainly on heterogeneous catalysts [4]. The product distribution, kinetics and selectivity of $NiMoP/Al_2O_3$ and $NiMoP/Al_2O_3$

catalysts with aniline, quinoline and decahydroquinoline have also been modelled [5]. It is understood that the removal of nitrogen from aromatic nitrogen-containing compounds occurs via the hydrogenation of the aromatic rings, C-N bond cleavage and ring opening, elimination of ammonia and olefin hydrogenation. Few studies of the heterogeneous catalysts look at the binding mode of the metal to the nitrogen heterocycle, although there is evidence that seems to indicate that this may play an important role in C-N bond cleavage. Just as studies of metal coordination to thiophene-like substrates has led to a better understanding of the activation of thiophene in dehydrosulfurisation, we hope to similarly expand on the knowledge of the coordination of the metal to nitrogen substrates in homogeneous solution.

The chemistry of pyridine with a variety of metals has been widely investigated. A metal centre can attach to a six-membered pyridine ring in various ways. The following modes of coordination have been identified: $\eta^1(N)$ [6], η^6 (π-N) [7], η^2 (N,C) [8], η^2 (C,C) [9] and μ-η^1 (N) [10].

Figure 4.1. Bonding modes of pyridine

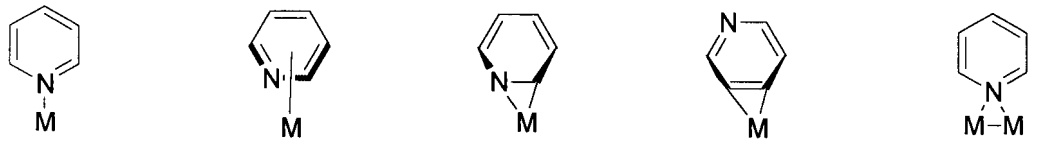

$\eta^1(N)$ $\eta^6(\pi\text{-}N)$ $\eta^2(N,C)$ $\eta^2(C,C)$ $\mu\text{-}\eta^1(N)$

Examples

[Ru(PCP){η^1(*N*),η^1(*N'*)η^1(*N''*)-terpy}]Cl where PCP = P,C,P terdentate "pincer" ligand 2,6-$(CH_2PPh_2)_2C_6H_3^-$ and terpy = 2,2':6',2''-terpyridine [6b]

[Ir(H){η^1(*N*)-thpy}(CO)(PPh_3)]PF_6 where thpy =2-(2'-thienyl)pyridine [6c]

[Cr(η^6-2,6-dimethylpyridine)$_2$]BF_4 [7]

[Ta{η^2-(*N,C*)- NC_5H_5}(silox)$_3$] where silox = OSi^tBu_3 [8]

[Os{η^2-(*C,C*)-lutidine}$(NH_3)_5$] where lutidine = 2,3-dimethylpyridine [9]

[Mo_2O_2{$S_2P(O^iPr)_2$}$_2$(μ-O){μ-η^1(*N*)-NC_5H_5}] [10]

Many examples of $\eta^1(N)$ type complexes with various transition metals, including platinum, have been characterised [11]. The synthesis [12], reactivity [13], spectroelectrochemical [14] and dynamic NMR properties [15] of platinum(II) complexes of pyridine have been reported.

The coordination of transition metals to pyrrole occurs mainly via π-bonding [16] of the η^5-pyrrolyl ligand [17] and less commonly via the neutral η^5-pyrrole ligand [18]. The pyrrolyl anion can also be σ-bonded as $\eta^1(N)$ [19], $\eta^1(C\text{-}2)$ [20] or $\eta^1(C\text{-}3)$ [21].

Figure 4.2. Bonding modes of pyrrole

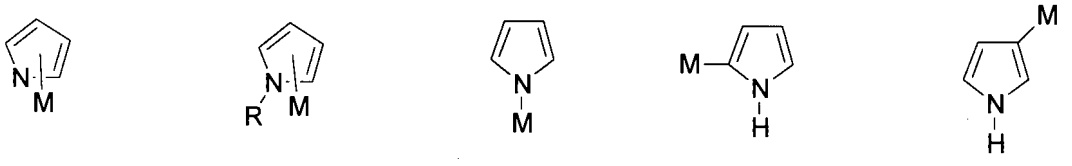

η^5-pyrrolyl η^5-pyrrole $\eta^1(N)$ $\eta^1(C\text{-}2)$ $\eta^1(C\text{-}3)$

Examples

$[Re(\eta^5\text{-}NC_4H_4)(H)(I)(PPh_3)_2]$	[17a]
$[Ru(\eta^5\text{-}NC_4H_4)Cl(PPh_3)_2]$	[17b]
$[M\ (\eta^5\text{-}MeNC_4Me_4)(\eta^6\text{-cymene})](OTf)_2$ where M = Ru, Os and cymene = 1-methyl-2-isopropylbenzene	[18a] (sandwich compound)
$[Re(\eta^5\text{-}MeNC_4H_4)H_2(PPh_3)_2]^+$	[18b] (sandwich compound)
$[Pd(\eta^1\text{-}NC_4H_4)_2(PPh_3)_2]$	[19a]
$[M(\eta^5\text{-}C_5H_5)_2(\eta^1\text{-}NC_4H_4)_2]$ where M = Ti, Zr	[19b]
$[M\{\eta^1(C\text{-}2)\text{-}C_4H_3N\}Cl(CO)_2(PPh_3)_2]$ where M = Ru, Os	[20a]
$[Hg\{\eta^1(C\text{-}2)\text{-}C_4H_3N(O)Me\}Cl]$	[20c]
$[Hg\{\eta^1(C\text{-}3)C_4H_3NSi^iPr_3\}Cl]$	[21]

This chapter focusses on the five-membered, nitrogen-containing, heteroaromatic molecules (1-methylpyrrole, 1*H*-pyrrole (pyrrole), indole, imidazole, pyrazole, and their annelated counterparts indole, benzimidazole and indazole) and their reactions with platinum(0).

Table 4.1 The nitrogen-containing heteroaromatic ligands investigated

1-methylpyrrole 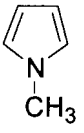	
pyrrole 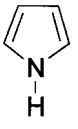	indole 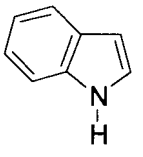
imidazole 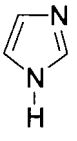	benzimidazole 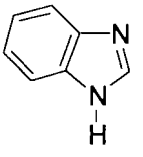
pyrazole 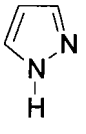	indazole 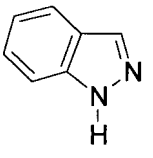

4.2 RESULTS AND DISCUSSION

In all cases, except for pyrrole and 1-methylpyrrole, complexes of the type *trans*-[PtH(*N*-heterocycle)(PEt_3)$_2$] were isolated. Under mild conditions the Pt(PEt_3)$_2$ moiety inserts into an N-H bond of the heterocycle and the oxidative insertion reaction is complete within minutes at room temperature. The resultant platinum(II) hydride complexes were characterised using NMR spectroscopy and mass spectrometry. Insertion into an N-C bond to form a metallacycle did not occur; this is in contrast to the thiaplatinacyles obtained with the analogous aromatic

five-membered sulfur heterocycles[1]. Neither was a heterocyclic C-H bond activation achieved, in contrast to the hydrides obtained with furan, thiazole- and oxazole-type molecules[2] (Figure 4.3).

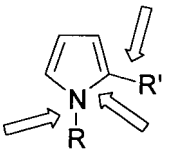

R = H, alkyl
R' = H

Figure 4.3 Potential sites for insertions of a $Pt(PR_3)_2$ moiety (R = alkyl)

As far as we know, only one example of a C-N bond activation is reported in the literature [22]. The reaction of $[Ir(\eta^5\text{-}C_5Me_5)Cl_2]$ with $[MgC_4H_6.2thf]$ at low temperature produces a mixture of $[Ir(\eta^5\text{-}C_5Me_5)(\eta^4\text{-}C_4H_6)]$ and $[Ir(\eta^5\text{-}C_5Me_5)(\eta^3\text{-}C_4H_7)R]$. The latter compound arises from C-H activation of solvent molecules, RH (RH = benzene, toluene, anisole, thiophene, furan and 1-methylpyrrole, pentane, cyclohexane, thf). In the case of pyrrole, C-N activation is reported to occur [22].

Although the activation of C-H bonds by low-valent transition metal complexes has been well studied [23], much less attention has been given to N-H bond activation. Several hydridoamido complexes [24] of the platinum group metals have been prepared and characterised, but the synthesis of these complexes follows various routes that generally do not involve the oxidative insertion of a metal centre into an N-H bond. For instance, platinum(II) hydridoamido complexes can be prepared by a ligand replacement reaction of a *trans*-hydrido(nitrato)-bis(triethylphosphine)platinum(II) complex [25]. The reaction of the cationic ammine complexes of the type *trans*-$[PtH(NH_3)(PR_3)_2]ClO_4$ with an amide ion gives rise to *trans*-

[1] Refer to Chapter 3

[2] Refer to Chapter 5

$[PtH(NH_2)(PR_3)_2]$, where R = Ph, Et or Cy [26].

A reduction reaction of *cis*-dichlorobis(triphenylphosphine)platinum(II) and 5-substituted tetrazoles in the presence of hydrazine results in the formation of *trans*-hydrido(tetrazolato)bis(triphenylphosphine)platinum(II) complexes, both *N*-(1)- and *N*-(2)-bonded (Figure 4.4) [27].

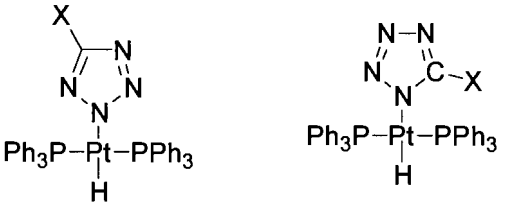

N-(2)-bonded N-(1)-bonded

X = Br, Cl, Ph

Figure 4.4 *trans*-hydrido(tetrazolato)bis(triphenylphosphine)platinum(II) complexes [27]

The intramolecular oxidative addition of an N-H bond to rhodium(I) and iridium(I) has been reported [28], but a chelating ligand was required to facilitate this oxidative addition [29]. Merola *et. al.* were later able to achieve heterocyclic amine N-H activation by reacting $[Ir(cod)(PMe_3)_3]Cl$ with pyrrole, indole, 3-methylindole and azaindole to yield octahedral iridium(III) hydrides [30]. In 1988, Milstein and co-workers were able to oxidatively insert an iridium(I) moiety into the N-H bond of aniline [31]. The stable *cis* hydride complex so generated was able to catalyse the amination of norbornylene, the first example of the amination of an olefin by a transition metal catalysed N-H activation. The platinum(II) and palladium(II) analogues could not be obtained. Indeed, only a couple of examples of N-H bond activation for aromatic heterocycles by platinum(0) have been reported in the literature [32, 33].

4.2.1 Reaction of $[Pt(PEt_3)_4]$ with 1-Methylpyrrole

Despite heating equimolar mixtures of 1-methylpyrrole and $[Pt(PEt_3)_4]$ in toluene for prolonged periods, no oxidative addition product could be isolated. Oxidative addition reactions of $[Pt(PEt_3)_4]$ are usually accompanied by a marked colour change (decolouration) of the solution, but no visual indication could be observed that a reaction had taken place to any appreciable extent. After a week of heating the reaction mixture under reflux, the solvent was removed *in vacuo* and the resultant brown residue analysed by NMR spectroscopy in deuterated chloroform.

A very low intensity, complex doublet of doublet of doublet (ddd) pattern was observed on magnification of the high-field region of the ^1H NMR spectrum. This pattern, centred at -5.13 ppm, indicated the presence of a hydride species. Furthermore, the accompanying satellite ddd patterns are indicative of coupling to the ^{195}Pt nucleus. The magnitudes of the observed couplings in the ddd pattern were: 977 Hz (due to ^{195}Pt-H coupling), 158 Hz, 24.8 Hz and 11.6 Hz. Since a hydrido *trans*-diphosphine species would give rise to a triplet resonance pattern (coupling of the hydride proton to two identical phosphorus atoms), the ddd pattern was tentatively identified as a *cis*-diphosphine platinum hydride.

The $^{31}P\{^1H\}$ NMR spectrum supported the argument for a *cis* isomer. Two doublets at 11.2 ppm and 0.21 ppm, each with satellites, corresponding to two nonequivalent phosphorus atoms were observed. The one-bond ^{135}Pt - ^{31}P coupling constants of 3887 Hz and 2996 Hz for the respective phosphine atoms are consistent with *cis*-phosphine couplings, where a value larger than 3000 Hz is generally observed, depending on the ligand *trans* to the phosphine. *Trans*-phosphines typically give coupling constants 1.5 times smaller than for the *cis*-analogues [34]. The $^2J_{P-P}$ coupling constant of 22 Hz is typical of a *cis*-phosphine coupling [35].

Since a *cis*-hydridobisphosphineplatinum(II) complex is expected to give rise to a simpler

doublet of doublet signal, rather than the observed ddd pattern, we turned to the literature in search of *cis*-hydrides with which comparisons could be made. The majority of complexes of the type $[Pt(H)(X)(PR_3)_2]$ (where X represents an anionic ligand) have the monodentate phosphine ligands mutually *trans* to each other [36]. When X is a halide, the complexes have the expected *trans* configuration [37a]. Interestingly, where X is thiocyanate it is *N*-bonded rather than *S*-bonded as the *trans* influence of the hydride proton favours more ionic bonding [37b]. A chelating phosphine ligand is usually required to obtain a mutually *cis* stereochemistry for the hydride and the anionic ligand X; an example is [PtHCl(dppe)] [37a].

Dihydridodi(phosphine)platinum(II) complexes, $[Pt(H)_2(PR_3)_2]$, also have a preference for the phosphines to adopt a *trans* geometry. Various theoretical studies have been done to calculate the relative stabilities of *cis* and *trans* platinum dihydrides [38]. A hydride has a strong *trans* influence and would thus prefer to be *cis* [39]. Calculations show that the *trans* isomer is only slightly more thermodynamically stable than the *cis* isomer, and that the preference for the *trans* geometry is probably a steric effect. Space-filling CPK models suggests that even with the relatively small trimethylphosphine, *cis*-$[Pt(H)_2(PMe_3)_2]$ is sterically crowded [40].

The only examples of *cis*-monohydride that could be found in the literature were silyl derivatives; *cis*-$[Pt(H)(SiEt_3)(PEt_3)_2]$ [41a] and *cis*-$[Pt(H)(SiH_2Ar)(PPh_3)_2)]$ were Ar = pentaphenylphenyl and 2,4,6-tris(trifluoromethyl)phenyl [41b]. Based on the coupling constants obtained for these complexes, as well as comparing it to the NMR data of *cis*-$[PtH_2(PMe_3)_2]$, the assignments were made as follows (Table 4.2):

A $J_{P\text{-}H}$ coupling constant of approximately 20 Hz is typical of a *cis* $M(PR_3)H$ arrangement [42]. It should be noted that there is a large difference in the $^2J_{P\text{-}H}$ coupling for the phosphines in the positions *cis* and *trans* to the hydridic proton. The stronger *trans* influence of the hydride leads to a weakening of the Pt-P *trans* to itself relative to the Pt-P in the *cis* position. This is manifested in a noticeably larger coupling constant for the P-atom *trans* to the hydride proton [43]. In general, the $^2J_{P\text{-}P}$ coupling for two *trans*-phosphines is smaller than for *cis* coupling of

the phosphorus atoms.

Table 4.2 NMR data for selected *cis*-$[Pt(H)(X)(PR_3)_2]$ complexes

High-field ^1H NMR data			
	cis-$[Pt(H)(SiEt_3)(PEt_3)_2]$ in C_6D_6 [41a]	*cis*-$[Pt(H)(X)(PEt_3)_2]$ X = $CH_3NC_4H_3$ in $CDCl_3$ **4-1**	*cis*-$[PtH_2(PMe_3)_2]$ in acetone-d_6 [40]
PtH δ / ppm	-2.29, dd	-5.13, ddd	-3.7, dd
$^2J_{Pa-H}$ (P_a *cis* to H)	23 Hz	24.6 Hz	24 Hz
$^2J_{Pb-H}$ (P_b *trans* to H)	154 Hz	158 Hz	179 Hz
$^1J_{Pt-H}$	942 Hz	977 Hz	1028 Hz
$^4J_{HH}$		11.6 Hz	
^{31}P NMR data			
δ / ppm			
P_a (*cis* to H)	22.8 d	0.21 d	-20.0, s
$^2J_{P-P}$	16.4 Hz	22 Hz	-
$^1J_{Pt-P}$	1432 Hz	2996 Hz	1875 Hz
δ / ppm	19.1	11.2, d	-20.0, s
P_b (*trans* to H)			
$^2J_{P-P}$	16.4 Hz	22 Hz	-
$^1J_{Pt-P}$	2392 Hz	3887 Hz	1875 Hz

Although the high field region of the ^{1}H NMR spectrum and the $^{31}P\{^{1}H\}$ spectrum gives sufficient evidence to reasonably identify the presence of a *cis*-$[Pt(H)(X)(PEt_3)_2]$ complex, some speculation surrounded the identity of the anionic X-ligand. As this compound exists in extremely low concentrations in a mixture containing excess 1-methylpyrrole, the downfield region of the ^{1}H NMR spectrum could not provide meaningful information. However, it is highly likely that the source of the hydride proton is the 1-methylpyrrole ligand, rather than the solvent (toluene), or indeed a triethylphosphine ligand that may arise from dissociation from $[Pt(PEt_3)_4]$. The chemical shift of the hydride proton indicates that the platinum centre is bonded to a carbon atom rather than a nitrogen atom (compare the ^{1}H NMR data in Table 4.11 and Table 5.7 for for N-H and C-H inserted complexes). We propose that the source of the hydridic proton is H-2 of 1-methylpyrrole, where the $Pt(PEt_3)_2$ moiety oxidatively inserts into the (C-2)-(H-2) bond to form *cis*-hydrido(2-{1-methylpyrrolyl})-bis(triethylphosphine)-platinum(II), **4-1**.

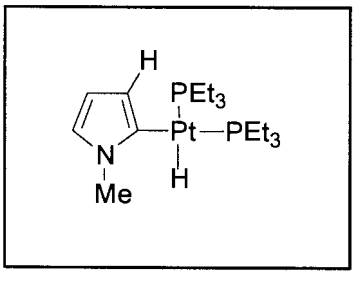

4-1

The C-H activation at position C-2 is highly plausible. Furan, the oxygen analogue of a five-membered, heteroaromatic ring also undergoes C-H activation at C-2 to generate *cis*-hydrido(2-furanyl)bis(triethylphosphine)platinum(II), **5-1**. Both 1-methylpyrrole and furan undergo metallation by *n*-butyllithium and derivatisation reactions at C-2. The heteroatom directs the metallation to the α-position [44]. It has been reported that the reaction of $[Rh(C_5Me_5)(H)Ph(PMe_3)]$ with 1-methylpyrrole leads to C-H activation at the α-position to yield $[Rh(C_5Me_5)(H)(2\text{-}\{1\text{-methylpyrrolyl}\})(PMe_3)]$ [45].

The ddd pattern observed in the ^{1}H NMR spectrum arises from the coupling of the hydride proton to three nonequivalent spin-½ nuclei. Two of these nuclei are the phosphorus atoms *cis*- and *trans*- to the hydride proton. We propose that the third coupled nucleus is the H-3 atom of 1-methylpyrrole. A coupling through the platinum metal centre, and through the double bond as a result of favourable bond angle and dihedral angle arrangement could give rise to the $^4J_{HH}$ coupling of 11.6 Hz.

This hypothesis can be tested by reacting 1,3,4-trimethylpyrrole with $[Pt(PEt_3)_4]$. In the absence of a proton on C-3, a dd rather than a ddd resonance pattern should be obtained. 1,3,4-Trimethylpyrrole is not commercially available, but can be synthesised by the lithiation and subsequent methylation of 3,4-dimethylpyrrole. It has been reported that 3,4-dimethylpyrrole was prepared in an overall yield of 20% by reducing 1-acetyl-3,4-di(carboethoxy)pyrrole [46] with lithium aluminium hydride [47] (Scheme 4.1).

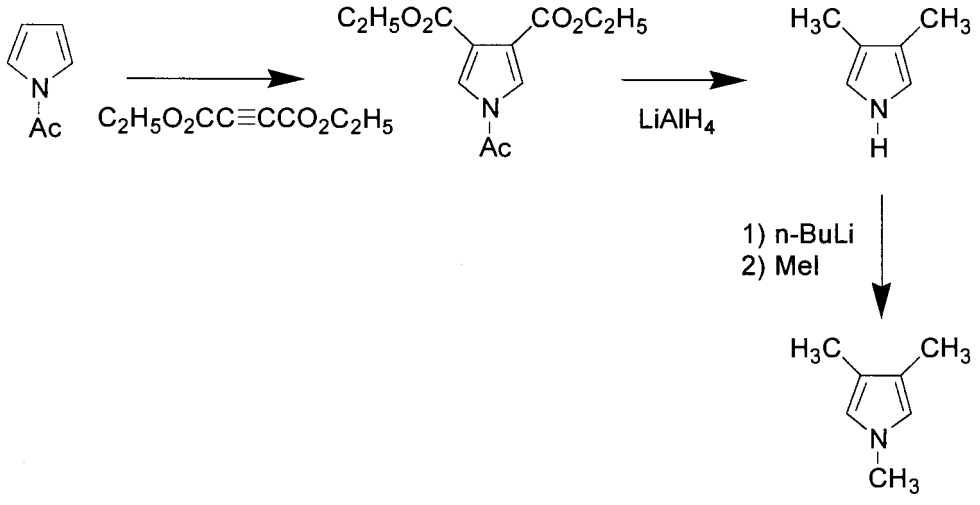

Scheme 4.1 Synthesis of 1,3,4-trimethylpyrrole

Due to time constraints, it was decided that it would not be worthwhile pursuing the option of synthesizing the 1,3,4-trimethylpyrrole with the purpose of testing the $^4J_{HH}$ coupling. The

reported yield is very low and the reaction of the 1,3,4-trimethylpyrrole with platinum(0) would take at least a week in order to obtain a trace amount of the probable *cis*-hydride complex within the reaction mixture.

Isotope labelling experiments could also be insightful. Replacing the proton on C-3 with a deuterium atom should lead to a dd in the high-field ^{1}H NMR spectrum. A pyrrole ring system can be constructed in several ways [48]. These methods generally lead to substituted pyrroles and the substituents have to be modified or degraded depending on the target pyrrole. Deuterium can be introduced at the C-3 position by dilithiation of 3,4-dibromo-1-methylpyrrole, followed by quenching with D_2O (Scheme 4.2). This is based on the assumption that migration to the lithium to the α-positions does not occur.

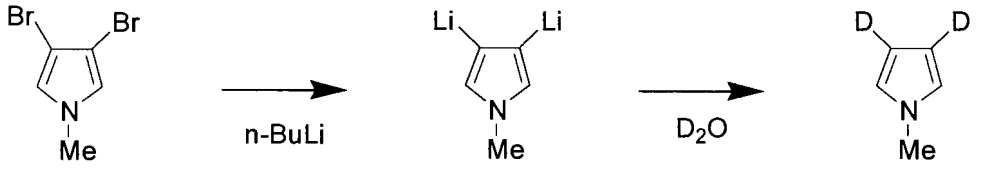

Scheme 4.2 Introduction of deuterium atoms at C-3 and C-4 of 1-methylpyrrole

Since the α-positions C-2 and C-5 are preferentially attacked by electrophilic substitution reagents, the synthesis of 3,4-dibromo-1-methylpyrrole would require an indirect, more challenging solution. It can readily be synthesized by bromination of the commercially available 1-(triisopropyl)silylpyrrole with *N*-bromosuccinimide [49]. Substitution of the silyl group by a methyl group would afford 3,4-dibromo-1-methylpyrrole (Scheme 4.3).

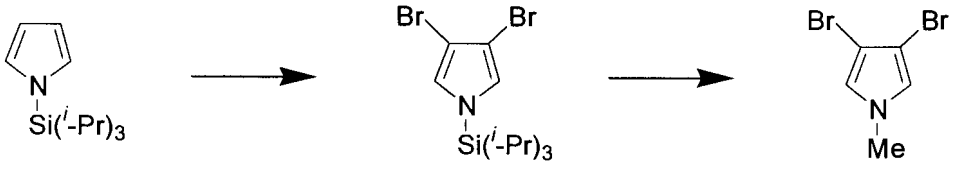

Scheme 4.3 Synthesis of 3,4-dibromo-1-methylpyrrole.

4.2.2 Reaction of $[Pt(PEt_3)_4]$ with Pyrrole

Pyrrole has been used as a ligand for transition metals mainly in the form of tetrapyrroles and porphyrins [50]. The structures of some of these macrocycles is show in Figure 4.5. Indeed, the organometallic chemistry of transition metal porphyrins is a well-developed field of research.

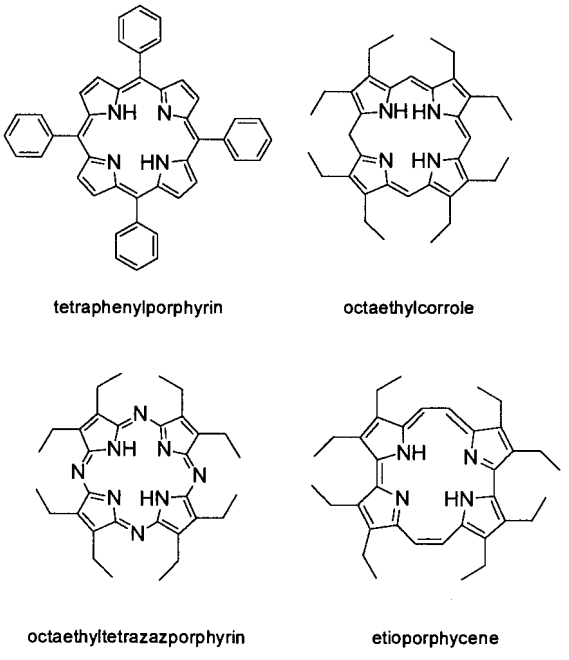

Figure 4.5 Pyrrole macrocycles

As a 'monomer', the bonding modes of pyrrole has been outlined in Figure 4.2.

Pyrrole is a π-excessive molecule; the electron densities on the ring atoms are all greater than in benzene (*i.e.* greater than 1) (Figure 4.6) and pyrrole is thus susceptible to electrophilic substitution whilst being substantially more inert to nucleophilic substitution.

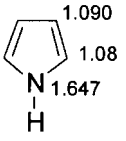

Figure 4.6 π-electron densities on the ring atoms of pyrrole [44]

The aromaticity of pyrrole is less than that of thiophene, but greater than that of furan. Despite having a larger resonance energy than furan, pyrrole generally undergoes electrophilic substitution reactions at a much faster rate than furan.

The hydrogen attached to the nitrogen-atom of pyrrole is weakly acidic with a pK_a of 17.5. This proton is readily removed by strong bases.

Freshly distilled pyrrole and $[Pt(PEt_3)_4]$ were refluxed in toluene for prolonged periods. The reaction was extremely sluggish and samples of the reaction mixture were periodically withdrawn and analysed by NMR spectroscopy in deuterated chloroform. The ^1H and $^{31}P\{^1H\}$ NMR spectra of the reaction mixture showed only partial conversion to the hydride. The ^1H NMR spectrum of the reaction mixture displayed an upfield triplet at -16.285 ppm with ^{195}Pt-satellites. The hydride proton that gives rise to this triplet has $^1J_{Pt-H}$ coupling of 922 Hz, and a $^2J_{Pt-H}$ coupling of 15.7 Hz. A singlet peak at 22.30 ppm, with a ^{31}P-^{135}Pt satellite coupling constant of 2734 Hz, was obtained in the $^{31}P\{^1H\}$ NMR spectrum. Again, this is consistent with a *trans* geometry. Although it was not possible to isolate the small amount of *trans*-hydride from the reaction mixture which contained excess reactants, on the basis of NMR data this compound could be identified as *trans*-hydrido(1-pyrrolyl)bis(triethylphosphine)-platinum(II), **4.2**.

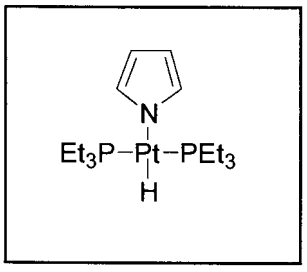

4-2

In addition to the hydride triplet resonance, a lower intensity doublet of doublet of doublets pattern was also observed at -5.108 ppm with $^{2}J_{Pa-H}$ (P_a *cis* to H) = 24.1 Hz, $^{2}J_{Pb-H}$ (P_b *trans* to H) = 159 Hz, $^{1}J_{Pt-H}$ = 973 Hz and $^{4}J_{HH}$ = 12.0 Hz. The $^{31}P\{^{1}H\}$ NMR showed two doublet resonances, each with Pt-satellites, at 21.70 ppm ($^{1}J_{Pt-P}$ = 2093 Hz and $^{2}J_{P-P}$ = 17.8 Hz) and at 15.20 ppm ($^{1}J_{Pt-P}$ = 1839 Hz and $^{2}J_{P-P}$ = 17.8 Hz). The ^{31}P NMR data differs somewhat to that of **4-1** because the platinum centre is nitrogen-bound rather than carbon-bound to the heterocycle. Using a similar argument that led to the identification of **4-1**, we propose that a similar type of *cis*-compound is obtained with pyrrole, viz *cis*-hydrido(1-pyrrolyl)bis-(triethylphosphine)platinum(II), **4-3**.

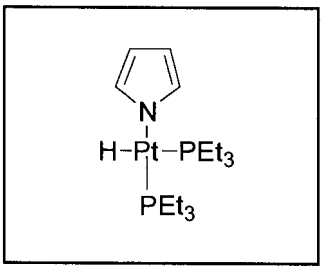

4-3

The coupling of 12.0 Hz is assigned to a four bond coupling between the hydride proton and the H-2 (or H-4) of the pyrrolyl ring. As the *trans*-isomer is the expected thermodynamically more stable isomer and a *cis-trans* isomerisation reaction thus occurred.

Insertion of a zerovalent platinum centre into the N-H bond of pyrrole has previously been

reported by Stone and co-workers [32], who were able to insert bis(tricyclohexylphosphine)-platinum(0) into the N-H bond of pyrrole and to isolate the resulting platinum(II) hydride. After 40 hours at room temperature *trans*-[PtH(C_4H_4N)(PCy_3)$_2$] was formed (^{1}H NMR (C_6D_6) δ for PtH -16.54 ppm, t, $^2J_{P-H}$ 13.4 Hz; $^{31}P\{^1H\}$ NMR δ -36.1 ppm, s with satellites, $^1J_{Pt-P}$ 2813 Hz). The coupling constants correspond well to the values obtained for the triethylphosphine analogue, **4-2**, generated *in situ* (2813 versus 2734 Hz). Exchanging the tricyclohexyl-phosphine with triethylphosphine, though, results in a large change in the chemical shift for the equivalent *trans* phosphorus atoms (-36.1 ppm versus 22.3 ppm), although a different deuterated solvent was used.

The reactivity of tertiary phosphine complexes of platinum(0), ML_n, is determined by the steric and electronic properties of the phosphine, L, as well as the coordination number *n*. In solution, [$Pt(PEt_3)_4$] readily loses one phosphine to give [$Pt(PEt_3)_3$] (a 16 electron species), but dissociation of a second phosphine to yield [$Pt(PEt_3)_2$] has not been observed spectroscopically. A 14-electron $Pt(PEt_3)_2$ moiety is sterically unhindered and is expected to be highly reactive. Trogler and co-workers [51] have developed a method of preparing [$Pt(PEt_3)_2$] *in situ*. Photolysis of the platinum(II) oxalate compound, [$Pt(PEt_3)_2(C_2O_4)$], releases carbon dioxide with the concomitant reduction of the platinum to the zerovalent state. In the presence of oxidative addition substates, XY (eg. X = HNR, Y= R), platinum(II) complexes containing two PEt_3 ligands, [$PtXY(PEt_3)_2$], can be prepared under mild conditions [52].

Stable two-coordinate platinum(0) phosphine species can be obtained where the phosphine is bulky. The complexes ML_2 where M = Pd, Pt and L = P^tBu_3, PPh^tBu_2, PCy_3 and $Pt(P^iPr_3)_2$ have been prepared and characterised [53]. In the solid state, complexes of the very bulky P^tBu_3 are relatively air stable, while the remaining complexes are readily dioxygenated. An enhanced reactivity is observed with the platinum(0) complexes of less bulky ligands, *eg.* a hydrogen molecule can add to bis(tricyclohexylphosphine)platinum(0) at room temperature to give the corresponding dihydride [54].

In the reaction with pyrrole, $[Pt(PCy_3)_2]$ is clearly more reactive than $[Pt(PEt_3)_3]$. In sharp contrast, $[Pt(PPh_3)_3]$ does not undergo a detectable reaction with pyrrole.

4.2.2.1 *Photochemistry*

It was attempted to achieve N-H activation under photochemical conditions. Jones *et. al.* [55] were able, by irradiation in C_6D_6, to activate a Si-C bond in the zerovalent complex, $[Pt(\eta^2\text{-}Me_3SiC{\equiv}CPh)(dcpe)]$ (where dcpe = (dicyclohexylphosphino)ethane) to generate the oxidative addition product $[Pt(SiMe_3)(C{\equiv}CPh)(dcpe)]$. Interestingly, upon heating, the reverse process of reductive elimination occurred to regenerate the Pt-η^2-alkyne complex. Similarly, irradiation of zerovalent Pt-η^2-alkyne complexes of diphenylacetylene and chelating P,N or P,P ligands causes cleavage of the C(sp^3) - C(sp) bond in diphenylacetylene [56].

Irradiation of a mixture of pyrrole and $[Pt(PEt_3)_4]$ in toluene under ultraviolet light, using a mercury lamp, for 18 hours, did not yield a platinum(II) hydride complex. A hydride proton resonance was absent from the ^{1}H NMR spectrum. A white precipitate settled out of the reaction mixture. The ^{31}P NMR spectra of this compound displayed a single resonance corresponding to two equivalent phosphine groups, coupled to ^{195}Pt. The $^1J_{Pt\text{-}P}$ value of 3469 Hz in this case suggests a *cis* rather than a *trans* geometry. Interpretation of the NMR spectra led to the conclusion that the compound is *cis*-[Pt(1-pyrrolyl)$_2$(PEt_3)$_2$], but this could not be confirmed by mass spectrometry.
^{1}H NMR in $CDCl_3$, δ / ppm: 6.465 (s br Pt sat., 2H, H-2 and H-5, $^3J_{Pt\text{-}H}$ = 16.5 Hz), 6.053 (d, 2H, H-3 and H-4, $^3J_{HH}$ = 1.65), 1.817 (m, 12H, CH_2), 1.15 (m, 18H, CH_3); ^{13}C NMR δ / ppm: 125.05 (C-2,C-5), 105.88 (C-3, C-4), 15.5 (m, CH_2), 8.09 (CH_3, $^3J_{Pt\text{-}C}$ = 26.0 Hz); ^{31}P{^{1}H} NMR δ / ppm: 3.52 (s, $^1J_{Pt\text{-}P}$ = 3469 Hz).

The formation of this complex would probably occur via a radical mechanism.

In certain instances thermal and photochemical activation can lead to different products. Heating a benzene solution of the complex [Rh(η^3-*N,N,N*-HBPz*$_3$)(CO)(η^2-C_2H_4)] where Pz* = 3,5-dimethylpyrazole leads to elimination of ethylene and the formation of [Rh(η^3-*N,N,N*-HBPz*$_3$)(H)Ph(CO)], while irradiation of the sample leads to [Rh(η^3-*N,N,N*-HBPz*$_3$)(CH_2CH_3)(Ph)(CO)] [57].

4.2.3 Reactions of [Pt(PEt_3)$_4$] with azoles resulting in N-H activation

A summary of the major products obtained when the respective azoles were reacted with [Pt(PEt_3)$_4$] is given below:

4-4

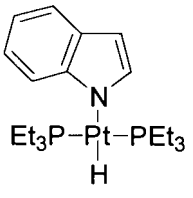

4-5

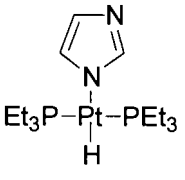

4-6

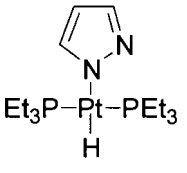

4-7

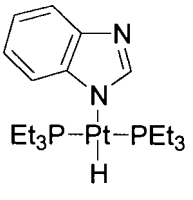

4-8

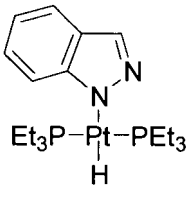

4.2.3.1 Indole

In this study, the reactivity of indole is remarkably different from that of pyrrole. Upon addition of $[Pt(PEt_3)_4]$ to a solution of indole in toluene at room temperature, an immediate decolouration of the solution occurred. The white solid obtained after removal of the solvent *in vacuo* was characterized by NMR spectroscopy and MS as *trans*-$[PtH(1\text{-indolyl})(PEt_3)_2]$, **4-4**. A solution of the hydride in deuterated chloroform soon adopts a blue colour which darkens upon standing. Similarly, in crystallization attempts, a solution of the hydride in dichloromethane, layered with hexane, degrades over time.

In 1998 Maitlis and co-workers [33] reported that PtL_3 (L = PEt_3 and PMe_3) inserts into the N-H bond of carbazole to form a platinum(II) hydride with the phosphines in *trans* positions. A single crystal X-ray structure confirmed the *trans* geometry of the trimethylphosphine complex. The only other example we could find of N-H bond activation by platinum(0) is attributed to Stone and co-workers, who reacted bis(tricyclohexylphosphine)platinum(0) with pyrrole, as discussed in 4.2.2 [32].

Thus, while pyrrole does not react with $[Pt(PEt_3)_4]$ to an appreciable extent, indole and carbazole both readily give platinum(II) hydrides. Structurally, the pyrrole and its benzo derivatives appear to be extremely similar; all three contain a five-membered, π-excessive, aromatic ring with an N-H moiety. The presence of fused benzene rings in indole and carbazole allows for the possibility of an additional mode of bonding to a transition metal moiety *viz*. η^2 or η^6 bonding to the fused benzene ring. However, this should not be a factor when considering the reactivity at the N-H site. The benzene rings do not sterically prevent approach of the metal centre, indeed, the reactivity is enhanced rather than diminished. The contribution of the benzene rings is likely to be an electronic effect. To explain the difference in reactivity, several properties of the three heterocycles were considered:

The pK_a value for the NH acid dissociation of carbazole is 17.06, which is similar to the pK_a of indole (16.97). Pyrrole is slightly less acidic NH group; pKa = 17.5. In dimethylsulfoxide, the pKa values of 19.9, 20.9 and 23.1 for carbazole, indole and pyrrole respectively show a similar trend in acidity [58].

On comparing the computed charge on each atom, as calculated by a PM3 semi-empirical calculation method and a Polak-Ribiere (conjugate gradient) algorithm [59] (Figure 4.7) the nitrogen atom of pyrrole carries a larger positive value than for indole or carbazole. The nitrogen atoms carry a fractional positive charge as a result of the small contribution to the overall structure from resonance hybrids in which a positive charge resides on the nitrogen atom (Scheme 4.4). In contrast, the NH-hydrogen carries a smaller positive charge in pyrrole than in either indole or carbazole. Hence there is greater polarisation of the N-H bond in pyrrole, and this decreases for indole and carbazole.

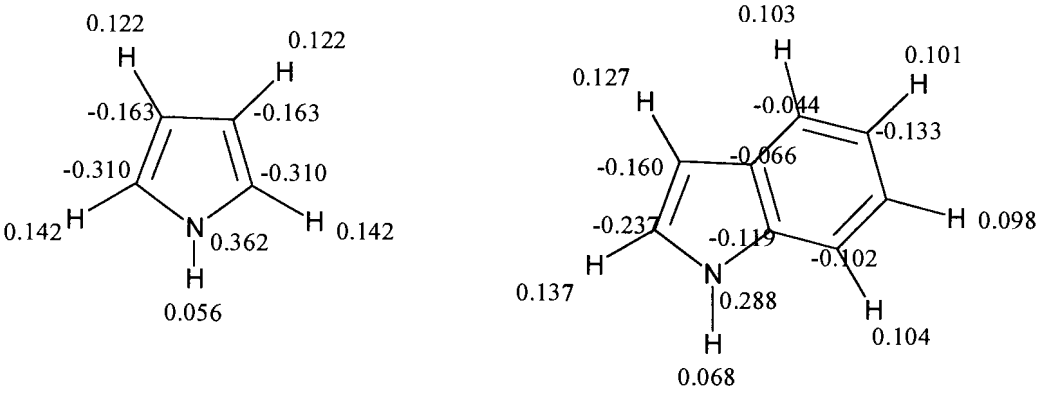

Figure 4.7 Calculated charges on each atom of pyrrole and indole

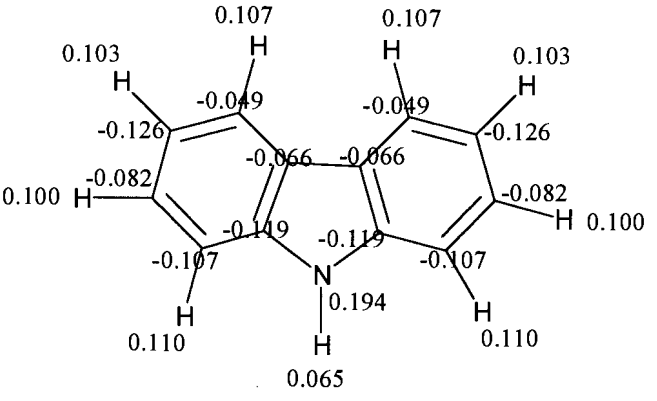

Figure 4.7 (continued) Calculated charges on each atom of carbazole

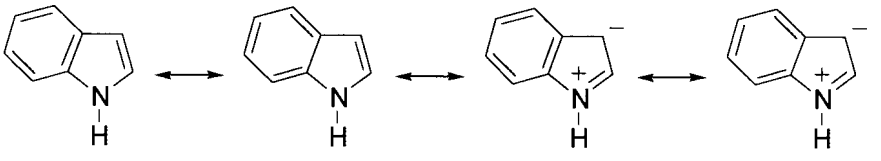

Scheme 4.4 Resonance hybrids of indole [58b]

The charge and NH acidity suggest that the N-H bond is stronger in pyrrole than in carbazole and indole. This helps to explain the poorer reactivity with platinum(0) at the N-H bond of pyrrole.

4.2.3.2 Imidazole

A popular use of the imidazole ligand in organometallic chemistry is as imidazole-derived carbenes. Carbene complexes in which bonding occurs via the C-2 atom, and where at least one of the nitrogen atoms of imidazole bears a proton or an alkyl group, are known [60]. However, the use of imidazole-based ligands in *N*-heterocyclic carbenes has flourished [61] since Arduengo *et. al.* [62] reported the first X-ray structure of the stable carbene, 1,3-di-

adamantylimidazol-2-ylidene in 1991. Imidazolium salts can be readily deprotonated to give imidazol-2-ylidene-type carbenes, which coordinate strongly to transition metals (Figure 4.8). Imidazolylidene complexes of Ru, Ir, Pd and Rh play an important role in homogeneous catalysis (hydrogenation, hydrocarbonylation, amination, olefin metathesis and various coupling reactions [63]). Imidazolium salts themselves are useful as ionic liquids.

Salts of 2-pyridylmethylimidazolium and $[IrH_5(PPh_3)_2]$ give an $[Ir(N\text{-}C)H_2PPh_3)_2]^+$ species with the imidazole ring bound at C-4 rather than at C-2 [67].

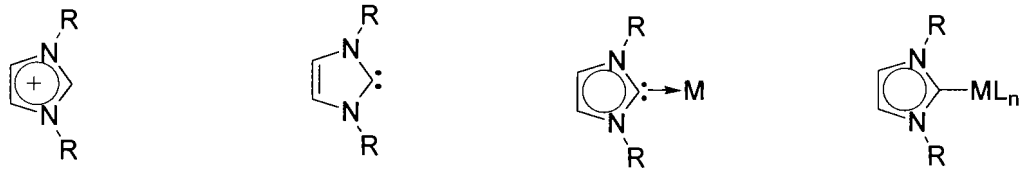

Figure 4.8 Imidazole-based carbenes complexes

Furthermore, certain transition metal complexes of imidazole derivatives have been shown to have biological activity. For example, [ImH][*trans*-$Rh(Im)_2Cl_4$] where Im = imidazole was found to exhibit antitumour activity *in vitro* [68a], whereas the complex [Au(1-imidazoyl)(PPh_3)] has antimicrobial activity [68b].

Imidazole has two types of nitrogen-donor atoms; one pyrrole-like and one pyridine-like. The coordinating possibilities are thus greater than for pyrrole. Coordination can occur via the pyridine-like nitrogen atom, where imidazole acts as a neutral ligand *eg* [ImH][*trans*-$Rh(Im)_2Cl_4$] [68a], or via the pyrrole nitrogen after deprotonation of the N-H group *eg* [Au(1-imidazoyl)(PPh_3)]. In the latter case, the imidazolyl group can act as a bidentate ligand, bridging two metal centres.

Like pyrrole, imidazole is a π-excessive aromatic heterocycle (Figure 4.9) [44]. The calculated point charges are given in Figure 4.10 [2].

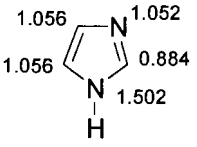

Figure 4.9 π-electron densities on the ring atoms of imidazole

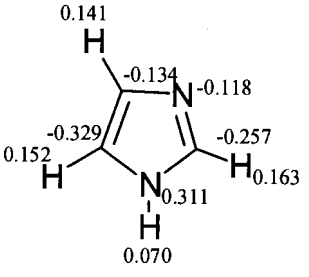

Figure 4.10 Calculated charge for each atom of imidazole

Imidazole displays annular tautomerism in solution (Figure 4.11). The transfer of a proton from position 1 to 3 is fast. An equilibrium is rapidly achieved at room temperature so that an average NMR signal for H-4 and H-5, as well as for C-4 and C-5, is obtained [44].

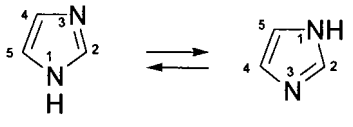

Figure 4.11 Tautomerism of imidazole

Such fluxional behaviour is also found for certain complexes of imidazole and imidazolyl (Figure 4.12). The ^{1}H NMR spectra of such compounds exhibit one broad resonance for H-4 and H-5, instead of the two expected signals, providing evidence of the metallotropy of the

ligand. Low temperature NMR experiments show a splitting of the broad signal into two separate resonances [69].

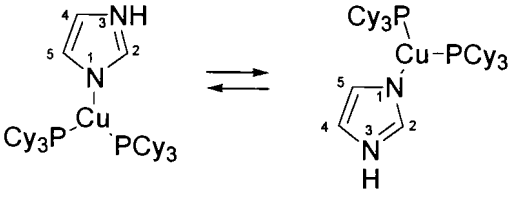

Figure 4.12 Metallotropy of a Cu(II) / imidazole complex

The pK_a of imidazole is 14.17 (measured spectrophotometrically at 25°C), making it a considerably stronger N-H acid than pyrrole (pK_a 17.5) [70]. This enhanced acidity is due to the introduction of the pyridinic nitrogen atom, which increases the ring's capacity to accept electronic charge.

It is thus not surprising then that the reaction of $[Pt(PEt_3)_4]$ with imidazole also led to N-H activation and resulted in the isolation of the complex, *trans*-hydrido(1-imidazolyl)-bis(triethylphosphine)platinum(II), **4-5**, which is analogous to that obtained for indole, **4-4**. The complex does not seem to be fluxional on the NMR time-scale.

4.2.3.3 Pyrazole

Like imidazole, pyrazole is a π-excessive, aromatic, five-membered heterocycle, but with its nitrogen atoms in positions 1 and 2 and bearing most of the electron density [44] (Figure 4.13).

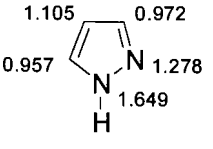

Figure 4.13 π-electron densities on the ring atoms of pyrazole

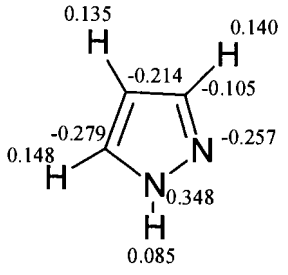

Figure 4.14 Calculated charge for each atom of pyrazole [59]

The modes of bonding of transition metals to pyrazole is very similar to that of imidazole [71]. An example of a platinum(II) complex of pyrazole is *cis*-[Pt(3-CF_3-5-CH_3pyrazolyl)$_2$(PEt_3)$_2$] which was synthesised in the reaction of *cis*-[$PtCl_2$(PEt_3)$_2$] with pyrazole and excess potassium hydroxide [72].

The incorporation of pyrazole into poly(pyrazol-1-yl)alkane and poly(pyrazol-1-yl)borate ligands and the use of these ligands in the organometallic chemistry of platinum has been well studied [73].

Pyrazole also exhibits annular tautomerism, where the protons in positions 3 and 5 give rise to one ^{1}H NMR resonance. Certain metal complexes containing an anionic η^1-pyrazolyl or a neutral monodentate pyrazole ligand also have the 3- and 5-positions equalised by a 1,2-metal shift. With complexes of the neutral pyrazoles, proton transfer is required in addition to metal exchange between nitrogen atoms (Figure 4.15) [74].

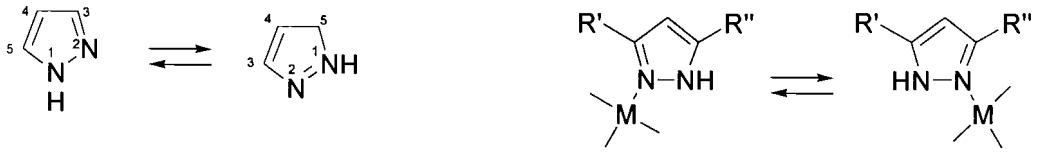

Figure 4.15 Tautomerism in pyrazole and pyrazole complexes.

Complexes of the type *cis*-$[M(pz)_2(L\text{-}L)]$ and *cis*-$[M(pzH)_2(L\text{-}L)]^{2+}$ where M = Pt, Pd, pz = pyrazolyl, pzH = pyrazole and L-L = dppe, bipy or cod do not exhibit fluxional behaviour [75]. Contrastingly, the complex cations *cis*-$[MCl(PEt_3)_2L]^+$ where L = pyrazole, 3,5-dimethyl-pyrazole, 3,4,5-trimethylpyrazole and bromo-3,5-pyrazole are fluxional when M = Pd, but static on the NMR timescale when M = Pt. Platinum complexes are generally less labile than the palladium analogues and the M-N bond is thought to be stronger for platinum than for palladium [76]. Platinum(II) complex cations that do undergo fluxional processes are *cis*-$[PtCl(PEt_3)_2L]^+$ where L = phenanthroline, naphtyridine and phthalazine [77].

As was the case for imidazole, the reaction of $[Pt(PEt_3)_4]$ with pyrazole led to N-H activation and *trans*-hydrido(1-pyrazolyl)bis(triethylphosphine)platinum(II), **4-6**, was isolated. The complex is not fluxional; the pyrazolyl protons give rise to three separate, distinguishable resonances in the ^1H NMR spectrum.

4.2.3.4 Benzimidazole

Benzimidazole is a stronger NH acid than imidazole (pKa = 12.75) [78]. Like imidazole it displays annular tautomerism in solution (Figure 4.16), and like imidazole it reacts rapidly with $[Pt(PEt_3)_4]$ to form *trans*-hydrido(1-benziimidazolyl)bis(triethylphosphine)platinum(II), **4-7**. This complex does exhibit metallotropy in solution.

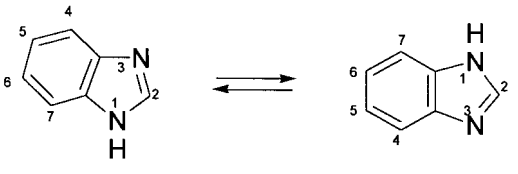

Figure 4.16 Tautomerism of benzimidazole [44]

4.2.3.5 Indazole

The tautomerism of indazole is somewhat different to that of pyrazole and imidazole (Figure 4.17) [44]:

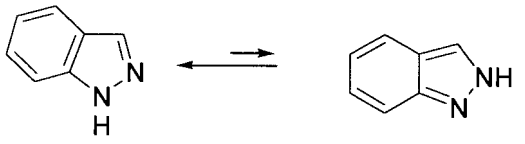

1*H*-indazole 2*H*-indazole (*o*-quinoid structure)

Figure 4.17 Tautomerism of indazole [44]

The equilibrium lies to the left, although the energy difference between the tautomers is quite small. A mixture of 1- and 2-alkylindoles is obtained when indazole is alkylated in the presence of bases. The ambidentate indazolyl anion is an intermediate in the alkylation reaction. This type of reactivity is mirrored in the reaction of indazole with $[Pt(PEt_3)_4]$. Two triplet resonance patterns with relative intensities of 8:1 were observed in the high-field region of the ^1H NMR spectrum (Table 4.3). The chemical shifts and the coupling constants are extremely similar, indicating the presence of two isomeric *trans*-hydride complexes of indazole *viz.* *trans*-[PtH(1-indazolyl)$(PEt_3)_2$] **4-8** and *trans*-[PtH(2-indazolyl)$(PEt_3)_2$] **4-9**. Similarly, the $^{31}P\{^1H\}$ NMR spectrum show two different *trans*-phosphine products (Table 4.3).

Table 4.3 High field ^{1}H and ^{31}P NMR data for *trans*-[PtH(indazolyl)(PEt_3)$_2$] isomers in $CDCl_3$

	major product, **4-8** 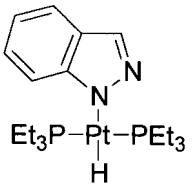	minor product, **4-9** 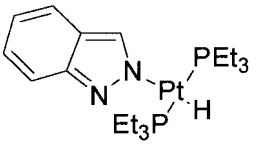
^{1}H (PtH) δ / ppm	-16.163	-16.821
$^{2}J_{P-H}$	15.3 Hz	15.3 Hz
$^{1}J_{Pt-H}$	958 Hz	958 Hz
^{31}P δ / ppm	23.0	21.8 Hz
$^{1}J_{Pt-P}$	2729 Hz	2733 Hz

As mentioned previously, *trans*-hydrido(tetrazolato)bis(triphenylphosphine)platinum(II) complexes exist as two isomers in solution (Figure 4.4) [27]. There, too, the chemical shifts and coupling constants for the N-1 and the N-2 bound isomers are very similar (Table 4.4).

trans-[PtH(X)(PPh_3)$_3$]	δ ^{1}H (PtH) / ppm	$^{2}J_{P-H}$	$^{1}J_{Pt-H}$
X = 5-phenyltetrazolato	-15.62, -16.13	13.2	964
X = 5-bromotetrazolato	-15.62, -16.13	12.5	~916
X = 5-chlorotetrazolato	-15.66, -16.38	10.2	

Table 4.4 High-field ^{1}H NMR data for the tetrazolato complexes *trans*-[PtH(X)(PPh_3)$_3$] in $CDCl_3$.

4.2.4 Reaction of $[Pt(PEt_3)_4]$ with 1,2,4-Triazole

Unexpectedly, the reaction of 1,2,4-triazole with tetrakis(triethylphosphine)platinum(0) did not yield a platinum(II) hydride complex, as evident from the absence of a hydride resonance in the ^1H NMR spectrum. The $^{31}P\{^1H\}$ NMR spectrum of the isolated white solid showed a single resonance at 2.38 ppm with a $^1J_{Pt\text{-}P}$ coupling of 3050 Hz. The value of this coupling constant indicates equivalent phosphine groups in *cis* positions, much like the product of the photochemical reaction of pyrrole with $[Pt(PEt_3)_4]$. NMR ^1H δ 7.941 (s, 1H), 7.476 (s, 1H) 1.717 (m, PCH_2), 1.118 (m PCH_2CH_3); $^{13}C\{^1H\}$ δ 151.52 (*C*H), 149.16 (*C*H), 15.14 (m, PCH_2), 8.21 (PCH_2CH_3, $^3J_{Pt\text{-}C}$ 22.4 Hz). This data is consistent with a $[Pt(1\text{-triazolyl})_2(PEt_3)_2]$, structure, although MS results could not verify this.

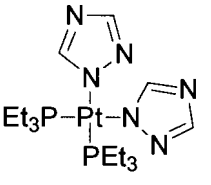

4.2.5 Reactions of $[Pt(PPh_3)_3]$ with selected Azoles

Since N-H activation for the azoles described in 4.2.3 was achieved relatively easily by $[Pt(PEt_3)_4]$, it was thought that it would be possible to obtain the triphenylphosphine analogues by employing harsher reaction conditions and longer reaction times. Solutions of tris(triphenylphosphine)platinum(0) with imidazole and pyrazole respectively were heated in toluene at 60 °C for a week without a N-Pt-H type hydride being detected in the high-field region of the ^1H NMR spectrum.

However low concentrations of a *cis*- and a *trans*- hydride platinum complex were detected in a $[Pt(PPh_3)_3]$ / indole toluene solution that had been stirring at room temperature for one

week. The ^{1}H NMR triplet pattern with ^{195}Pt satellites, centred at -14.144 ppm, is slightly more downfield than the triplet patterns obtained for the *trans*-[Pt(H)(1-azolyl)(PEt_3)$_2$] complexes **4.4 - 4.8**, which resonate at *ca.* -15 to -16 ppm (See Table 4.7). However, it corresponds well with *trans*-[Pt(H)(succinimidyl)(PPh_3)$_2$]-type complexes (Table 4.5) [79]. The coupling values of 15.3 Hz and 838 Hz were assigned to $^{2}J_{P\text{-}H}$ and $^{1}J_{Pt\text{-}H}$ respectively. The $^{1}J_{Pt\text{-}H}$ value is lower than that obtained for the triethylphosphine complexes but falls within the range of 660 - 970 Hz reported for various hydrides in this dissertation. The $^{2}J_{P\text{-}H}$ value is typical of a *trans*-phosphine hydrido platinum(II) species.

A second resonance, a ddd pattern with satellites, also appeared in the high-field region, albeit in very low concentration. Centred at -11.126 ppm, it had couplings of 3.2 Hz, 8.4 Hz, 83 Hz and 727 Hz. These values are somewhat smaller than the couplings measured for the ddd pattern of **4-3**, but of the correct order of magnitude. The value of 727 Hz is not unusual for $^{1}J_{Pt\text{-}H}$ coupling. The remaining coupling constants were assigned as follows: $^{2}J_{Pa\text{-}H}$ (P_a *cis* to H) = 8.4 Hz, $^{2}J_{Pb\text{-}H}$ (P_b *trans* to H) = 83 Hz and $^{4}J_{HH}$ = 3.2 Hz.

Based on the ^{1}H and $^{31}P\{^{1}H\}$ NMR data, the complexes were identified as follows:

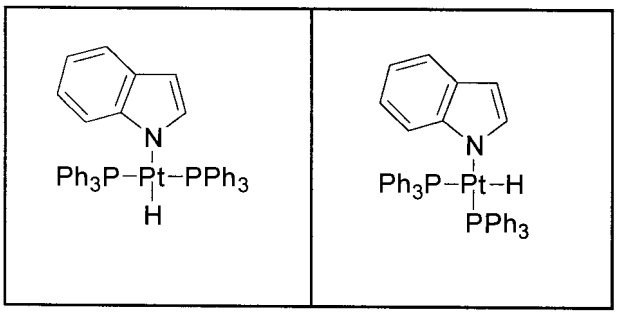

4-9 **4-10**

Although triphenylphosphine is not basic enough to effect facile oxidative addition into a heterocyclic aromatic N-H bond, [$Pt(PPh_3)_3$] is known to activate the N-H bonds of succinimide, phthalimide (by refluxing for 24 hours), saccharin (within minutes at room

temperature) and parabanic acid (after several hours at room temperature) to form *trans*-hydridoimidobis(triphenylphosphine)platinum(0) complexes (Table 4.6) [79]. These cyclic, nitrogen compounds are secondary amines and are stronger bases through their respective nitrogen atoms than aromatic nitrogen-containing heterocycles. They are also considerably stronger NH acids: pK_a (succinimide) = 9.5; pK_a (phthalimide) = 8.3 [80].

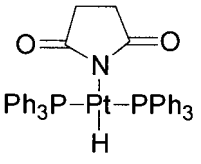

(i)

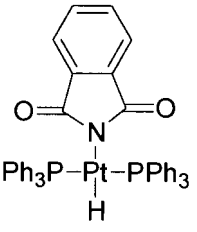

(ii)

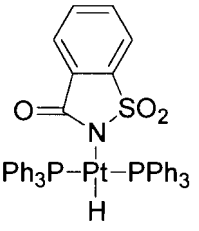

(iii)

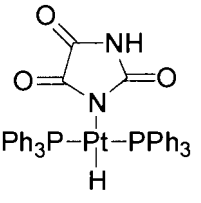

(iv)

δ PtH	-14.1 ppm	-14.0 ppm	-15.7 ppm	-14.6 ppm
$^2J_{P\text{-}H}$	poorly resolved	12.3 Hz	12.8 Hz	poorly resolved
$^1J_{Pt\text{-}H}$	unresolved	unresolved	unresolved	unresolved

Table 4.5 Complexes resulting from the N-H activation of (i) succinimide (ii) phthalimide (iii) saccharin and (iv) parabanic acid by $[Pt(PPh_3)_3]$ and their corresponding hydride ^1H NMR data (in $CDCl_3$).

4.2.6 NMR Spectroscopy of Complexes 4-4 to 4-8

All NMR spectra were recorded in $CDCl_3$, unless stated otherwise. The ^1H NMR data for indole and the Pt(II) indolyl hydride, **4-4**, is presented in Table 4.6. For comparative purposes

the data for the analogous carbazolyl hydride, *trans*-[PtH($C_{12}H_8N$)(PEt_3)$_2$], which has been reported in the literature [33], is also included.

Table 4.6 ^{1}H NMR data for indole and the Pt(II) indolyl hydride, **4-4**, δ / ppm

	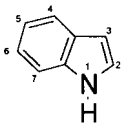	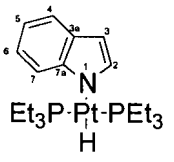	*trans*-[PtH($C_{12}H_8N$)(PEt_3)$_2$] [32]
H-4	7.881 (dd, $^3J_{HH}$ = 7.50 Hz, $^4J_{HH}$ = 0.78 Hz)	6.85 (m,overlaps with H-6)	*8.25*
H-5	7.42-7.34 (m)	7.612 (m)	*7.6*
H-6		6.91 (m,overlaps with H-4)	*7.58*
H-7		7.365 (d, br, $^3J_{HH}$ = 7.78 Hz)	*7.02*
H-2	7.143 (m)	7.155 (d, Pt-sat, $^3J_{Pt-H}$ = 13.8 Hz)	-
H-3	6.732 (m)	6.501 (m)	-
CH_2	-	1.536 (m)	*1.5*
CH_3	-	1.006 (m)	*0.95*
N-H / Pt-H	7.753 (br s)	-15.660 (t, Pt-sat, $^2J_{P-H}$ 15.7 Hz $^1J_{Pt-H}$ 945 Hz)	*-14.4* $^2J_{P-H}$ = *17 Hz* $^1J_{Pt-H}$ = *940 Hz*

On comparing the hydride resonance of complex **4-4** with the hydride resonances of the analogous pyrrolyl and carbazoyl complexes (Table 4.7), there is a clear trend to a less negative value for the hydride proton's chemical shift on moving from pyrrole to indole to carbazole.

Table 4.7 High-field ^{1}H NMR data for pyrrolyl, indolyl and carbazolyl Pt(II) hydrides

trans-[PtHX(PEt_3)$_2$] complex	δ /ppm	$^2J_{P-H}$ / Hz	$^1J_{Pt-H}$ / Hz
X = pyrrolyl, **4-2**	-16.285	15.7	922
X= indolyl, **4-4**	-15.660	15.7	945
X = carbazolyl [32]	-14.4	17	940

The $^2J_{P-H}$ coupling constant has the same value for complexes **4-2** and **4-4**, and is only slightly larger for the carbazolyl hydride. While the $^1J_{Pt-H}$ coupling constants do not follow a particular trend, the values are all of the same order.

The ^{1}H NMR data for the imidazolyl hydride, **4-5**, the pyrazolyl hydride **4-6**, the benzimidazolyl hydride **4-7**, and the indazolyl hydride **4-8** are presented in Tables 4.8 to 4.10, together with data for the nonbonded ligands. Furthermore, Table 4.11 summarises the high-field ^{1}H NMR data for the hydride protons of complexes **4-4** and **4-8** . The chemical shifts for the hydride protons of the imidazolyl and pyrazolyl complxes are both at higher field than for their annelated counterparts - the hydrides of benzimidazolyl and indazolyl. This follows the same trend found for the analogous pyrrolyl-, indolyl- and carbazolyl-complexes. Similarly, the $^1J_{Pt-H}$ values are smaller for imidazolyl- and pyrazolyl- than for the corresponding benzimidazolyl- and indazolyl-complexes. The $^2J_{P-H}$ values are slightly larger though for imidazolyl- and pyrazolyl- than for the corresponding benzimidazolyl- and indazolyl-complexes.

Table 4.8 ^{1}H NMR data for the imidazolyl hydride, **4-5**, δ / ppm

	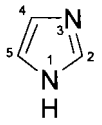	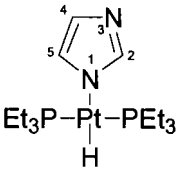	
H-2	7.716 (s)	7.133	(s, br)
H-4	7.116 and 7.113 (s)	7.213	(br, Pt-sat., $^3J_{Pt-H}$ unresolved)
H-5		6.721	(br, Pt-sat., $^3J_{Pt-H}$ 11.5 Hz)
CH_2	-	1.615	(m)
CH_3	-	1.018	(m)
N / Pt-H	not detected	-16.326	(t, Pt-sat., $^2J_{P-H}$ 15.5 Hz, $^1J_{Pt-H}$ 966 Hz)

Table 4.9 ^{1}H NMR data for the pyrazolyl hydride, **4-6**, δ / ppm

	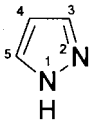	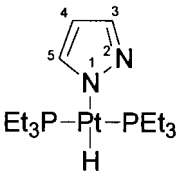	
H-3	7.11 (s)	7.338	(m)
H-5		6.764	(d, Pt-sat as shoulders, $^3J_{HH}$ 1.91 Hz, $^3J_{Pt-H}$ unresolved)
H-4	6.331 (s)	5.83	(m)
CH_2	-	1.53	(m)
CH_3	-	0.94	(m)
N/Pt-H	12.223 (s, br)	-17.011	(t, Pt-sat.,$^2J_{P-H}$ 15.6 Hz, $^1J_{Pt-H}$ 942 Hz)

Table 4.10 ^{1}H NMR data for benzimidazole, the benzimidazolyl hydride **4-7**, indazole and the indazolyl hydride **4-8**, δ / ppm

	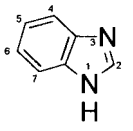	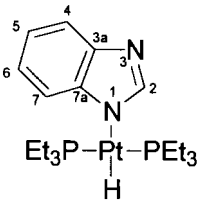	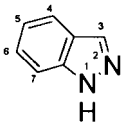	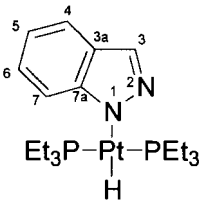
H-2	8.066 (s)	7.72-7.7 (m)	-	-
H-3	-	-	8.076 (s)	8.125 (s)
H-4	7.656 (dd)	7.04-7.01 (m)	7.754 (d)	7.663 (d $^3J_{HH}$ 8.1 Hz)
H-7	J 6.1; 3.2 Hz		7.489 (dd)	7.500 (d $^3J_{HH}$ 8.1 Hz)
H-6	7.283 (dd)	7.72-7.70 (m)	7.379 (td)	7.040 (t $^3J_{HH}$ 7.6 Hz)
H-5	J 5.7, 3.1 Hz	7.47-7.44 (m)	7.161 (td)	6.837 (t $^3J_{HH}$ 7.1 Hz)
CH_2	-	1.546 (m)	-	1.532 (m)
CH_3	-	0.992 (m)	-	0.966 (m)
N-H or Pt-H	1.899 (s, br)	-15.831 (t, Pt-sat.) $^2J_{P-H}$ 15.3 Hz $^1J_{Pt-H}$ 989 Hz	10.235 (br)	-16.163 (t, Pt-sat.) $^2J_{P-H}$ 15.3 Hz $^1J_{Pt-H}$ 958 Hz

Table 4.11 Summary of high-field ^{1}H NMR data complexes **4-4** to **4-8**

Complex	δ /ppm	$^2J_{P-H}$ / Hz	$^1J_{Pt-H}$ / Hz
4-4 indolyl hydride	-15.660	15.7	945
4-5 imidazolyl hydride	-16.326	15.5	966
4-7 benzimidazolyl hydride	-15.831	15.3	989
4-6 pyrazolyl hydride	-17.011	15.6	942
4-8 indazolyl hydride	-16.163	15.3	958

Table 4.12 ^{13}C NMR data for indole and the Pt(II) indolyl hydride, **4-4**, δ / ppm

	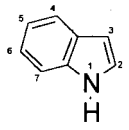	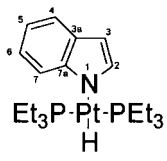	*trans*-[PtH($C_{12}H_8N$)(PEt_3)$_2$] [32]
C-7a	135.60	145.42	149.5
C-3a	127.67	130.36	125.3
C-2	124.215	136.48 ($^2J_{Pt-C}$ 24.2 Hz)	-
C-5	121.80	119.14	122
C-4	120.59	116.90	118.7
C-6	119.69	115.64	113.5
C-7	110.03	114.89 ($^3J_{Pt-C}$ 20.5 Hz)	113
C-3	102.20	98.98 ($^3J_{Pt-C}$ 26.0 Hz)	-
CH_2	-	17.4 m	20 .0 m
CH_3	-	8.38 ($^3J_{Pt-C}$ 0.6 Hz)	10.3

Table 4.13 ^{13}C NMR data for imidazole and **4-5**; and pyrazole and **4-6**, δ / ppm

	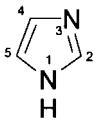	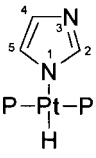		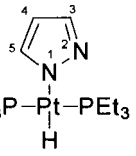
C-2	135.15	143.26 ($^2J_{Pt-C}$ 26.9 Hz)	-	-
C-3	-	-	133.48	137.44 ($^3J_{Pt-C}$ 46.7 Hz)
C-4	121.73	127.45 ($^3J_{Pt-C}$ 30.6 Hz)	104.87	102.30 ($^3J_{Pt-C}$ 25.2 Hz)
C-5		125.10 ($^2J_{Pt-C}$ 21.5 Hz)	133.48	135.36 ($^2J_{Pt-C}$ 50.3 Hz)
CH_2	-	17.65	-	17.11
CH_3	-	8.36 ($^3J_{Pt-C}$ 30.5 Hz)	-	7.74

Table 4.14 ^{13}C NMR data for indazole, the indazolyl hydride **4-8**, benzimidazole and the benzimidazolyl hydride **4-7**, δ / ppm

	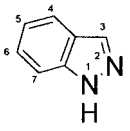	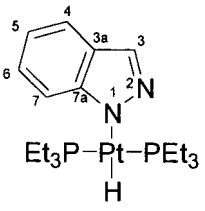		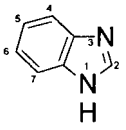	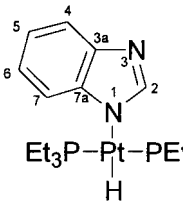
C-7a	140.09	148.86	C-2	140.39	150.51 $^{2}J_{Pt-C}$ 26.4 Hz
C-3	134.90	132.73 $^{3}J_{Pt-C}$ 34.1 Hz	C-3a C-7a	137.9	145.34 148.18
C-6	126.82	121.51	C-5 C-6	122.96	118.21 114.49 $^{4}J_{Pt-C}$ 17.1 Hz
C-3a	123.23	125.95	C-4 C-7	115.31	119.06
C-5	120.99	116.99	CH_2	-	17.66 m
C-4	120.87	119.89	CH_3	-	8.33 $^{3}J_{Pt-C}$ 30.5 Hz
C-7	109.68	113.44 $^{3}J_{Pt-C}$ 17.1 Hz			
CH_2	-	17.84 m			
CH_3	-	8.35 $^{3}J_{Pt-C}$ 30.5 Hz			

The preceding tables (Table 4.12 to 4.14) contain the ^{13}C NMR data for complexes **4-4** to **4-8**. The spectra of the free ligands were also recorded and tabulated above. The assignment of chemical shifts were aided by two-dimensional NMR ^{1}H / ^{13}C correlation (HETCOR) experiments. J_{Pt-C} couplings were not always clearly resolved.

Table 4.15 ^{31}P NMR data for complexes **4-4** to **4-8**		
Complex	δ / ppm	$^{1}J_{Pt-P}$ / Hz
4-4 (indolyl)	22.62	2715
4-5 (imidazolyl)	21.65	2705
4-7 (benzimidazolyl)	22.03	2691
4-6 (pyrazolyl)	22.41	2744
4-8 (indazolyl)	22.98	2729

The ^{31}P NMR data, summarised in Table 4.15, consist of a single resonance peak accompanied by satellites, indicating equivalent phosphine moieties. The $[PtHX(PEt_3)_2]$ complexes must therefore have the phosphines in mutually *trans* positions. The magnitude of the $^{1}J(^{195}Pt\text{-}^{31}P)$ coupling constants also indicate a *trans*-geometry, and compare favourably with the value of 2693 Hz reported for an analogous carbazole Pt(II) hydride [33]. Similarly the chemical shift values for these complexes corresponds closely to the 22.6 ppm reported for *trans*-$[PtH(C_{12}H_8N)(PEt_3)_2]$ [32]. Very little variation in magniture for the chemical shift and the coupling constants are observed for the complexes. A slight increase in chemical shift, and a concomitant decrease in coupling constant occurs upon annelation of the nitrogen heterocycle (*viz.* from the imidazolyl to the benzimidazolyl and from pyrazolyl to the indazolyl complex). This reflects the same trend as the ^{1}H NMR data for the hydride proton.

4.2.7 Mass Spectrometry

The complexes are analysed by fast atom bombardment mass spectrometry (FAB-MS), the results of which are presented in Tables 4.16 and 4.17.

Table 4.16 High-resolution MS for complexes **4-4** to **4-8**

Complex	Molecular Formula	Accurate Mass - Calculated	Accurate Mass - Observed	Intensity	Ion
4-4 (indolyl)	$C_{20}H_{37}NP_2Pt$	548.2049	547.1971	47	M^+-1
4-5 (imidazolyl)	$C_{15}H_{34}N_2P_2Pt$	499.1845	498.1766	58	M^+-1
4-7 (benzimidazolyl)	$C_{19}H_{36}N_2P_2Pt$	549.2002	550.2079	40	M^++1
4-6 (pyrazolyl)	$C_{15}H_{34}N_2P_2Pt$	499.1845	499.1853	18	M^+
4-8 (indazolyl)	$C_{19}H_{36}N_2P_2Pt$	549.2002	549.2002	62	M^+

The $[M^+-1]$ ion for the indolyl and imidazolyl complexes are an anomaly. The molecular ion has lost a hydrogen atom.. The $[M^+ +1]$ observed for the benzimidazolyl complex is not as uncommon; a hydrogen atom has been gained.

Table 4.17 MS fragmentation ions of complexes **4-4** to **4-8**

	m/z (intensity) [fragment ion]		m/z (intensity) [fragment ion]
4-4	547 (47) $[M]^+$	**4-5**	498 (58) $[M - H]^+$
	432 (100) $[M - C_8H_5N]^+$		432 (88) $[M - C_4H_4N]^+$ *ie* $[HPt(PEt_3)_2]^+$
	429 (93) $[M - PEt_3]^+$		403 (31) $[HPt(PEt_3)_2 - Et]^+$
	399 (36) $[M - PEt_3 - C_2H_6]^+$		374 (29) $[HPt(PEt_3)_2 - 2Et]^+$
	371 (23) $[M - PEt_3 - 2Et]^+$		345 (24) $[HPt(PEt_3)_2 - 3Et]^+$
	341 (18) $[M - PEt_3 - 2Et - C_2H_6]^+$		313 (25) $[Pt(PEt_3)]^+$
	284 (8) $[Pt(PEt_3) - Et]^+$		284 (13) $[Pt(PEt_3) - Et]^+$
	255 (5) $[PtPEt]^+$		256 (9) $[Pt(PEt_3) - Et - C_2H_4]^+$
	135 (24) $[HOPEt_3]^+$		135 (100) $[HOPEt_3]^+$
	119 (21) $[HPEt_3]^+$		119 (34) $[HPEt_3]^+$

4-6	499 (18) $[M]^+$ 430 (100) $[M - C_3H_4N_2H]^+$ 402 (28) $[M - C_3H_4N_2 - Et]^+$ 374 (28) $[M - C_3H_4N_2H - 2C_2H_4]^+$ 347 (25) $[M - C_3H_4N_2H - 2C_2H_4 - C_2H_3]^+$ 314 (20) $[HPt(PEt_3)]^+$ 283 (13) $[Pt(PEt_3) - C_2H_6]^+$ 255 (9) $[PtPEt]^+$ 135 (15) $[HOPEt_3]^+$ 119 (20) $[HPEt_3]^+$	**4-7**	550 (40) $[M + H]^+$ 432 (100) $[M + H - PEt_3]^+$ 375 (18) $[M + H - PEt_3 - Et - C_2H_4]$ 347 (16) $[M + H - PEt_3 - Et - 2C_2H_4]^+$ 314 (11) $[HPt(PEt_3)]^+$ 283 (7) $[Pt(PEt_3) - C_2H_6]^+$ 255 (4) $[PtPEt]^+$ 119 (27) $[HPEt_3]^+$ or $[C_7H_6N_2H]^+$
4-8	549 (62) $[M]^+$ 518 (10) $[M - H - C_2H_6]^+$ 491 (5) $[M - H - C_2H_6 - C_2H_4]^+$ 462 (9) $[M - H - C_2H_6 - C_2H_4 - Et]^+$ 431 (24) $[M - PEt_3]^+$ or $[M - C_7H_6N_2]^+$ 428 (98) $[M - 3H - C_7H_6N_2]^+$ 399 (50) $[M - 3H - C_7H_6N_2 - Et]^+$		370 (41) $[M - 3H - C_7H_6N_2 - 2Et]^+$ 313 (28) $[Pt(PEt_3)]^+$ 283 (21) $[Pt(PEt_3) - C_2H_6]^+$ 255 (11) $[PtPEt]^+$ 135 (100) $[HOPEt_3]^+$ 119 (43) $[HPEt_3]^+$

In general the main fragmentation pathway (Table 4.17) involves the loss of the azolyl ligand, followed by stepwise loss of C_2-units as ethyl, C_2H_6 or even C_2H_4 fragments to give the m/z metal ions: 313 $[Pt(PEt_3)]^+$, 284 $[PtPEt_2]^+$ and 255 $[PtPEt]^+$.

4.3 CONCLUSIONS

Interesting platinum(II) hydrides of the type *trans*-$[PtH(1\text{-azolyl})(PEt_3)_2]$, where azolyl = indolyl, imidazolyl, benzimidazolyl, pyrazolyl and indazolyl (**4-4** to **4-8**), were obtained by

a rapid oxidative insertion of platinum(0) into the N-H bond of the respective azole at ambient temperature. This illustrated that N-H activation is more facile than either C-S or C-H activation and this is consistent with the relatively weaker strength of N-H bonds. In contrast to the abovementioned azoles, pyrrole acts in an anomolous fashion, undergoing only partial N-H activation, despite the employment of harsher reaction conditions. The presence of both *cis*- and *trans*-isomers of [PtH(1-pyrrolyl)(PEt_3)$_2$] (**4-2** and **4-3**) was detected by NMR spectroscopy, with the *trans* isomers being thermodynamically more stable. Substitution of the *N*-bonded hydrogen of pyrrole by a methyl group deactivated the pyrrole ring even further towards oxidative insertion by platinum(0). A *cis*-hydride, **4-8**, was formed in an extremely low concentration. The strength of the N-C bond rules out activation at this site, and the platinum was thus directed to the alpha C-H bond.

4.4 REFERENCES

[1] J.G. Speight in *The Desulfurization of Heavy Oils and Residua*, Chemical Industries Vol. 4, ed. H. Heinemann, Marcel Dekker Inc., New York, 1981

[2] (a) C. Bianchini and A. Meli; *Acc. Chem. Res.*, **1998**, *31*, 109-116 (b) S. Harris, *Polyhedron*, **1997**, *16*, 3219-3233

[3] K.J. Weller, P.A. Fox, S.D. Gray and D.E. Wigley; *Polyhedron*, **1997**, *16*, 3139-3163

[4] (a) C.N. Satterfield, *Heterogeneous Catalysis in Industrial Practice*, 2nd ed. McGraw-Hill, New York, 1991 (b) R.J. Angelici in *Encyclopedia of Inorganic Chemistry*, Vol. 3, ed. R.B. King, John Wiley and Sons, New York, 1994, pp1433-1443 (c) S. Kasztelan, T. des Courières and M. Breysse; *Catal. Today*, **1991**, *10*, 433-445 (d) R. Prins; *Adv. Catal.* **2001**, *46*, 399-464 (e) R.M. Laine; *Catal. Rev.-Sci. Eng.*, **1983**, *25*, 459-474

[5] R. Prins, M. Jian and M. Flechsenhar; *Polyhedron*, **1997**, *16*, 3235-3246

[6] (a) J. Reedijk in *Comprehensive Coordination Chemistry*, Vol. 2, ed. G. Wilkinson, R.D. Gillard and J. McCleverty. Pergamon Press, Oxford, 1987, p.73 (b) T. Karlen, P. Dani, D.M. Grove, P. Steenwinkel and G. van Koten; *Organometallics*, **1996**, *15*, 5687-5694
(c) F. Neve, M. Ghedini and A. Crispini; *J. Organomet. Chem.*, **1994**, *466*, 259-263

[7] E.J. Wuchere and E.L. Muetterties; *Organometallics*, **1987**, *6*, 1696-1702

[8] P.T. Wolczanski; *Polyhedron*, **1995**, *14*, 3335-3362

[9] R. Cordone and H. Taube; *J. Am. Chem. Soc.*, **1987**, *109*, 8101-8102

[10] (a) M.G.B Drew, P.C.H,. Mitchell and A.R. Read.; *J. Chem. Soc. Chem. Commun.*, **1982**, 238-239 (b) M.G.B. Drew, P.J. Baricelli, P.C.H. Mitchell and A.R. Read.; *J. Chem. Soc. Dalton Trans.*, **1983**, 649-655

[11] W. Sliwa and M. Deska; *Collect. Czech. Chem. Commun.*, **1999**, *64*, 435-458

[12] a) M. Schmülling and R. van Eldik; *Chem. Ber.*, **1997**, *130*, 1791-1799 (b) M. Bonivento, L. cattalini, G. Maragoni, B. Pitteri and T. Bobbo; *Transition Met. Chem.*, **1997**, *22*, 46

[13] (a) J. Vicente, J.A. Abad, M.-T. Chicote, M.-D. Abrisqueta, J.-A. Lorca and M.C. Barmirez de Arellano; *Organometallics*, **1998**, *17*, 1564-1568 (b) S. Narayan, V.K. Jain and B. Varghese; *J. Chem. Soc. Dalton Trans.*, **1998**, 2359-2366 (c) S.L. James, M. Younus, P.R. Raithby and J. Lewis; *J. Organomet. Chem.*, **1997**, *543*, 233-235 (d) G.M. Kapteijn, M.D. Meijer, D.M.

Grove, N. Veldman, A.L. Spek and G. van Koten; *Inorg. Chim. Acta*, **1997**, *264*, 211-217

[14] (a) J.A. Weinstein, N.N. Zheligovskaya, M.Y. Mel'nikov and F. Hartl; *J. Chem. Soc. Dalton Trans.*, **1998**, 2459-2466 (b) A. Klein, S. Hasenzahl, W. Kaim and J. Fiedler; *Organometallics*, **1998**, *17*, 3532-3538 (c) W.-H. Leung, T.S. Hun, S. Fung, I.D. Williams and K.-Y Wong; *Polyhedron*, **1997**, *16*, 3641-3648

[15] (a) A. Gelling, M.D. Olsen, K.G. Orrell, A.G. Osborne and V. Šik; *J. Chem. Soc. Dalton Trans.*, **1998**, 3479-3488 (b) A. Gelling, K.G. Orrell, A.G. Osborne and V. Šik; *J. Chem. Soc. Dalton Trans.*, **1998**, 937-945

[16] M. Rakowski DuBois; *Coord. Chem. Rev.*, **1998**, *174*, 191-205

[17] (a) J. Zakrzewski; *J. Organomet. Chem.*, **1987**, *327*, C41 (b) M.Rakowski DuBois, K.G. Parker, C. Ohman, B.C. Noll; *Organometallics*, **1997**, *16*, 2325-2334

[18] (a) F. Kvietok, V. Allured, V. Carperos and M. Rakowski DuBois; *Organometallics*, **1994**, *13*, 60-68 (b) H. Felkin, J. Zakrzewski; *J. Am. Chem. Soc.*, **1985**, *107*, 3374-3375

[19] (a) G. Mann, J.F. Hartwig, M.S. Driver and C. Fernández-Rivas; *J. Am. Chem. Soc.*, **1998**, *120*, 827-828 (b) R. Vann Bynum, W. E. Hunter, R.D. Rogers and J.L Atwood; *Inorg. Chem.*, **1980**, *19*, 2368-2374

[20] (a) T.J. Johnson, A.M. Arif and J.A. Gladysz; *Organometallics*, **1993**, *12*, 4728-4730 (b) M.M.P. Ng, W.R. Roper and L.J. Wright; *Organometallics*, **1994**, *13*, 2563-2565 (c) G.R. Clark, M.M.P. Ng, W.R. Roper and L.J. Wright; *J. Organomet. Chem.*, **1995**, *491*, 219-229

[21] K. Hübler, U. Hübler, W.R. Roper and L. J. Wright; *J. Organomet. Chem.*, **1996**, *526*, 199-202

[22] J. Muller, P.E. Gaede and K. Qiao; *Z. Naturforsch., B: Chem. Sci.*, **1994**, *49*, 1645-1653

[23] (a) G. Dyker; *Angew. Chem. Int. Ed.*, **1999**, *38*, 1698-1712 (b) A.E. Shilov and G.B. Shul'pin; *Chem. Rev.*, **1997**, *97*, 2879-2932 (c) A.D. Ryabov; *Chem. Rev.*, **1990**, *90*, 403-424

[24] (a) H.E. Bryndza and W. Tam; *Chem. Rev.* **1988**, *88*, 1163-1188 (b) M.D. Fryzuk and C.D. Montgomery; *Coord. Chem. Rev.*, **1989**, *95*, 1-40

[25] R.L. Cowan and W.C. Trogler; *J. Am. Chem. Soc.*, **1989**, *111*, 4750-4761

[26] S. Park, D.M. Roundhill and A.L Rheingold; *Inorg. Chem.*, **1987**, *26*, 3974-3976

[27] J. H. Nelson, D.L. Schmitt, R.A. Henry, D.W. Moore and H.B. Jonassen; *Inorg. Chem.*, **1970**, *9*, 2678-2681

[28] (a) D. Hedden and D.M. Roundhill; *Inorg. Chem.*, **1986**, *25*, 9-15 (b) S. Park, D. Hedden and D.M. Roundhill; *Organometallics*, **1986**, *5*, 2151-2152 (c) D. Hedden, W.C. Fultz, A.L.

Rheingold and D.M. Roundhill; *J. Am. Chem. Soc.*, **1984**, *106*, 5014-5016

[29] R.L. Cowan and W.C. Trogler, *Organometallics*, **1987**, *6*, 2451-2453

[30] J.S. Merola and F. T. Ladipo; *Inorg. Chem.*, **1990**, *29*, 4172-4173

[31] A.L. Casalnuovo, J.C. Calabrese and D. Milstein; *J.Am. Chem. Soc.*, **1988**, *110*, 6738-6744

[32] J. Fornies, M. Green, J.L. Spencer and F.G.A. Stone; *J. Chem. Soc. Dalton Trans.*, **1977**, 1006-1009

[33] J.J. Garcia, A.L.Casado, A. Iretskii, H. Adams and P.M. Maitlis; *J. Organomet. Chem.*, **1998**, *558*, 189-192

[34] A. Pidcock, R.E. Richards and L.M. Venanzi; *J. Chem. Soc. A*, **1966**, 1707-1710

[35] G.N. Glavee, L.M Daniels and R.J. Angelici; *Organometallics*, **1989**, *8*, 1856-1865

[36] D.M. Roundhill, *Adv. Organomet. Chem.*, **1975**, *13*, 273-361

[37] (a) A.F. Clemmitt and F. Glockling; *J. Chem. Soc. A*, **1969**, 2163-2165 (b) J. Chatt and B.L. Shaw; *J. Chem. Soc.*, **1962**, 5075 (c) W. Beck and M. Bauder; *Chem. Ber.*, **1970**, *103*, 583-589

[38] (a) J.O. Noell and P.J. Hay; *J. Am. Chem. Soc.*, **1982**, *104*, 4578-4584 (b) J.J. Low and W.A. Goddard; *J. Am. Chem. Soc.*, **1984**, *106*, 6928-6937 (c) S. Obara, K. Kitaura and K. Morokumna; *J.Am. Chem. Soc.*, **1984**, *106*, 7482-7492

[39] T.G. Appleton, H.C. Clark and L.E. Manzer; *Coord. Chem. Rev.*, **1973**, *10*, 335-422

[40] D.L. Packett, C.M. Jensen, R.L. Cowan, C.E. Strouse and W.C. Trogler; *Inorg. Chem.*, **1985**, *24*, 3578-3583

[41] (a) R.S. Paonessa and W.C. Trogler; *Organometallics*, **1982**, *1*, 768-770 (b) J. Braddock-Wilking, Y. Levchinsky and N.P. Rath; *Organometallics*, **2000**, *19*, 5500-5510

[42] S. Gründemann, A. Kovacevic, M. Albrecht, J.W. Faller and R.H. Crabtree; *Chem. Commun.*, **2001**, 2274-2275

[43] (a) E.O. Greaves, R. Bruce and P.M. Maitlis; *J. Chem. Soc.Chem. Commun.*, **1967**, 860 (b) R. H. Crabtree in *The Organometallic Chemistry of the Transition Metals*, John Wiley and Sons, New York, 1988, p. 53

[44] T. Eicher and S. Hauptmann in *The Chemistry of Heterocycles*, Georg Thieme Verlag, Stuttgart, 1995, pp 86-89 (pyrrole), 165-167 (imidazole), 180-181 (pyrazole), 175 (benzimidazole), 185 (indazole)

[45] W.D. Jones, L. Dong and A.W. Myers; *Organometallics*, **1995**, *14*, 855-861

[46] N.W. Gable, *J. Org. Chem.*, **1962**, *27*, 301-303

[47] R. L. Hinman and S. Theodoropulos; *J. Org. Chem.*, **1963**, *28*, 3052-3058

[48] A.H. Jackson in *Comprehensive Organic Chemistry*, ed. P.G. Sammes, Pergamon Press, Oxford, 1979, pp 296-300

[49] P.W. Shum and A. P. Kozikowski, *Tetrahedron Lett.*, **1990**, *31*, 6785-6788

[50] P.J. Brothers; *Adv. Organomet. Chem.*, **2001**, *46*, 224-315

[51] R.S. Paonessa, A.L. Prignano and W.C. Trogler; *Organometallics*, **1985**, *4*, 647-657

[52] D.R. Schaad and C.R. Landis; *Organometallics*, **1992**, *11*, 2024-2029

[53] S. Otsuka, T. Yoshida, M. Matsumoto and K. Nakatsu; *J. Am. Chem. Soc.*, **1976**, *98*, 5850-5858

[54] T. Yoshida and S. Otsuka; *J. Am. Chem. Soc.*, **1977**, *99*, 2134-2140

[55] C. Müller, R.J. Lachicotte and W.D. Jones; *Organometallics*, **2002**, 21, 1190-1196

[56] C. Müller, C.N. Iverson, R.J. Lachicotte and W.D. Jones; *J. Am. Chem. Soc.*, **2001**, *123*, 9718-9719

[57] (a) C.K.Ghosh, D.P.S. Rodgers and W.A.G. Graham; *J. Chem. Soc. Chem. Commun.*, **1988**, 1511-1512 (b) C.K.Ghosh and W.A.G. Graham; *J. Am. Chem. Soc.*, **1989**, 111, 375-376

[58] (a) R.A. Jones in *Comprehensive Heterocyclic Chemistry*, ed. K.T. Potts, editorial board A.R. Katritzky and C.W. Rees; Vol. 5 Part 4A, Pergamon Press, Oxford, 1984, p235

[59] HyperChem ® Pro 6, Hypercube Inc., Gainsville, U.S.A.

[60] (a) W.P. Fehhammer, A. Völkl, U. Plaia and G. Beck; *Chem. Ber.* **1987**, *120*, 2031 (b) F. Bonati, A. Burini, B.R. Pietroni and B. Bovio; *J. Organomet. Chem.*, **1989**, *375*, 147 (c) J. Muller and R. Stock; *Angew. Chem., Int. Ed. Engl.*, **1983**, *22*, 993 (d) H.G. Raubenheimer, M. Desmet and L. Lindeque; *J. Chem. Res.*, **1995** (5), 184-185

[61] D. Bourissou, O. Guerret, F.P. Gabbai and G. Bertrand; *Chem. Rev.*, **2000**, *100*, 39-91

[62] A.J. Arduengo, III., R.L. Harlow and M. Kline; *J.Am. Chem. Soc.*, **1991**, *113*, 361-

[63] (a) T.M. Trnka and R.H. Grubbs; *Acc. Chem. Res.*, **2001**, *34*, 18 (b) A. Fürster; *Angew. Chem., Int. Ed.*, **2000**, *39*, 3012-3042

[67] G. Sini, O. Eisenstein and R.H. Crabtree; *Inorg. Chem.*, **2002**, *41*, 602-604

[68] (a) G. Mestroni, E. Alessio, A. Sessanta o Santi, S. Geremia, A. Bergamo, G. Sava, A. Boccarelli, A. Schettino, M. Coluccia; *Inorg. Chim. Acta*, **1998**, *273*, 62-71 (b) K. Nomiya, R. Noguchi, K. Ohsawa, K. Tsuda, M. Oda; *J. Inorg. Biochem.*, **2000**, *78*, 363-370

[69] C. Pettinari, F. Marchetti, R. Polimante, A. Cingolani, G. Portalone and M. Colapietro, *Inorg. Chim. Acta*, **1996**, *249*, 215-229

[70] (a) K. Schofield, M.R. Grimmett and B.R.T. Keene in *Heteroaromatic nitrogen compounds: the azoles*, Cambridge University Press, 1976, p 22 (b) T. Yagil; *Tetrahedron*, **1967**, *23*, 2855-2861

[71] S. Trofimenko; *Chem. Rev.*, **1972**, *72*, 497-509

[72] J.L. Atwood, K.R. Dixon, D.T. Eadie, S.R. Stobart and M.J. Zaworotko; *Inorg. Chem.*, **1983**, *22*, 774-779

[73] P.K. Byers, A.J. Cantry and R.J. Honeyman; *Adv. Organomet. Chem.*, **1992**, *34*, 1-63

[74] (a) M. Cano, J.A. Campo, J.V. Heras, J. Lafuente, C. Rivas and E. Pinilla; *Polyhedron*, **1995**, *14*, 1139-1147 (b) M.A. Angaroni, G.A. Ardizzoia, T. Beringhelli, G.D'Alfonso, G. La Monica, N. Masciocchi and M.Moret; *J. Organomet. Chem.*, **1989**, *363*, 409-418

[75] (a) F. Bonati and H.C. Clark, *Can. J. Chem.*, **1978**, *56*, 2513-2515 (b) G. Minghetti, G. Banditelli and F. Bonati; *J. Chem. Soc, Dalton Trans.*, **1979**, 1851-1856 (c) A.L. Bandini, G. Banditelli, G. Minghetti and F. Bonati; *Can. J. Chem.*, **1979**, *57*, 3237-3242

[76] G.W. Bushnell, K.R. Dixon, D.T. Eadie and S.R. Stobart; *Inorg Chem.*, **1981**, *20*, 1545-1552

[77] K.R. Dixon; *Inorg. Chem.*; **1977**, *16*, 2618-2624

[78] J. Catalan, R.M. Claramunt, J. Elguero, J. Laynez, M. Menendez, F. Anvia, J.H. Quian, M. Taajepera and R.W. Taft; *J. Am. Chem. Soc.*, **1988**, *110*, 4105-4111

[79] D.M. Roundhill; *Inorg. Chem.*, **1970**, *9*, 254-258

[80] Merck index, 12th ed., Merck and Co. Inc., 1996

/ End of Chapter 4 //

CHAPTER 5

Homogeneous C-H Activation of Aromatic Heterocycles by $[Pt(PEt_3)_4]$

5.1 INTRODUCTION

As discussed in previous chapters, C-S and N-H bond activations by zerovalent platinum complexes have been observed with thiophenes and with azoles respectively. In addition, evidence of C-H activation was obtained for 1-methylpyrrole. We now consider other aromatic, π-excessive heterocycles (*eg.* oxygen-containing heteroaromatic compounds) and their reactions with tetrakis(triethylphosphine)platinum(0). Although C-O bond cleavage is proposed as being a key step in the hydrodeoxygenation of oil feedstocks [1], relatively few examples of C-O bond activation have been reported in the literature.

Transition metal-mediated cleavage of C(allyl)-O bonds occurs fairly readily and is widely utilised in catalytic organic synthetic processes by combining it with subsequent other reactions *eg.* nucleophilic attack [2]. Examples of stoichiometric processes are more limited. C-O single bonds of esters, lactones and anhydrides also react with low valent transition metal complexes to give oxidative addition products. These reactions are facilitated by the electron-withdrawing carbonyl group. In contrast, C-O single bond activation of ethers, alcohols and acetals are relatively rare. Insertion into C(alkyl)-O and C(aryl)-O ether bonds by palladium(II) and rhodium(I) complexes respectively, is aided by chelation to substituents on the ether molecule *i.e.* ether derivatives of PCP-pincer type molecules (Figure 5.2, where R' = OMe or

OPh) [3]. $Ta(silox)_3$ (where silox = $^tBu_3SiO$) oxidatively inserts into the C(sp^2)-O bond of 1,2-dihydrofuran and into the C-O bond of 3,3-dimethyloxetane. Six- and five-membered metallacycles are formed respectively [4].

The first, and only, example of an aromatic heterocyclic C-O bond activation has recently been reported in the literature [5a,b]. A $Pt(PPh_3)_2$ moiety is able to oxidatively insert into the C(vinyl)-O bond of a η^6-$Mn(CO)_3^+$ bonded benzofuran complex (Figure 5.1). Coordination of the manganese to the carbocyclic ring has previously been found to activate benzo- and dibenzothiophene towards C-S insertion by metal nucleophiles.[5b, c]. In the absence of pre-coordination by the η^6-$Mn(CO)_3^+$ group, C-O activation is considerably less favourable than C-S cleavage due to the high C-O bond strength and to the fact that late transition metals prefer bonding to S than to O. The bonds more accessible to oxidative addition by a platinum(0) centre would more likely be the C-H and C-C bonds of the oxygen heterocycle.

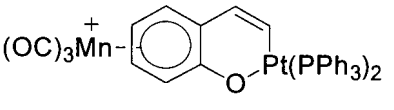

Figure 5.1 Insertion of $Pt(PPh_3)_2$ into activated benzofuran

A theoretical study of the mechanism of C-C and C-H reductive elimination and oxidative addition of Pt(II) / Pt(IV) systems was undertaken by Puddephatt and Hill [6]. From density functional theory (DFT) calculations they concluded that C-H reductive elimination and oxidative addition are much easier than C-C reductive elimination and oxidative addition. A review by Milstein and Rybtchinski addresses the thermodynamic and kinetic factors which favour C-H over C-C bond activation [7]. The C-H bonds are more amenable to oxidative addition as it is generally easier for the metal centre to approach a C-H bond than a C-C bond and C-H bonds are also statistically more abundant. Oxidative additions into C-C bonds are accompanied by considerably larger activation energy barriers as a result of the more directed nature of C-C bonds. Contrastingly, in the transition state, the hydrogen atom in a C-H bond can bond simultaneously, via its 1*s* orbital, to both the carbon atom and the metal centre. The

formation of an M-H bond (where M = transition metal centre) is thermodynamically favoured over M-C bond formation as M-H bonds are generally much stronger than M-C(alkyl) bonds and usually stronger than M-C(aryl) bonds [8], although an M-C(aryl) bond where M = Rh or Ir has been found to be even stronger than the corresponding M-H bonds [9].

Although C(aryl)-C(aryl) bonds are very strong, the reaction of $[Pt(PEt_3)_3]$ with biphenylene leads to C-C activation rather than C-H activation [10]. Insertion into the C-C bond reduces the ring strain and leads to the formation of two new Pt-C(aryl) bonds, which are relatively strong bonds. Another example where a C-C site is preferred over a C-H bond is the unusual transition metal buckybowl complex $[Pt(\eta^2\text{-}\sigma\text{-}C_{30}H_{12})(PPh_3)_2]$. It is formed in the reaction of a semibuckminsterfullerene ($C_{30}H_{12}$) molecule with the zerovalent platinum complex $[Pt(CH_2{=}CH_2)(PPh_3)_2]$ [11]. Activation of C-C bonds by soluble metal complexes is not only driven by relief of steric strain, but can also be achieved when energy is gained by aromatisation [12], or when coupled to an exothermic process (C-C activation followed by reductive elimination). Other unstrained systems which lead to C-C activation are complexes stabilised by agostic interactions [13], certain cluster complexes [14], and electrochemically induced systems [15].

In complexes of PCP and PCN "pincer" ligands (Figure 5.2), C-C and C-H activation processes compete with each other depending on the nature of the ligand substituents [7,16].

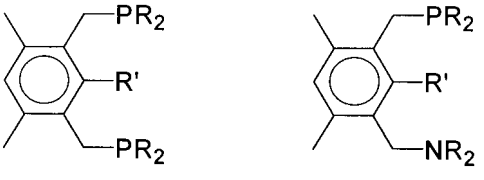

Figure 5.2 PCP and PCN pincer type ligands, where R′ = H or Me

In the absence of driving forces such as relief of steric strain or energy gain from aromatisation, C-H bond activation is likely to prevail over C-C bond activation. For the heterocycles to be considered, it is thus expected that C-H rather than C-C bond activation would occur. The C-H bond most reactive to oxidative insertion by a low-valent transition

metal complex has been highlighted in each case.

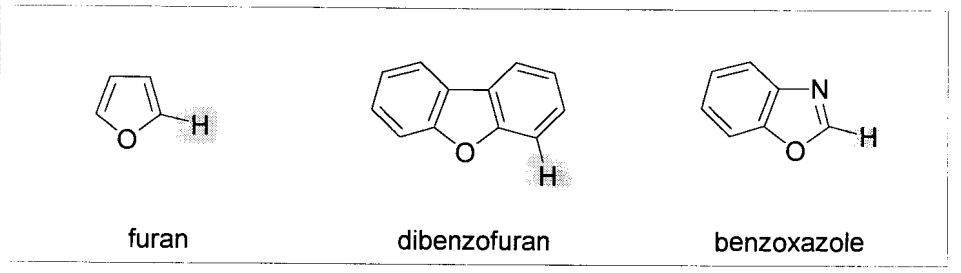

furan dibenzofuran benzoxazole

The activation and functionalisation of C-H bonds (as well as C-C and C-heteroatom bonds) in homogeneous solution is an important challenge as it could lead to the design of new processes for the utilisation of hydrocarbons and small organic molecules. The catalytic activation and cleavage of C-H bonds by transition metal catalysts has led to the development of efficient C-C coupling processes [17]. Other examples of the application of C-H activation for catalysis include the Heck reaction, hydrovinylation, and C-heteroatom coupling.

C-H bond activation by metal complexes can be classified into three main groups according to the mechanism of cleavage [18].

- "True" activation results in the formation of σ-organyl metal hydride complexes $RH + [M^{n+}] = R\text{-}[M^{(n+2)+}]\text{-}H$.
- A metal complex may cleave a C-H bond without a C-[M] intermediate being generated directly.
- A metal complex may promote the formation of a reactive species which then attacks a C-H bond.

Intramolecular activation of C-H bonds (also called cyclometallation [19]) occurs more easily than intermolecular activation. The intramolecular activation of aryl C-H bonds has been well-studied and is facilitated by coordination to donor substituents attached to the aryl ligand (*eg.* "pincer ligands", Figure 5.2) [16]. This chelation-assisted C-H (or C-C) bond activation is not limited to pincer-type ligands. A mixture of $[RhL_3Cl]$, 2-amino-3-picoline and a ketone or aldehyde leads to the formation of a cyclometallated aldimine hydride complex which is capable of catalytic hydroacylation [20].

Examples of aromatic C-H bond activation are more numerous than that of alkyl (or benzyl) C-H bonds. This phenomenon has been explained in terms of kinetics where coordination to the arene via the π-electrons is considered to be a "pre-activation" which leads to oxidative addition (Figure 5.3) [21].

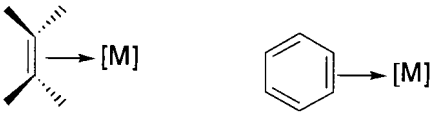

Figure 5.3 Pre-coordination leading to C-H oxidative addition

Alkyl C-H bonds form much weaker adducts (*eg.* agostic complexes) to transition metal complexes. M-C(alkyl) bonds are weaker than M-C(aryl) bonds [8] and the bond dissociation energy of an aryl C-H bond is smaller than, or comparable to, the sum of the M-H and M-C(aryl) bond dissociation energies, thus favouring C(aryl)-H bond cleavage.

This chapter focusses on reactions of furan, dibenzofuran, benzoxazole, benzothiazole and thiazole with tetrakis(triethylphosphine)platinum(0). It should be borne in mind that divalent platinum can also effect C-H activation, but it does so through electrophilic and nucleophilic means [19]. The activation of C-H bonds by platinum(0), though, is considered to be a "true" oxidative addition.

5.2 RESULTS AND DISCUSSION

The oxidative addition products obtained from the reactions of [$Pt(PEt_3)_4$] with furan, benzothiazole and benzoxazole respectively were isolated after heating the reaction mixtures under reflux. Oxidative insertions into a C-H bond was achieved in each of the three cases to yield complexes of the type *trans*-[$PtHX(PEt_3)_2$] where X is a carbon-σ-bonded furanyl, benzoxazolyl and benzothiazolyl respectively, **5-1** to **5-3**. The complexes were characterised by NMR spectroscopy and MS.

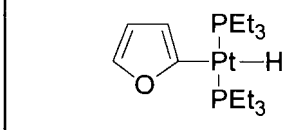

5-1

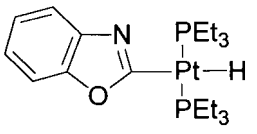

5-2

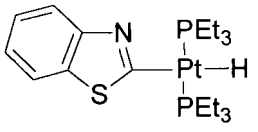

5-3

These reactions contrast markedly with the kinetics of the reactions of [$Pt(PEt_3)_4$] with the nitrogen heterocycles[1], which were generally rapid at room temperature. More rigorous conditions were required to activate C-H bonds than N-H bonds; N-H bonds being weaker and the NH hydrogen atom more acidic.

The activation of C-H bonds of a variety of saturated and unsaturated hydrocarbons (*eg.* benzene, cyclohexane) by the transient platinum(0) complex bis(dicyclohexylphosphino-ethane)platinum(0) has been described [22]. This platinum(0) intermediate is formed *in situ* by the reductive elimination of neopentane from *cis*-[PtH(neopentyl){bis(dicyclo-hexylphosphino)ethane}]. The chelating phosphine ligand imposes a bent geometry on the bis(phosphine)platinum(0) complex, considerably enhancing the reactivity. Linear bis(phosphine) complexes, in turn, do not activate the C-H bonds of benzene and toluene. The chelating ligand is thus thought to be a prerequisite for such reactions. In 2001, Cavell *et al* reported the first example of a C-H activation by a platinum(0) complex that did not contain a chelating ligand [23]. The hydrido platinum(II) carbenes, *cis*- and *trans*-[PtH(1,3-dimethylimidazolin-2-ylidene(PPh_3)$_2$]BF_4 were formed (*ca.* 15% by NMR) by heating equimolar quantities of [$Pt(PPh_3)_4$] and 1,3-methyl-imidazolium tetrafluoroborate.

5.2.1 Reaction of [$Pt(PEt_3)_4$] with Furan

Furan, like its sulfur- and nitrogen- five-membered counterparts thiophene and pyrrole, is π-excessive (the π-electron density on each atom is greater than that on benzene), aromatic

[1] Refer to Chapter 4

compound (Figure 5.4).

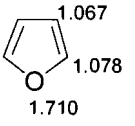

Figure 5.4 π-electron densities of furan

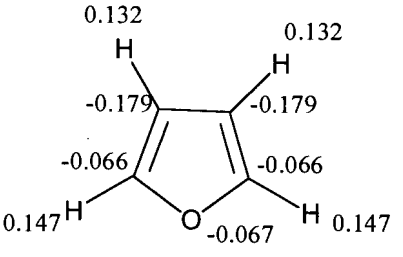

Figure 5.5 Point charges on each atom of furan [25]

Although furan is an extremely weak Brønsted acid, its pK_a has been estimated to be 35.6 in tetrahydrofuran [24], the $Pt(PEt_3)_2$ moiety is basic enough to achieve C-H activation and the complex *trans*-hydrido(2-furanyl)bis(triethylphosphine)platinum(II), **5-1**, was isolated when [$Pt(PEt_3)_4$] was reacted with excess furan. The position of attachment of platinum to the furanyl ring is at C-2, the carbon atom in the α-position with respect to the heteroatom. This is also the site for lithiation by butyllithium where the butylate base essentially abstracts the proton from C-2 (See Figure 5.5 for point charges on each atom of furan [25]). A C-H activation at the α-position of furan was reported for the thermolysis (60°C for 23 hours) of [$Rh(C_5Me_5)(H)Ph(PMe_3)$] in the presence of excess furan [26]. When furan was blocked at positions C-2 and C-5 by methyl substituents, a C-H activation at the β-position occurred to generate the complex [$Rh(C_5Me_5)(H)(3\text{-}\{2,5\text{-dimethylfuranyl}\})(PMe_3)$].

The π-excessive nature of furan, and the fact that furan has a lower resonance energy than benzene allows for furan to attach a platinum centre at C-2, whilst benzene does not undergo a reaction under similar conditions. In fact, benzene or toluene is used as the solvent in oxidative addition reactions of this type.

A compound similar to **5-1** has been reported in the literature [27]. *Trans*-hydrido-2-(5-phenyloxycarbonylfuranyl)bis(triethylphosphine)platinum(II), Figure 5.6, was prepared from phenyl 2-furoate and *trans*-[PtH(NHPh)(PEt$_3$)$_2$].

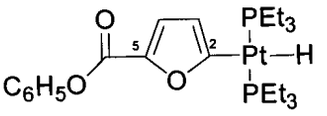

Figure 5.6 *Trans*-hydrido-2-(5-phenyloxycarbonylfuranyl)bis(triethylphosphine)platinum(II)

The authors regards this reaction as a C-H activation rather than a process involving deprotonation of the phenyl 2-furoate by the anilide anion followed by coordination of the resultant furanyl carbanion to the platinum centre. The driving force for the reaction is probably the formation of a stronger Pt-C bond which has been shown to be thermodynamically more stable than a Pt-N bond [28]. Interestingly, the complex mentioned above, [Rh(C$_5$Me$_5$)(H)Ph(PMe$_3$)], in the presence of stoichiometric amounts of pyrrole, forms [Rh(C$_5$Me$_5$)(H)(1-pyrrolyl)(PMe$_3$)] after 22 hours at 60°C by oxidative insertion into the N-H bond of pyrrole [26]. The hydride resonance of the N-Rh-H system is more downfield than the C-Rh-H systems, and the Rh-N bond is considered to be stronger than the Rh-C bond.

The catalytic C-C coupling of furan to acrylate by palladium(II) has been documented [29a]. Although this process proceeds via a C-H activation at C-2 of furan, this intermediate was not isolated as palladium readily undergoes reductive elimination to yield the C-C coupled product. Gold(III) chloride similarly catalyses the coupling of 2-methylfuran to methyl vinyl ketone at C-5 [29b].

5.2.2 Reaction of [Pt(PEt$_3$)$_4$] with Benzoxazole

Benzoxazole is similar to the anellated furan *viz.* benzo[*b*]furan, but with a pyridine-like nitrogen atom at position 3. Benzoxazole rather than oxazole was chosen as a ligand because it is commercially available. It can also be compared to benzimidazole where an NH group takes the position of the oxygen atom. Benzoxazole undergoes a similar type of reaction with

$[Pt(PEt_3)_4]$ as does furan. Oxidative insertion into a C-H bond at the most acidic hydrogen atom (Figure 5.6) *viz.* at position C(2)-H(2), to yield (2-benzoxazolyl)hydridobis-(triethylphosphine)platinum(II), **5-2**.

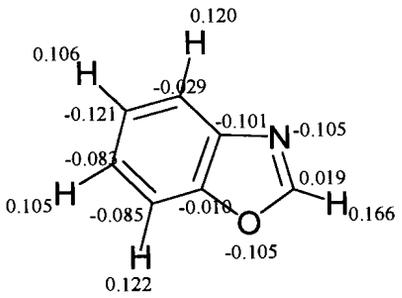

Figure 5.6 Point charges on each atom of benzoxazole [25]

5.2.3 Reaction of $[Pt(PEt_3)_4]$ with Benzothiazole

Thiazoles have been used as neutral *N*-donor ligands with transition metals *eg. cis*- and *trans*-[Pt(dmso)(*N*-thiazole)Cl_2] (dmso = dimethylsulfoxide) [30]. Benzothiazole carbenes have also been used as ligands in a similar way as has imidazole and triazole. Recently the first palladium benzothiazole carbene, bis(2,3-dihydro-3-methlbenzothiazole-2-ylidine)palladium(II) diiodide, has been found to catalyse Heck coupling reactions [31].

The reaction of benzothiazole with $[Pt(PEt_3)_4]$ is an interesting case. The activation of the C-N bond of an aromatic heterocycle is difficult and is extremely rare [32]. There are thus two possible bonds into which the $Pt(PEt_3)_2$ group can oxidatively insert (Figure 5.7). The first possible reactive site is at a C-S bond, in which case a thiaplatinacycle analogous to **3-1** would be expected to form. A $Pt(PEt_3)_2$ moiety is able to oxidatively insert into a C(aryl)-S bond of dibenzothiophene, but where there is a choice of a C(aryl)-S and a C(vinyl)-S bond as in benzothiophene, the C(vinyl)-S bond is the preferred site of attack[2] [33a]. There are two explanations for the C(vinyl)-S bond being favoured: a steric effect, and the weakening of the C(vinyl)-S bond relative to the C(aryl)-S bond as a result of pre-coordination, Figure 5.3 [33].

[2] Refer to Chapter 3

The second possibility is a C-H activation at position C-2 to form a complex analogous to the hydride complex obtained for benzoxazole **5-2**.

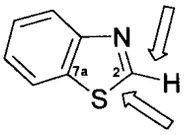

Figure 5.7 Possible reactive sites for insertion of a $Pt(PEt_3)_2$ moiety

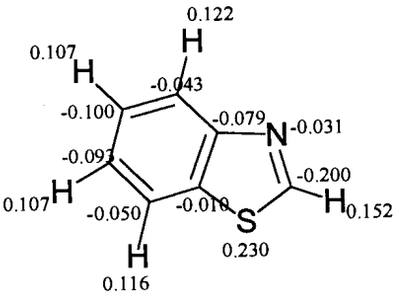

Figure 5.8 Point charges on each atom of benzothiazole

In fact, the second scenario was found to be applicable and a C-H activation at C-2 resulted in the isolation of (2-benzoxazolyl)hydridobis(triethylphosphine)platinum(II), **5-3**.

Column chromatography of **5-3** on silica gel (diethyl ether/ hexane eluent) caused this complex to undergo a change to form a bridging hydride species. For comparative purposes, a short discussion of the μ-hyride decomposition product follows: While the ^1H NMR spectrum terminal hydride of **5-3** showed a triplet resonance signal, the decomposition product's ^1H NMR spectrum displayed a doublet of doublet of doublet pattern centred at -5.455 ppm and flanked by two sets of ^{195}Pt-satellites (Figure 5.9).

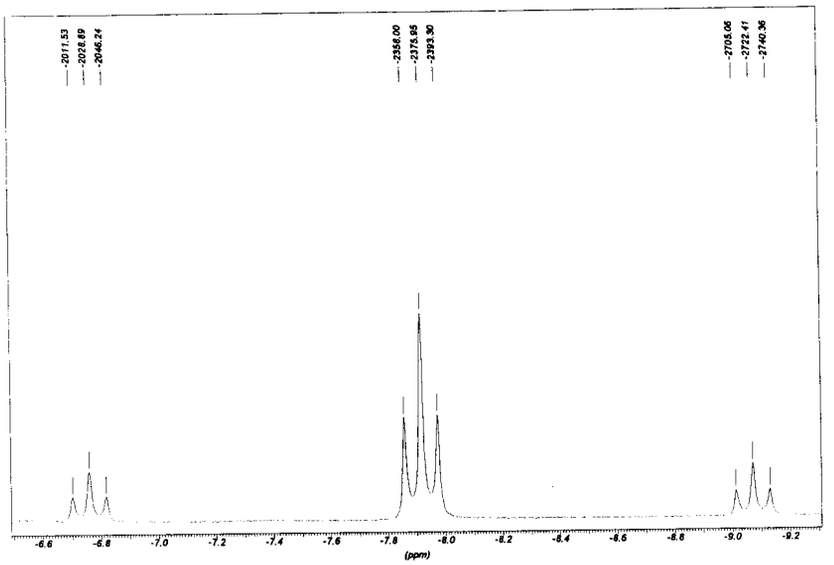

a) Terminal hydride of **5-3**

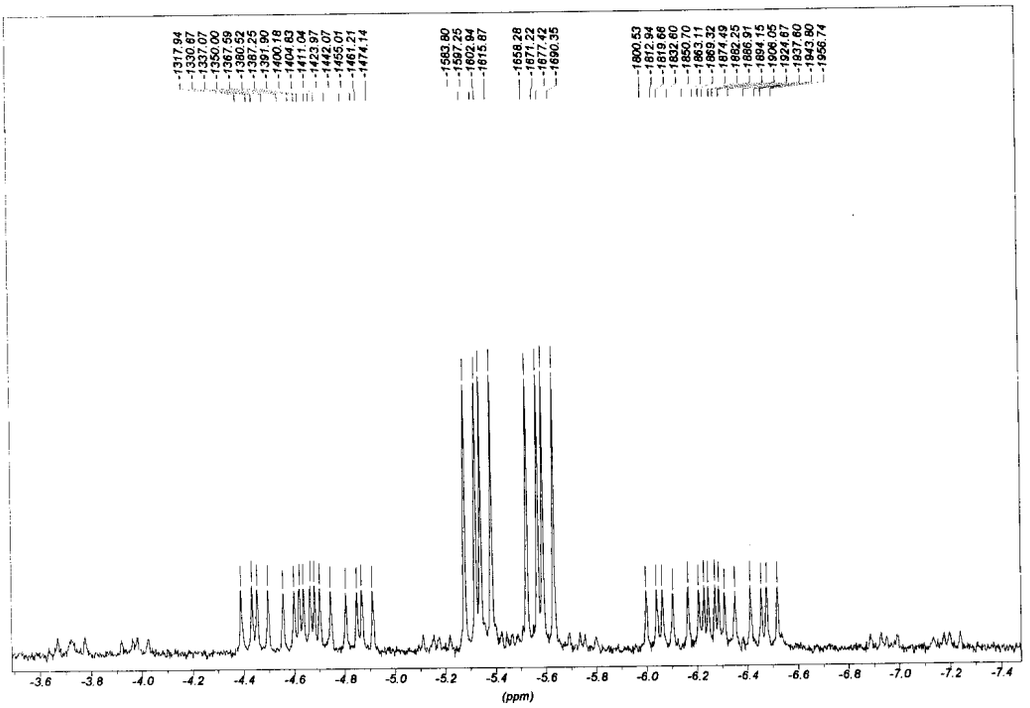

b) Bridging hydride of decomposition product

Figure 5.9 Comparison of the high-field ^1H NMR spectrum for terminal and bridging hydrides

This pattern of three superimposed subspectra arises from the three different isotopomeric combinations of platinum nuclei having different nuclear spins (Pt/Pt 43.8%, ^{195}Pt/Pt 22.4%, Pt/^{195}Pt 22.4% and ^{195}Pt/^{195}Pt 11.4%). The whole resonance thus has a pseudo quintet structure, 1:8:18:8:1 (central ddd {18}, outer ddd {1} and overlapping ddd for the remaining {4:4}). The magnitudes of the $^1J_{Pt\text{-}H}$ coupling constants are 533 Hz and 432 Hz. These values fall within the range previously found for other $Pt_2(\mu\text{-}H)$ complexes [34]. The couplings pattern also indicates that the hydride proton is coupled to three nonequivalent phosphines: $^2J_{P\text{-}H}$ *trans* to H = 74.5 Hz, $^2J_{P\text{-}H}$ *cis* to H = 19.1 Hz and $^2J_{P\text{-}H}$ *cis* to H = 12.9 Hz (J *trans* > J *cis* [35]). This is further substantiated by the presence of three different phosphorus resonances in the $^{31}P\{^1H\}$ NMR spectrum; the chemical shifts of which are typical of phosphines. Although the spectrum is complicated, the coupling pattern could be resolved to indicate a bimetallic complex (Table 5.1). This data indicates that a bridging phosphido group is not present as such groups resonate far downfield (> 100 ppm) [36].

Table 5.1 $^{31}P\{^1H\}$ NMR data for μ-hydride complex

	P_a	P_b	P_c
δ / ppm	23.63	3.40	1.95
J	$J_{P\text{-}P}$ 33.1 Hz $J_{P\text{-}P}$ 2.5 Hz $^2J_{Pt\text{-}P}$ 488 Hz $^1J_{Pt\text{-}P}$ 4705 Hz	$J_{P\text{-}P}$ 24.2 Hz $J_{P\text{-}P}$ 2.5 Hz $^2J_{Pt\text{-}P}$ 96 Hz $^1J_{Pt\text{-}P}$ 2458 Hz	$J_{P\text{-}P}$ 24.2 Hz $J_{P\text{-}P}$ 33.1 Hz $^2J_{Pt\text{-}P}$ 120 Hz $^1J_{Pt\text{-}P}$ 2411 Hz

Values of $J_{P\text{-}P}$ coupling constants fall into a wide range depending on the identity of the co-ligands. The coupling constants of P_c seems to indicate that the values of 33.1 Hz and 24.2 Hz are $^{3\text{ or }4}J_{P\text{-}P}$ coupling and that 2.5 Hz is a $^2J_{P\text{-}P}$ coupling, although the latter value is smaller than would be expected for a *cis*-phosphine coupling [37]. P_a and P_c would thus have to be mutually *cis* and P_a is mostly likely *trans* to the bridging hydride (Figure 5.10). Although the $^1J_{Pt\text{-}P}$ coupling for a phosphine *trans* to a bridging hydride is expected to be larger than when it is *trans* to a terminal hydride ligand, the value for P_a is unusually large, thus indicating that the Pt(1)-H interaction is weak [38]. The $^1J_{Pt\text{-}P}$ coupling for P_b and P_c (*cis* to bridging hydride) fall

into the usual range [37a]. $^2J_{Pt\text{-}P}$ values are generally considerably smaller than $^1J_{Pt\text{-}P}$ [37].

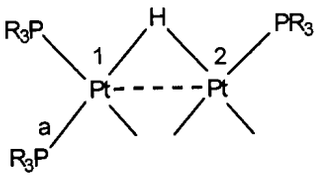

Figure 5.10 Partial structure of the μ-hydride bimetallic complex

The ^{1}H NMR spectrum also indicated the presence of a benzothiazolyl ligand (8.386 d, 1H, 7.590 dd 1H, 7.178 td 1H, 7.018 td 1H). The information was not sufficient to accurately deduce the structure of this bimetallic μ-hyride decomposition product.

5.2.4 Reaction of [Pt(PEt$_3$)$_4$] with 2-Methylbenzothiazole

The effect of blocking the 2-position of benzothiazole on the oxidation reaction of [Pt(PEt$_3$)$_4$] was then considered. A methyl group was thus attached to C-2 (Scheme 5.1).

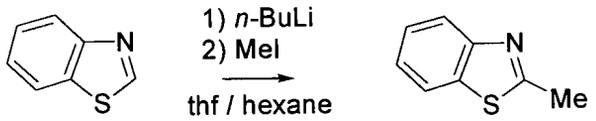

Scheme 5.1 Preparation of 2-methylbenzothiazole

With 2-methylthiophene, C-S activation is directed to the less crowded C-5 position [39]. With 2-methylbenzothiophene, the C(vinyl)-S rather than the C(aryl)-S bond is again the site of attack despite crowding of the α-carbon by the methyl group. Thus, a [Pt(*C*,*S*-C_9H_8S)(PEt$_3$)$_2$] thiaplatinacycle can be obtained with 2-methylbenzothiophene, though it slowly rearranges to give a dimeric thiaplatinacycle [{Pt(*C*,μ-*S*-C_9H_8S)(PEt$_3$)$_2$}$_2$] [40].

The methyl group is known to be acidic and can be readily deprotonated by butyllithium. However, no evidence of a hydride or other oxidative insertion product could be detected by

NMR spectroscopy. In this instance, the Pt(PEt$_3$)$_2$ moiety is not basic enough to activate an alkyl C-H bond.

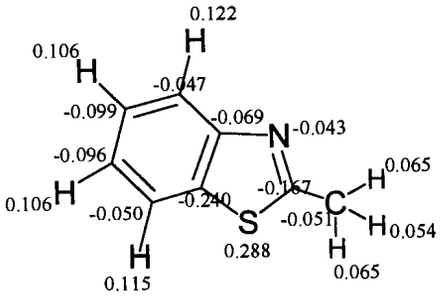

Figure 5.11 Point charges on each atom of 2-methylbenzothiazole [25]

5.2.5 Reaction of [Pt(PEt$_3$)$_4$] with Thiazole

Unlike the reaction of benzothiazole with [Pt(PEt$_3$)$_4$], thiazole did not give a "clean" reaction and a mixture of complexes was obtained. When considering the possible bonds which can be activated, there is a greater probability for C-S activation than in the case of benzothiazole (Figure 5.11).

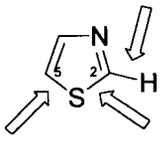

Figure 5.12 Possible sites for activation by Pt(0)

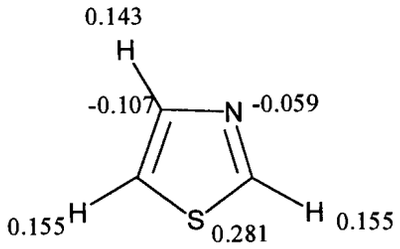

Figure 5.13 Point charges on each atom of thiazole [25]

The hydride region of the NMR spectrum showed a broadened resonance with accompanying ^{195}Pt-satellites at -7.995 ppm ($^1J_{Pt-H}$ coupling = 698 Hz). This is unlike the clearly resolved triplet resonances obtained for **5-3** (and indeed for all the *trans*-hydrides described). Yet the chemical shift and coupling constant correspond very well to the values obtained for the benzothiazolyl hydride, **5-3**. The $^{31}P\{^1H\}$ NMR spectrum showed several different Pt-coupled resonances. A broadened peak at 18.88 ppm with a $^1J_{Pt-P}$ of 2687 Hz could possibly be due to the equivalent phosphines of a *trans*-hydride. Because of the overlapping of signals it was difficult to distinguish the presence of two doublet resonances of approximately equal intensity characteristic of two nonequivalent *cis*-phosphines of a thiaplatinacyle.

The line broadening seems to suggest that exchange process occur in solution. It thus appears that thiazole undergoes C-H bond insertion, but activation of the C-S bond cannot be ruled out.

5.2.6 Reaction of [$Pt(PEt_3)_4$] with Dibenzofuran

After refluxing a mixture of dibenzofuran and [$Pt(PEt_3)_4$] for ninety minutes, the high-field region of the ^1H NMR spectra, when magnified, indicated the presence of hydride species in low concentrations. A doublet of doublet of doublet pattern similar to that obtained for **4-1** and a triplet of doublet pattern (both patterns being accompanied by platinum satellites) indicated a *cis*- and a *trans*-hydrido platinum complex respectively. Furthermore, another triplet pattern of very low intensity was also observed. Table 5.2 summarises the relevant data.

The ^1H and $^{31}P\{^1H\}$ NMR data for the *cis*-hydride complex, **a**, corresponds very well to the data for **4-1** (1-methylpyrrolyl hydride) and the assignments of coupling constants were made accordingly.

Table 5.2 NMR data for Dibenzofuran / Pt(0) reaction mixture (90 min, reflux)

^{1}H NMR (high-field region)			
	cis-hydride, **a**	*trans*-hydride, **b**	*trans*-hydride, **c** (very minor)
PtH δ /ppm	-5.114 ddd	-6.928 td	-6.786 t
$^2J_{Pa-H}$ (P_a *cis* to H)	25.0 Hz	18.0 Hz	18.0 Hz
$^2J_{Pb-H}$ (P_b *trans* to H)	158.1 Hz		
$^1J_{Pt-H}$	977 Hz	683 Hz	653 Hz
other	$^4J_{H-H}$ = 11.1 Hz	1.85 Hz	-
$^{31}P\{^1H\}$ NMR data[3]			
δ /ppm (P_a *cis* to H)	0.21 d	18.3 s	17.5 s
$^2J_{P-P}$	21.6 Hz		
$^1J_{Pt-P}$	2996 Hz	2722 Hz	2819 Hz
δ /ppm (P_b *trans* to H)	11.2 d		
$^2J_{P-P}$	21.6		
$^1J_{Pt-P}$	3886 Hz		

The doublet of triplet pattern for the *trans*-hydride complex, **b**, was puzzling, as it had not been observed for any of the other platinum(II) hydrides presented thus far. Otherwise, the chemical shift and coupling constants (except for the 1.85 coupling) correspond closely to the data for the furanyl hydride, **5-1**. The 1.85 Hz may be a $^4J_{HH}$ coupling.

The very minor *trans*-hydride product, **c**, resonates at a very similar frequency to the *trans*-hydride, **b**, and it is difficult to account for this complex. The proton at positions 4 (or 6) is the acidic proton and activation of the other C-H bonds is not expected to occur (Figure 5.14).

[3] As the reaction of dibenzofuran had not gone to completion, the ^{31}P NMR spectrum was complicated by resonances due to the unreacted $[Pt(PEt_3)_4]$ species and its side-products.

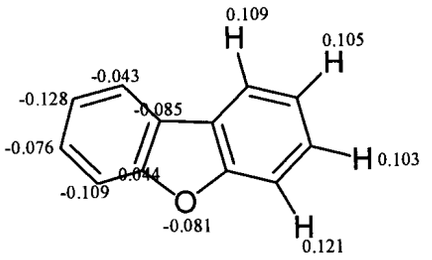

Figure 5.14 Point charges of dibenzofuran [25]

The experiment was therefore repeated; stoichiometric amounts of dibenzofuran and [$Pt(PEt_3)_4$] were refluxed in toluene over a period of several days. The ^1H NMR spectra showed that the reaction had not gone to completion but a single triplet hydride resonance with satellites was present. The relevant data is presented in Table 5.3.

Table 5.3 NMR data for Dibenzofuran / Pt(0) reaction mixture (4 days, reflux)	
^1H NMR (high-field region)	
	trans-hydride
PtH δ /ppm	-6.915
$^2J_{P-H}$	17.9 Hz
$^1J_{Pt-H}$	684 Hz
^{31}P {^1H} NMR data[3]	
δ /ppm	17.5
$^1J_{Pt-P}$	2820 Hz

It thus appears that the *cis*-isomer is formed first but undergoes *cis-trans* isomerisation to form the thermodynamically stable *trans*-isomer. Based on the NMR data, the most likely structures for the hydrides **a** and **b** are:

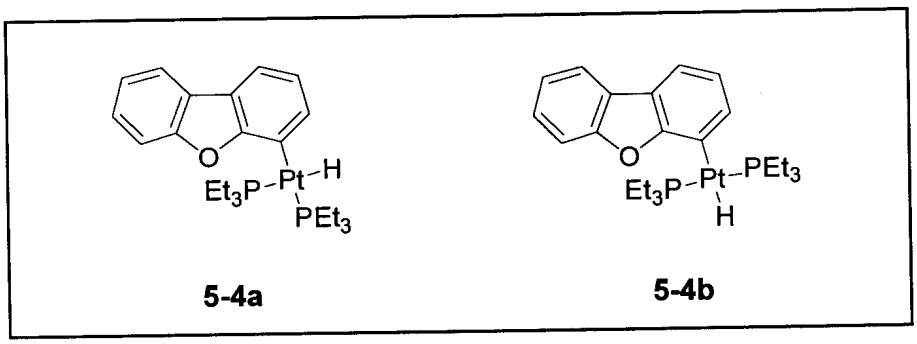

5-4a **5-4b**

5.2.7 NMR Spectroscopy of complexes 5-1 to 5-3

The NMR spectra of the ligands and the complexes were recorded in $CDCl_3$, unless stated otherwise. Refer to Tables 5.4, 5.5 and 5.5 for ^1H, $^{13}C\{^1H\}$ and $^{31}P\{^1H\}$ NMR data for complexes **5-1**, **5-2** and **5-3** respectively. The NMR data for the free ligands are included for comparative purposes. Two-dimensional correlation experiments (COSY and HETCOR) were used to assign peaks were necessary. In general J_{P-C} and J_{Pt-C} couplings were not observed or were unresolved. Hydride ^1H NMR resonances appeared as triplets with accompanying satellites. Phosphines gave singlet resonances with ^{195}Pt satellites in the $^{31}P\{^1H\}$ NMR spectra.

The NMR data of **5-1** compares favourably with the data reported for the complex *trans*-hydrido-2-(5-phenyloxycarbonylfuryl)bis(triethylphosphine)platinum(II) [27]. The latter was recorded in C_6D_6: ^1H NMR δ PtH -6.80 ppm (t, Pt-sat., $^2J_{P-H}$ 18 Hz, $^1J_{PtH}$ 663 Hz), $^{31}P\{1H\}$ NMR δ 20.4 ppm (s, Pt-sat., $^1J_{Pt-P}$ 2690 Hz).

Table 5.4 NMR data for furan and the Pt(II) furanyl hydride **5-1**

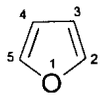	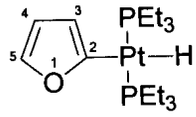
^{1}H NMR δ / ppm	
7.483 d, H-2 & H-5, $^3J_{HH}$ = 1.3 Hz 6.428 d, H-3 & H-4, $^3J_{HH}$ = 1.3 Hz	7.651 m, H-5 6.268 m, H-4 5.794 d, H-3, $^3J_{HH}$ 3.2 Hz 1.71-1.60 m, CH_2 1.05-0.974 m, CH_3 -7.059 t, Pt-sat., PtH, $^2J_{P-H}$ 17.8 Hz, $^1J_{Pt-H}$ = 666 Hz
^{13}C{^{1}H} NMR δ / ppm	
142.48 C-2, C-5 109.37 C-3, C-4	- C-2, not observed 142.22 C-5 111.42 C-3 110.65 C-4 17.9 m, CH_2 8.4 m, CH_3, $^3J_{Pt-C}$ = 31.4 Hz
	^{31}P{^{1}H} NMR δ / ppm
	20.27 s, Pt-sat., $^1J_{PtP}$ 2695 Hz

Table 5.5 NMR data for benzoxazole and the Pt(II) benzoxazolyl hydride **5-2**

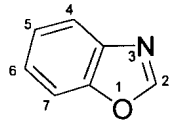

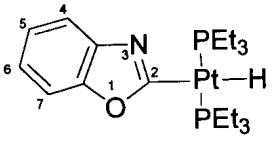

^{1}H NMR δ / ppm	
8.041	s, H-2
7.742	m, H-7
7.511	m, H-4
7.32-7.29	m, H-5 and H-6
7.506	d, H-7, $^3J_{HH}$ = 7.12 Hz
7.321	d, H-4, $^3J_{HH}$ = 6.10 Hz
7.050	t, H-5, $^3J_{HH}$ = 7.12 Hz
6.982	t, H-6, $^3J_{HH}$ = 6.10 Hz,
1.654	m, CH_2
1.000	m, CH_3
-7.490	t, Pt-sat, PtH, $^2J_{PH}$ 17.3 Hz, $^1J_{PtH}$ = 682 Hz

^{13}C{^{1}H} NMR δ / ppm	
152.36	C-2
149.81	C-7a
139.88	C-3a
125.39	C-5
124.38	C-6
120.41	C-7
110.75	C-4
152.81	*ipso*-C, J_{Pt-C} = 24.2 Hz
144.25	*ipso*-C, J_{Pt-C} = 44.9 Hz
	ipso-C not resolved
121.33	C-5
120.46	C-6
116.99	C-7
108.62	C-4, $^4J_{Pt-C}$ = 55.7 Hz
19.21	m, CH_2
8.51	CH_3, $^3J_{Pt-C}$ = 29.4 Hz

^{31}P{^{1}H} NMR δ / ppm	
20.34	$^1J_{PtP}$ 2650 Hz

Table 5.6 NMR data for benzothiazole and the Pt(II) benzothiazolyl hydride **5-3**

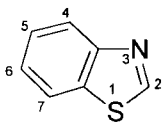

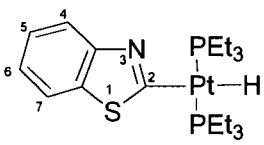

^{1}H NMR δ / ppm	
8.962 s, H-2	7.748 d, H-4, $^3J_{HH}$ = 7.8 Hz
8.124 d, H-4, $^3J_{HH}$ = 7.6 Hz	7.590 d, H-7, $^3J_{HH}$ = 7.6 Hz
7.922 dd, H-7	7.119 dt, H-5
$^3J_{HH}$ = 7.9 Hz, $^4J_{HH}$ = 0.8 Hz	$^3J_{HH}$ = 7.56 Hz, $^4J_{HH}$ = 1.1 Hz
7.490 dt, H-5	7.700 dt, H-6
$^3J_{HH}$ = 7.7 Hz, $^4J_{HH}$ = 1.3 Hz	$^3J_{HH}$ = 7.49 Hz, $^4J_{HH}$ = 1.1 Hz
7.403 dt, 1H, H-6	1.521 m, CH_2
$^3J_{HH}$ = 7.6 Hz, $^4J_{HH}$ = 1.0 Hz	0.959 m, CH_3
	-7.916 t, Pt-sat, PtH,
	$^2J_{P-H}$ 17.7 Hz, $^1J_{Pt-H}$ = 694 Hz
^{13}C{^{1}H} NMR δ / ppm	
153.78 C-2	155.41 C-3a
153.15 C-3a	137.19 C-7a
133.64 C-7a	123.92 C-5
126.09 C-5	121.67 C-6
125.47 C-6	120.23 C-4
123.55 C-4	120.04 C-7
121.79 C-7	117.27 C-2
	18.41 m, CH_2
	8.14 CH_3, $^3J_{Pt-C}$ = 28.3 Hz
	^{31}P{^{1}H} NMR δ / ppm
	15.32 $^1J_{Pt-P}$ 2585 Hz

The hydride protons for complexes **5-1** to **5-3** resonate at *ca* -7.0 ppm (Table 5.7) in the ^1H NMR spectra. This is *ca* 7-8 ppm more downfield than for the hydride protons of the *trans* (H-Pt-N)-type complexes (**4-4** to **4-8**). On comparison of the rhodium hydride complexes of [$Rh(C_5Me_5)(H)Ph(PMe_3)$] and [$Rh(C_5Me_5)(H)$(1-pyrrolyl(PMe_3)], the ^1H NMR hydride resonance of the N-Rh-H system is more downfield than the C-Rh-H systems, and this was interpreted as being due to the greater strength of the Rh-N bond over the Rh-C bond. Using this argument, the Pt-N bond is expected to be weaker than the Pt-C bond. The $^2J_{P-H}$ coupling is *ca* 2 Hz larger for the Pt-C than the Pt-N hydrides, while the $^1J_{Pt-H}$ coupling constants are smaller by *ca* 300 Hz. Larger $^1J_{Pt-H}$ values have been associated with a weaker *trans*-influence [41].

$^{31}P\{^1H\}$ NMR for complexes **5-1** to **5-3** are summarised in Table 5.7. For the furanyl hydride, the phosphine chemical shift is more downfield than for the benzoxazolyl hydride complex. The delocalization of electrons on the nitrogen atom into the benzoxazolyl ring thus increases the shielding on the phosphorus atoms. When the more electronegative oxygen atom of benzoxazolyl is replaced by a sulfur atom in the benzothiazolyl hydride complex, the phosphorus atom is even more shielded and thus shifts more upfield.

When comparing the $^{31}P\{^1H\}$ NMR data for these *trans* (C-Pt-H)-type complexes with that of *trans* (N-Pt-H)-type complexes, there is less variation between the two types of hydride complexes than was observed for their ^1H NMR data. The chemical shift of complexes **5-1** to **5-3** are only slightly more upfield and the $^1J_{Pt-P}$ Hz coupling is somewhat less (roughly 2650 Hz versus 2750 Hz -average values).

Table 5.7 Summary of pertinent NMR data for **5-1** to **5-3**

	^1H NMR PtH, δ /ppm	$^2J_{P-H}$	$^1J_{Pt-H}$	^{31}P NMR δ / ppm	$^1J_{Pt-P}$
5-1	-7.059	17.8 Hz	666 Hz	20.27	2695 Hz
5-2	-7.490	17.3 Hz	682 Hz	20.34	2650 Hz
5-3	-7.916	17.7 Hz	694 Hz	15.32	2585 Hz

5.2.8 Mass Spectrometry

Table 5.8 FAB-MS data for **5.1** - **5.3**

	Molecular Formula	Accurate Mass - Calculated	Accurate Mass - Observed	Intensity [peak assignment]
5-1 furanyl hydride	$C_{16}H_{34}OP_2Pt$	499.1945	498.1767	16 $[M^+-1]$
5-2 benzoxazolyl hydride	$C_{19}H_{35}NOP_2Pt$	550.1842	551.1920	76 $[M^+ +1]$
5-3 benzothiazolyl hydride	$C_{19}H_{35}NP_2SPt$	566.1613	566.1614	62 $[M^+]$

Complex **5.1** loses a hydrogen atom in the mass spectrometer so that the "molecular ion" recorded is an $[M^+-1]$ fragment. Complex **5.2** gains a hydrogen atom and the accurate mass of the $[M^+-1]$ fragment was observed.

Table 5.9 MS Fragmentation Ions of **5.1** - **5.3**

	m/z (intensity) [fragment ion]		m/z (intensity) [fragment ion]
5-1	498 (16) $[M^+-H]$ 467 (5) $[M - H - C_2H_6]^+$ 431 (39) $[M - H - C_4H_3O]^+$ or $[Pt(PEt_3)_2]^+$ 402 (27) $[Pt(PEt_3)_2 - Et]^+$ 373 (19) $[Pt(PEt_3)_2 - 2Et]^+$ 344 (13) $[Pt(PEt_3)_2 - 3Et]^+$ 314 (11) $[HPt(PEt_3)]^+$ 284 (10) $[Pt(PEt_2)]^+$ 255 (7) $[Pt(PEt)]^+$ 135 (100)$[OPEt_3^+]$ 119 (33) $[HPEt_3^+]$	**5-2**	551 (76) $[M^+ + H]$ 428 (58) $[M - 3H - C_7H_5NO]^+$ 402 (44) $[M - C_7H_5NO - C_2H_6]^+$ 398 (40) $[M - 4H - C_7H_5NO - C_2H_6]^+$ 374 (34) $[M - C_7H_5NO - C_2H_6 - C_2H_4]^+$ 370 (40) $[M - 4H - C_7H_5NO - 2Et]^+$ 344 (19) $[Pt(PEt_3)_2 - 3Et]^+$ 314 (17) $[HPt(PEt_3)]^+$ 284 (10) $[Pt(PEt_2)]^+$ 135 (100)$[OPEt_3^+]$ 120 (13) $[C_7H_5ONH]^+$ 119 (36) $[HPEt_3^+]$

5-3	566 (62) $[M^+]$	314 (13) $[HPt(PEt_3)]^+$
	429 (39) $[M - H_2 - C_7H_5NS]^+$	285 (7) $[HPt(PEt_2)]^+$
	401 (22) $[M - H_2 - C_7H_5NS - C_2H_4]^+$	255 (5) $[Pt(PEt)]^+$
	371 (16) $[M - H_2 - C_7H_5NS - 2Et]^+$	135 (100) $[OPEt_3^+]$ or $[C_7H_5NS]^+$
		119 (51) $[HPEt_3^+]$

The fragmentation pattern generally involves the loss of the carbon-α-bonded ligand. Stepwise cleavage of C_2 units then occurs, until an entire phosphine is lost. The second bonded phosphine then loses its C_2 units.

5.3 CONCLUSIONS

The C-O bond in furan is stronger than the C-S bond in thiophene, so that upon reacting furan with $[Pt(PEt_3)_4]$, insertion into the C-O bond did not occur and a six-membered platinacycle was not obtained. Instead, C-H activation at the α-carbon was observed and the platinum(II) hydride, **5.1** (*trans* isomer), was isolated. Attack at the C-H bond of the α-carbon had also been observed with 1-methylpyrrole, although in that case, the platinum(II) *cis*-hydride complex, **4.1**, was observed. Complexes of the type *trans*-$[Pt(H)(X)(PEt_3)_2]$ (where X = anionic ligand) are in general thermodynamically favoured over their corresponding *cis* isomers. Dibenzofuran was found to be less reactive to C-H activation than furan.

The reaction of $[Pt(PEt_3)_4]$ with benzoxazole was similar to that of furan; C-H activation resulted in the *trans*-hydride complex, **5-2**. Benzothiazole, like benzoxazole, also exhibited C-H activation to yield **5-3** despite the presence of a C-S bond in the molecule. It was reported in Chapter 3 that a heteroaromatic compound containing a thienyl ring leads to the formation of a thiaplatinacycle, as well as, in certain cases, a C-H activation product. The fine line between C-S and C-H activation was tipped in the favour of C-H insertion when an additional heteroatom, *viz.* the nitrogen atom in benzoxazole, was introduced to the sulfur-containing ring.

Oxidative insertion of $[Pt(PEt_3)_4]$ into C-O (of furans) and C-N bonds (of azoles) did not occur, and would require pre-coordination by another metal fragment to be effected [5].

/ References for Chapter 5 follow.....

5.4 REFERENCES

[1] (a) E. Furimsky, *Catal. Rev. Sci. Eng.*, **1983**, *25*, 421-458 (b) T.E. Caldwell, I.M. Abdelrehim and D.P. Land, *J. Am. Chem. Soc.*, **1996**, *118*, 907-908

[2] Y.-S. Lin and A. Yamamoto in *Topics in Organometallic Chemistry*, Vol. 3, ed. S. Murai, 1999, pp 162-192

[3] M.E. van der Boom, S.-Y. Liou, Y. Ben-David, A. Vigalok and D. Milstein; *Angew. Chem. Int. Ed.*, **1997**, *36*, 625-626

[4] J.B. Bonanno, T.P. Henry, D.R. Neithamer, P.T. Wolczanski and E.B. Lobkovsky; *J. Am. Chem. Soc.*, **1996**, 118, 5132-5133

[5] K. Yu, H. Li, E.J. Watson, K.L. Virkaitis, G.B. Carpenter and D.A. Swiegart; *Organometallics*, **2001**, *20*, 3550-3559 (b) X. Zhang, E.J. Watson, C.A. Dullaghan, S.M. Gorun and D.A. Swiegart; *Angew. Chem. Int. Ed.*, **1999**, *38*, 2206-2208 (c) C.A. Dullaghan, S. Sun, G.B. Carpenter and D.A. Swiegart, *ibid*, **1996**, *35*, 212-214

[6] G.S. Hill and R.J. Puddephatt; *Organometallics*, **1998**, *17*, 1478-1486

[7] B. Rybtchinski and D. Milstein; *Angew. Chem. Int. Ed.*, **1999**, *38*, 870-883

[8] (a) J.A. Martinho Simões and J.L. Beauchamp; *Chem. Rev.*, **1990**, *90*, 629-688 (b) J. Halpern; *Inorg. Chim. Acta*, **1985**, *100*, 41-48 (c) S.P. Nolan, C.D. Hoff, P.O. Stoutland, L.J. Newman, J.M. Buchanan, R.G. Bergman, G.K. Yang and K.S. Peters; *J. Am. Chem. Soc.*, **1987**, *109*, 3143-3145 (d) W.D. Jones and F.S. Feher; *J. Am. Chem. Soc.*, **1984**, *106*, 1650-1663

[9] P.O. Stoutland, R.G. Bergman, S.P. Nolan and C.D. Hoff; *Polyhedron*, **1988**, *7*, 1429-1440

[10] B.L. Edelbach, R.J. Lachicotte and W.D. Jones; *J. Am. Chem. Soc.*, **1998**, *120*, 2843-2853

[11] R.M. Shaltout, R. Sygula, A. Sygula, F.R. Fronczek, G.G. Stanley and P.W. Rabideau; *J. Am. Chem. Soc.*, **1998**, *120*, 835-836

[12] (a) P. Eilbracht; *Chem. Ber.*, **1980**, *113*, 542 (b) R.H. Crabtree and R.P. Dion, *J. Chem. Soc., Chem. Commun.*, **1984**, 1260-1261 (c) F. Urbanos, M.A. Halcrow, J. Fernandez-Baeza, F. Dahan, D. Labroue and B. Chaudret; *J. Am. Chem. Soc.*, **1993**, *115*, 3484-3493

[13] (a) M.A. Bennett, J.C. Nicholls, A.K.F. Rahman, A.D. Redhouse, J.L. Spencer and A.C. Willis; *J. Chem. Soc., Chem. Commun.*, **1989**, 1328-1330 (b) J.C. Nicholls and J.L. Spencer; *Organometallics*, **1994**, 13, 1781-1787

[14] (a) S. Pulst, F.G. Kirchbauer, B. Heller, W. Baumann and U. Rosenthal, *Angew. Chem. Int. Ed.*, **1998**, *37*, 1925-1927 (b) H. Suzuki, Y. Takaya and T. Takemori; *J. Am. Chem. Soc.*, **1994**, *116*, 10779-10780

[15] W.E. Geiger, A. Salzer, J. Edwin, W. von Philipsborn, U. Piantini and A.L. Rheingold; *J. Am.*

Chem. Soc., **1990**, *112*, 7113-71121

[16] P. Steenwinkel, R.A. Gossage and G. van Koten; *Chem. Eur. J.*, **1998**, *4*, 759-762

[17] G. Dyker; *Angew. Chem. Int. Ed.*, **1999**, *38*, 1698-1712

[18] A.E. Shilov and G.B. Shul'pin; *Chem. Rev.*, **1997**, *97*, 2879-2932

[19] A.D. Ryabov; *Chem. Rev.*, **1990**, *90*, 403-424

[20] C.-H. Jun, C.W. Moon and D.-Y. Lee; *Chem. Eur. J.*, **2002**, *8*, 2422-2428

[21] (a) W.D. Jones and F.J. Feher; *J. Am. Chem. Soc.*, **1982**, *104*, 4240-4242 (b) M. Lavin, E.M. Holt and R.H. Crabtree, *Organometallics*, **1989**, *8*, 99-104

[22] M. Hackett and G.M. Whitesides; *J. Am. Chem. Soc.*, **1988**, *110*, 1449-1462

[23] D.S. McGuiness, K.J. Cavell and B.F. Yates; *Chem. Commun.*, **2001**, 355-356

[24] R.R. Fraser, T.S. Mansour and S. Savard; *Can. J. Chem.*, **1985**, *63*, 3505

[25] HyperChem ® Pro 6, Hypercube Inc., Gainsville, U.S.A.

[26] W.D. Jones, L. Dong and A.W. Myers; *Organometallics*, **1995**, *14*, 855-861

[27] R.L. Cowan and W.C. Trogler; *J. Am. Chem. Soc.*, **1989**, *111*, 4750-4761

[28] H.E. Bryndza, L.K. Fong, R.A. Pacielli, W. Tam and J.E. Bercaw; *J. Am. Chem. Soc.*, **1987**, *109*, 1444-1456

[29] (a) J. Tsuji and H. Nagashima; *Tetrahedron*, **1984**, *40*, 2699-2702 (b) G. Dyker; *Angew. Chem. Int. Ed.*, **2000**, *39*, 4237-4239

[30] A. Cornia, A.C. Fabretti, M. Bonivento and L. Cattalini; *Inorg. Chim. Acta.*, **1997**, *255*, 405-409

[31] (a) V. Caló, R. Del Sole, A. Nacci, E. Schingaro and F. Scordari; *Eur. J. Org. Chem.*, **2000**, 869-871 (b) V. Caló, A. Nacci, L. Lopez and N. Mannarini; *Tetrahedron Lett.*, **2000**, *41*, 8973-8976

[32] J. Muller, P.E. Gaeda and K. Qiao; *Z. Naturforsch. B: Chem. Sci.*, **1994**, *49*, 1645-1653

[33] (a) J.J. Garcia, B.E. Mann, H. Adams, N.A. Bailey and P.M. Maitlis; *J. Am. Chem. Soc.*, **1995**, *117*, 2179-2186 (b) M.-G. Choi and R.J. Angelici; *Organometallics*, **1992**, *11*, 3328-3334

[34] I. Ara, L.R. Falvello, J. Forniés, E. Lalinde, A. Martin, F. Martinez and M.T. Moreno; *Organometallics*, **1997**, *16*, 5392-5405 and references therein.

[35] R.H. Crabtree in *The Organometallic Chemistry of the Transition Metals*, John Wiley and Sons, New York, 1988, pp 53, 121-132

[36] A.L. Bandini, G. Banditelli and G. Minghetti; *J. Organomet. Chem.*, **2000**, *595*, 224-231

[37] (a) P. Leoni, S. Manetti and M. Pasquali; *Inorg Chem.*, **1995**, *34*, 749-752 (b) F. Bachechi, G. Bracher, D.M. Grove, B. Kellenberger, P.S. Pregosin, L.M. Venanzi and L. Zambonelli; *Inorg. Chem.*, **1983**, *22*, 1031-1037

[38] J.Jans, R. Naegeli, L.M. Venanzi and A. Albinati; *J. Organomet. Chem.*, **1983**, *247*, C37-C41

[39] J.J. Garcia, A. Arevalo, S. Capella, A. Chehata, M. Hernandez, V. Montiel, G. Picazo, F. Del Rio, R.A. Toscano, H. Adams and P.M. Maitlis; *Polyhedron*, **1997**, *16*, 3185-3195

[40] A. Arévalo, S. Bernès, J.J. Garcia and P.M. Maitlis; *Organometallics*, **1999**, *18*, 1680-1685

[41] T.G. Appleton, H.C. Clark and L.E. Manzer; *Coord. Chem. Rev.*, **1973**, *10*, 335-422

/ End of Chapter 5 //

CHAPTER 6

Platinum(II) Complexes of Heteroarylphosphine Ligands[1]

6.1 INTRODUCTION

The development of new ligands is becoming increasingly important to fine tune metal activity in coordination chemistry [1]. Following on with the idea of using thiophene-based ligands as rigid A-frame skeletons to which two metal centres can be attached (Chapter 2), we were interested in using a diphosphine-substituted thiophene molecule as a spacer. Bidentate, bridging ligands such as bis(diphenylphosphino)methane, dppm, and bis(diphenylphosphino)-ethane, dppe, have been incorporated as A-frame ligands in complexes of symmetrical and unsymmetrical palladium and platinum dimers (See Figure 2.1, Chapter 2) [2].

Phosphine ligands bearing pyridinyl substituents, such as 2-pyridinylphosphine, are widely exploited in binuclear complex formation as bridging ligands. Platinum(I) and palladium(I) homo- and heterobinuclear complexes from head-to-head or head-to-tail isomers with 2-pyridinylphosphine (Figure 6.1a). The neutral, potentially tridentate 2,6-bis(diphenyl-

[1] The content of this chapter has been published:
J. Chantson, H. Görls and S. Lotz; *Inorg. Chim. Acta*, **2000**, *305*, 32-37

phosphino)pyridine has also been used to synthesise binuclear complexes (Figure 6.1b) [3].

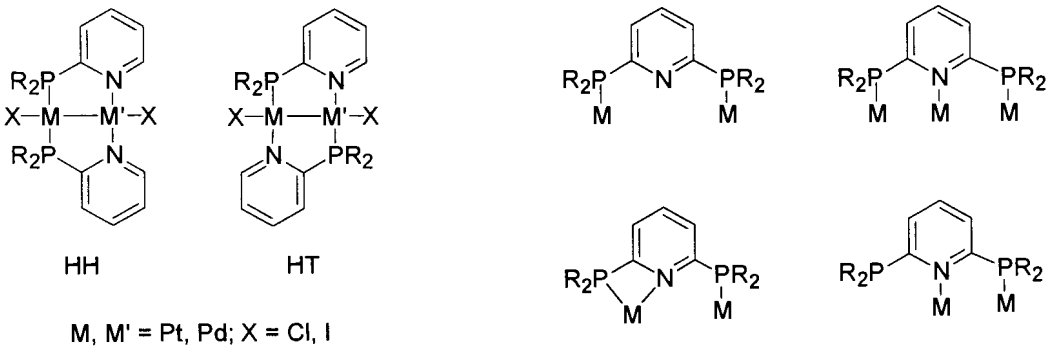

a) Binuclear A-frame complexes with 2-pyridinylphosphines

b) Di- and tri-nuclear complexes with bridging 2,6-diphosphinopyridine

Figure 6.1 Di- and tri-nuclear complexes of bridging phosphine ligands.

Other heteroaryl substituents such as 2-thienyl, 2-furyl and 2-(1-methylpyrrolyl) are less inclined to coordinate in a similar fashion through their respective heteroatoms [4]. Bis(diphenylphosphino)-containing molecules with polythiophenes (2,2′-bithiophene, 2,2′:5′,2″-terthiophene) and thienylpyridines (2-(2′-thienyl)pyridine and 2,6-di-2′-thienyl-pyridine) as spacers have been prepared by Field and co-workers [5]. Van Leeuwen and co-workers have investigate the effect of "bite-angle" of rigid bidentate phosphine ligands in mononuclear rhodium complexes on catalytic hydroformylation [6].

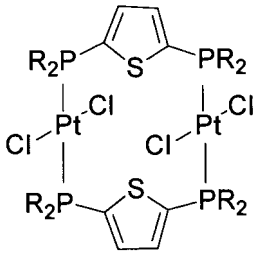

I

Using thiophene as a spacer, it is aimed to construct an A-frame complex of the type depicted in **I** above.

In general, 2-thienyl and 2-furyl groups behave as moderately strong electron-withdrawing units and a comparative study [7] of the magnitude of ^{1}J (^{77}Se-^{31}P) coupling constants for heteroarylphosphine selenides established an electron-withdrawing effect which follows an ordering of 2-furyl > 2-thienyl > phenyl > 2-(1-methylpyrrolyl). Platinum(II) complexes prepared in polar solvents from tetrachloroplatinate(II) and bis(phosphine) ligands containing 2-furyl or 2-thienyl substituents invariably afforded *cis*-products, *cis*-$[Pt(PR_2R')_2Cl_2]$, which did not spontaneously convert into the *trans*-isomers. The mechanisms of *cis-trans* isomerizations have been the subject of rigorous investigations and any of the precursor, the solvent, phosphine substituents or auxiliary ligands in the complex may determine the structure of the final product [8]. For complexes of the type $[PtL_2X_2]$, the *cis*-isomers are generally enthalpy-driven, while the *trans*-isomers are entropy-favoured. The position of 2-(1-alkylpyrrolyl) in the above sequence as well as the omission of phosphine ligands displaying this substituent in the literature in complexes of the type $[Pt(PR_2R')_2Cl_2]$, is noteworthy. Furthermore, we observed in structural studies that 2,5-(1-methylpyrrolydene), in sharp contrast to 2,5-thienylene, displayed a passiveness to stabilize the carbocationic centres in biscarbene complexes [9]. Hence, it was of some interest to reinvestigate and compare the structures of $[Pt(P\{monoheteroaryl\}R_2)_2Cl_2]$ (R = dialkyl and diaryl) complexes. In order to minimize variables all reactions were studied by utilizing the *cis*-directing precursor, dichloro-η^4-1,5-cyclooctadieneplatinum(II), as well as the same reaction conditions and solvent. The

cis isomers were isolated as expected except for the case of *trans*-[Pt(P{2-(1-methylpyrrolyl)}^{i}Pr$_2$)$_2$Cl$_2$], the structure of which was confirmed by a crystal structure determination.

6.2 RESULTS AND DISCUSSION

Early on in this investigation, attempts to isolate the binuclear A-frame complex, **I**, was unsuccessful. When 2,5-bis(diphenylphosphoryl)thiophene was reacted with an equivalent of dichloro(η^4-1,5-cyclooctadiene)platinum(II) in dichloromethane, a white solid was obtained which proved to be insoluble in common organic solvents. Consequently this complex could not be characterised and was suspected to be a polymer of the type depicted in **II**. The focus of the study thus shifted to the monoheteroarylphosphines and their complexes with platinum(II).

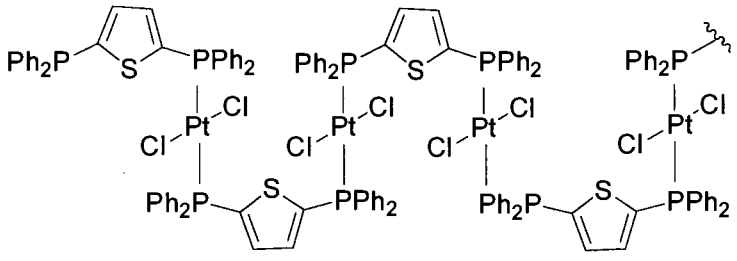

II

6.2.1 Synthesis of Phosphine Ligands

The phosphine ligands were prepared by utilizing standard synthetic organic methods [10] which involved the monolithiation of 1-methylpyrrole, 2-methylthiophene, and 2,6-dibromopyridine, followed by quenching with the chlorodiphenylphosphine or chlorodiisopropylphosphine electrophile (Scheme 6.1). To prevent the formation of 2,5-bis-

(diisopropylphosphino)thiophene, 2-methylthiophene rather than thiophene was used in order to block the 5-position from attack by the lithiating agent [11]. Whereas the thiophene ring undergo metallation at room temperature, the pyrrole ring requires heating to 50 °C and the presence of *N,N,N′,N′*-tetramethylethylenediamine. 2,6-Dibromopyridine is much more reactive to lithiation and the reaction was carried out in dichloromethane at −78 °C. The lithiated heterocycle reaction mixtures were cooled before the chlorophosphine was added.

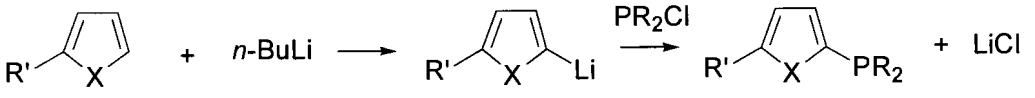

X = NMe, S
R = Ph, ^{i}Pr
R' = H, Me

Scheme 6.1

2,5-Bis(triphenylphosphino)thiophene was prepared by dilithiation of thiophene in the presence of tmeda followed by the addition of two equivalents of chlorodiphenylphosphine.

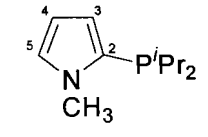

P1

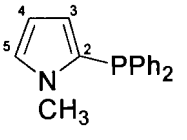

P2

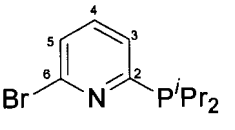

P5

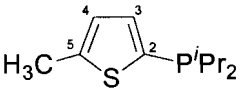

P3

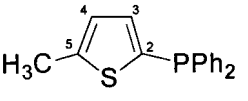

P4

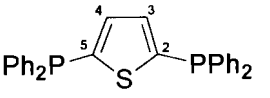

P6

6.2.2 Synthesis of Pt(II) Complexes

The platinum(II) complexes were obtained by the displacement of cod from [Pt(η^4-cod)Cl_2] by two equivalents of the appropriate phosphine ligand at ambient temperature in dichloromethane (Scheme 6.2).

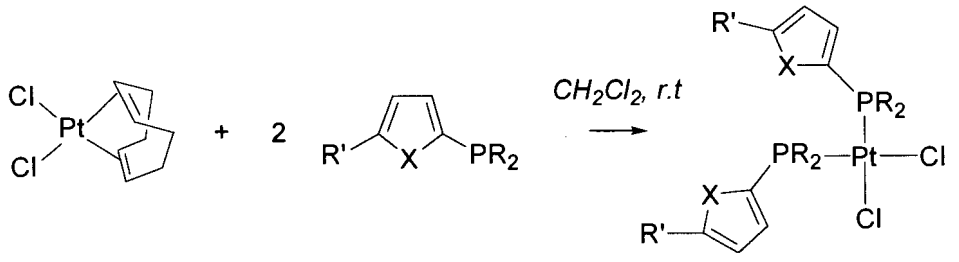

X = NMe, S
R = Ph, ^{i}Pr
R' = H, Me

Scheme 6.2

All the complexes were isolated as white solids and purified by washing with various solvents. *Cis*-products were expected to form from the direct replacement of a cod ligand in the metal precursor by two phosphine ligands. This was indeed the case in all the reactions with the exception of *trans*-dichlorobis[diisopropyl-2-(1-methyl-pyrrolyl)phosphine]platinum(II), **6-1**.

Grim and co-workers showed that aryl substituents promote, to an extent, the stabilisation of the *cis*-isomers [12]. The synthesis of bis(phosphine)platinum(II) complexes under analogous reaction conditions, with 2-(1-methylpyrrolyl)diphenylphosphine, 2-(5-methylthienyl)-diisopropylphosphine and 2-(5-methylthienyl)diphenylphosphine respectively, led to the isolation of *cis*-dichlorobis[2-(1-methylpyrrolyl)diphenylphosphine]platinum(II), **6-2**, *cis*-dichlorobis[2-(5-methylthienyl)diisopropylphosphine]platinum(II), **6-3** and *cis*-dichlorobis[2-(5-methylthienyl)diphenylphosphine]platinum(II), **6-4**.

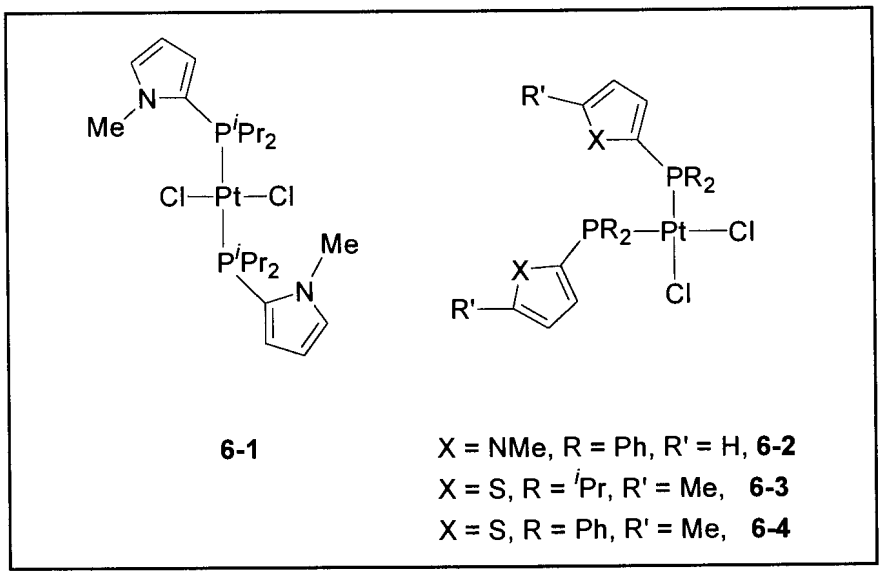

6-1

X = NMe, R = Ph, R' = H, **6-2**
X = S, R = ^{i}Pr, R' = Me, **6-3**
X = S, R = Ph, R' = Me, **6-4**

The magnitude of the $^1J_{Pt-P}$ coupling constants of 3644 and 3696 Hz for **6-2** and **6-4** respectively, fit into the range of $^1J_{Pt-P}$ values reported for other *cis*-dichlorobis(phosphine)-platinum(II) complexes [13]. A heteroaryl substituent with strong coordinating power via the N-heteroatom, such as a pyridinyl derivative [14] also yields a *cis*-product, bis(2-{6-bromopyridinyl}diphenylphosphine)dichloroplatinum(II), **6-5** ($^1J_{Pt-P}$ = 37112Hz). It is interesting to note that in **6-5** there is evidence (the resonance is broadened and shifted upfield) from the ^{1}H NMR spectrum that hydrogen bonding occurs between methyl hydrogen atoms of the isopropyl group and the nitrogen atom of the pyridine ring. On comparison with related complexes reported in the literature, the $^1J_{Pt-P}$ coupling constants for **6-4** and for **6-5** correspond favourably with the 3681 Hz observed for *cis*-bis(diphenyl-2-thienylphosphine)-dichloroplatinum(II) [15] and 3675.6 Hz for *cis*-bis(diphenyl-2-pyridinylphosphine)-dichloroplatinum(II), respectively (dichloromethane-d_2) [16]. Incomplete spectroscopic data were reported for the former complex. On replacing the two phenyl groups on the heteroarylphosphine ligands with isopropyl groups, *cis*-dichlorobis(2-{5-methylthienyl}-diisopropylphosphine)platinum(II), **6-3**, was obtained. Its $^1J_{Pt-P}$ coupling constant of 3763 Hz is once again indicative of a *cis*-configuration. However, replacement of phenyl groups of the 2-(1-methylpyrrolyl)phosphine ligand by isopropyl groups results in a platinum(II) complex,

6-1, displaying a significantly smaller $^{1}J_{Pt-P}$ coupling constant of 2430.0 Hz. This value is characteristic of *trans*-dichlorobis(phosphine)platinum(II) complexes [13].

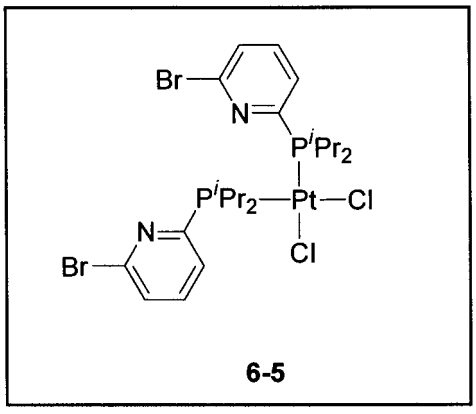

6-5

The reason for **6-1** assuming a *trans*-conformation while **6-2** to **6-5** are *cis*-isomers, we believe, lies in electronic rather than steric effects. Even large bulky phosphines can stabilize the *cis*-isomer. For example, the intermeshing ability of the phosphine ligand in *cis*-dichlorobis(di-*tert*-butylphenylphosphine)platinum(II) alleviates steric hinderance and allows for the *cis*-configuration to be adopted [17]. An example of a case where electronic interactions lead to quite different properties in pyrrole- or thiophene-like molecules is given by comparison of the 2,2′-diaryl molecules. A twisted conformation is observed for 2,2′-bi(1-methylpyrrole) in the biscarbene complex $[(CO)_5WC(OEt)C_5H_5N\text{-}C_5H_5NC(OEt)W(CO)_5]$, where the two pyrrole rings are twisted away from each other [9]. By contrast, the analogous biscarbene complex with a 2,2′-biphenyl spacer [18] and 5,5′-substituted 2,2′-bithiophene compounds [19] have planar structures with rotation about the 2,2′-linkage bond severely restricted. This implies that the π-orbitals of the sulfur atom are involved in delocalization of electron density over the two thiophene rings, whereas this is not the case for dipyrroles. The difference in the electronic properties between the 5-membered heterocycles of 2-methylthiophene and 1-methylpyrrole determines the bonding properties of these phosphine ligands and plays a role in the reasons for **6-1** adopting a *trans*-configuration.

The *cis*-complexes do not spontaneously undergo *cis-trans* isomerisation to the thermodynamically more stable *trans*-isomer. It is difficult to establish a trend amongst the various interrelating factors that affect the isomerisation equilibrium, although the effect of the substituent at phosphorus is marked. As discussed below, the diisopropyl-2-(1-methylpyrrolyl)phosphine ligand is the most shielded of the series of phosphines in this investigation, suggesting that the phosphine ligand is a relatively stronger electron-donor. This may affect the reaction kinetics leading to the *trans*- rather than the *cis*-isomer. The presence of a trace amount of free phosphine known to catalyse the isomerisation [8]. It can thus be argued that platinum(II), being a relatively electron-rich metal centre, could have a greater tendency to labilise the stronger donor phosphine ligand.

6.2.3 Crystal Structure of *trans*-dichlorobis[diisopropyl-2-(1-methylpyrrolyl)-phosphine]platinum(II), 6-1

Confirmation of the *trans*-configuration of phosphine ligands in **6-1** was obtained from a single crystal X-ray structure determination. X-ray quality crystals of **6-1** were grown from a dichloromethane solution layered with hexane. The crystals were isolated as colourless prisms. Ball-and-stick representations of **6-1** are given in Figure 6.2, one with atom numbering. Selected bond lengths and angles are listed in Table 6.1. Full details of the aquisition, refinement and structural parameter data are tabulated in the Appendix. A square planar structure is adopted with two molecules of phosphine ligands occupying *trans*-positions.

Deviations of the bond angles at platinum from 90° are minimal and the P-Pt-Cl atoms are almost co-planar. The Pt-Cl and Pt-P bond lengths are 2.321(2) and 2.334(1) Å, respectively. Both bond lengths are in the normal range for *trans*-Pt-Cl and *trans*-Pt-P bonds [20]. In the analogous compound *trans*-dichlorobis(triethylphosphine)platinum(II) the Pt-Cl bond length is also reported to be slightly shorter than the Pt-P bond length [21]. The average P-

C(isopropyl) bond distance is 1.857(6) Å, which is 0.049 Å longer than the P-C(pyrrolyl) bond length of 1.808(6) Å. This feature has been observed in other alkyl-aryl phosphines [17].

The two isopropyl groups attached to a phosphorus atom display slightly different orientations. One methyne group has a C-P-Pt angle of 116.2°(2) while the other is 109.7°(2). Furthermore, while the C(7)-C(6)-P and C(10)-C(9)-P angles are identical at 112.1°(4), the other methyl group of each isopropyl substituent give different angles *viz.* 109.3°(4) for C(11)-C(9)-P and 111.3°(4) for C(8)-C(6)-P. The 1-methyl group is slightly tilted away from the phosphorus and inclined to the far side of the pyrrole ring; C(1)-N-C(5) = 128.8°(5) and C(4)-N-C(5) = 122.2°(5).

Table 6.1 Selected bond lengths and angles for **6-1**

Selected Bond lengths / Å		Selected bond angles / °	
Pt-Cl(1)	2.321 (1)	Cl(1A)-Pt-Cl(1)	180.0
Pt-P(1)	2.334 (1)	Cl(1A)-Pt-P(1)	89.49 (5)
P(1)-C(1)	1.808 (6)	Cl(1)-Pt-P(1)	90.52 (5)
P(1)-C(9)	1.855 (6)	C(1)-P(1)-Pt	116.2 (2)
P(1)-C(6)	1.858 (6)	C(9)-P(1)-Pt	109.7 (2)
N(1)-C(1)	1.385 (8)	C(6)-P(1)-Pt	116.5 (2)
N(1)-C(4)	1.380 (7)	C(8)-C(6)-P(1)	111.3 (4)
N(1)-C(5)	1.467 (7)	C(7)-C(6)-P(1)	112.0 (4)
		C(10)-C(9)-P(1)	112.1 (4)
		C(11)-C(9)-P(1)	109.3 (4)

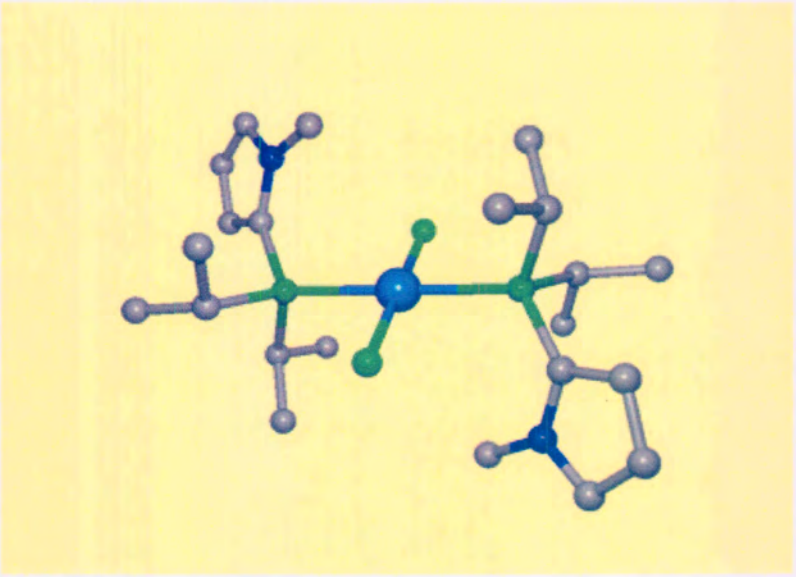

Figure 6.2 The ball-and-stick depictions of **6-1**

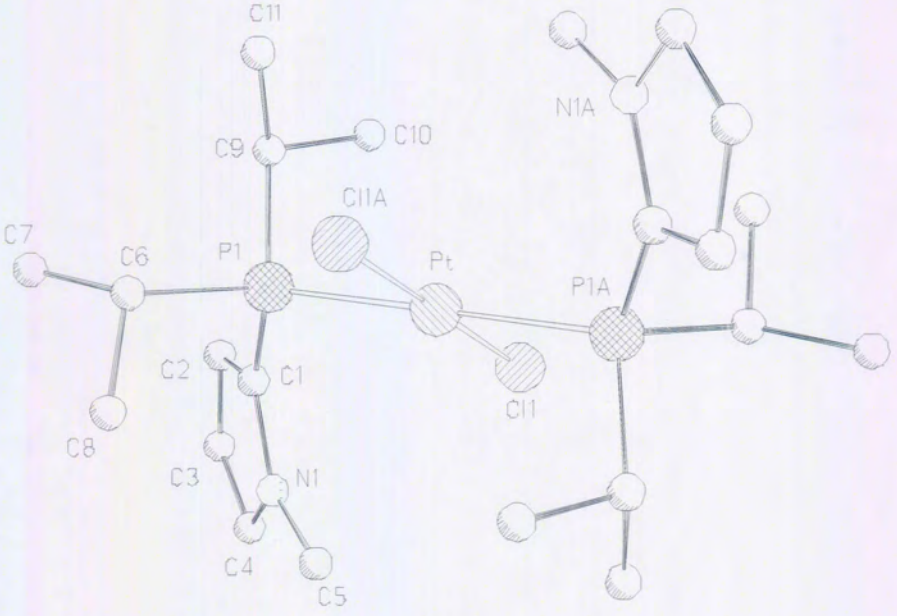

The *cis*-complexes did not afford crystals suitable for single crystal X-ray diffraction studies. We ascribe this to better packing of the molecules resulting from the centrosymmetric *trans*-complex compared to the *cis*-complexes.

6.2.4 NMR Spectroscopy

Spectra were recorded in deuterated chloroform. See Tables 6.2 to 6.6 for ^{1}H NMR data, Table 6.7 for ^{31}C{^{1}H} NMR data and Tables 6.8 and 6.9 for ^{31}P{^{1}H} NMR data.

Table 6.2 ^{1}H NMR data for phosphine ligands, **P1** and **P2**, δ / ppm (J in Hz)

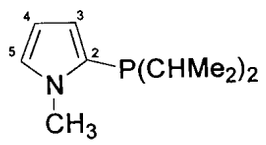	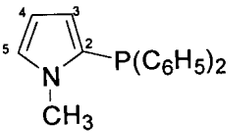
6.14 dd, H-3, 1H, $^{3}J_{HH}$ 3.2, $^{3}J_{P-H}$ 6.6	5.88 dd, H-3, 1H, $^{3}J_{HH}$ 3.6, $^{3}J_{P-H}$ 1.8
6.26 m, H-4, 1H	6.15 m, H-4, 1H
6.72 m, H-5, 1H	6.84 m, H-5, 1H
3.70 s, CH_3, 3H	3.62 s, CH_3, 3H
1.96 heptet of d, PC*H*, 2H, $^{3}J_{HH}$ 6.9, $^{2}J_{P-H}$ 0.9	7.63 m, Ph, 10H
0.99 - 0.90 dd, Me, 6H, $^{3}J_{HH}$ 7.1, $^{3}J_{P-H}$ 16.3 dd, Me, 6H $^{3}J_{HH}$ 7.0, $^{3}J_{P-H}$ 11.7	

Table 6.3 ^{1}H NMR data for phosphine ligands, **P3** and **P4**, δ / ppm (J in Hz)

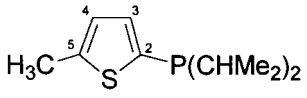		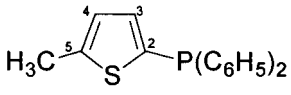	
7.07	dd, H-3, 1H, $^3J_{HH}$ 3.2, $^3J_{P-H}$ 6.6	7.13	dd, H-3, 1H, $^3J_{HH}$ 3.4, $^3J_{P-H}$ 6.6
6.71	m, H-4, 1H	6.75	m, H-4, 1H
2.47	s, CH_3, 3H	2.45	s, CH_3, 3H
2.00	heptet of d, PC*H*, 2H, $^3J_{HH}$ 7.0, $^2J_{P-H}$ 1.1	7.35	m, Ph, 10H
1.09 - 0.96	m, Me, 12H		

Table 6.4 ^{1}H NMR data for phosphine ligand, **P5** and **P6**, δ / ppm (J in Hz)

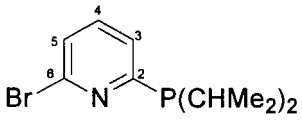		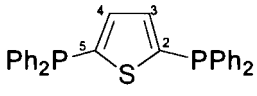	
7.40	d, H-3, 1H, $^3J_{HH}$ 2.4	7.36-7.29	m, Ph, 20H
7.35	m, H-4,1H	7.13	dd, H-3, H-4, 2H, $^3J_{HH}$ 2.3, $^3J_{P-H}$ 4.2
7.42	d, H-5, 1H, $^3J_{HH}$ = 3.0		
2.25	heptet of d, PC*H*, 2H, $^3J_{HH}$ 7.1, $^2J_{P-H}$ 2.6		
1.09	dd, Me, 6H, $^3J_{HH}$ 7.1, $^3J_{P-H}$ 14.7		
0.92	dd, Me, 6H $^3J_{HH}$ 7.0, $^3J_{P-H}$ 12.7		

Table 6.5 ^{1}H NMR data for Pt(II) complexes, **6-1** and **6-2**, δ / ppm (J in Hz)

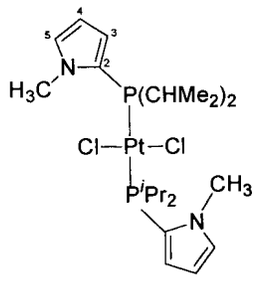 **6-1**		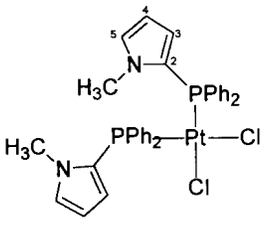 **6-2**	
6.34	dd, H-3, 2H, $^{3}J_{HH}$ 1.3, $^{3}J_{P-H}$ 8.8	6.74	m, H-3, 2H
6.22	m, H-4, 2H	5.99	m, H-4, 2H
6.84	m, H-5, 2H	5.96	m, H-5, 2H
4.16	s, CH_3, 6H	3.48	s, CH_3, 6H
2.79	m, PC*H*, 4H	7.44	Ph *o*-H, m, 8H
		7.32	Ph *p*-H, m, 4H
1.22	m, Me, 24H	7.13	Ph *m*-H, m, 8H

Table 6.6 ^{1}H NMR data for Pt(II) complexes, **6-3 - 6-5**, δ / ppm (J in Hz)

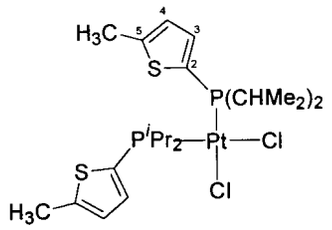

6-3

6.71	dd, H-3, 2H, $^3J_{HH}$ 3.5, $^3J_{P-H}$ 6.1
6.42	d, H-4, 2H, $^3J_{HH}$ 3.5
2.41	s, CH_3, 6H
3.08	m, PC*H*, 4H
1.49	dd, Me, 12H, $^3J_{HH}$ 7.1, $^3J_{P-H}$ 17.1
1.11	dd, Me, 12H, $^3J_{HH}$ 6.9, $^3J_{P-H}$ 16.3

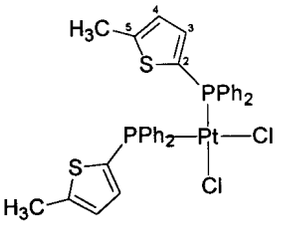

6-4

6.77	m, H-3 and H-4, 4H
2.42	s, CH_3, 6H
7.46	Ph *o*-H, m, 8H
7.30	Ph *p*-H, t, 4H, $^3J_{HH}$ 7.6
7.15	Ph *m*-H, td, 8H, $^3J_{HH}$ 7.6 , $^3J_{HH}$ 2.0

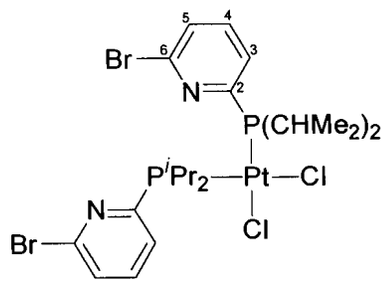

6-5

7.13	m, H-3 H-4 and H-5, 6H
3.06	m, PC*H*, 4H
1.55	dd, Me, 12H, $^3J_{HH}$ 7.2, $^3J_{P-H}$ 16.3
1.07	m, Me, 12H

Table 6.7 ^{13}C NMR data for Pt(II) complexes, δ / ppm (J in Hz)

	6-1	**6-2**	**6-4**	**6-3**	**6-5**
C-2	114.7	unresol.	128.4	121.3 d $^{1}J_{P-C}$ 46.4	139.8
C-3	119.1	122.7	141.0	135.9	128.4
C-4	108.1	108.2	125.7	126.3	137.3
C-5	128.2	128.7	149.6	145.4	125.6
CH_3	37.4	37.5	15.0	15.0	141.7
PCH	22.3	-	-	27.7 d $^{1}J_{PC}$ 39.7 $^{3}J_{Pt-C}$ unresolved)	25.6
PC*Me*	18.6 17.7	-	-	19.6 d $^{1}J_{P-C}$ 39.7 $^{3}J_{Pt-C}$ unresolved	19.5 19.0
Ph	-	134.4 *o*-C 130.9 *p*-C 129.7 *ipso*-C 128.1 *m*-C	134.2 *o*-C 130.6 *p*-C 130.0 *ipso*-C 127.9 *m*-C	-	-

Table 6.8 ^{31}P NMR data of phosphine ligands δ / ppm			
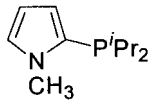	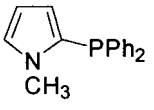	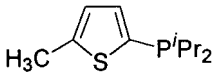	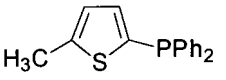
-18.8	-29.3	1.2	-18.7
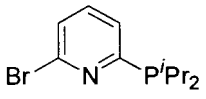		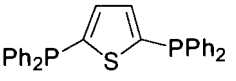	
16.4		-18.2	

Chemical shifts of phosphines in the ^{31}P NMR spectra (Table 6.8) are affected by the electronegativity of the group attached to phosphorus. The increased shielding of the phosphorus centre in the order triphenylphosphine (-4.7 ppm [3]), 2-{5-methylthienyl}-diphenylphosphine (-18.7 ppm) and 2-{1-methylpyrrolyl}diphenylphosphine (-29.3 ppm) suggests that the electron donor ability of the aryl substituents increases from phenyl, to 5-methylthienyl, to 1-methylpyrrolyl. From the view of group electronegativities of the heteroatom of thienyl and pyrrolyl compared to phenyl, the observed trend is in apparent contradiction. Studies of quarterisation kinetics by Allen *et. al* has shown that diphenyl-2-thienylphosphine reacts half as fast as does triphenylphosphine, indicating that the thienyl substituent behaves as a stronger electron withdrawing substituent than phenyl [22]. However, as thienyl, and pyrrolyl, are classified as "π-excessive" systems, these studies suggest that electron density is returned to phosphorus via the π-system by $p\pi$-$d\pi$ interactions. Electron-withdrawing or -donating abilities of aryl and heteroaryl sustituents involves both σ (inductive) and π (resonance) properties [22]. Cone angles also affect ^{31}P NMR chemical shifts [16b]. For example, the phenyl groups in triphenylphosphine are more electron-withdrawing than the isopropyl groups in triisopropylphosphine, yet the phosphorus centre in the latter is more deshielded than in the former. This is due to the increase in cone angle from 145° in

triphenylphosphine to 160° in triisopropylphosphine [23]. An analogous type of effect is presumed to account for the differences in $^{31}P\{^{1}H\}$ NMR chemicals shifts for 2-{5-methyl-thienyl}diphenylphosphine (-18.7 ppm) and 2-{5-methylthienyl}diisopropylphosphine (1.2ppm); and 2-{1-methylpyrrolyl}diisopropylphosphine) (-18.3ppm) and 2-{1-methylpyrrolyl}diphenylphosphine (-29.3 ppm). Upon coordination with platinum, the phosphorus is deshielded in each of the complexes (Table 6.9).

Table 6.9 ^{31}P NMR data of Platinum(II) complexes

δ / ppm

$^{1}J_{Pt-P}$ (Hz)

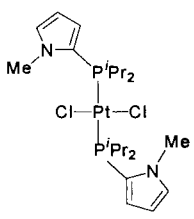	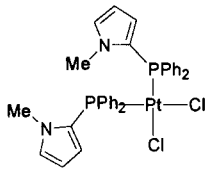	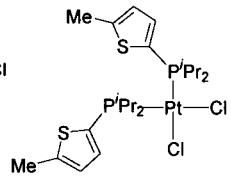	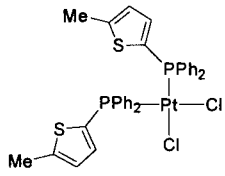	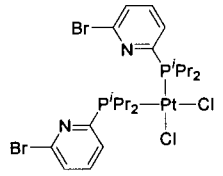
6-1	**6-2**	**6-3**	**6-4**	**6-5**
14.4	-3.5	5.1	19.2	28.2
2430	3644	3696	3763	3712

6.2.5. Mass spectrometry

In general the molecules fragment by loss of Cl ligands, followed by the scission of successive ^{i}Pr or Ph phosphine groups (Table 6.10).

Table 6.10 EI-MS Mass peaks m/z (% Intensity) [Fragment]

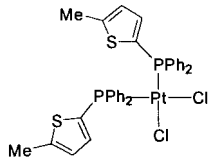 **6-4**	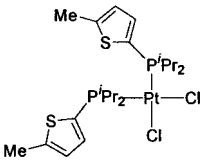 **6-3**	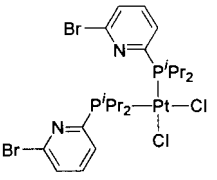 **6-5**
835 (5) [M^++1]*	694 (8) [M^+]	817 (63) [M^+]*
797 (3) [M^+ - H^{37}Cl]	659 (2) [M^+ - Cl]	780 (26) [M^+ - ^{37}Cl]
759 (1) [M^+ - 2Cl]	624 (2) [M^+ - 2Cl]	744 (26) [M^+ - Cl - HCl]
574 (0.1) [M^+ - 2Cl - PPh_2]	581 (1) [M^+ - 2Cl - ^{i}Pr]	702 (7) [M^+ - 2 Cl - ^{i}Pr]
477 (0.4) [Pt($MeSC_4H_2PPh_2$)$^+$]	538 (1) [M^+ - 2Cl - 2^{i}Pr]	659 (2) [M^+ - 2 Cl - 2 ^{i}Pr]
282 (100) [$MeSC_4H_2PPh_2^+$]	410 (0.2) [Pt($MeSC_4H_2P^iPr_2$)$^+$]	616 (1) [M^+ - 2 Cl - 3 ^{i}Pr]
205 (42) [$MeSC_4H_2PPh^+$]	367 (1) [Pt($MeSC_4H_2P^iPr$)$^+$]	310 (100) [PtBrCl$^+$]
97 (12) [$MeSC_4H_2^+$]	323 (4) [Pt($MeSC_4H_2$)$^+$]	232 (84) [BrpyP^iPr^+]
	214 (100) [$MeSC_4H_2P^iPr_2^+$]	230 (100 [PtCl$^+$]
	129 (72) [$MeSC_4H_2P^+$]	
	97 (4) [$MeSC_4H_2^+$]	
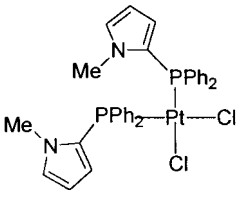 **6-2**	[M^+] of 795 not observed	380 (16) [$PtPPh_2$+]
	723 (72) [M^+ - 2 HCl] or	303 (24) [$PtPPh^+$]
	[M^+ - Cl - ^{37}Cl]	265 (61) [$MeNC_4H_3PPh_2^+$]
	645 (24) [M^+ - 2 HCl - PhH]	188 (18) [$MeNC_4H_3PPh^+$]
	494 (50) [M^+ - 2 Cl - 3 Ph]	80 (49) [$MeNC_4H_3^+$]
	460 (12) [Pt($MeNC_4H_3PPh_2$)$^+$]	

* based on ^{37}Cl isotope

6.3 REFERENCES

[1] (a) G. Van Koten; *Pure Appl. Chem.*, **1989**, *61*, 1681-1694 (b) G. Van Koten, *New J. Chem.*, **1997**, *21*, 751-771

[2] (a) K.A. Fallis, C. Xu and G.K. Anderson; *Organometallics*, **1993**, *12*, 2243 (b) J.K. Stille in *The Chemistry of the Metal-Carbon Bond*, Ed. F.R. Hartley and S. Patia, John Wiley and Sons Ltd., 1985, pp 716-717 (c) H.-K. Yip, C.M. Che and S.-M. Peng; *J. Chem. Soc., Dalton Trans.*, **1993**, 179-187 (d) P.K. Byers; *Coord. Chem. Rev.*, **1995**, *146*, 431-450

[3] F.A. Cotton, E.V. Dikarev, G.T. Jordan IV, C.A. Murilo and M.A. Petrukhina; *Inorg. Chem.*, **1998**, *37*, 4611-4616

[4] G.R. Newkome; *Chem. Rev.*, **1993**, *96*, 2067-2089

[5] J.S. Field, R.J. Haines, E.I. Lakoba and M.H. Sosabowski; *J. Chem. Soc., Perkin Trans. 1*, **2001**, 3352-3360

[6] (a) M. Kranenburg, W.E.M. van der Burgt, P.C.J. Kamer and P.W.N.M. van Leeuwen; *Organometallics*, **1995**, *14*, 3081-3089 (b) L.A. van der Veen, P.C.J. Kamer and P.W.N.M. van Leeuwen; *Angew. Chem. Int. Ed.*, **1999**, *38*, 336-338

[7] D.W. Allen, B.F. Taylor; *J. Chem. Soc., Dalton Trans.*,**1982**, 51-54

[8] G.K. Anderson and R.J. Cross; *Chem. Soc. Rev.*, **1980**, 9,185-215

[9] A. Olivier, M.Sc. thesis, **2000**

[10] L. Brandsma and H. Verkruijsse in *Preparative Polar Organometallic Chemistry 1*, Springer-Verlag, Berlin Heidelberg, 1987, pp.115-136

[11] S. Lotz, Y. Terblans and H.M. Roos; *J. Organometal. Chem.*, **1998**, *566*,133

[12] S.O. Grim and R. L. Keiter; *Inorg. Chim. Acta*, **1970**, *4*, 56-60

[13] S. Berger, S. Braun and H. Kalinowski in *NMR Spektroskopie von Nichtmetallen*, Georg Thieme Verlag, 1993, p169 (b) C.A.Tolman; *Chem. Rev., **1977**, 77*, 313-348

[14] Z-Z. Zhang and Hui Cheng; *Coord. Chem. Rev.*, **1996**, *147*,1-39

[15] A. Varshney and G.M. Gray; *Inorg. Chim. Acta*, **1988**, *148*, 215-222

[16] J.P. Farr, M.M. Olmstead, F.E. Wood and A.L. Balch; *J. Am. Chem. Soc., **1983**, 105*, 792-798

[17] (a) W. Porzio, A. Musco, A. Immirzi; *Inorg. Chem.*, **1980**, *19*, 2537-2540 (b) S. Otsuka, T. Yoshida, M. Matsumoto and K. Nokatsu; *J. Am. Chem. Soc.*, **1976**, *98*, 5850-5857

[18] N. Hoa Tran Huy, P. Lefloch, F. Robert and Y. Jeannin; *J. Organometal. Chem.*, **1987**, *327*, 211-221

[19] (a) J. Lewis, N.J. Long, P.R. Raithby, G.P. Shields, W.-Y. Wong and M. Younus; *J. Chem. Soc., Dalton Trans.*, **1997**, 4283-4288 (b) S.V. Meille, A. Farina, F. Bezziccheri and M.C. Gallazzi; *Adv. Mater.*, **1994**, *6*, 848-851

[20] a) G.A. Wilkinson, R.D. Gillard and J.A. McCleverty in *Comprehensive Coordination Chemistry*, New York Pergamon Press, 1987, p 439

[21] G.G Messmer and E.I. Amma; *Inorg. Chem.*, **1966**, *5*, 1775-1781

[22] D.W. Allen and D.F. Ashford; *J. Inorg. Nucl. Chem.*, **1976**, *38*, 1953-1956

[23] P.S. Pregosin and R.W. Kunz in *^{31}P and ^{13}C NMR of Transition Metal Phosphine Complexes*, Springer-Verlag, New York, 1978, p 50

/ End of Chapter 6 //

CHAPTER 7

Experimental

7.1 INSTRUMENTATION AND GENERAL TECHNIQUES

7.1.1 Nuclear Magnetic Resonance Spectroscopy

NMR spectra of the ligands and complexes reported in Chapter 6 were recorded on a Bruker AC-300 spectrophotometer operating at 300.135 MHz for ^{1}H, 75.469 MHz for ^{31}P and 121.496 MHz for ^{13}C. All other spectra were recorded on a Bruker ARX-300 (7.0 T) operating on 1D WIN NMR and 2D WIN NMR release 6.0 software.

Chemical shifts are reported as δ values in parts per million (ppm) using the deuterated solvent signal as the internal reference. For $CDCl_3$, the ^{1}H NMR spectra were calibrated at $\delta_H = 7.2400$ and the ^{13}C spectra at $\delta_C = 77.000$ ppm. ^{31}P NMR spectra were referenced to the deuterated lock solvent, which had been previously referenced to 85 % H_3PO_4.

The ^{1}H NMR signals were assigned according to first-order analysis of the spin systems and further information was obtained, when necessary, from two-dimensional (^{1}H, ^{1}H) homonuclear chemical shift correlation (COSY) experiments. The allocation of signals was further substantiated by integration values. The ^{13}C and ^{31}P NMR spectra were obtained as proton-decoupled spectra. The multiplicities of the ^{13}C resonances were deduced from proton-

decoupled CH, CH_2 and CH_3 subspectra obtained using DEPT pulse sequences. The signals of proton-bearing carbon atoms were correlated with specific proton resonances through two-dimensional heteronuclear correlation (HETCOR) experiments. Abbreviations used for spectral coupling patterns are:

br	broad	m	multiplet
d	doublet	q	quartet
dd	doublet of doublets	s	singlet
ddd	doublet of doublets of doublets	sat.	satellites
dt	doublet of triplets	t	triplet

7.1.2 Mass Spectrometry

Mass spectrometry analyses were outsourced, and depending on the availability of the service, either the Electron Impact (EI) or the Fast Atom Bombardment (FAB) method of ionisation was used. EI mass spectra were recorded on a Finnigan Mat 8200 mass spectrometer operating at approximately 70 eV (1.12×10^{-17} J). FAB mass spectra were measured on a VG 7070-E instrument (Xe beam, *m*-nitrobenzyl alcohol matrix, detection of positive ions with $m/z > 99$).

7.1.3 Melting Point Determination

Melting points were determined using a Kofler hot stage microscope and are uncorrected.

7.1.4 Single Crystal X-ray Crystallography

The intensity data for the platinum(II) complexes, **6-1** and **3-1**, were collected on a Nonius KappaCCD diffractometer, using graphite-monochromated Mo-K_α radiation. Data was corrected for Lorentz, polarization and absorption effects [1]. The structure was solved by direct methods and refined by full-matrix least squares techniques against Fo^2 [2, 3]. The

hydrogen atoms of the compounds were included at calculated positions with fixed thermal parameters. All nonhydrogen atoms were refined anisotropically [3]. XP (SIEMENS Analytical X-ray Instruments, Inc.) was used for structure representations. Further details of the crystal structure investigations for **6-1** are available on request from the director of the Cambridge Crystallographic Data Center, 12 Union Road, GB-Cambridge CB2 1 EZ (depository number CCDC-136338 (**1**) J.T.Chantson, H. Görls, S. Lotz; *Inorg. Chim. Acta.*, **2000**, *305*, 32-37)

An Enraf-Nonius CAD4 diffractometer operating with graphite-monochromatized MoKα radiation ($\lambda = 0.7107$ Å) was used for single crystal structure determination of **3**. The intensity data was collected using ω-2θ techniques, and was corrected for absorption and Lorentz-polarization effects. The structures were solved using conventional Patterson and Fourier techniques on SHELX86 [4]. All non-hydrogen atoms were refined anisotropically and the hydrogen atoms were placed in calculated positions and refined with a common isotropic thermal parameter. X-ray diffraction data for **2** was collected on a SMART CCD 1K diffractometer and refined by full-matrix, least squares techniques against F^2 as for **3** (CCDC-157702).

7.1.5 General

Solvents were dried and distilled prior to use: Hexane, benzene and toluene were dried over sodium metal, dichloromethane over phosphorus pentoxide, and ether and tetrahydrofuran over sodium/dibenzophenone.

All reactions generating novel platinum(II) complexes were carried out using standard vacuum-line and Schlenk techniques under nitrogen [5]. The preparation of certain metal precursors were also carried out under an inert atmosphere. All lithiation reactions were preformed under a positive argon pressure.

7.2 SYNTHESIS OF PLATINUM PRECURSORS

7.2.1. (η^4-cycloocta-1,5-diene)dichloroplatinum(II), [Pt(cod)Cl_2]

$$K_2[PtCl_4] + cod \rightarrow [Pt(cod)Cl_2] + 2\ KCl$$

A sample of 1.026 g (2.47 mmol) of potassium tetrachloroplatinate(II) was dissolved in 18 mL of water. To this solution was added 12.5 mL of *n*-propanol, 2.0 mL of cod and 0.0176 g (0.088 mmol) of tin(II) chloride dihydrate. The mixture was stirred for 2 days after which the solution had become colourless and a precipitate had formed. The white solid was filtered, washed with 10 mL of water and then with 3 mL of ethanol, and air-dried [6].

Yield 0.81 g (87 %, yields generally range from 80 - 92 %) white, air-stable solid

7.2.2 Tetrakis(triethylphosphine)platinum(0), [Pt(PEt_3)$_4$]

$$K_2[PtCl_4] + 4\ PEt_3 + 2\ KOH + EtOH \rightarrow [Pt(PEt_3)_4] + 4\ KCl + CH_3CHO + 2\ H_2O$$

Under an argon atmosphere, 1.5 g (3.6 mmol) of potassium tetrachloroplatinate(II) was dissolved in 10 mL of water. This solution was added dropwise to a solution of 0.7 g (12.5 mmol) of potassium hydroxide in 30 mL ethanol / 1 mL water and 3.0 mL (20 mmol) triethylphosphine. The solution became colourless whilst stirring for 1 hr at room temperature The reaction mixture was then heated at 60 °C for 3 hr, and evaporated to dryness *in vacuo*, also at room temperature (This takes about 2-3 hr.) An orange oil / solid residue was obtained which was extracted with three 10 mL portions of hexane. The extracts were combined and filtered by the Schlenk-flask method [5]. After reducing the volume of the filtrate by 75 %, 0.50 mL (3.4 mmol) of triethylphosphine was added and the mixture cooled at -78 °C for at least 4 hr, during which time a white precipitate formed. The supernatant was removed via a syringe, three 2 mL portions of hexane was used to wash the precipitate at -78°C and the precipitate was dried *in vacuo* at -40 °C [7].

Yield generally 2.0 - 2.2g (80 - 92 %) white, air-sensitive solid.

7.2.3 Tris(triphenylphosphine)platinum(0), $[Pt(PPh_3)_3]$

Step 1: $K_2[PtC\ell_4] + 4\ PPh_3 + 2\ KOH + EtOH \rightarrow [Pt(PPh_3)_4] + 4\ KC\ell + CH_3CHO + 2\ H_2O$

Working under a nitrogen atmosphere a mixture of 8.40 g (32.0 mmol) of triphenylphosphine and 120 mL of absolute ethanol was heated at 65 °C until the solution was clear. A solution of 0.777g (13.8 mmol) of potassium hydroxide in 16 mL ethanol / 4 mL water was added. To this mixture, at 65 °C, a solution of 2.86 g (6.88 mmol) of potassium tetrachloroplatinate(II) in 25 mL of water was slowly added over a period of 10 min. Within minutes a pale yellow compound began to separate out. After allowing the mixture to cool to room temperature, the compound was filtered; the filtration process proceeded very slowly, even under a high vacuum. The compound was washed with 70 mL of warm ethanol, followed by 20 mL of cold water and then by 20 mL of cold ethanol, and dried *in vacuo* [8].
Yield 8.0 g (93 %) yellow solid, stored under nitrogen.

Step 2: $[Pt(PPh_3)_4] \rightarrow [Pt(PPh_3)_3] + PPh_3$

A 8.0 g (6.4 mmol) sample of tetrakis(triphenylphosphine)platinum(0) was suspended in 250 mL of absolute ethanol and boiled under a nitrogen atmosphere for 2 hr. The dark yellow suspension was filtered whilst hot and the precipitate collected was washed with 30 mL of cold ethanol and dried *in vacuo* for 2 hr [8].
Yield 5.0 g (79 %) bright-yellow, air-sensitive solid.

7.2.4 *N,N*-(2,2'-bipyridyl)dimethylplatinum(II), $[PtMe_2(bipy)]$

Step 1: $K_2[PtC\ell_4] + 2\ SMe_2 \rightarrow$ *cis*- and *trans*-$[PtC\ell_2(SMe_2)_2] + 2\ KC\ell$

Under a nitrogen atmosphere, a 500 mL 3-neck, round-bottomed flask was charged with 5.76g

(13.9 mmol) of potassium tetrachloroplatinate and 100 mL water. Once all the solid had dissolved, 6.4 mL (87 mmol) of dimethylsulfide was introduced via a syringe. Upon heating, a yellow solution was obtained. Once the solution had cooled to room temperature, it was extracted with four portions (50 mL each) of dichloromethane. The organic fractions were combined and dried over anhydrous sodium sulfate. The solvent was removed under reduced pressure [9].

Yield 4.9 g (91 %) yellow, air-stable solid.

Step 2: *cis*- and *trans*-$[PtCl_2(SMe_2)_2]$ + 4 MeLi → $[Pt_2Me_4(\mu\text{-}SMe_2)_2]$

The entire procedure was performed under an atmosphere of dry nitrogen. A mixture of *cis*- and *trans*-$[PtCl_2(SMe_2)_2]$ from Step 1 was finely powdered and 3.88 g (9.94 mmol) of the powder was suspended in 160 mL of dry, freshly-distilled diethyl ether. The suspension was immersed in an ice-bath and 14.9 mL (21 mmol) of a 1.4 M solution of methyllithium in diethylether was added dropwise over a period of 10 min. The mixture was stirred for 20 min before 4.0 mL of a cold solution of saturated, aqueous ammonium chloride was added. Approximately 100 mL of cold water was added and the mixture extracted with three 50 mL portions of cold diethylether (0 °C). The organic portions were combined and dried over anhydrous magnesium sulfate. A spatula-tip quantity of decolourising charcoal was added and the black mixture filtered into a 1-L round-bottomed flask. The solvent was removed *in vacuo* without external heating [9].

Yield 1.7 g (60%) off-white solid stored under nitrogen at -20 °C.

Step 3: $[Pt_2Me_4(\mu\text{-}SMe_2)_2]$ + 2 (2,2′-bipy) → 2 $[PtMe_2(2,2'\text{-bipy})]$ + 2 SMe_2

To a suspension of 1.7 g (2.98 mmol) $[Pt_2Me_4(\mu\text{-}SMe_2)_2]$ in 60 mL of benzene was added a solution of 1.7 g (10.1 mmol) of 2,2′-bipyridine in 40 mL of dry diethyl ether. A red colouration occurred immediately. The mixture was stirred for several minutes and stored in the fridge overnight. The bright red precipitate was filtered, washed with a small volume of

diethyl ether and dried *in vacuo* [10].
Yield 1.17 g (51 %) red, air-stable solid.

7.3 SYNTHESIS OF PALLADIUM PRECURSORS

7.3.1 Tetrakis(triphenylphosphine)palladium(0), [$Pd(PPh_3)_4$]

$$2\,[PdCl_2] + 8\,PPh_3 + 5\,NH_2NH_2.H_2O \rightarrow 2\,[Pd(PPh_3)_4] + 4\,NH_2NH_2HCl + N_2 + 5\,H_2O$$

A 500 mL, three-necked, round-bottomed flask containing 1.82 g (10.2 mmol), 13.4 g (51.1 mmol) triphenylphosphine and 140 mL of dimethylsulfoxide was heated at 135 °C until a yellow-orange coloured suspension was obtained. The mixture was removed from the heat and stirred for 15 min. Hydrazine hydrate (2 mL) was added and to ensure that nitrogen evolution did not occur too vigorously or that the mixture did not overheat, the temperature of the flask was regulated by immersion into a water-bath. The mixture was stirred for 1 hr and then filtered under nitrogen. The collected precipitate was washed with two 5 mL portions of ethanol and three 4 mL aliquots of diethyl ether, and dried *in vacuo* for 20 min [11].
Yield 8.4 g (72 %) yellow solid stored under nitrogen.

7.3.2 Tris(dibenzylideneacetone)dipalladium(0), [$Pd_2(dba)_3$.dba]

$$2\,PdCl_2 + 4\,dba \xrightarrow[NaOAc]{MeOH\ /} Pd_2(dba)_3.dba + 4\,NaCl$$

A solution of 4.49 g (19.2 mmol) of dba and 3.80 g (46.4 mmol) of sodium acetate was heated (*ca* 50 °C) in 150 mL of methanol before 1.02 g (5.79 mmol) of palladium dichloride was added. The mixture was heated for 3 ½ hr at 45 °C and allowed to cool to room temperature

The purple precipitate obtained was filtered, and washed with water, and acetone before it was dried *in vacuo* [12].

Yield 3.1 g (93 %) purple, air-stable solid.

7.4 LIGAND SYNTHESIS

7.4.1 Preparation of dibenzothiophene-based ligands (Chapter 2)

1. *4,6-Bis(trimethylsilyl)dibenzothiophene*, **2**

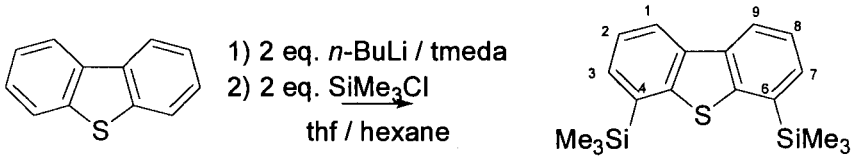

A 250-mL round-bottomed flask was charged with 11.9 mL (78.8 mmol) of tmeda and 40 mL of dry hexane under nitrogen. With the aid of a dropping funnel, 49.6 mL (79 mmol) of a 1.6 M solution of n-butyllithium in hexane was added to the tmeda-solution at 0 °C. The mixture was stirred at 0 °C for 30 min and for a further 30 min at room temperature. The mixture was then diluted by the addition of 60 mL of hexane, and 4.83 g (26.2 mmol) of dibenzothiophene was introduced via a powder funnel [13]. After heating the mixture at 60 °C for 2 hr, it was cooled to -70 °C, and 10.0 mL (78.8 mmol) of chlorotrimethylsilane was added dropwise. The mixture was stirred for 20 min at -65 °C after which the cold bath was removed and the mixture stirred for an additional 40 min. The reaction was quenched upon pouring the mixture into a separating funnel containing 250 mL of water. The organic layer was separated, the aqueous layer extracted with hexane, the hexane fractions combined, dried over anhydrous sodium sulfate and concentrated under reduced pressure. White crystals of

2 were obtained upon cooling the resulting yellow solution at -20 °C. The product was purified by column chromatography on silica gel using *n*-pentane as eluent.
Yield 2.64 g (30 %) $C_{18}H_{24}SSi_2$ FM 328.63; mp 97-98°C

2. *4,6-Dibromodibenzothiophene*, **3**

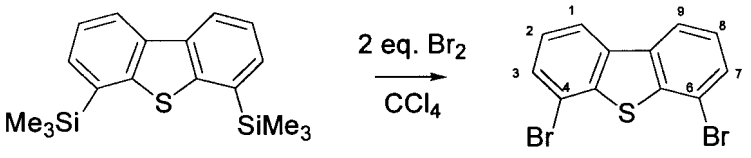

To a solution of 0.480 g of 4,6-bis(trimethylsilyl)dibenzothiophene (1.46 mmol) in 3.0 mL of carbon tetrachloride at -15 °C was added 1.20 mL (2.96 mmol) of a 2.47 M bromine / carbon tetrachloride solution. The mixture was stirred in the cold for 60 min, the cold bath was removed and the mixture stirred for a further 60 min. The volume of the mixture was increased by the addition of 45 mL of carbon tetrachloride before the reaction was quenched with water. After washing the organic layer with brine, drying over anhydrous sodium sulfate and evaporating to dryness, **3** was obtained as a pure, white crystalline solid.
Yield 0.444 g (89 %) $C_{12}H_6Br_2S$ FM 342.05; mp 177-178 °C

3. *2,8-Dibromodibenzothiophene*, **1**

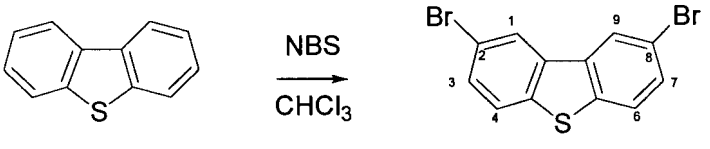

A mixture of 9.95 g (54 mmol) of dibenzothiophene and 20.3 g (114 mmol) of *N*-bromosuccinimide was stirred in 500 mL of chloroform at ambient temperature for 24 hr [14]. The reaction mixture was hydrolysed and the organic phase separated off and dried over anhydrous sodium sulfate. The volume of the solution was reduced by rotary vaporisation and a pure crystalline white solid precipitated upon cooling the solution to -25 °C.

Yield 12 g (65 %) $C_{12}H_6Br_2S$ FM 342.05

4. *4,6-Bis(trimethylstannyl)dibenzothiophene,* **4**

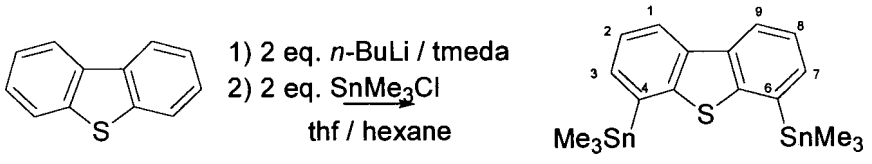

A mixture of 5.0 mL (33 mmol) of tmeda and 20 mL of hexane was cooled to 0 °C under argon and 20.6 mL (33 mmol) of a 1.6 M *n*-butylllithium / hexane solution was added. The mixture was stirred for 30 min at 0 °C, and for a further 30 min after removal of the cold-bath. Solid dibenzothiophene (2.006 g, 10.9 mmol) and a further 20 mL of hexane was added. After refluxing the mixture for 2 hr, a dark brown suspension was obtained. This was cooled to -78 °C before 6.573 g (33 mmol) of chlorotrimethylstannane was added. The mixture was stirred for 30 min at -78 °C, followed by 30 min at room temperature and 30 min at refluxing temperature. Once the mixture had cooled to ambient temperature it was poured onto 100 mL of a saturated aqueous ammonium chloride solution. Three 80 mL portions of hexane was used to extract the target compound from the aqueous phase. The combined hexane fractions were dried over anhydrous sodium sulfate and the solvent was removed under reduced pressure. The ligand undergoes extensive protodestannylation on silica gel.

While purifying the compound by fractional distillation, sublimated dibenzothiophene was collected which significantly reduced the yield.

Yield 1.36 g (24 %) yellow oil $C_{18}H_{24}SSn_2$ FM 509.87

7.4.2 Thiophene based ligands

1. *3,6-Dimethylthieno[3,2-b]thiophene*, **L1**

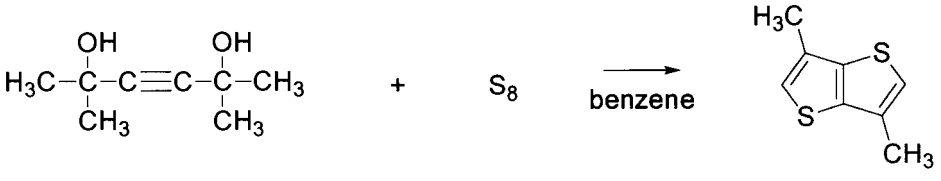

A mixture of 17.0 g (120 mmol) of 2,5-dihyroxy-2,5-dimethyl-3-hexyne, 9.52 g elemental sulfur (S_8) and 130 mL of benzene was sealed in an autoclave. The mixture was heated at 200 °C overnight. The reaction proceeds via dehydration of the hexyne to form 2,5-dimethyl-1,5-hexadiene-3-yne as a probable reaction intermediate. After cooling to room temperature, the autoclave was opened and the brown residue obtained was extracted with benzene. The benzene was removed *in vacuo* and the resulting residue was dissolved in warm hexane and filtered. Purification by column chromatography on silica gel with hexane as the eluent resulted in the isolation of a white solid [15].

Yield 3.55 g (21 %) $C_8H_8S_2$ FM 168.28

2. *1-Methyl-2-(2-thienyl)pyrrole*, **L3**

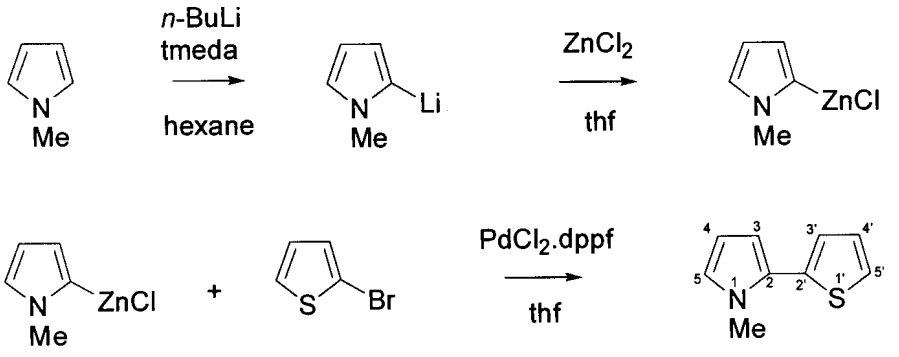

Under an atmosphere of argon, 4.02 g (49.6 mmol) of freshly distilled 1-methylpyrrole was slowly added to a Schlenk flask containing 38 mL (60 mmol) of a 1.6 M *n*-butyllithium and 8.30 mL (55 mmol) of tmeda in 60 mL of hexane. The solution was heated under reflux for 20 min. After allowing the solution to cool to room temperature, 40 mL of freshly-distilled tetrahydrofuran (thf) was added. The solution was vigorously stirred as 9.0 g (66 mmol) of anhydrous zinc chloride was added. The temperature of the mixture was controlled by an external bath so that the temperature did not rise above 20 °C. To the 2-(1-methylpyrrolyl)zinc chloride that had formed *in situ*, 4.8 mL (50 mmol) of 2-bromothiophene and 0.54 g (0.74 mmol) of the $PdCl_2$.dppf catalyst were added. The mixture was heated to reflux for 6 hr. After cooling to room temperature the solution was poured onto a 2.8 M aqueous ammonium chloride solution to which a small amount of ammonia had been added. The organic layer was separated and the aqueous phase was treated consecutively with four 100 mL portions of diethyl ether. The organic fractions were combined and dried over anhydrous potassium carbonate. The solvent was removed under reduced pressure and the product isolated by distillation (B.p. 125°C / 15 mm Hg) [16a].

Yield 5.51 g (68 %) slight brown oil kept under argon C_9H_9NS FM 163.24

2.1 *Preparation of the catalyst, dichloro-1,1'-bis(diphenylphosphino)-ferrocene palladium(II), $PdCl_2$.dppf*

$$PdCl_2 + dppf \rightarrow PdCl_2.dppf$$

5.60 g (10.0 mmol) of 1,1'-bis(diphenylphosphino)ferrocene (dppf) was dissolved in 75 mL of hot toluene. A solution of 1.77 g (10.0 mmol) of palladium(II) chloride and 1.48 g (35.0 mmol) of anhydrous lithium chloride was dissolved in 100 mL of 96 % ethanol by heating at 70 °C. This solution was then added to the dppf / toluene solution at 70 °C. After stirring for 30 min at this temperature, the suspension was cooled to room temperature before it was filtered. The precipitate was washed three times with 10 mL portions of ethanol, and then twice with two 10 mL portions of diethyl ether. The orange-red solid was dried *in vacuo* with external heating at 40 °C [16b].
Yield 6.6 g (90 %) $C_{34}H_{28}P_2FePdCl_2$ FM 731.71

2.2 *Preparation of 1,1'-bis(diphenylphosphino)ferrocene, dppf*

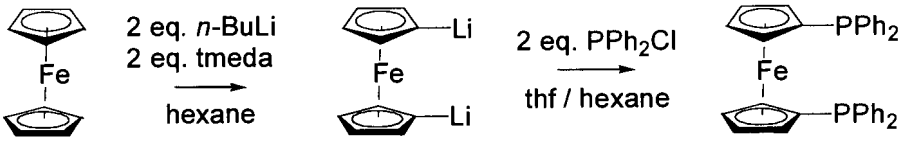

A 3.7 g (20 mmol) portion of ferrocene and 125 mL of hexane was introduced into a 500 mL round bottom flask under nitrogen. An aliquot of 27 mL (43 mmol) of 1.6 M *n*-butyllithium in hexane was added at room temperature via a syringe. This was followed by the addition of 6.2 mL (41 mmol) of tmeda to the resulting red suspension. The temperature of the mixture quickly rose to 35 °C. The mixture was heated at 60 °C for 1 hr. After cooling to room temperature, 60 mL of dry thf was added and the orange suspension cooled to

-40°C before a mixture of 9.6 g (44 mmol) of chlorodiphenylphosphine in 30 mL of thf was slowly added. The cold-bath was removed and the reaction mixture was stirred for an additional 15 min at room temperature. It was then concentrated under reduced pressure and filtered. The precipitate was washed with 20 mL of 2 M hydrochloric acid, 20 mL of water, 20 ml ethanol and finally with 20 mL of diethyl ether. The orange solid was dried *in vacuo* [16c].
Yield 8.0 g (72 %) $C_{34}H_{28}P_2Fe$ FM 554.39

3. *2-Methylbenzothiazole*

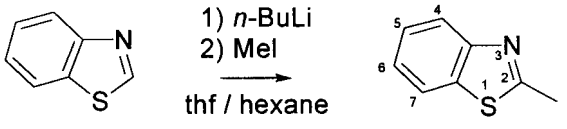

Under an atmosphere of nitrogen and at a temperature of -70°C, 9.80 mL (12.1 g, 89.7 mmol) of benzothiazole was added over several seconds to 60.0 mL (96.0 mmol) of a 1.6 M of an *n*-butyllithium / hexane solution in 70 mL of freshly distilled thf. The mixture was stirred for 15 min at -70 °C, after which 5.60 mL (12.8 g, 89.9 mmol) of methyl iodide was introduced via a syringe. A further 20 min of stirring at -70°C elapsed before the cold-bath was removed and the mixture allowed to warm to room temperature. The reaction was quenched by the addition of 200 mL of a saturated aqueous ammonium chloride solution. The aqueous layer was extracted with diethyl ether (4 × 100 mL) . The combined ether extracts was washed with 100 mL of water. The ether phase was separated and dried over anhydrous sodium sulfate. The solvent was removed under reduced pressure and the crude 2-methylbenzothiazole obtained was purified by column chromatography on silica gel; the eluent being a mixture of diethyl ether / hexane [17].
Yield 9.52 g (71 %) C_8H_7NS FM 149.22
NMR in $CDCl_3$ ^1H δ / ppm: 7.930 (d, 1H, H-4, $^3J_{HH}$ = 7.7 Hz), 7.799 (d, 1H, H-7, $^3J_{HH}$

= 7.7 Hz), 7.423 (dt, 1H, H-5, $^{3}J_{HH}$ = 7.7 Hz, $^{4}J_{HH}$ = 1.29 Hz), 7.318 (td, 1H, H-6, $^{3}J_{HH}$ = 7.7 Hz, $^{4}J_{HH}$ = 1.04 Hz), 2.816 (s, 3H, Me); ^{13}C δ / ppm: 153.81 (C-2), 153.44 (C-3a), 135.97 (C-7a) 125.86 (C-5), 124.67 (C-6), 122.40 (C-4), 121.36 (C-7), 20.07 (Me)

7.4.3 **Preparation of heteroaylphosphine ligands** (Chapter 6)

The phosphine ligands were prepared according to the following generalized reaction scheme:

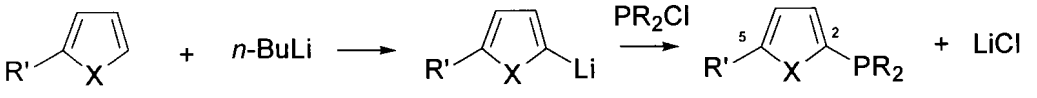

X = NMe, S
R = Ph, ^{i}Pr
R' = H, Me

The reaction conditions (solvent, temperature and reaction times) for the lithiation step were chosen according to literature methods [14].

1. *Diisopropyl-2-(5-methylthienyl)phosphine,* **P3**

A solution of *n*-butyllithium (14.2 mL of 1.6 M in hexane, 22.7 mmol) was added dropwise to a solution of 2-methylthiophene (2.00 mL, 20.7 mmol) in thf (10 mL) at room temperature. No external cooling was applied and the resultant mixture was stirred for 1 hr. The reaction mixture was then cooled to 0 °C in an ice-bath before chlorodiisopropylphosphine (3.30 mL, 20.7 mmol) was introduced. After allowing the reaction to proceed for an additional hour at room temperature, the solvent was removed under reduced pressure. Diethyl ether was added, the mixture filtered through silica gel layered with anhydrous sodium sulfate and the filtrate vacuum-evaporated

to dryness. The orange oil that was obtained was distilled under reduced pressure to give a colourless liquid.

Yield 3.4 g (77 %) $C_{11}H_{19}PS$ FM 214.31

2. *2-(5-Methylthienyl)diphenylphosphine,* **P4**

A procedure similar to that described above was followed, using chlorodiphenyl-phosphine (3.80 mL, 20.6 mmol) instead of chlorodiisopropylphosphine.

Yield 4.9 g (84 %) $C_{17}H_{15}PS$ FM 282.35

3. *Diisopropyl-2-(1-methylpyrrolyl)phosphine*, **P1**

1-Methylpyrrole (2.50 mL, 28.2 mmol) was reacted with *n*-butyllithium (16.0 cm^3 of a 1.6 M hexane solution, 25.6 mmol) in the presence of tmeda (3.84 mL, 25.6 mmol). The reaction mixture was heated for 20 min at 50 °C. The reaction mixture was then allowed to cool to room temperature before the temperature was decreased to -60 °C (acteone/dry ice bath) and chlorodiisopropylphosphine (4.07 mL, 25.6 mmol) was added. The product was filtered through silica gel.

Yield 2.5 g (50 %) $C_{11}H_{20}NP$ FM 197.26

4. *2-(1-Methylpyrrolyl)diphenylphosphine,* **P2**

The phosphine ligand was prepared as described above using chlorodiisopropylphosphine (4.60 mL, 25.6 mmol) instead of chlorodiisopropyl-phosphine was added. The product was purified as described above.

Yield 5.6 g (82 %) $C_{17}H_{16}NP$ FM 265.29

5. *2-(6-Bromopyridinyl)diisopropylphosphine,* **P5**

2,6-Dibromopyridine (1.137 g, 4.80 mmol) was reacted with *n*-butyllithium (3.30 mL of a 1.6 M hexane solution, 5.28 mmol) in dichloromethane at -78 °C for 20 min. Thereafter, chlorodiisopropylphosphine (0.76 mL, 4.8 mmol) was added and after 30 min the reaction mixture was allowed to equilibrate to room temperature. Water was added and the aqueous layer extracted with diethyl ether. The combined organic fractions was dried over anhydrous sodium sulfate, filtered and the solvents were removed by rotary evaporation under reduced pressure. The ligand was purified by column chromatography (silica gel with diethyl ether / hexane mixtures as eluent).
Yield 0.79 g (60.0 %) $C_{11}H_{17}BrNP$ FM 274.14

6. *2,5-Bis(diphenylphosphino)thiophene,* **P6**

A 3-necked, 100-mL, round-bottomed flask was charged with 0.98 mL (12.3 mmol) of thiophene and 15 mL thf. The solution was cooled to -78 °C and 20.0 mL (32 mmol) of a 1.6 M *n*-butyllithium/ hexane solution was added dropwise. After stirring the solution for 30 min at -78 °C, 4.54 mL of chlorodiphenylphosphine was added via a syringe. The reaction mixture was allowed to equilibrate to ambient temperature overnight. Water was added to the flask in order to quench the reaction. The solvent volume was reduced *in vacuo* and the resulting solution was extracted three times with diethyl ether. The combined ether extracts was dried over anhydrous sodium sulfate , filtered and the solvent removed under reduced pressure. The resultant brown oil was purified by column chromatography on silica gel using hexane / diethyl ether solutions as the eluent.
Yield 1.4 g (25 %) colourless liquid $C_{28}H_{22}P_2S$ FM 452.50

7.5 PREPARATION OF PLATINUM(II) COMPLEXES

7.5.1 Preparation of Binuclear Pt(II) complexes (Chapter 2)

1. *μ-Dibenzothienyl-1κC⁴:2κC⁶-bis[*trans-*bromobis(triethylphosphine)-platinum(II)]*, **2-1**

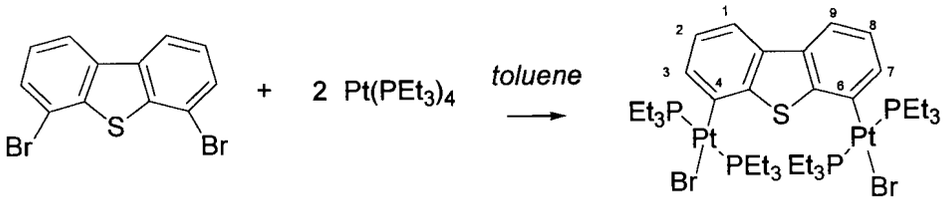

At ambient temperature and under a nitrogen atmosphere, 0.283 g (0.827 mmol) of 4,6-dibromodibenzothiophene was added to a solution of 1.09 g (1.63 mmol) of tetrakis(triethylphosphine)platinum(0) in 10 mL toluene. An additional 10 mL of toluene was added and the solution refluxed for 1 hr. The solvent was removed *in vacuo* and the resultant white solid was washed twice with 2 mL portions of hexane and dried *in vacuo*. Colourless, cubic crystals of the compound were grown from a cold (-20 °C) toluene / hexane solution. However the crystals became amorphous upon removal of the mother liquour or on exposure to air.

Yield 0.87 g (87 %). $C_{36}H_{66}Br_2P_4SPt_2$ FM 1204.85; mp > 220 °C

2. *μ-Dibenzothienyl-1κC⁴:2κC⁶-bis[*cis-*chloro(η⁴-cycloocta-1,5-diene)-platinum(II)]*, **2-2**

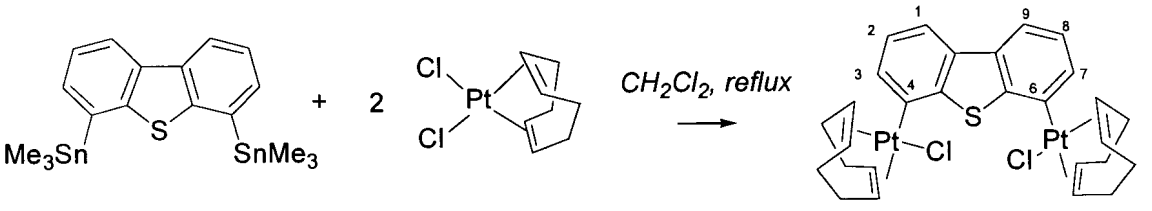

+ 2 $SnMe_3Cl$

To a Schlenk-flask containing 0.82 g (1.6 mmol) of 4,6-bis(trimethylstannyl)-dibenzothiophene was added 1.21 g (3.23 mmol) of dichloro-η^4-cycloocta-1,5-dieneplatinum(II) and 25 mL dichloromethane. The mixture was refluxed for 3 days. The solvent was removed *in vacuo* and the white solid obtained was washed with hexane.

Yield 1.3 g (%) $C_{28}H_{30}Cl_2SPt_2$ FM 859.68

3. *Reaction of 4,5-dibromo-2,7-di-*tert*-butyl-9,9-dimethylxanthene with [Pt(PEt₃)₄]*

Experiment 1: 2.80 mmol of $[Pt(PEt_3)_4]$ and 0.673 g (1.40 mmol) of 4,5-dibromo-2,7-di-*tert*-butyl-9,9-dimethylxanthene was refluxed for 24 hr in 10 mL of toluene.

Experiment 2: A 20 mL toluene solution of 3.30 mmol of $[Pt(PEt_3)_4]$ and 0.721 g (1.50 mmol) of the dibromoxanthene compound was refluxed for 1 week. A single oxidative insertion into a C-Br bond by "$Pt(PEt_3)_2$" resulted.

7.5.2 **Reaction of Pt(0) with thiophene-based ligands** (Chapter 3)

1. *Reaction of [Pt(PEt$_3$)$_4$] with 3,6-dimethylthieno[3,2-*b*]thiophene* (**3-1**)

Under an argon atmosphere 0.55 g (0.82 mmol) of tetrakis(triethylphosphine)-platinum(0) was weighed into a clean, dry Schlenk flask and dissolved in 5 mL of toluene. To the Schlenk was added 0.278 g (1.65 mmol) of solid 3,6-dimethylthieno-[3,2-*b*]thiophene and 10 mL of toluene. The mixture was heated to 80 °C under high vacuum for 6 hr. It was then refluxed for 3 hr. Thereafter the heat source was removed and the mixture stirred overnight at room temperature to form an off-white solid precipitate. The supernatant was removed and the precipitate washed with two 1 mL portions of hexane and dried *in vacuo*. Ivory-coloured crystals suitable for X-ray crystallography studies were obtained from a saturated toluene / hexane solution of **3-1** at -20 °C.
Yield 0.33 g (67 %) $C_{20}H_{38}P_2S_2Pt$ RM 599.68; mp 185-187 °C

2. *Reaction of [Pt(PEt$_3$)$_4$] with 2,2'-Bithiophene* (**3-2**)

Solid 2,2′-bithiophene (0.42 g, 2.5 mmol) was added to a Schlenk flask containing 1.87 g (2.8 mmol) of tetrakis(triethylphosphine)-platinum(0) in 20 mL of toluene. The mixture was stirred for 5 hr at 80°C and then at room temperature overnight. The solvent was removed *in vacuo* to yield a brown oil, containing a mixture of **3-2a** and **3-2b**.

3. *Reaction of [Pt(PEt$_3$)$_4$] with 1-methyl-2-(2-thienyl)pyrrole* (**3-3**)

To a solution of 2.26 mmol of tetrakis(triethylphosphine)platinum(0) in 10 mL of toluene was added 0.56 g (3.4 mmol) of 1-methyl-2-(2-thienyl)pyrrole, **L3**. The reaction mixture was stirred under reflux for 48 hr. A mixture of **3-3a** and **3-3b** was

obtained after removal of the solvent *in vacuo*.

7.5.3 **Preparation of Platinum(II) hydrides** (Chapters 4 and 5)

All reactions involving $[Pt(PEt_3)_4]$ were carried out under an atmosphere of dry nitrogen. A general reaction scheme for the preparation of *trans*-diphosphine platinum(II) hydride complexes is given below:

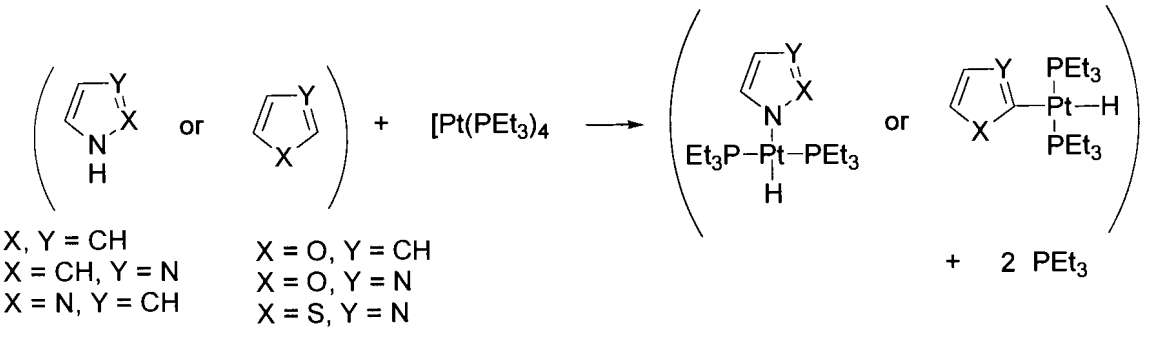

1. *Reaction of 1-methylpyrrole with $[Pt(PEt_3)_4]$*

A 0.120 mL aliquot of freshly distilled 1-methylpyrrole was added via a syringe to 5mL of a toluene solution containing $[Pt(PEt_3)_4]$ (1.4 mmol). A further 5 mL of toluene was added. The solution was heated at 80 °C for 3 weeks. The colour of the mixture darkened over this time period. After removal of the solvent *in vacuo*, a brown oily solid was obtained. This residue was washed with hexane and dried *in vacuo*. The presence of **4-1** was detected by NMR spectroscopy.

2. *Reaction of pyrrole with $[Pt(PEt_3)_4]$*

An aliquot of 0.175 mL (2.52 mmol) of pyrrole was added to a solution of 1.95 mmol of $[Pt(PEt_3)_4]$ in 5 mL of toluene. An additional 5 mL of toluene was added and the solution heated under reflux for 72 hr. The solvent was removed *in vacuo* and the brown residue triturated with two portions (1 mL) of hexane. A mixture of **4-2** and **4-3**

was obtained in low concentrations.

3. *Indolyl hydride* **4-4**

A solution of 1.72 mmol of $[Pt(PEt_3)_4]$ in 5 mL of toluene was added to a solution of 0.267 g (2.28 mmol) of indole in 2 mL toluene. The mixture was stirred at room temperature for 10 min, after which the solvent was removed *in vacuo*. The residue was washed with two portions of hexane (1 mL) and dried *in vacuo*. A white waxy solid was obtained, which gradually assumed a green/blue tinge. The compound also develops a blue colour whilst standing in $CDCl_3$.

Yield 0.8 g (87 %) $C_{20}H_{37}NP_2Pt$ FM 548.50; mp 53-55 °C

4. *Imidazolyl hydride* **4-5**

A solution of 1.95 mmol of $[Pt(PEt_3)_4]$ in 5 mL of toluene was added to a solution of 0.174 g (2.55 mmol) of imidazole in 2 mL toluene. Decolouration of the orange $[Pt(PEt_3)_4]$ solution occurred during the addition. The mixture was stirred at room temperature for 10 min, after which the solvent was removed *in vacuo*, leaving an oily solid.

Yield 0.7 g (76%) $C_{15}H_{34}N_2P_2Pt$ FM 499.48; mp 47-50 °C

5. *Pyrazolyl hydride* **4-6**

A solution of 1.55 mmol of $[Pt(PEt_3)_4]$ in 5 mL of toluene was added to a solution of 0.107 g (1.57 mmol) of pyrazole in 2 mL toluene. Decolouration of the orange $[Pt(PEt_3)_4]$ solution occurred immediately. The mixture was stirred at room temperature for 10 min, after which the solvent was removed *in vacuo*. An air-sensitive clear yellow oil was obtained.

Yield 0.5 g (68 %) $C_{15}H_{34}N_2P_2Pt$ FM 499.48

6. *Benzimidazolyl hydride* **4-7**

A solution of 1.25 mmol of $[Pt(PEt_3)_4]$ in 5 mL of toluene was added to a solution of

0.154 g (1.30 mmol) of benzimidazole in 5 mL of toluene. After decolourisation of the solution it was stirred for 30 min. The solvent was removed *in vacuo*. The white solid was obtained, washed with hexane and dried *in vacuo*.
Yield 0.6 g (87 %) $C_{15}H_{34}N_2P_2Pt$ FM 549.54; mp 82-85 °C

7. *Indazolyl hydride* **4-8**

A solution of 1.60 mmol of $[Pt(PEt_3)_4]$ in 5 mL of toluene was added to a suspension of 0.188 g (1.59 mmol) of indazole in 5 mL toluene. The solution decolourised and was stirred at room temperature for 3 hr, after which the solvent was removed *in vacuo*. A white solid was obtained, which was washed with hexane and dried *in vacuo*.
Yield 0.5 g (61 %) $C_{19}H_{36}N_2P_2Pt$ FM 549.54; mp 192-194 °C

8. *Reaction of $[Pt(PEt_3)_4]$ with 1,2,4-triazole*

Triazole (0.08 g, 1.16 mmol) was added to 1.19 mmol of $[Pt(PEt_3)_4]$ in 5 mL of toluene. An additional 5 mL of toluene was added. The colour change from orange to yellow was gradual (the triazole is not very soluble). After stirring at room temperature, work-up of the reaction mixture yielded a white solid which was washed with hexane and dried *in vacuo*. $[Pt(1\text{-azolyl})_2(PEt_3)_2]$ rather than a platinum(II) hydride was obtained.

9. *Furanyl hydride* **5-1**

To a solution of 0.155g (2.23 mmol) of furan in 10 mL toluene was added a solution of $[Pt(PEt_3)_4]$ (1.13 mmol) in 5 mL of toluene. The mixture was heated to reflux for 17 hr. The dark brown **5-1** was placed under vacuum and the solvent removed.
Yield 0.7 g (63 %) $C_{16}H_{34}OP_2Pt$ FM 499.48

10. *Benzoxazolyl hydride* **5-2**

To a solution of 0.1964 g (1.65 mmol) benzoxazole in 10 mL toluene was added a solution of $[Pt(PEt_3)_4]$ (1.62 mmol) in 5 mL of toluene. The mixture was heated to

reflux for a total of 40 hr. The colour of the solution changed gradually from light yellow to brown. After removal of the solvent *in vacuo*, a red-brown oil **5-2** was obtained.

Yield 0.8 g (90 %) $C_{19}H_{35}NOP_2Pt$ FM 550.52

11. *Benzothiazolyl hydride* **5-3**

Benzothiazole (0.70 mL, 6.4 mmol) was added to a solution of 3 mmol of $[Pt(PEt_3)_4]$ in 20 mL of toluene. The mixture was reluxed for 4 ½ hr and then stirred at room temperature for 16 hr. After work-up a red oil **5-3** was isolated.

Yield = 1.3 g (76 %) $C_{19}H_{35}NP_2SPt$ FM 566.59

12. *Reaction of dibenzofuran with $[Pt(PEt_3)_4]$*

Experiment 1: A solution of dibenzofuran (0.237 g, 1.41 mmol) in 5 mL of toluene was added to a solution of 1.4 mmol of $[Pt(PEt_3)_4]$ in 5 mL of toluene. The mixture was stirred for 90 min at 80 °C, by which time the solution had adopted a brown colour. The solvent was removed *in vacuo* and the residue triturated with hexane.

Experiment 2: The procedure was repeated using 1.5 mmol of $[Pt(PEt_3)_4]$ and 0.253 g (1.51 mmol) of dibenzothiophene and with refluxing for 1 week. Compound **5-4** was identified by NMR spectroscopy.

13. *Reaction of 2-methylbenzothiazole with $[Pt(PEt_3)_4]$*

A 5.0 mL toluene solution of 1.19 mmol of $[Pt(PEt_3)_4]$ was added to a Schlenk flask containing 0.20 g (1.3 mmol) of 2-methylbenzothiazole and 5 mL of toluene. The red solution, which gradually darkened, was stirred at room temperature for 34 hr and heated at 60 °C for 68 hr. After removal of the solvent *in vacuo*, no evidence of a hydride or a thiaplatinacycle could be detected by NMR analysis.

14. *Reaction of thiazole with $[Pt(PEt_3)_4]$*

Experiment 1: A solution of 1.6 mmol of $[Pt(PEt_3)_4]$ and 0.114 mL (1.61 mmol) of

thiazole was heated in 10 mL of toluene to reflux for 24 hr. The solvent was removed *in vacuo* and the brown oily residue triturated with hexane.

Experiment 2: The procedure was repeated, but using excess thiazole (0.230 mL, 3.24 mmol) and with refluxing for 4 days. A mixture of products were obtained. Line broadening in the ^{1}H NMR spectrum complicated the identification.

7.5.4 **Preparation of Pt(II) complexes of heteroarylphosphines** (Chapter 6)

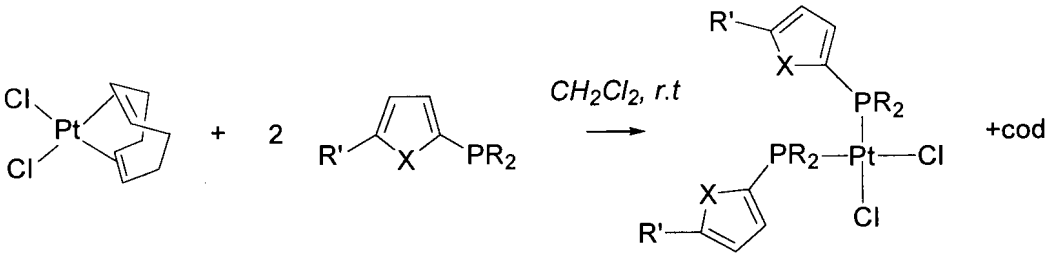

X = NMe, S
R = Ph, ^{i}Pr
R' = H, Me

1. *Dichlorobis[diisopropyl-2-(1-methylpyrrolyl)phosphine]platinum(II),* **6-1**

A solution of diisopropyl(1-methylpyrrolyl)phosphine (0.274 g, 1.39 mmol) in 5 mL of dichloromethane was slowly added to a suspension of [Pt(cod)Cl_2] (0.260 g, 0.695 mmol) in 5 mL dichloromethane. The resulting mixture was stirred at room temperature for 14 hr. After removal of the solvent, a solid was obtained which was washed with hexane and with diethyl ether. X-ray quality crystals were grown from a solution of **6-1** in dichloromethane layered with hexane at -20 °C over several days.

Yield 0.42 g (91.0 %) $C_{22}H_{40}N_2P_2PtCl_2$ FM 660.51

2. *Dichlorobis[2-(1-methylpyrrolyl)diphenylphosphine]platinum(II),* **6-2**

A solution of (1-methylpyrrolyl)diphenyl phosphine (0.56 g, 2.11 mmol) in 10 mL dichloromethane was slowly added to a suspension of $[Pt(cod)Cl_2]$ (0.376 g, 1.00 mmol) in 5 mL dichloromethane. After work-up, **6-2** was isolated.

Yield 0.66 g (83 %) $C_{34}H_{32}N_2P_2PtCl_2$ FM 796.57

3. *Dichlorobis[diisopropyl-2-(5-methylthienyl)phosphine]platinum(II),* **6-3**

Complex **6-3** was formed from diisopropyl-2-(5-methylthienyl)phosphine (0.520 g, 2.4 mmol) and $[Pt(cod)Cl_2]$ (0.425 g, 1.14 mmol) using the same procedure as for **6-2**. A white powder was obtained.

Yield 0.75 g (95 %) $C_{22}H_{38}P_2S_2PtCl_2$ FM 694.61

4. *Dichlorobis[2-(5-methylthienyl)diphenylphosphine]platinum(II)* , **6-4**

Complex **6-4** was isolated as a white solid from 2-(5-methylthienyl)diphenylphosphine (0.700 g, 2.48 mmol) and $[Pt(cod)Cl_2]$ (0.464 g, 1.24 mmol) under the same reaction conditions as for **6-1**.

Yield 0.94 g (91 %) $C_{34}H_{30}P_2S_2PtCl_2$ FM 830.69

5. *Dichlorobis[5-(2-bromopyridinyl)diisopropylphosphine]platinum(II),* **6-5**

A similar procedure was followed as described above. $[Pt(cod)Cl_2]$ (0.386 g, 1.03 mmol) was reacted with 2-(6-bromopyridinyl)diisopropylphosphine (0.565 g, 2.06 mmol). The complex **6-5** was isolated as white, crystalline flat needles.

Yield 0.80 g (95 %) $C_{22}H_{34}Br_2N_2P_2PtCl_2$ FM 814.27

6. *Reaction of 2,5-bis(diphenylphosphino)thiophene with $[Pt(cod)Cl_2]$*

A solution of 0.53 g (1.2 mmol) of 2,5-bis(diphenylphosphino)thiophene in 10 mL of dichloromethane was added to a solution of 0.201 g (0.537 mmol) of $[Pt(cod)Cl_2]$ in 10 mL of dichloromethane. The solution was stirred for 3 hr at room temperature,

during which time a suspension formed. The solvent was removed *in vacuo* and a white solid was obtained. This compound proved to be very insoluble in common organic solvents.

7.5.5 Photochemical reaction, $[Pt(PEt_3)_4]$ and pyrrole

A toluene solution (10 mL) containing 1.72 mmol of $[Pt(PEt_3)_4]$ and 0.160 mL (2.31 mmol) of pyrrole was stirred at room temperature under ultraviolet radiation (Hg lamp) for 18 hours. During this time the colour of the solution adopted a brown colour and a white suspension was formed. The supernatant was removed and the white solid was washed with hexane (two 2 mL portions) and dried *in vacuo*. $[Pt(1\text{-pyrrolyl})_2(PEt_3)_2]$ rather than a platinum(II) hydride was obtained.

7.5.6 Reactions of azoles with $[Pt(PPh_3)_3]$

1. *With indazole*

To a solution of 0.107 g (0.916 mmol) of indole in 10 mL of toluene, was added a slurry of 0.90 g (0.90 mmol) of $[Pt(PPh_3)_3]$ in 20 mL of toluene. The mixture was refluxed overnight. The volume of the solution was halved by evaporation *in vacuo* and the solution stirred at room temperature for a further 5 days. The solvent was removed *in vacuo* and the red residue washed with three portions (2 mL) of hexane. Compounds **4-9** and **4-10** were identified by NMR spectroscopy.

2. *With imidazole*

A mixture of 0.90 g (0.92 mmol) of $[Pt(PPh_3)_3]$ and 0.0674 (0.99 mmol) of imidazole was heated in 40 mL of toluene at 60 °C for 1 week. A red oil was obtained after work-up. No reaction occurred.

3. *With pyrazole*

The reaction was carried out as described above, using 1.0 g (1.0 mmol) of $[Pt(PPh_3)_3]$ and 0.073 g (1.07 mmol) of pyrazole. No reaction occurred.

7.6 REACTIONS OF PALLADIUM(0)

Various attempts were made at isolated a single or double oxidative insertion product of palladium(0) with bromo-substituted heteroaromatic compounds. The reactions are briefly outlined below:

1. A benzene solution (15 mL) of 1.30 g (1.13 mmol) of $[Pd(PPh_3)_3]$ and 0.063 mL (0.56 mmol) of 2,5-dibromothiophene was stirred at room temperature for 6 days.
2. A mixture of 1.49 g (1.29 mmol) of $[Pd(PPh_3)_3]$ and 0.313 g (0.65 mmol) of 4,5-dibromo-2,7-di-*tert*-butyl-9,9-dimethylxanthene in 15 mL of benzene was stirred at room temperature for 2 days.
3. A mixture of 1.43 g (1.24 mmol) of $[Pd(PPh_3)_3]$ and 0.215 g (0.63 mmol) of 4,6-dibromodibenzothiophene in 20 mL of benzene was stirred at room temperature for 4 days.
4. A mixture containing 1.012 g (1.76 mmol) of "$Pd(dba)_2$", 0.704 g (1.77 mmol) of dppe and 0.099 mL (0.880 mmol) of 2,5-dibromothiophene in 20 mL of toluene was stirred at room temperature for 90 min.
5. A toluene solution (20 mL) containing 1.048 g (1.82 mmol) "$Pd(dba)_2$", 0.275 mL (1.82 mmol) tmeda and 0.103 mL (0.91 mmol) 2,5-dibromothiophene was heated at 60 °C for 40 hr.

After work-up of the reaction mixtures, NMR and MS analysis was unable to indicate the presence of the target palladium(II) complexes.

7.7 REFERENCES

[1] Z. Otwinowski and W. Minor, "Processing of X-Ray Diffraction Data Collected in Oscillation Mode", in *Methods in Enzymology*, Vol. 276, Macromolecular Crystallography, Part A, edited by C.W. Carter & R.M. Sweet, Academic Press, 1997, pp. 307-326

[2] G.M. Sheldrick, *Acta Crystallogr. Sect. A, 46* (1990) 467

[3] G.M. Sheldrick, SHELXL-97, University of Göttingen, Germany, 1993

[4] (a) G.M. Sheldrick; SHELX86, University of Göttingen, Göttingen, Germany, 1986 (b) C.K. Johnson; ORTEP. Report ORNL-3794, Oak Ridge National Laboratory, Oak Ridge, TN, USA, 1965

[5] R.J. Errington in *Advanced Practical, Inorganic and Metalorganic Chemistry*, Blackie Academic and Professional, London, 1997

[6] H.C. Clark and L.E. Manzer; *J. Organomet. Chem.*, **1973**, *59*, 411-428

[7] T. Yoshida, T. Matsuda and S. Otsuka; *Inorg Synth.*, **1990**, *28*, 122

[8] R. Ugo, F. Cariati and G. La Monica; *Inorg Synth.*, **1990**, *28*, 124-125

[9] G.S. Hill, M.J. Irwin, C.J. Levy, L.M. Rendina and R.J. Puddephatt; *Inorg. Synth.* **1998**, *32*, 149-150

[10] P.K. Monaghan and R.J. Puddephatt; *Organometallics*, **1984**, *3*, 444-449

[11] D.R. Coulson, *Inorg Synth.*, **1990**, *28*, 107-108

[12] W.A. Herrmann and C. Zybill in *Synthetic Methods of Organometallic and Inorganic Chemistry*, ed. W.A Herrmann and A. Salzer; Vol 1., Georg Thieme Verlag, Stuttgart, 1996, p 160

[13] C. Kuehm-Caubère, S. Adach-Becker, Y. Fort and P. Caubère; *Tetrahedron*, **1996**, *52*, 9087-9092

[14] R.H. Mitchell, Y. Chen and J. Zhang; *Oppi Briefs*; **1997**, *29*, 715-719

[15] K.S. Choi, K. Sawada, H.B. Dong, M. Hoshino and J. Nakayama; *Heterocycles*, **1994**, *38*, 143-149

[16] (a) L. Brandsma, S.F. Vasilevsky and H.D. Verkruijsse in *Applications of Transition Metal Catalysts in Organic Synthesis*, Springer-Verlag, Berlin, 1998, p 264 and (b) p 5 and (c) p 8

[17] adapted from: *Modern Synthetic Methods*, ed. Rolf Scheffold, Verlag Helvetica Chemica Acta, Basel, 1992, p386

[18] L. Brandsma and H. Verkruijsse in *Preparative Polar Organometallic Chemistry*, Vol.1,

Springer-Verlag, Berlin, 1987

/ End of Chapter 7 //

APPENDIX

Single crystal X-ray structure determination: acquisition and structural parameters

4,6-bis(trimethylsilyl)dibenzothiophene, **2**

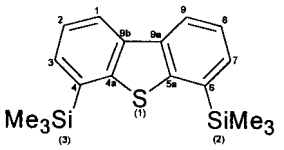

4,6-dibromodibenzothiophene, **3**

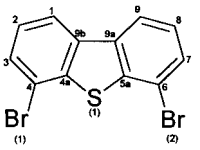

thiaplatinacycle of $Pt(PEt_3)_2$ with 3,6-dimethylthieno[3,2-*b*]thiophene, **3-1**

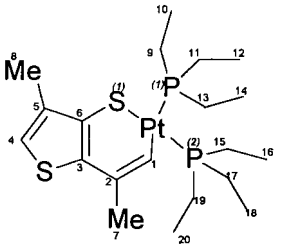

trans-dichlorobis[diisopropyl-2-(1-methyl-pyrrolyl)phosphine]-platinum(II), **6-1**

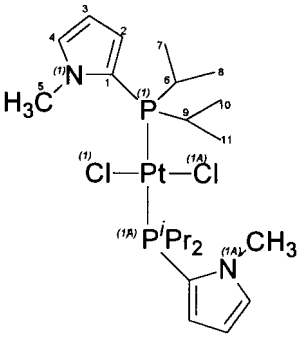

Table A1 Crystal Data Acquisition and Refinement for **2**

Empirical formula	$C_{18}\ H_{24}\ S\ Si_2$
Formula weight	328.61
Temperature	294(2) K
Wavelength	0.71073 Å
Crystal system	Monoclinic
Space group	$P2_1/n$
Unit cell dimensions: a,b,c (Å) α, β, γ (°)	15.169 (2), 8.4610 (13), 15.288 (2) 90 , 94.228 (3) , 90
Volume	1956.8 (5) $Å^3$
Z	4
Density (calculated)	1.115 g/cm^3
Absorption coefficient	0.281 mm^{-1}
F(000)	704
Crystal size	0.50 × 0.48 × 0.44 mm
Θ range for data collection	1.83 to 28.30°
Index ranges	$-20 \le h \le 11$, $-11 \le k \le 9$, $-20 \le l \le 19$
Reflections collected	13152
Independent reflections, R(int)	4839, 0.0162
Reflections observed (>2σ)	3566
Absorption correction	Empirical
Max. and min. transmission	0.8864 and 0.8677
Refinement method	Full-matrix least-squares on F^2
Data / restraints / parameters	4839 / 0 / 202
Goodness-of-fit on F^2	1.026
Final R indices [I > 2σ(I)]	$R_1 = 0.0394$, $wR_2 = 0.1026$
R indices (all data)	$R_1 = 0.0588$, $wR_2 = 0.1152$
Largest difference. peak and hole	0.234 and -0.201 $e.Å^{-3}$

Table A2 Atomic coordinates ($\times 10^4$) and equivalent isotropic displacement parameters ($Å^2 \times 10^3$) for **2**

Atom	x	y	z	U(eq)
S(1)	923(1)	1980(1)	3790(1)	59(1)
Si(2)	1224(1)	2578(1)	6043(1)	58(1)
Si(3)	62(1)	2900(1)	1685(1)	65(1)
C(9a)	1937(1)	-501(2)	4033(1)	53(1)
C(4)	817(1)	1185(2)	2001(1)	58(1)
C(5a)	1562(1)	723(2)	4499(1)	51(1)
C(4a)	1148(1)	859(2)	2865(1)	52(1)
C(6)	1679(1)	884(2)	5419(1)	54(1)
C(9b)	1700(1)	-424(2)	3099(1)	54(1)
C(8)	2582(1)	-1512(2)	5396(1)	72(1)
C(7)	2201(1)	-288(2)	5840(1)	64(1)
C(3)	1091(1)	125(2)	1376(1)	68(1)
C(9)	2454(1)	-1633(2)	4499(1)	67(1)
C(1)	1946(1)	-1438(2)	2437(1)	67(1)
C(2)	1645(2)	-1151(3)	1585(2)	74(1)
C(10)	649(2)	4792(2)	1920(2)	81(1)
C(13)	28(2)	2877(3)	5732(2)	89(1)
C(14)	1859(2)	4371(3)	5778(2)	89(1)
C(15)	1369(2)	2157(3)	7241(2)	94(1)
C(12)	-938(2)	2785(3)	2318(2)	98(1)
C(11)	-289(2)	2788(4)	496(2)	120(1)

U(eq) is defined as one third of the trace of the orthogonalized U_{ij} tensor.

Table A3 Bond lengths [Å] and angles [°] for **2**

S(1)-C(4a)	1.7561(17)	C(4a)-S(1)-C(5a)	92.24(8)
S(1)-C(5a)	1.7586(16)	C(14)-Si(2)-C(13)	110.19(12)
Si(2)-C(14)	1.857(2)	C(14)-Si(2)-C(15)	110.17(12)
Si(2)-C(13)	1.858(2)	C(13)-Si(2)-C(15)	108.64(12)
Si(2)-C(15)	1.864(2)	C(14)-Si(2)-C(6)	107.24(10)
Si(2)-C(6)	1.8812(19)	C(13)-Si(2)-C(6)	111.19(9)
Si(3)-C(10)	1.854(2)	C(15)-Si(2)-C(6)	109.39(10)
Si(3)-C(11)	1.859(3)	C(10)-Si(3)-C(11)	109.42(14)
Si(3)-C(12)	1.861(3)	C(10)-Si(3)-C(12)	110.05(12)
Si(3)-C(4)	1.890(2)	C(11)-Si(3)-C(12)	108.71(15)
C(9a)-C(9)	1.399(2)	C(10)-Si(3)-C(4)	109.87(9)
C(9a)-C(5a)	1.401(2)	C(11)-Si(3)-C(4)	109.56(11)
C(9a)-C(9b)	1.448(2)	C(12)-Si(3)-C(4)	109.20(10)
C(3)-C(4)	1.396(3)	C(9)-C(9a)-C(5a)	118.69(17)
C(4)-C(4a)	1.406(2)	C(9)-C(9a)-C(9b)	128.47(17)
C(5a)-C(6)	1.410(2)	C(5a)-C(9a)-C(9b)	112.82(15)
C(4a)-C(9b)	1.401(2)	C(3)-C(4)-C(4a)	114.48(17)
C(6)-C(7)	1.396(2)	C(3)-C(4)-Si(3)	121.62(14)
C(1)-C(9b)	1.398(2)	C(4a)-C(4)-Si(3)	123.90(13)
C(8)-C(9)	1.375(3)	C(9a)-C(5a)-C(6)	123.53(15)
C(7)-C(8)	1.388(3)	C(9a)-C(5a)-S(1)	111.03(12)
C(2)-C(3)	1.390(3)	C(6)-C(5a)-S(1)	125.43(13)
C(1)-C(2)	1.370(3)	C(9b)-C(4a)-C(4)	123.81(16)
		C(9b)-C(4a)-S(1)	111.15(13)
		C(4)-C(4a)-S(1)	125.04(14)
C(7)-C(8)-C(9)	120.69(19)	C(7)-C(6)-C(5a)	114.66(16)
C(6)-C(7)-C(8)	123.11(18)	C(7)-C(6)-Si(2)	121.57(14)
C(2)-C(3)-C(4)	123.13(19)	C(5a)-C(6)-Si(2)	123.71(13)
C(8)-C(9)-C(9a)	119.32(19)	C(1)-C(9b)-C(4a)	118.50(17)
C(2)-C(1)-C(9b)	119.4(2)	C(1)-C(9b)-C(9a)	128.75(17)
C(1)-C(2)-C(3)	120.64(19)	C(4a)-C(9b)-C(9a)	112.76(15)

Table A4 Anisotropic displacement parameters ($Å^2 \times 10^3$) for **2**

Atom	U11	U22	U33	U23	U13	U12
S(1)	69(1)	53(1)	54(1)	-2(1)	-2(1)	13(1)
Si(2)	56(1)	60(1)	56(1)	-2(1)	0(1)	-3(1)
Si(3)	74(1)	61(1)	58(1)	0(1)	-10(1)	1(1)
C(9a)	48(1)	47(1)	64(1)	2(1)	3(1)	-2(1)
C(4)	64(1)	52(1)	58(1)	-4(1)	0(1)	-8(1)
C(5a)	47(1)	46(1)	60(1)	4(1)	0(1)	-2(1)
C(4a)	54(1)	46(1)	56(1)	-4(1)	4(1)	-5(1)
C(6)	52(1)	53(1)	57(1)	4(1)	0(1)	-6(1)
C(9b)	51(1)	47(1)	64(1)	-3(1)	7(1)	-4(1)
C(8)	74(1)	61(1)	78(1)	13(1)	-7(1)	11(1)
C(7)	67(1)	63(1)	62(1)	9(1)	-5(1)	-2(1)
C(3)	82(1)	65(1)	57(1)	-11(1)	1(1)	-9(1)
C(9)	65(1)	55(1)	81(1)	1(1)	4(1)	10(1)
C(1)	67(1)	56(1)	79(1)	-11(1)	7(1)	5(1)
C(2)	84(1)	65(1)	74(1)	-21(1)	11(1)	1(1)
C(10)	89(2)	58(1)	96(2)	0(1)	4(1)	2(1)
C(13)	62(1)	116(2)	88(2)	-16(1)	4(1)	8(1)
C(14)	93(2)	67(1)	106(2)	-10(1)	12(1)	-16(1)
C(15)	115(2)	104(2)	61(1)	-4(1)	4(1)	20(2)
C(12)	69(1)	104(2)	120(2)	22(2)	0(1)	11(1)
C(11)	171(3)	107(2)	73(2)	-7(1)	-41(2)	26(2)

The anisotropic displacement factor exponent takes the form:
$-2\,\pi^2\,[h^2\,a^{*2}\,U11 + \ldots + 2\,h\,k\,a^*\,b^*\,U]$

Table A5 Hydrogen coordinates ($\times 10^4$) and isotropic displacement parameters ($Å^2 \times 10^3$) for **2**

Atom	x	y	z	U(eq)
H(8)	2921(9)	-2240(20)	5702(8)	86
H(7)	2303(2)	-243(3)	6482(13)	77
H(3)	894(5)	280(4)	790(14)	82
H(9)	2713(6)	-2470(20)	4200(8)	80
H(1)	2309(9)	-2290(20)	2573(4)	81
H(2)	1820(5)	-1844(17)	1123(12)	89
H(10A)	830(3)	4849(3)	2526(9)	122
H(10B)	266(5)	5647(12)	1766(3)	122
H(10C)	1152(7)	4847(3)	1589(5)	122
H(13A)	-266(5)	2025(14)	5861(3)	133
H(13B)	-49(2)	3060(5)	5166(10)	133
H(13C)	-165(4)	3687(14)	6021(5)	133
H(14A)	2448(9)	4212(4)	5935(3)	133
H(14B)	1660(3)	5220(13)	6082(5)	133
H(14C)	1783(2)	4568(4)	5187(9)	133
H(15A)	1057(6)	1288(16)	7363(3)	140
H(15B)	1173(4)	2987(15)	7542(6)	140
H(15C)	1946(10)	1993(4)	7399(3)	140
H(12A)	-776(3)	2828(3)	2891(11)	147
H(12B)	-1219(5)	1878(16)	2197(3)	147
H(12C)	-1296(7)	3592(15)	2172(3)	147
H(11A)	-583(7)	1850(20)	379(3)	179
H(11B)	203(11)	2837(4)	175(7)	179
H(11C)	-661(8)	3624(19)	343(4)	179

Table A6 Crystal Data Acquisition and Refinement for **3.**

Empirical formula	$C_{12}\ H_6\ Br_2\ S$
Formula weight	342.05
Temperature	293 (2) K
Wavelength	0.71073 Å
Crystal system	Monoclinic
Space group	$P2_1/c$
Unit cell dimensions: a,b,c (Å) α, β, γ (°)	10.4977 (17), 8.5629 (14), 12.947 (2) 90 , 106.813 (3) , 90
Volume	1114.0 (3) $Å^3$
Z	4
Density (calculated)	2.039 g/cm^3
Absorption coefficient	7.423 mm^{-1}
F(000)	656
Crystal size	0.32 × 0.20 × 0.05 mm
Θ range for data collection	2.03 to 28.32°
Index ranges	$-13 \le h \le 12$, $-11 \le k \le 11$, $-10 \le l \le 17$
Reflections collected	7581
Independent reflections	2766
R(int)	0.0462
Reflections observed (>2σ)	1860
Max. and min. transmission	0.7079 and 0.1998
Refinement method	Full-matrix least-squares on F^2
Data / restraints / parameters	2766 / 0 / 136
Goodness-of-fit on F^2	0.954
Final R indices [I > 2σ(I)]	$R_1 = 0.0514$, $wR_2 = 0.1319$
R indices (all data)	$R_1 = 0.0779$, $wR_2 = 0.1470$
Largest difference. peak and hole	0.889 and -1.010 $e.Å^{-3}$

Table A7 Atomic coordinates ($\times 10^4$) and equivalent isotropic displacement parameters ($Å^2 \times 10^3$) for **3**

Atom	x	y	z	U(eq)
S(1)	5129(1)	-219(1)	7040(1)	43(1)
Br(1)	1927(1)	389(1)	6854(1)	56(1)
Br(2)	8399(1)	299(1)	8149(1)	60(1)
C(1)	3372(5)	-2877(5)	4515(4)	51(1)
C(2)	2036(6)	-2679(6)	4388(4)	58(1)
C(3)	1579(5)	-1709(5)	5078(4)	51(1)
C(4)	2495(4)	-934(5)	5900(4)	43(1)
C(4a)	3841(4)	-1117(4)	6045(3)	40(1)
C(5a)	6316(4)	-1137(4)	6534(3)	41(1)
C(6)	7681(5)	-1005(5)	6938(4)	44(1)
C(7)	8509(5)	-1814(6)	6469(4)	53(1)
C(8)	7942(6)	-2772(6)	5583(4)	57(1)
C(9)	6595(5)	-2922(5)	5164(4)	47(1)
C(9a)	5749(5)	-2110(4)	5639(3)	41(1)
C(9b)	4312(5)	-2093(4)	5352(3)	41(1)

U(eq) is defined as one third of the trace of the orthogonalized U_{ij} tensor.

Table A8 Bond lengths [Å] and angles [°] for **3**

S(1)-C(4a)	1.753(4)	C(4a)-S(1)-C(5a)	90.6(2)
S(1)-C(5a)	1.752(4)	C(4a)-C(4)-Br(1)	118.8(3)
Br(1)-C(4)	1.894(5)	C(3)-C(4)-Br(1)	120.6(4)
Br(2)-C(6)	1.894(4)	C(5a)-C(6)-Br(2)	118.8(3)
C(1)-C(2)	1.374(7)	C(7)-C(6)-Br(2)	120.6(4)
C(2)-C(3)	1.403(7)	C(1)-C(2)-C(3)	121.5(5)
C(3)-C(4)	1.381(6)	C(2)-C(3)-C(4)	119.0(5)
C(4)-C(4a)	1.379(6)	C(3)-C(4)-C(4a)	120.5(4)
C(5a)-C(6)	1.381(6)	C(4)-C(4a) -C(9b)	120.9(4)
C(6)-C(7)	1.382(6)	C(4a)-C(9b)-C(1)	118.2(4)
C(7)-C(8)	1.396(7)	C(5a)-C(6)-C(7)	120.6(4)
C(8)-C(9)	1.367(7)	C(6)-C(7)-C(8)	118.9(5)
C(9)-C(9a)	1.402(6)	C(7)-C(8)-C(9)	121.8(5)
C(5a)-C(9a)	1.412(6)	C(8)-C(9)-C(9a)	119.6(4)
C(9a)-C(9b)	1.445(6)	S(1)-C(4a)-C(9b)	112.8(3)
C(4a)-C(9b)	1.416(6)	S(1)-C(4a)-C(4)	126.3(3)
C(1)-C(9b)	1.407(6)	S(1)-C(5a)-C(9a)	113.2(3)
		S(1)-C(5a)-C(6)	126.4(3)
		C(4a)-C(9b)-C(9a)	111.9(4)
		C(5a)-C(9a)-C(9b)	111.5(4)
		C(1)-C(9b)-C(9a)	129.9(4)
		C(9)-C(9a)-C(9b)	129.7(4)
		C(6)-C(5a)-C(9a)	120.3(4)
		C(2)-C(1)-C(9b)	119.9(5)
		C(9)-C(9a)-C(5b)	118.9(4)

TableA9 Anisotropic displacement parameters ($Å^2 \times 10^3$) for **3**

Atom	U11	U22	U33	U23	U13	U12
S(1)	50(1)	43(1)	35(1)	-7(1)	9(1)	-2(1)
Br(1)	55(1)	61(1)	52(1)	-1(1)	16(1)	8(1)
Br(2)	63(1)	63(1)	50(1)	-9(1)	8(1)	-17(1)
C(1)	69(3)	40(2)	37(2)	-6(2)	7(2)	-5(2)
C(2)	66(3)	52(3)	43(3)	-4(2)	-6(2)	-9(3)
C(3)	51(3)	49(3)	44(3)	5(2)	2(2)	-4(2)
C(4)	51(3)	36(2)	41(2)	9(2)	11(2)	2(2)
C(4a)	52(3)	34(2)	31(2)	4(2)	7(2)	0(2)
C(5a)	53(3)	34(2)	34(2)	2(2)	12(2)	-2(2)
C(6)	50(3)	39(2)	42(2)	3(2)	12(2)	-5(2)
C(7)	51(3)	56(3)	58(3)	9(2)	23(2)	-2(2)
C(8)	71(3)	54(3)	55(3)	-3(2)	31(3)	3(3)
C(9)	64(3)	41(2)	39(2)	-3(2)	18(2)	0(2)
C(9a)	57(3)	32(2)	34(2)	1(2)	13(2)	0(2)
C(9b)	56(3)	30(2)	30(2)	0(2)	4(2)	-1(2)

The anisotropic displacement factor exponent takes the form:
$-2\pi^2 [h^2 a^{*2} U11 + ... + 2 h k a^* b^* U]$

Table A10 Hydrogen coordinates ($\times 10^4$) and isotropic displacement parameters ($Å^2 \times 10^3$) for **3**

Atom	x	y	z	U(eq)
H(1)	3654	-3527	4049	61
H(2)	1422	-3201	3832	70
H(3)	672	-1589	4983	61
H(7)	9429	-1722	6739	64
H(8)	8497	-3324	5269	69
H(9)	6241	-3559	4568	557

Table A11 Crystal Data Acquisition and Refinement for **3-1**

Empirical formula	$C_{20}\ H_{38}\ P_2\ Pt\ S_2$
Formula weight	599.65
Temperature	183(2) K
Wavelength	0.71073 Å
Crystal system	Orthorhombic
Space group	$P2_12_12_1$
Unit cell dimensions: a,b,c (Å) α, β, γ (°)	9.8621 (4), 13.3149 (6), 18.6497 (8) 90 , 90, 90
Volume	2448.9 (2) $Å^3$
Z	4
Density (calculated)	1.626 g/cm^3
Absorption coefficient	6.033 mm^{-1}
F(000)	1192
Crystal size	0.12 × 0.12 × 0.12 mm
Θ range for data collection	3.01 to 27.41°
Index ranges	$-12 \le h \le 12$, $-15 \le k \le 17$, $-24 \le l \le 20$
Reflections collected	13153
Independent reflections, R(int)	5516, 0.0786
Completeness to θ = 27.41	99.4%
Max. and min. transmission	0.5313 and 0.4098
Refinement method	Full-matrix least-squares on F^2
Data / restraints / parameters	5516 / 0 / 226
Goodness-of-fit on F^2	1.062
Final R indices [$I > 2\sigma(I)$]	$R_1 = 0.0809$, $wR_2 = 0.0881$
R indices (all data)	$R_1 = 0.1146$, $wR_2 = 0.0943$
Absolute structure parameter	-0.007(12)
Largest difference. peak and hole	3.862 and -1.958 $e.Å^{-3}$

Table A12 Selected bond lengths (Å) and angles (°) for **3-1**

Pt-C(1)	2.035(10)	C(11)-P(1)-C(13)	104.3(5)
Pt-P(2)	2.279(3)	C(11)-P(1)-C(9)	101.6(5)
Pt-S(1)	2.290(2)	C(13)-P(1)-C(9)	101.1(5)
Pt-P(1)	2.342(2)	C(11)-P(1)-Pt	116.3(4)
P(1)-C(11)	1.826(10)	C(13)-P(1)-Pt	115.3(4)
P(1)-C(13)	1.822(10)	C(9)-P(1)-Pt	116.2(4)
P(1)-C(9)	1.839(10)	C(19)-P(2)-C(15)	103.1(6)
P(2)-C(19)	1.825(12)	C(19)-P(2)-C(17)	100.8(6)
P(2)-C(15)	1.834(11)	C(15)-P(2)-C(17)	103.3(6)
P(2)-C(17)	1.844(11)	C(19)-P(2)-Pt	111.8(4)
S(1)-C(6)	1.753(12)	C(15)-P(2)-Pt	114.5(4)
S(2)-C(3)	1.740(10)	C(17)-P(2)-Pt	121.0(4)
S(2)-C(4)	1.734(15)	C(6)-S(1)-Pt	112.0(4)
C(1)-C(2)	1.291(15)	C(3)-S(2)-C(4)	90.8(6)
C(2)-C(3)	1.420(17)	C(2)-C(1)-Pt	137.6(10)
C(2)-C(7)	1.553(15)	C(1)-C(2)-C(3)	122.9(10)
C(3)-C(6)	1.371(16)	C(1)-C(2)-C(7)	122.0(12)
C(4)-C(5)	1.331(17)	C(3)-C(2)-C(7)	115.1(11)
C(5)-C(6)	1.430(17)	C(6)-C(3)-C(2)	129.4(9)
C(5)-C(8)	1.480(19)	C(6)-C(3)-S(2)	109.6(10)
C(9)-C(10)	1.527(15)	C(2)-C(3)-S(2)	120.9(10)
C(11)-C(12)	1.508(17)	C(5)-C(4)-S(2)	114.1(11)
C(13)-C(14)	1.542(14)	C(4)-C(5)-C(6)	110.5(14)
C(15)-C(16)	1.531(18)	C(4)-C(5)-C(8)	125.1(14)
C(17)-C(18)	1.541(15)	C(6)-C(5)-C(8)	124.3(12)
C(19)-C(20)	1.509(16)	C(3)-C(6)-C(5)	114.9(11)
		C(3)-C(6)-S(1)	125.7(9)
		C(5)-C(6)-S(1)	119.4(10)
C(1)-Pt-P(2)	85.4(4)	C(10)-C(9)-P(1)	116.4(8)
C(1)-Pt-S(1)	89.8(4)	C(12)-C(11)-P(1)	111.9(7)
P(2)-Pt-S(1)	173.67(11)	C(14)-C(13)-P(1)	112.2(8)
C(1)-Pt-P(1)	176.1(3)	C(16)-C(15)-P(2)	112.1(9)
P(2)-Pt-P(1)	97.73(9)	C(18)-C(17)-P(2)	116.1(9)
S(1)-Pt-P(1)	87.24(9)	C(20)-C(19)-P(2)	113.5(9)

Table A13 Torsion angles (°) for **3-1**

C(1)-Pt-P(1)-C(11)	-158(6)	C(4)-S(2)-C(3)-C(2)	175.5(9)
P(2)-Pt-P(1)-C(11)	59.8(4)	C(3)-S(2)-C(4)-C(5)	1.5(10)
S(1)-Pt-P(1)-C(11)	-116.3(4)	S(2)-C(4)-C(5)-C(6)	-2.1(14)
C(1)-Pt-P(1)-C(13)	79(6)	S(2)-C(4)-C(5)-C(8)	-178.6(11)
P(2)-Pt-P(1)-C(13)	-62.8(4)	C(2)-C(3)-C(6)-C(5)	-176.2(11)
S(1)-Pt-P(1)-C(13)	121.2(4)	S(2)-C(3)-C(6)-C(5)	-0.6(12)
C(1)-Pt-P(1)-C(9)	-39(6)	C(2)-C(3)-C(6)-S(1)	3.3(17)
P(2)-Pt-P(1)-C(9)	179.2(4)	S(2)-C(3)-C(6)-S(1)	178.9(6)
S(1)-Pt-P(1)-C(9)	3.2(4)	C(4)-C(5)-C(6)-C(3)	1.8(14)
C(1)-Pt-P(2)-C(19)	53.4(5)	C(8)-C(5)-C(6)-C(3)	178.3(12)
S(1)-Pt-P(2)-C(19)	12.4(11)	C(4)-C(5)-C(6)-S(1)	-177.8(8)
P(1)-Pt-P(2)-C(19)	-129.0(4)	C(8)-C(5)-C(6)-S(1)	-1.2(16)
C(1)-Pt-P(2)-C(15)	-63.4(6)	Pt-S(1)-C(6)-C(3)	12.0(10)
S(1)-Pt-P(2)-C(15)	-104.4(10)	Pt-S(1)-C(6)-C(5)	-168.5(8)
P(1)-Pt-P(2)-C(15)	114.2(5)	C(11)-P(1)-C(9)-C(10)	-49.7(10)
C(1)-Pt-P(2)-C(17)	171.9(6)	C(13)-P(1)-C(9)-C(10)	57.5(10)
S(1)-Pt-P(2)-C(17)	130.9(9	Pt-P(1)-C(9)-C(10)	-176.9(7)
P(1)-Pt-P(2)-C(17)	-10.6(5)	C(13)-P(1)-C(11)-C(12)	-174.3(9)
C(1)-Pt-S(1)-C(6)	-13.8(5)	C(9)-P(1)-C(11)-C(12)	-69.6(10)
P(2)-Pt-S(1)-C(6)	27.0(10)	Pt-P(1)-C(11)-C(12)	57.5(10)
P(1)-Pt-S(1)-C(6)	168.8(4)	C(11)-P(1)-C(13)-C(14)	172.4(9)
P(2)-Pt-C(1)-C(2)	-166.6(12)	C(9)-P(1)-C(13)-C(14)	67.3(10)
S(1)-Pt-C(1)-C(2)	9.2(11)	Pt-P(1)-C(13)-C(14)	-58.8(10)
P(1)-Pt-C(1)-C(2)	51(6)	C(19)-P(2)-C(15)-C(16)	-178.8(10)
Pt-C(1)-C(2)-C(3)	3.6(18)	C(17)-P(2)-C(15)-C(16)	76.5(11)
Pt-C(1)-C(2)-C(7)	-179.5(9)	Pt-P(2)-C(15)-C(16)	-57.1(12)
C(1)-C(2)-C(3)-C(6)	-13.5(18)	C(19)-P(2)-C(17)-C(18)	-61.7(11)
C(7)-C(2)-C(3)-C(6)	169.5(11)	C(15)-P(2)-C(17)-C(18)	44.7(12)
C(1)-C(2)-C(3)-S(2)	171.4(8)	Pt-P(2)-C(17)-C(18)	174.5(8)
C(7)-C(2)-C(3)-S(2)	-5.6(13)	C(15)-P(2)-C(19)-C(20)	175.3(10)
C(4)-S(2)-C(3)-C(6)	-0.5(8)	C(17)-P(2)-C(19)-C(20)	-78.1(10)
		Pt-P(2)-C(19)-C(20)	51.8(11)

Table A14 Crystal Data Acquistion and Refinement for **6-1**

Empirical formula	$C_{22}\ H_{40}\ Cl_2\ N_2\ P_2\ Pt$
Formula weight	660.49
Temperature	183(2) K
Wavelength	0.7103 Å
Crystal system	Monoclinic
Space group	$P2_1/n$
Unit cell dimensions:	
a,b,c (Å)	8.1993 (3), 8.2423 (3), 19.4461(6)
α, β, γ (°)	90 , 94.303 (2) , 90
Volume	1310.48 (8) $Å^3$
Z	2
Density (calculated)	1.674 g/cm^3
μ (Mo-K_α) Absorption coefficient	56.92 cm^{-1}
F(000)	656
Crystal size	0.14 × 0.12 × 0.10 mm^3
Θ range for data collection	3.51 to 26.32°
Index ranges	$-10 \le h \le 10$, $-10 \le k \le 8$, $-24 \le l \le 23$
Reflections collected	6702
Independent reflections	2638
R(int)	0.0418
Completeness to Θ = 26.32°	99.0 %
Absorption correction	Semiempirical
Max. and min. transmission	0.968 and 0.553
Refinement method	Full-matrix least-squares on F^2
Data / restraints / parameters	2638 / 0 / 133
Goodness-of-fit on F^2	1.12
Final R indices [$I > 2\sigma(I)$]	R1 = 0.0325, wR^2 = 0.0723
R indices (all data)	R1 = 0.0420, wR^2 = 0.0768
Largest difference. peak and hole	1.246 and -1.779 $e.Å^{-3}$

Table A15 Atomic coordinates ($\times 10^4$) and equivalent isotropic displacement parameters ($Å^2 \times 10^3$) for **6-1**

	x	y	z	U(eq)
Pt	0	0	0	15(1)
Cl(1)	2427(1)	-212(1)	688(1)	26(1)
P(1)	-1364(1)	664(2)	974(1)	17(1)
N(1)	824(4)	3084(5)	1534(2)	25(1)
C(1)	-189(5)	1776(6)	1643(2)	22(1)
C(2)	-167(6)	1551(6)	2351(2)	28(1)
C(3)	880(6)	2734(7)	2668(2)	32(1)
C(4)	1464(6)	3656(7)	2157(3)	33(1)
C(5)	1263(6)	3771(6)	875(2)	33(1)
C(6)	-3293(5)	1827(6)	821(2)	23(1)
C(7)	-4143(6)	2105(7)	1498(2)	34(1)
C(8)	-3004(6)	3443(6)	463(3)	35(1)
C(9)	-1988(5)	-1210(5)	1405(2)	20(1)
C(10)	-527(6)	-2334(6)	1604(3)	33(1)
C(11)	-3284(6)	-2119(6)	932(3)	29(1)

U(eq) is defined as one third of the trace of the orthogonalized U_{ij} tensor.